THE EFFECT OF DISSOLVED OXYGEN CONCENTRATION ON MONOCLONAL ANTIBODY GLYCOSYLATION IN SERUM-FREE CONTINUOUS CULTURE

by

JEREMY PAUL KUNKEL

A Thesis Submitted to the
Faculty of Graduate Studies in Partial Fulfillment of the
Requirements for the Degree of

DOCTOR OF PHILOSOPHY

Department of Chemistry
University of Manitoba
Winnipeg, Manitoba
Canada

THE UNIVERSITY OF MANITOBA

FACULTY OF GRADUATE STUDIES

*****

COPYRIGHT PERMISSION PAGE

THE EFFECT OF DISSOLVED OXYGEN CONCENTRATION ON MONOCLONAL ANTIBODY GLYCOSYLATION IN SERUM-FREE CONTINUOUS CULTURE

BY

Jeremy Paul Kunkel

A Thesis/Practicum submitted to the Faculty of Graduate Studies of The University of Manitoba in partial fulfillment of the requirements of the degree of

DOCTOR OF PHILOSOPHY

A day will come in which zealous research over long periods of time will bring to light things that now still lie hidden. The life of a single man, even if he devotes it entirely to the heavens, is insufficient to fathom so broad a field. Knowledge will thus unfold only over the course of generations. But there will come a time when our descendants will marvel that we did not know the things that seem so simple to them. Many discoveries are reserved for future centuries, however, when we are long forgotten. Our universe would be deplorably insignificant had it not offered every generation new problems. Nature does not surrender her secrets once and for all.

– Lucius Annaeus Seneca, 4 BC – 65 AD

Just as we do not inquire for what useful purpose the birds sing, because they were created to sing and song is a delight for them, so we should also not ask why the human spirit strives to ascertain the secrets of heaven. Natural phenomena are so diverse, and heaven is so rich in hidden treasures, in order that the human spirit will never want for fresh nourishment.

– Johannes Kepler, 1571 – 1630

A work such as this is actually never complete. One must declare it complete when one has done all that is possible given the time and the circumstances.

– Johann Wolfgang von Goethe, 1749 – 1832

Scientists do not study nature because it is useful to do so. They study it because they take pleasure in it, and they take pleasure in it because it is beautiful.

– Jules-Henri Poincaré, 1854 – 1912

Where is the wisdom we have lost in knowledge?
Where is the knowledge we have lost in information?

– Thomas Stearns Eliot, 1888 – 1965

The vision of the mind authoritatively supplements the vision of the eye. By a necessity engendered and justified by science I cross the boundary of the experimental evidence.

– John Tyndall, 1820 – 1893

Table of contents

Acknowledgements

The completion of this, my Ph.D. thesis, would not have been possible without the assistance and support of many people. I would like to extend my gratitude to everyone who helped me in this endeavour, your efforts and contributions are deeply appreciated.

Prof. James Jamieson, my supervisor, is especially recognized for his encouragement and support. His enthusiasm, good nature, and patience have been greatly appreciated and admired.

Prof. Michael Butler, my 'co-supervisor', and the two other members of my advisory committee, Prof. Hélène Perreault and Dr. Keith Lewis, are also thanked for the time and effort they invested in various meetings, and for their careful perusal of this work and thoughtful advice in the various stages of the research.

Dr. T. Shantha Raju, my external thesis examiner, is thanked for his meticulous and valuable examination of this work, and for his kind comments at several conferences.

Also recognized are: Dr. David Jan, for cell culture in the laboratory of Prof. Butler; Dr. William Yan, for cell culture and base galactosyltransferase assays in the laboratory of Prof. Butler; Julian Saba, for mass spectrometry in the laboratories of Prof. Perreault and Profs. Standing and Ens.

The members of the Jamieson laboratory and my various other friends in the department, past and present, too numerous to name here, whom I have had the good fortune of knowing, are thanked for their friendship and comradery.

To my parents, Johann and Elisabeth, for everything, from the beginning until now, and forever: I love you. My siblings, Deborah, Dorcas, Lois, Kathryn, and John Adam, are thanked for their love and support.

My partner and spouse, Tamara Schroeder, is cherished for her unlimited support, complete faith, and everything she has done for me. To her parents, Siegfried and Esther, for providing many meals and doses of common sense, thank you.

Thanks also to my dear friends, Todd and Jennifer Long, and Sean Garrity, for years and years of sharing.

This work was partially supported by grants to JCJ and MB from the Natural Sciences and Engineering Research Council (NSERC) of Canada.

Portions of this work have been previously published by the author, and are reproduced with kind permission from Elsevier Science and the American Chemical Society.

Abstract

The majority of diagnostic and therapeutic monoclonal antibodies (mAbs) are of the immunoglobulin G (IgG) class and are produced in cell cultures. The glycosylation of these mAbs can have major influences on their physicochemical and functional properties.

The murine B-lymphocyte hybridoma cell line, CC9C10, was grown in serum-free continuous culture in steady-state dissolved oxygen (DO) concentrations of 10, 50, and 100% of air saturation in a LH Series 210 (LH) bioreactor and in 1, 2, 5, 10, 25, 50, 100, 125, and 150% DO in a New Brunswick Scientific (NBS) CelliGen bioreactor. The secreted mAb, an IgG_1, was subjected to both enzymatic deglycosylation by peptide N-glycosidase F (PNGase F) digestion and chemical deglycosylation by hydrazinolysis. Both methods resulted in quantitative removal of asparagine-linked (N-linked) oligosaccharides and produced identical glycan profiles.

The N-linked oligosaccharides were analyzed qualitatively and quantitatively by fluorophore-assisted carbohydrate electrophoresis (FACE) and high-pH anion-exchange chromatography with pulsed amperometric detection (HPAEC-PAD). These two methods provided complementary and corroborating information. Only the heavy chains were glycosylated and there was no evidence for threonine- or serine-linked (O-linked) glycosylation. The predominant N-linked oligosaccharides were core-fucosyl asialyl biantennary glycans with varying galactosylation. There were also minor amounts of monosialyl oligosaccharides, and trace contributions from afucosyl and bisected oligosaccharides. Identification of the glycans was confirmed by matrix-assisted laser desorption/ionization tandem quadrupole time-of-flight mass spectrometry (MALDI-QqTOF-MS).

The level of DO affected the glycosylation of the mAb. A definite shift

towards decreased galactosylation of the glycans was observed in steady-state DO concentrations below and above 100% DO, establishing an optimum for maximum galactosylation. The DO effect was observed in both bioreactors but was less pronounced in the NBS bioreactor.

The DO effect was not a result of alterations in β1,4-galactosyltransferase (β1,4-GalT) activities, which were remarkably consistent. However, changes in the DO concentration may have affected the redox environments of the endoplasmic reticulum (ER) and Golgi, causing variations in the rate and timing of formation of the disulfide bonds and subsequent disulfide bond shuffling. Perturbations in the disulfide bond formation of immunoglobulins have previously been shown to affect their glycosylation. The interdependence of glycosylation and glycoprotein folding is discussed.

List of figures

List of tables

Abbreviations

α_1-AGP	α1-acid glycoprotein
ADCC	antibody-dependent cell-mediated cytotoxicity
ADP	adenosine diphosphate
AMP	adenosine monophosphate
ANTS	8-aminonaphthalene-1,3,6-trisulfonic acid
Asn	asparagine
Asn-X-Thr/Ser-Y	amino acid N-glycosylation consensus sequence (sequon)
ATCC	American Type Culture Collection
ATP	adenosine triphosphate
BALB/c	mouse strain
BCA	bicinchoninic acid
BHK	baby hamster kidney
BiP	immunoglobulin heavy chain binding protein
BSA	bovine serum albumin
CCD	charge-coupled device
CG	chorionic gonadotropin
CHO	Chinese hamster ovary
CMCL	complement-mediated cell lysis
CMP	cytidine monophosphate
cpm	counts-per-minute
DDW	distilled-deionized water
DHB	2,5-dihydroxybenzoic acid
D-MEM	Dulbecco's Modified Eagle's Medium
DMSO	dimethyl sulfoxide
DNA	deoxyribonucleic acid
DO	dissolved oxygen

Dol-P	dolichylphosphate
Dol-PP	dolichylpyrophosphate
DP	degree of polymerization
dpm	disintegrations-per-minute
DTT	dithiothreitol
EBV	Epstein-Barr virus
EDTA	ethylenediaminetetraacetic acid
ELISA	enzyme-linked immunosorbent assay
EPO	erythropoietin
ER	endoplasmic reticulum
ERp57	endoplasmic reticulum protein 57 kD
ERp72	endoplasmic reticulum protein 72 kD
ESI	electrospray ionization
Fab	antibody antigen-binding fragment
FACE	fluorophore-assisted carbohydrate electrophoresis
Fc	antibody C-terminal fragment
FSH	follicle stimulating hormone
Fuc	fucose
FucT	fucosyltransferase
Gal	galactose
GalNAc	*N*-acetylgalactosamine
GalT	galactosyltransferase
GDP	guanidine diphosphate
Glc	glucose
GlcT	glucosyltransferase
Glcase	glucosidase
GlcNAc	*N*-acetylglucosamine
GlcNAcase	*N*-acetylglucosaminidase

GlcNAcPT	phospho-*N*-acetylglucosaminyltransferase
GlcNAcT	*N*-acetylglucosaminyltransferase
GSH	glutathione, reduced form
GSSG	glutathione, oxidized form
GU	glucose units
HAT	hypoxanthine, aminopterin, and thymidine
HGPRT	hypoxanthine guanine phosphoribosyl transferase
HPAEC	high-pH anion-exchange chromatography
IgA	immunoglobulin A
IgG	immunoglobulin G
IUBMB	International Union of Biochemistry and Molecular Biology
LacNAc	*N*-acetyllactosamine
LH	LH Series 210 bioreactor
LH	luteinizing hormone
mAb	monoclonal antibody
MALDI	matrix-assisted laser desorption/ionization
Man	mannose
Manase	mannosidase
MBL	mannose-binding lectin
MR	mannose receptor
MS	mass spectrometry
MWCO	molecular weight cut-off
NBS	New Brunswick CelliGen bioreactor
Neu5Ac	5(*N*)-acetylneuraminic acid
Neu5Gc	5(*N*)-glycoylneuraminic acid
NK	natural killer
N-linked	asparagine-linked
NS0	murine cell line

O-linked	threonine- or serine-linked
OST	oligosaccharyltransferase
PAD	pulsed amperometric detection
PAGE	polyacrylamide gel electrophoresis
PBS	phosphate-buffered saline
pCO_2	partial pressure of carbon dioxide
PDI	protein disulfide isomerase
PI	proportional-integral
PID	proportional-integral-differential
PMSF	phenylmethylsulfonyl fluoride
PMP	1-phenyl-3-methyl-5-pyrazolone
PNGase F	peptide N-glycosidase F
pO_2	partial pressure of oxygen
Qq	tandem quadrupole
RA	rheumatoid arthritis
RF	rheumatoid factor
RNA	ribonucleic acid
SA	sialic acid
SAT	sialic acid transferase
SDS	sodium dodecyl sulfate
Ser	serine
THAP	2',4',6'-trihydroxyacetophenone
Thr	threonine
TK	thymidine kinase
TOF	time-of-flight
t-PA	tissue-type plasminogen activator
TRP-1	tyrosinase-related protein-1
UDP	uridine diphosphate

UMP	uridine monophosphate

Chapter 1 – Introduction

1.1 Glycoproteins and glycobiology

Complex carbohydrates were as recently as a few decades ago ascribed the status of cellular debris. Even today, the majority of life scientists think of carbohydrates as relatively simple molecules with energy storage and structural functions. This viewpoint is increasingly changing as scientists elucidate elaborate systems of enzymes in the endoplasmic reticulum (ER) and Golgi, the function of which is to systematically assemble highly complex oligosaccharides. Many biologically important molecules are glycosylated. It is now known that the nature of the oligosaccharides present on glycoproteins, glycolipids, and other glycoconjugates may drastically alter their biological function. The field of glycobiology has emerged as one of the 'final frontiers' of biochemistry.

The majority of proteins secreted by mammalian cells are glycoproteins – they contain covalently attached carbohydrates. Glycoproteins have functions that span the entire spectrum of protein activities including those of enzymes, transport proteins, receptors, hormones, and structural proteins. Their oligosaccharide moieties can have important biological roles, but in many cases these remain enigmatic. In contrast to the protein chains of glycoproteins, which are synthesized under strict genetic control, the oligosaccharides are enzymatically generated and covalently linked without the rigid guidance of nucleic acid templates. The synthesis of specific oligosaccharide linkages depend on factors such as the availability of the various processing enzymes, the identity of glycoprotein itself, and the cell environment. Because of this, each type of glycoprotein has a unique population of glycans and even individuals of the same glycoprotein species do not often display uniformity of their glycans. This glycan heterogeneity extends to specific glycan attachment sites within a single glycoprotein, leading to the phenomenon known as

microheterogeneity, which often complicates the purification and characterization of the glycoprotein.

The great diversity of oligosaccharides indicates there is some adaptive evolutionary benefit in oligosaccharide heterogeneity. A large amount of energy, in the form of adenosine triphosphate (ATP), is required to synthesize an oligosaccharide. This implies some advantage from evolutionary preservation of at least some of these large and complex structures. Since there is a limited number of genes available in the genome for the generation of functional diversity, it should not be surprising that a protein resulting from a single gene may be modified by oligosaccharide attachment to modulate its function, activity, bioavailability, biodistribution, *etc.* It should also not be surprising that a particular oligosaccharide structure may be used in different contexts to generate a wide variety of functions in different tissues at different times in the life cycle. However, the survival of certain molecules and structures may be due to relatively minor and undetectable selective advantages.

Genetic defects in glycosylation are surprisingly rare. There are few other biochemical pathways in which naturally occurring mutants are so uncommon. In the few instances in which glycosylation mutants have been observed in intact complex multicellular organisms, the consequences have been highly variable, from severely lethal to relatively minor. The rarity of such naturally occurring mutations is because the great majority of them cause lethal aberrations that prevent completion of embryogenesis.

The glycosylation state of a glycoprotein can have significant effects on its: protein folding (secondary and tertiary structure) and quality control; final macromolecular structure (tertiary and quaternary structure); solubility and stability; intracellular transport and secretion rate; extracellular transport and biodistribution; clearance rate (circulation time); immunogenicity (innate immune system) and antigenicity (adaptative immune system); specific activity;

resistance to proteolytic degradation and/or catabolism (Brockhausen, 1993; Lis & Sharon, 1993; Varki, 1993). Particular oligosaccharide sequences on the surfaces of cells can also be crucial for cell differentiation, signal transduction, and cell-cell recognition (important in cell growth and migration) (Brockhausen, 1993; Lis & Sharon, 1993; Varki, 1993).

Glycosylation is known to be cell and tissue specific, glycoprotein specific, and site specific within a particular glycoprotein. Appreciation of these factors are necessary for a better understanding of glycoprotein structure and function, and for the development and manufacture of biological products for human diagnostic and therapeutic use. The glycoforms of recombinant glycoproteins, which are due to the heterogeneity of the attached oligosaccharides, vary depending on the cell expression system used and the growth conditions in which they are expressed.

Pharmaceutical manufacturers are obliged to provide assurance to regulatory authorities that drug products intended for clinical trials and commercial distribution are of appropriate quality, safety, and efficacy. Process validation of a cell culture operation for the production of a biological therapeutic involves thorough examination of a number of different elements associated with the successful and reproducible manufacture of the drug. A whole battery of physicochemical and functional assays are now routinely used for the characterization of biological products (Schaffner *et al.*, 1995; Center for Biologics Evaluation and Research, 1997; Moran *et al.*, 2000). Glycoform analysis is an essential element of monoclonal antibody characterization, and indeed for all glycoproteins intended for therapeutic use, due to the known dependence of such glycoprotein characteristics as conformation, bioactivity, and pharmacokinetic profile on oligosaccharide structure.

1.2 Biosynthesis and processing of glycoprotein oligosaccharides

With respect to glycoproteins, the two major types of glycosylation are termed N- and O-linked oligosaccharides. Other types of glycosylation and glycosylated molecules, which will not be discussed, include glycosphingolipids, glycophospholipid anchors, proteoglycans, glycosaminoglycans, nuclear and cytoplasmic glycosylation, and a few other less common Golgi-derived classes (Varki *et al.*, 1999).

1.2.1 Building blocks and connectivity of oligosaccharides

Glycoprotein oligosaccharides are polymers of monosaccharides (*i.e.* simple sugars). Monosaccharides are polyhydroxyalcohols with a terminal aldehyde or penultimate ketone group capable of internal cyclization (*i.e.* hemiacetal or acetal formation), generating a chiral centre. Two possible cyclic forms of each monosaccharide can therefore occur via a process termed mutarotation, resulting in the α- and β-anomers (Figure 1-1). The preferred anomeric form for a given monosaccharide is dependent on thermodynamic, steric, and electronic effects. The carbon backbone of a monosaccharide is numbered starting with the terminal carbon nearest the anomeric carbon (Figure 1-1). For the monosaccharides common in glycoproteins, the terminal carbon is the anomeric carbon – except for the sialic acids, where the terminal carbon is the carboxyl carbon. While each hydroxyl of the monosaccharide is potentially available for cyclization, ring strain essentially precludes all but the C-4 and C-5 hydroxyls, yielding furanose (*i.e.* 5-member) and pyranose (*i.e.* 6-member) ring forms, respectively. Epimers are structural isomers formed by inversion at one carbon atom. Therefore, α- and β-anomers are C-1 epimers. Epimers at the C-5 carbon are another special case generating the 'D' and 'L' absolute configurations. In mammalian glycoproteins, it is reasonable to assume that all monosaccharides are in the pyranose form and have the 'D' absolute

configuration (except fucose, which has the 'L' absolute configuration) (Figure 1-2).

Oligosaccharides are generated by glycosidic bond formation between the anomeric hydroxyl of one monosaccharide and a ring hydroxyl of a another monosaccharide. Each of the ring hydroxyls is potentially available to form a glycosidic bond. Common linkages are between carbons 1-2, 1-3, 1-4, and 1-6 for neutral monosaccharides; carbons 2-3, 2-6, and 2-8 for sialic acids. Each linkage may also have either an α- or β-anomeric configuration. In addition, more than one ring hydroxyl of a given monosaccharide constituent may be involved in a glycosidic bond, generating a branched, non-linear polymer – unlike proteins and nucleic acids, which are linear polymers. Depending on the structure, up to four of the linkage positions may be used simultaneously. However, not all combinations and permutations of these factors are actually observed in mammalian glycoproteins (Table 1-1). The remaining possibilities still generate a vast potential for the structural diversity of oligosaccharides (Figure 1-3).

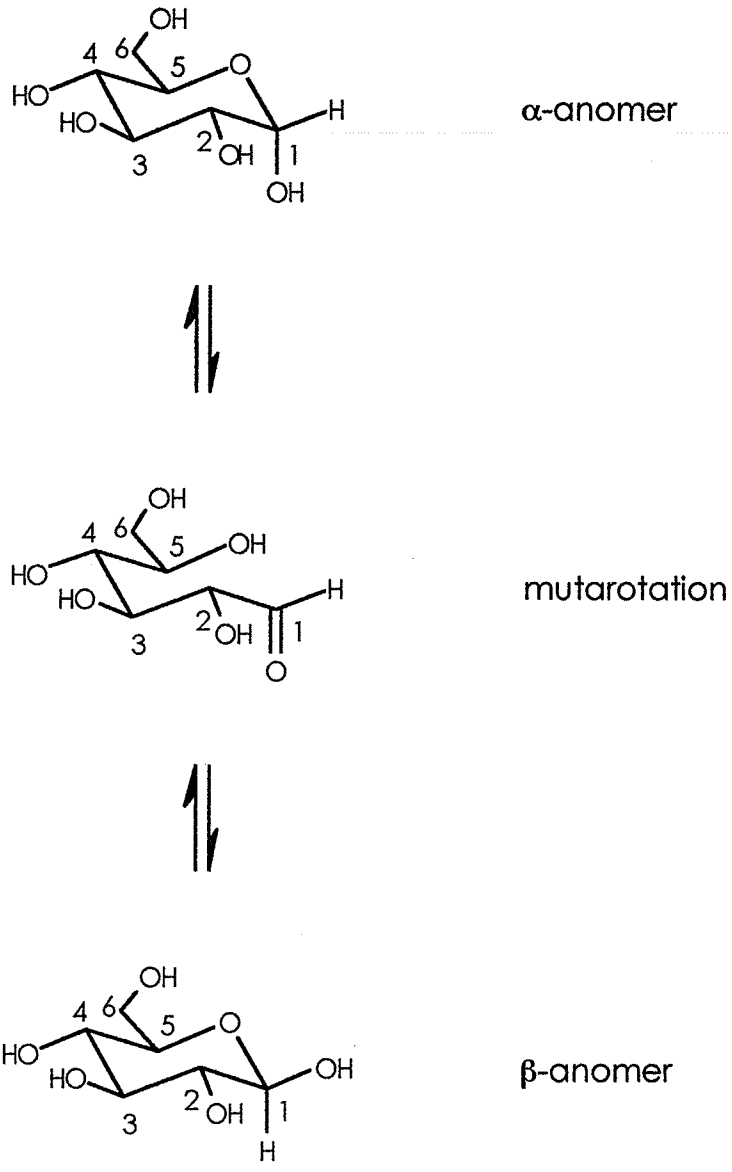

Figure 1-1. Monosaccharide numbering and mutarotation. The monosaccharide in the example is glucose.

Figure 1-2. Monosaccharides commonly found in mammalian glycoproteins.

The C-2 and C-4 epimers of glucose are mannose and galactose, respectively. *N*-acetylglucosamine and *N*-acetylgalactosamine are C-4 epimers of each other.

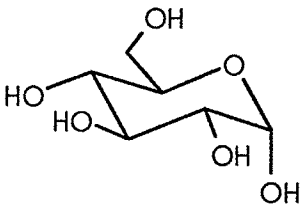

α-D-glucose

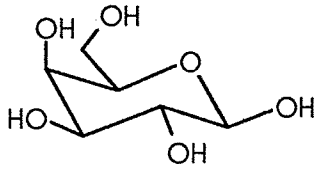

β-D-galactose

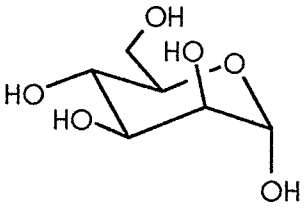

α-D-mannose

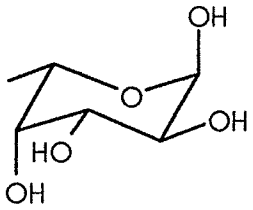

α-L-fucose

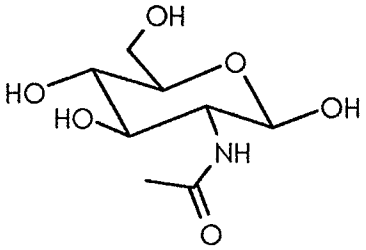

N-acetyl-β-D-glucosamine

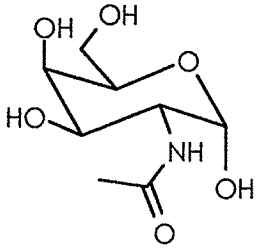

N-acetyl-α-D-galactosamine

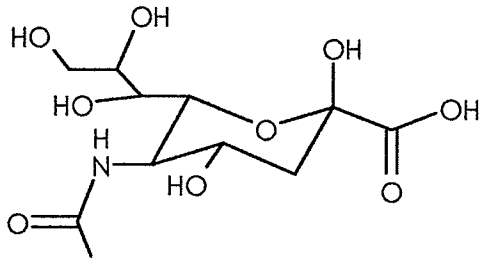

N-acetyl-α-neuraminic acid

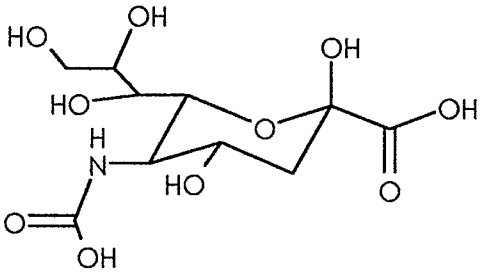

N-glycolyl-α-neuraminic acid

Table 1-1. Glycosidic linkages commonly found in mammalian glycoproteins.

			Glycosidic Bond	
Monosaccharide	Abbreviation	Symbol	Anomers	Linkages
D-glucose	Glc	▲	α	2, 3
D-galactose	Gal	●	α	3
			β	3, 4, 6
D-mannose	Man	○	α	2, 3, 6
			β	4
L-fucose	Fuc	△	α	2, 3, 4, 6
N-acetyl-D-glucosamine	GlcNAc	■	β	2, 3, 4, 6
N-acetyl-D-galactosamine	GalNAc	□	α	3
			β	4
5(*N*)-acetylneuraminic acid	Neu5Ac	◆	α	3, 6, 8
5(*N*)-glycolylneuraminic acid	Neu5Gc		α	3, 6, 8

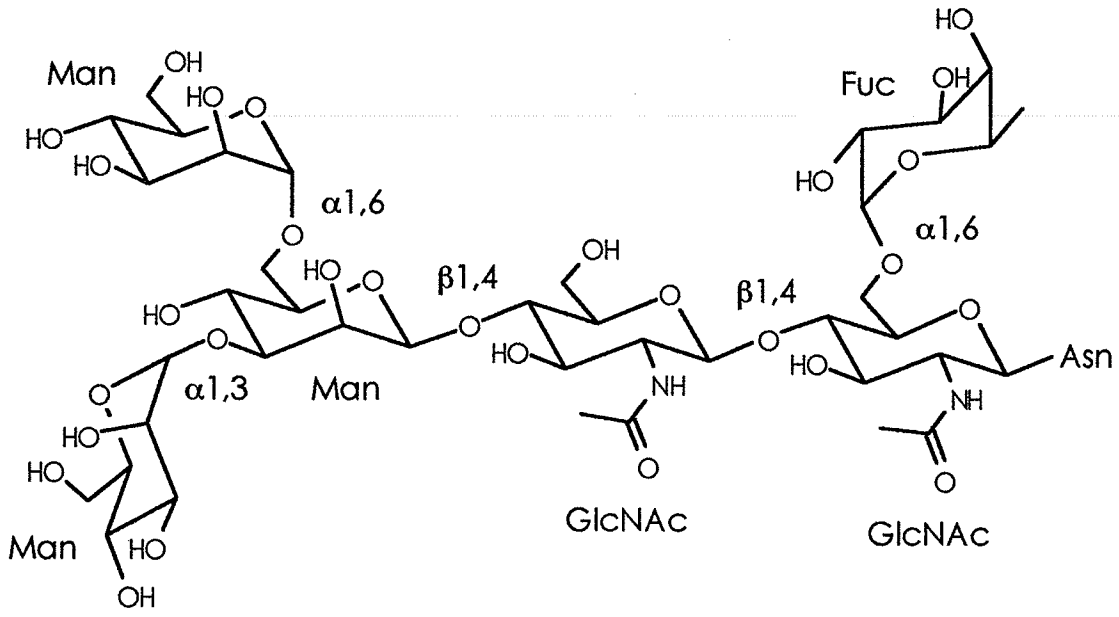

Figure 1-3. Origins of oligosaccharide structural diversity. The main components of the structural diversity of glycans include:

- the identity of the constituent monosaccharides (e.g. Man, GlcNAc, Fuc) and their sequence
- the anomeric configuration (*i.e.* α or β) of the glycosidic bonds between monosaccharides
- the linkage positions of the glycosidic bonds between monosaccharides
- the type and degree of glycan branching

Shown is the trimannosylchitobiose ($Man_3GlcNAc_2$) core common to all N-linked oligosaccharides – with the addition of Fuc α1,6-linked to the proximal GlcNAc.

1.2.2 Biosynthesis and processing

1.2.2.1 Asparagine-linked oligosaccharides

The first important carbohydrate linkage is the β1,*N* (N-glycosidic) bond between a reducing terminal GlcNAc and the side chain amide nitrogen of an asparagine residue.

The initial core structure of all aparagine-linked (N-linked) glycans ($Glc_3Man_9GlcNAc_2$) is built from the sequential addition of GlcNAc, Man, and Glc residues onto the dolichylphosphate (Dol-P) lipid using phosphorylated intermediates (Kornfeld & Kornfeld, 1985; Hirschberg & Snider, 1987; Roth, 1987; Paulson & Colley, 1989; Abeijon & Hirschberg, 1992; Cummings, 1992; Varki *et al.*, 1999) (Figures 1-4 & 1-5). The biosynthesis of the dolichylpyrophosphate- (Dol-PP)-linked oligosaccharide begins on the cytoplasmic side of the ER. Seven consecutive monosaccharide additions from activated nucleotide sugar donors lead to the heptasaccharide that is linked to Dol-PP. The heptasaccharide is translocated across the membrane into the ER lumen, where seven additional monosaccharide attachments, using Dol-P-linked donors, yield the $Glc_3Man_9GlcNAc_2$ intermediate (Figure 1-5).

The Dol-P-linked sugar donors for the lumenal additions are formed on the cytosolic side from nucleotide sugars and subsequently flipped to the lumenal side. The membranes of the ER and Golgi also contain transporters specific for the transfer of each nucleotide sugar across the membrane (Capasso & Hirschberg, 1984; Hirschberg & Snider, 1987; Verbert *et al.*, 1987; Abeijon *et al.*, 1997; Hirschberg *et al.*, 1998; Kawakita *et al.*, 1998) (Table 1-2; Figure 1-6).

Various inhibitors can block the pathway at specific steps. For example, the nucleoside antibiotic tunicamycin inhibits the initial step of Dol-PP-GlcNAc synthesis, while amphomycin inhibits the synthesis of Dol-P-Man (Elbein, 1987a, 1987b, 1991a, 1991b).

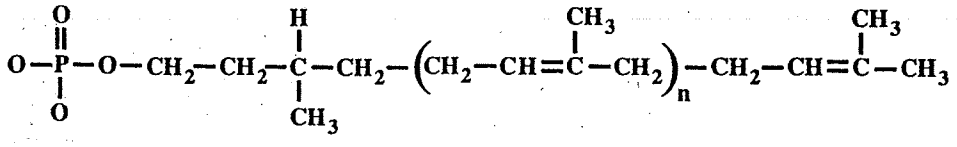

Figure 1-4. Structure of dolichylphosphate. The number of isoprene repeats (n) varies between 15 and 19. (From Varki *et al.*, 1999.)

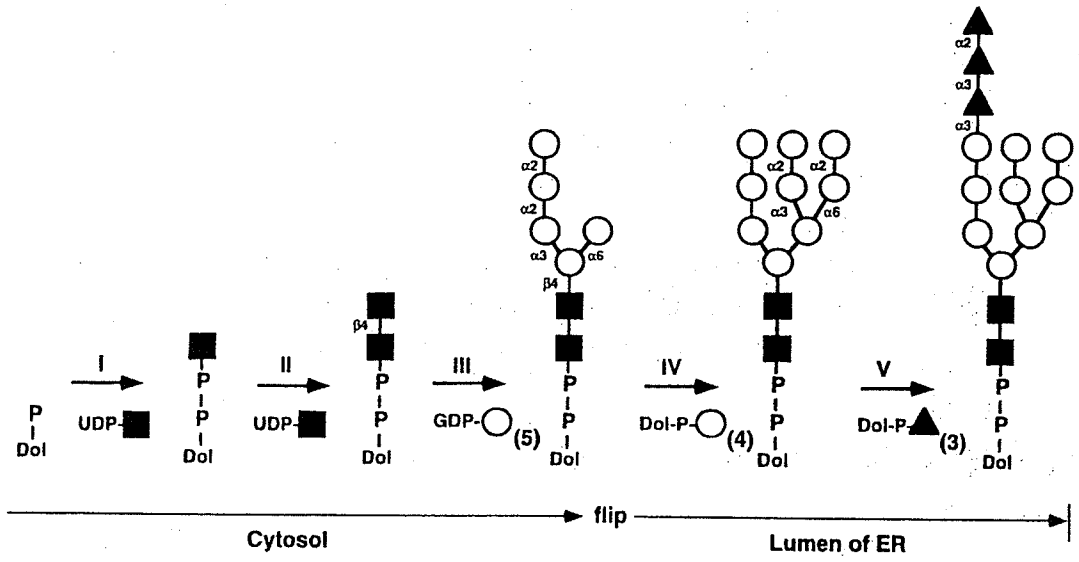

Figure 1-5. Biosynthesis of the dolichylpyrophosphate oligosaccharide precursor. (From Varki *et al.*, 1999.) Monosaccharide symbols are defined in Table 1-1.

Table 1-2. Nucleotide sugar donors and transport in the ER and Golgi.

		Nucleotide sugar transport	
Monosaccharide	Nucleotide sugar	ER	Golgi
Glc	UDP-Glc	++++	+
Gal	UDP-Gal	–	++++
Man	GDP-Man	–	++++
Fuc	GDP-Fuc	–	++++
GlcNAc	UDP-GlcNAc	++	++++
GalNAc	UDP-GalNAc	++	++++
Neu5Ac	CMP-Neu5Ac	–	++++
Neu5Gc	CMP-Neu5Gc	–	++++

UDP: uridine diphosphate

GDP: guanidine diphosphate

CMP: cytidine monophosphate

The relative distribution of nucleotide sugar transporters in the ER and Golgi is indicated by the number of plus signs (+). A minus sign (–) indicates that the transporter is not found in that organelle. (Adapted from Hirschberg *et al.*, 1998.)

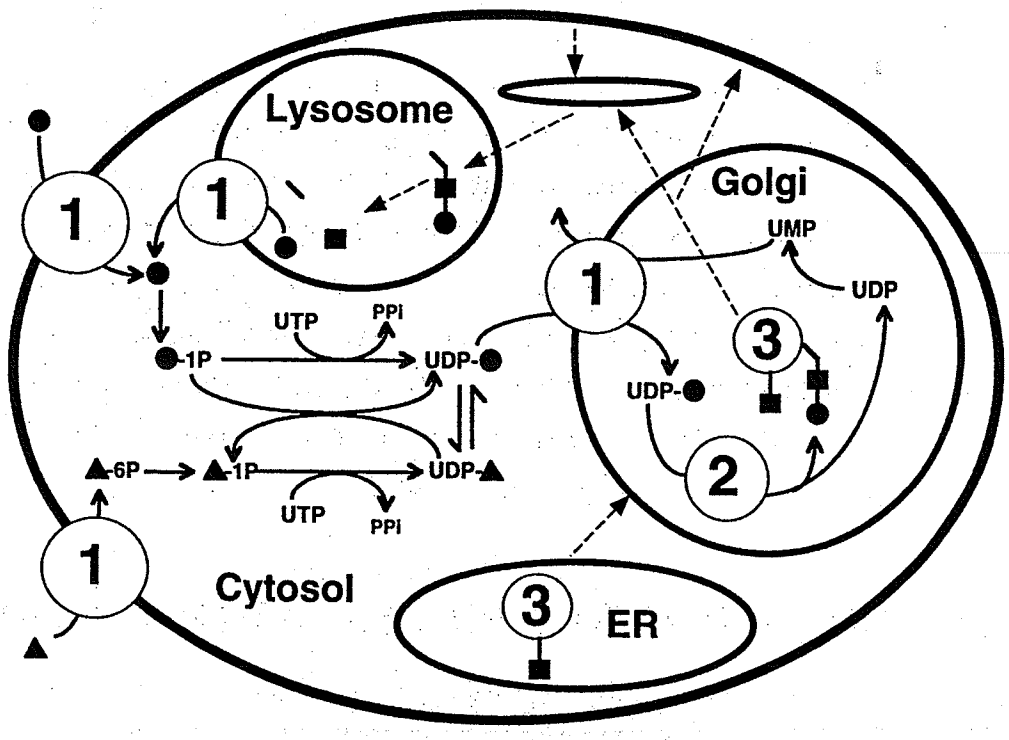

Figure 1-6. Biosynthesis, utilization, and turnover of galactose. This schematic shows the biosynthesis, fate, and turnover of one common monosaccharide constituent of mammalian glycoproteins, Gal. Although small amounts of Gal can be taken up from outside of the cell, most is either synthesized *de novo* from Glc or recycled from degradation of glycoconjugates in the lysosome. This schematic presents a simplified view of the generation of UDP-Gal, its equilibrium state with UDP-Glc, and its uptake and utilization in the Golgi for synthesis of new glycans. (From Varki *et al.*, 1999.) Monosaccharide symbols are defined in Table 1-1.

1: transporter; 2: transferase; 3: acceptor

Solid lines: biochemical pathways

Dashed lines: pathways for the trafficking of membranes and glycans

The oligosaccharide is then transferred, *en bloc* and co-translationally, from the Dol-PP carrier to the nascent protein by the oligosaccharyltransferase (OST) complex in the ER. The OST complex is comprised of three subunits, two of which are ribophorins, abundant integral ER transmembrane proteins whose cytosolic domains bind tightly to the larger ribosomal subunit and thus localize the third subunit, the actual transferase, within the ER lumen near the growing peptide chain.

OST recognizes the amino acid glycosylation consensus sequence (sequon) asparagine-X-threonine/serine-Y (Asn-X-Thr/Ser-Y). However, not all sequons are glycosylated (Bause & Legler, 1981; Bause, 1983; Gavel & Von Heijne, 1990; Silberstein & Gilmore, 1996; Shakin-Eshleman *et al.*, 1996; Kasturi *et al.*, 1997; Mellquist *et al.*, 1998). Glycosylation is greatly reduced by the presence of proline in positions X or Y, and moderately reduced when X is aspartic or glutamic acid. The Asn-X-Thr-Y sequence is preferred over Asn-X-Ser-Y, especially when positions X or Y are occupied by large hydrophobic or negatively-charged amino acids. Glycosylation of Asn-X-cysteine-Y has also been observed.

The glycosylation potential of a particular primary sequence is related to its ability to adopt and/or stabilize a turn or loop conformation. This Asx-turn motif is analogous to the β-turn conformation, whereby the hydroxyl (Thr or Ser) or thiol (cysteine) amino acid stabilizes the Asx-turn via a hydrogen bond network, permitting activation of the the Asn amide nitrogen by OST (Bause & Legler, 1981; Bause, 1983; Abbadi *et al.*, 1991; Imperiali & Shannon, 1991; Silberstein & Gilmore, 1996; Imperiali, 1997). In addition, sequons which are nearer the N-terminus (*i.e.* translated first) are more likely to be occupied than those nearer the C-terminus (Pollack & Atkinson, 1983). Because the initial oligosaccharide transfer is co-translational, this reflects temporal competition between protein

folding and initiation of N-glycosylation, and is partially due to steric effects related to the secondary (and higher order) structure of the protein.

Molecular chaperones are large oligomeric structures whose basic function is to prevent incorrect associations within and between polypeptide chains during *de novo* protein folding. Two different classes of chaperones assist folding and transport pathways for proteins in the ER: a membrane-associated pathway and a lumenal pathway. Newly synthesized proteins are transiently bound by these molecular chaperones. Non-glycosylated proteins, misfolded proteins, and aggregated proteins are associated with the lumenal molecular chaperones. Calnexin, a membrane-bound chaperone of the ER, and calreticulin, its lumenal homolog, play a major role in the quality control mechanism for secretory or membrane-associated glycoproteins, directing them to the membrane pathway (Ou *et al.*, 1993; Bergeron *et al.*, 1994, 1998; Ware *et al.*, 1995; Vassilakos *et al.*, 1998; Michalak *et al.*, 1999). Thus, the lectins calnexin and calreticulin have been determined to assist the correct folding/refolding, transport, sorting, and secretion of glycoproteins with N-linked glycans, while having little affinity for non-glycosylated proteins.

After transfer to the sequon, the oligosaccharide is trimmed by α-glucosidases (α-Glcases) I and II in the ER. Quality control of glycoprotein folding is accomplished by a deglucosylation-reglucosylation cycle (Figure 1-7). This entails selective reglucosylation of misfolded proteins and the specific binding by calnexin and calreticulin of these glucosylated forms (Hammond *et al.*, 1994; Helenius, 1994; Ware *et al.*, 1995; Helenius *et al.*, 1997; Bergeron *et al.*, 1998; Parodi, 1998, 1999, 2000a, 2000b; Trombetta & Helenius, 1998, 2000). Chronically misfolded glycoproteins are transported back into the cytosol from the ER, where they are deglycosylated (Suzuki *et al.*, 1998a, 1998b; Cacan & Verbert, 2000; Suzuki & Lennarz, 2000; Cacan *et al.*, 2001). The released oligosaccharides are then directed to lysosomes, while the protein and peptide portions are directed

to proteasomes. After deglucosylation the oligosaccharide is further trimmed by an α-mannosidase (α-Manase) I in the ER (Figure 1-8). When synthesis of the protein portion is complete, the glycoprotein is transferred from the lumen of the ER to the lumen of the *cis*-Golgi. Some glycans that have escaped the action of α-Glcase II and the α-Manase I in the ER are acted upon by an endo-α-Manase in the Golgi (Figure 1-8).

For most glycoproteins, subsequent processing and maturation of the $Man_8GlcNAc_2$ oligosaccharide occurs as the glycoprotein transits through the Golgi. However, lysosomal enzymes are recognized by a phospho-*N*-acetylglucosaminyltransferase (GlcNAcPT), which transfers GlcNAc-1-P to the C-6 of one or two of several possible Man residues (Figure 1-8). Subsequently, an α-*N*-acetylglucosaminidase (GlcNAcase) removes the GlcNAc(s), exposing the Man-6-P residue(s). These are recognized by Man-6-P receptor(s) in the *trans*-Golgi, which direct the enzymes to the lysosome (Varki *et al.*, 1999). Lysosomal enzymes may have several N-linked glycans, some of which are converted to typical complex oligosaccharides in the later compartments of the Golgi.

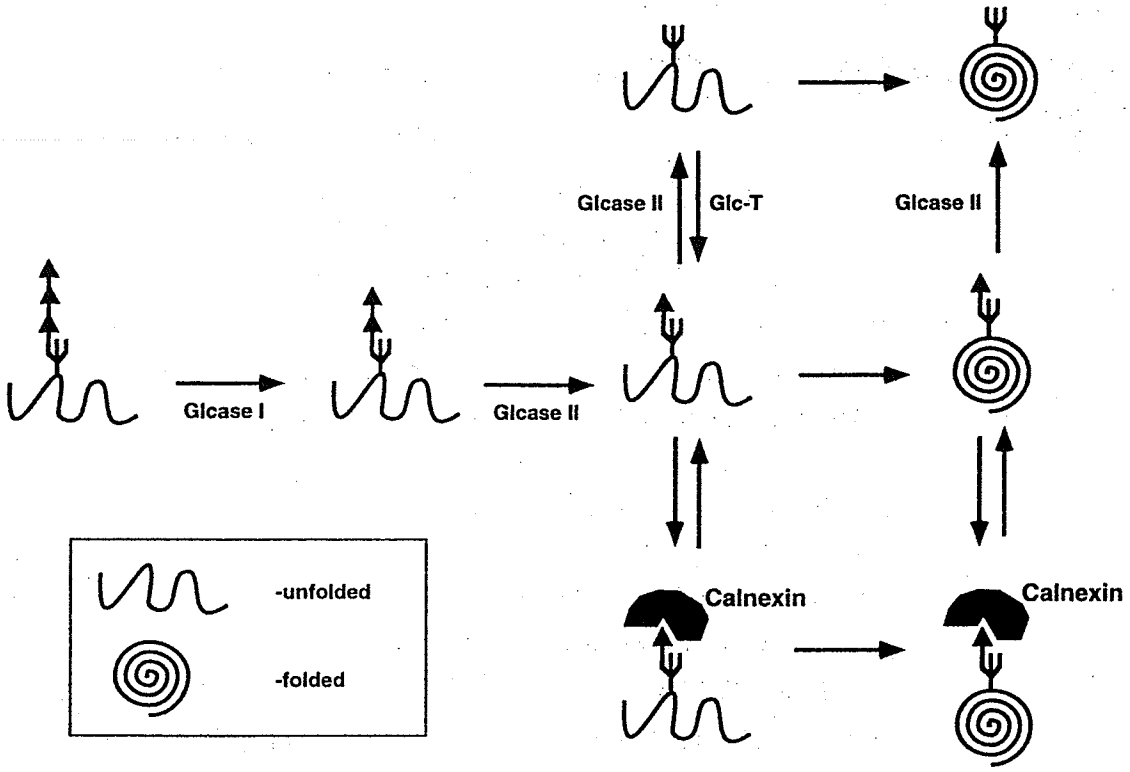

Figure 1-7. Calnexin functions during glycoprotein folding in the ER. After removal of Glc by Glcases I and II, the glycoprotein is either properly folded and ready for further processing, or is reglucosylated by a glucosyltransferase (GlcT). Calnexin binds preferentially to the Glc α1,3-linked to Man and retains the glycoprotein in the ER for correct folding. Calreticulin functions in a similar manner. (From Varki *et al.*, 1999.)

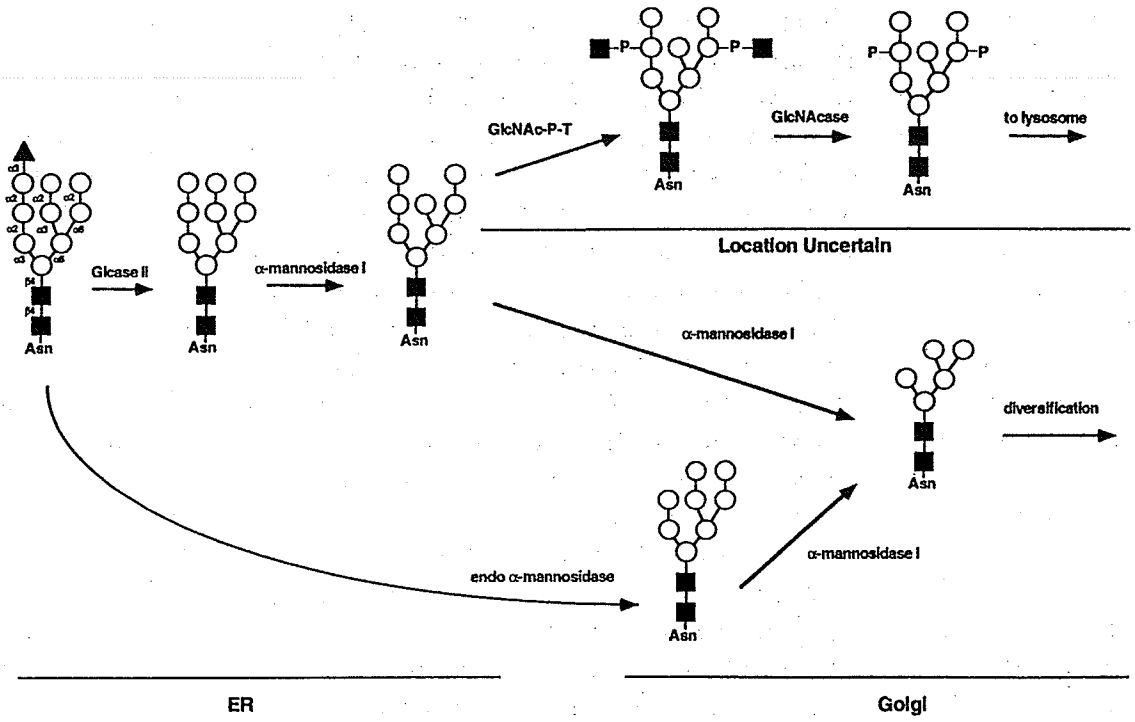

Figure 1-8. Processing of mammalian N-linked oligosaccharides. Most N-glycan processing takes place through the action of an α-Manase I in the ER followed by an α-Manase I in the Golgi. Some glycans that have escaped the action of Glcase II and α-Manase I in the ER are acted upon by an endo-α-Manase in the Golgi. Glycoproteins bound for the lysosome are modified by a GlcNAcPT and subsequently by an α-GlcNAcase to carry the Man-6-P signal. (From Varki *et al.*, 1999.) Monosaccharide symbols are defined in Table 1-1.

Most N-linked oligosaccharides can be placed into one of three classes, going from least to most processed: high-mannose, hybrid, and complex (with or without *N*-acetyllactosamine repeats) (Figure 1-9). All categories of N-linked oligosaccharides share a common 'core' structure consisting of the innermost three Man residues and two GlcNAc residues (chitobiose) – also known as the trimannosylchitobiose ($Man_3GlcNAc_2$) core – which is the attachment structure to the protein. It is distal to this core where the classes differ. High-mannose glycans contain only Man outside the core, while complex glycans contain GlcNAc, Gal, Fuc, and sialic acid. The hybrid class of glycans is, as the name suggests, intermediate between the two. Sialic acid (SA) is actually the term for a group of structurally similar negatively-charged neuraminic acid derivatives, of which the most common in mammals are Neu5Ac and Neu5Gc. Glycosylation sites which are nearer the N-terminus are more likely to be occupied by complex rather than high-mannose glycans (Pollack & Atkinson, 1983). Again, this reflects competition between protein folding and glycan processing. Each category comprises a diverse array of structures that can differ in numbers of glycosyl residues, substitution patterns, or branching patterns. Complex glycans may also contain polyLacNAc antennae comprised of Galβ1,4GlcNAcβ1,3 repeating units.

In the *cis*- and *medial*-Golgi enzymatic processing of the oligosaccharide occurs by various monosaccharide removals and additions to yield the biantennary structure terminating in GlcNAc (Kornfeld & Kornfeld, 1985; Hirschberg & Snider, 1987; Roth, 1987; Paulson & Colley, 1989; Cummings, 1992; Rabouille *et al.*, 1995; Colley, 1997; Varki *et al.*, 1999) (Figure 1-9). Also in the *medial*-Golgi, additional GlcNAc residues may be added to the core Man residue, leading to multiantennary structures (Schachter *et al.*, 1983; Schachter, 1986, 1991a, 1991b; Brockhausen *et al.*, 1988) (Figure 1-10). Fuc, Gal, and SA residues are added in the *medial*-Golgi, *trans*-Golgi, and *trans*-Golgi network

by fucosyltransferases (FucTs), galactosyltransferases (GalTs), and sialyltransferases (SATs) (Kornfeld & Kornfeld, 1985; Hirschberg & Snider, 1987; Roth, 1987; Paulson & Colley, 1989; Cummings, 1992; Rabouille *et al.*, 1995; Colley, 1997; Varki *et al.*, 1999) (Figure 1-11).

The addition of β1,2GlcNAc to the α1,3Man antenna by *N*-acetylglucosaminyltransferase I (GlcNAcT I) is a requirement for the action of α-Manase II (and thus GlcNAcT II), core α1,6-FucT, GlcNAcT III, and GlcNAcT IV. Therefore, GlcNAcT I is the signal for the production of hybrid and complex oligosaccharides. In contrast, the addition of a bisecting β1,4-GlcNAc to the core Man by GlcNAcT III prohibits the action of α-Manase II, core α1,6-FucT, GlcNAcT II, GlcNAcT IV, and GlcNAcT V. There are many such crossroads and roadblocks during oligosaccharide biosynthesis.

Inhibitors can block the pathway at specific steps, causing the accumulation of biosynthetic intermediates (Elbein, 1987a, 1987b, 1991a, 1991b; Kaushal & Elbein, 1994; Varki *et al.*, 1999). For example, castanospermine inhibits the α-Glcases I and II that remove Glc residues from the $Glc_3Man_9GlcNAc_2$ intermediate, while australine and deoxynojirimycin preferentially inhibit α-Glcases I and II, respectively. Deoxymannojirimycin and kifunensin inhibit the α-Manases I that remove Man residues from the $Man_8GlcNAc_2$ intermediate (Figures 1-7 & 1-8). Swainsonine and mannostatin A inhibit the α-Manase II that removes Man residues from the $GlcNAcMan_5GlcNAc_2$ intermediate (Figure 1-9). In the presence of swainsonine, only high-mannose and hybrid N-linked glycans are synthesized.

Defects in glycosylation have also been observed in mutant cell lines (Stanley, 1984, 1987, 1989, 1992; Stanley & Ioffe, 1995; Lee *et al.*, 2001; Oelmann *et al.*, 2001). Deficiencies in nucleotide-sugar synthesis and transport, glycosyltransferase activity, glycosidase activity, altered compartmentalization, *etc.* have been identified.

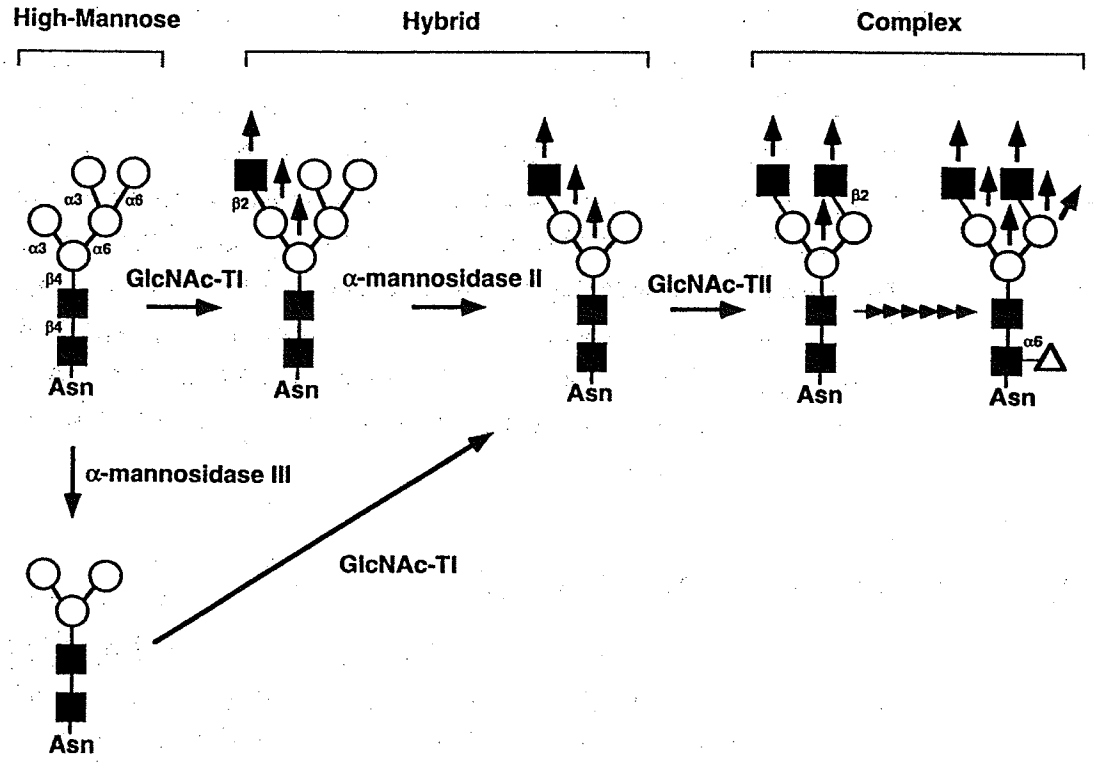

Figure 1-9. Diversification of mammalian N-glycans in the Golgi. Three N-glycan subtypes are generated: high-mannose, hybrid, and complex. Note that the trimannosylchitobiose core is common to all three subtypes. Most secreted and cell surface N-glycans are of the complex type and are generated by one of the two possible routes. (From Varki *et al.*, 1999.) Monosaccharide symbols are defined in Table 1-1.

The vertical arrows depict locations of branch formation in N-glycan diversification, not all of which occur on any single N-glycan.

Fucose can be added earlier than indicated.

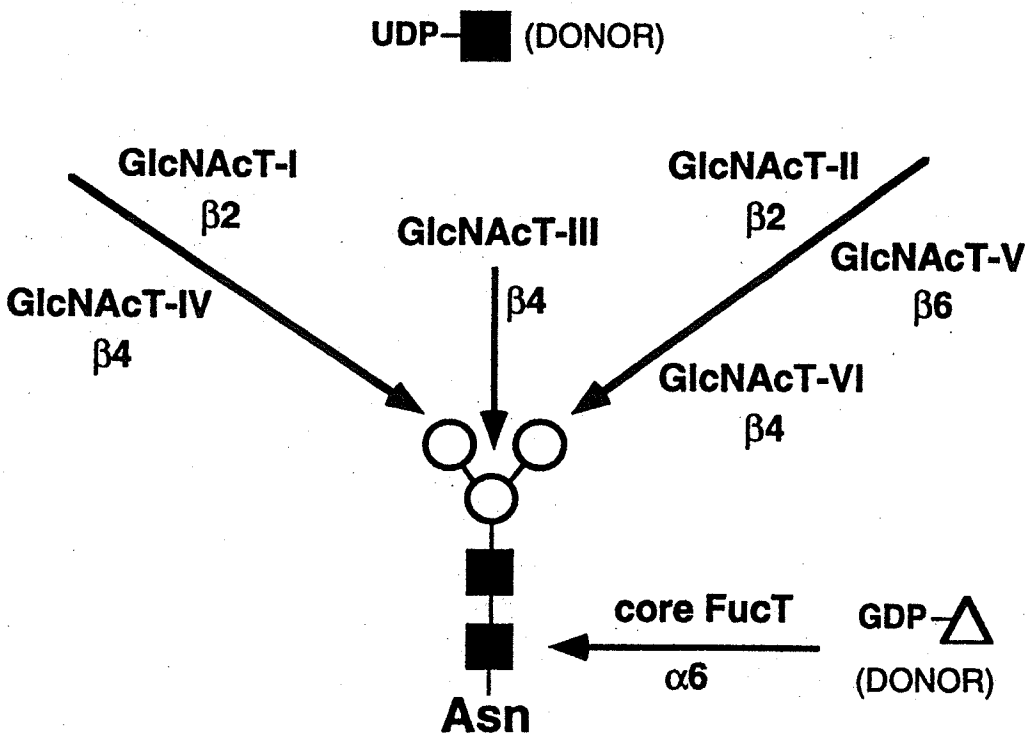

Figure 1-10. 'Branching' GlcNAc transferases. Up to five branches have been observed on N-glycans of some mammalian glycoproteins. There are five 'antennae' and one 'bisecting' GlcNAcTs. GlcNAcT VI is uncommon in mammals. Another GlcNAcT, GlcNAcT VII is responsible for the addition of β1,3-linked GlcNAc in polyLacNAc structures. (From Varki *et al.*, 1999.) Monosaccharide symbols are defined in Table 1-1.

Not all GlcNAcT reactions shown occur on any given N-glycan as some glycosyltransferases compete for the same substrate, and products may inhibit the action of other glycosyltransferases.

Addition of Fuc only occurs in hybrid and complex N-glycans, and is inhibited by the prior addition of a bisecting GlcNAc.

Figure 1-11. Idealized N-linked oligosaccharide biosynthetic pathway. Biosynthesis begins in the ER and proceeds through the *cis-*, *medial-*, and *trans-*Golgi. Some of the enzymes and steps in the process are numbered as follows: 1. transfer of oligosaccharide from Dol-PP to nascent protein by OST; 2. α-Glcase I; 3. α-Glcase II; 4. reglucosylation of improperly folded glycoproteins; 5. ER α-Manase I; 6. Golgi α-Manase I; 7. addition of phosphoGlcNAc by a GlcNAcPT; 8. removal of GlcNAc by an α-GlcNAcase to produce Man-6-P signal for transfer to lysosomes; 9. GlcNAcT I; 10. α-Manase II; 11. GlcNAcT II; 12. core α1,6-FucT; 13. β1,4-GalT; 14. terminal sialylation by SATs. Additional branching and terminal structures may be produced by the action of other GlcNAcTs, GalTs, and SATs. (Adapted from Kornfeld & Kornfeld, 1985.)

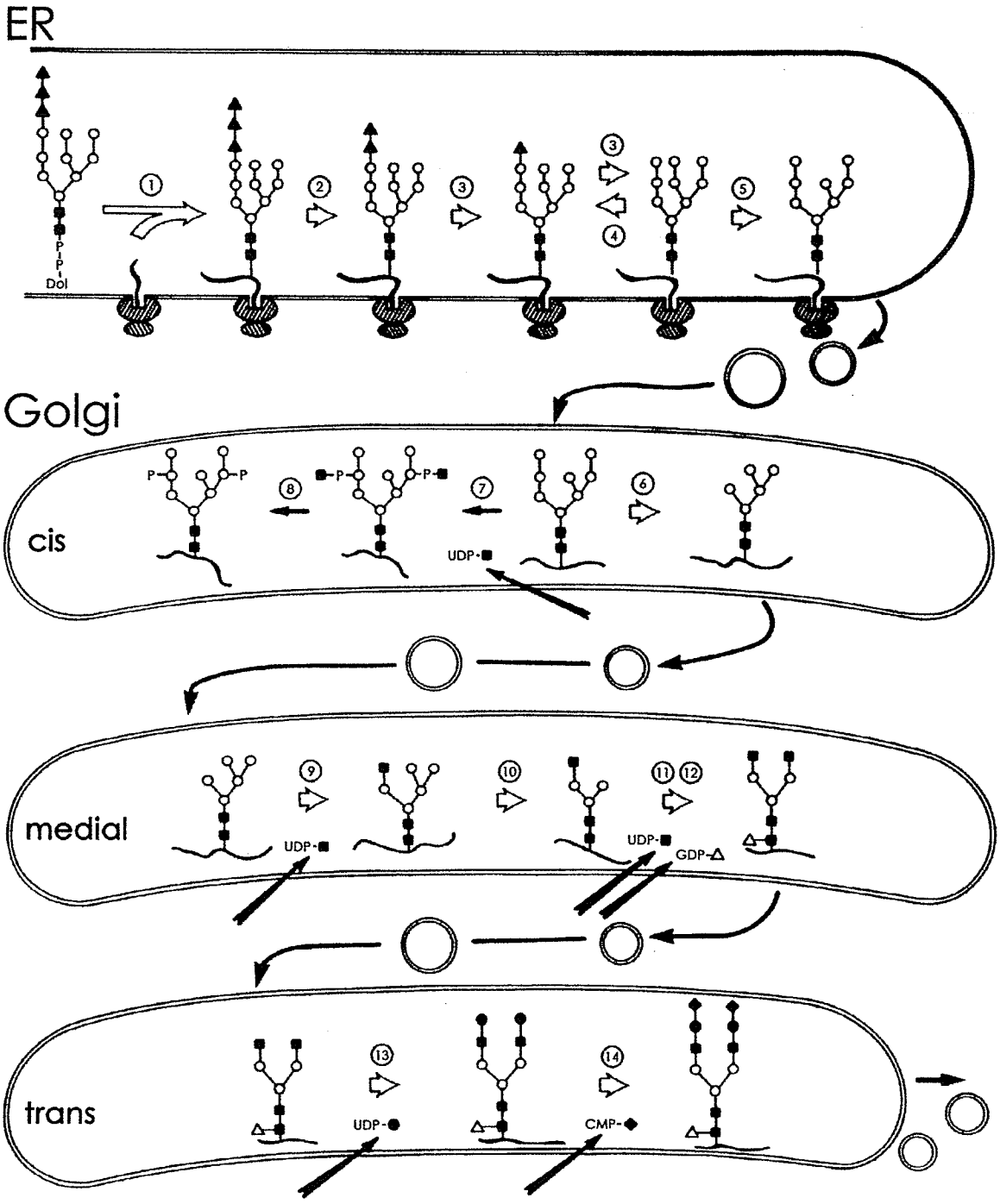
ER
P
P
P
Dol
1
2
3
4
3
5
Golgi
cis
P
P
P
P
8
7
6
UDP-■
medial
9
10
11
12
UDP-■
UDP-■
GDP-△
trans
13
14
UDP-●
CMP-◆

The division of biosynthesis and processing between the ER and Golgi represents an evolutionary adaptation that allows efficient exploitation of the potential of oligosaccharides (Helenius & Aebi, 2001). In the ER, where the repertoire of oligosaccharide structures is still quite small, the glycans play a pivotal role in protein folding, oligomerization, quality control, sorting, and transport. In the Golgi, the glycans acquire more complex structures and more glycoprotein-specific functions.

The highly branched nature of oligosaccharides has important implications concerning their synthesis. Proteins and nucleic acids are linear molecules and are synthesized by a highly accurate template mechanism: deoxyribonucleic acid (DNA) acts as a template for ribonucleic acid (RNA) and RNA acts as a template for protein. Because they are branched, oligosaccharides cannot be made in this way. Genetic information is transferred via an indirect non-template pathway. Genes code for the protein backbone of the glycoprotein, for the glycosyltransferases and glycosidases that form the oligosaccharides, for substrate and cofactor availability, and for the construction of the assembly lines within which all oligosaccharides are made. Regulational control of biosynthesis appears to be governed primarily by the availability and activity of the respective enzymes, which are under transcriptional control. The end result is that nucleic acid and protein assembly tends to be very accurate, while the assembly of oligosaccharides is prone to variation.

With rare exceptions, glycosidases and glycosyltransferases act in a regio- and stereo-specific manner (*i.e.* branch specificity). However, often there is competition for a common substrate (van den Eijnden & Joziasse, 1993; Moremen *et al.*, 1994; Yeh & Cummings, 1997). Also, conversion of a potential substrate to a non-substrate, and *vice versa*, is common. This highlights an important point to consider in oligosaccharide synthesis: the cascade action of

enzymes is highly dependent on previous steps (Schachter *et al.*, 1983; Schachter, 1986, 1991a, 1991b; Brockhausen *et al.*, 1988; van den Eijnden & Joziasse, 1993). Factors that are known to affect N-linked glycosylation are the availability of the various processing enzymes and their cofactors, and the kinetic characteristics and compartmentalization of the enzymes within the ER and Golgi – which are all variably dependent on the age, health, species, and type of cell (Schachter, 1986, 1991a, 1991b; Brockhausen *et al.*, 1988; Paulson & Colley, 1989; van den Eijnden & Joziasse, 1993; Kitagawa & Paulson, 1994; Moremen *et al.*, 1994; Colley, 1997). In addition, due to clonal variation in glycosylation capabilities, each cell within a given population of like cells may express a subset of potential structures (Endo *et al.*, 1989; Rothman *et al.*, 1989; Jefferis *et al.*, 1990; Tandai *et al.*, 1991; Cole *et al.*, 1993; Cant *et al.*, 1994; Bergwerff *et al.*, 1995).

In addition to influencing the level of occupancy of a potential glycosylation site, the protein milieu may also affect the type and extent of oligosaccharide processing at that site, leading to site-specific glycosylation (Schachter, 1986, 1991a, 1991b; Yet *et al.*, 1988; Lee *et al.*, 1990; Yet & Wold, 1990; Baenziger, 1994; Do *et al.*, 1994). There is significant interdependence between the state of glycosylation and correct protein folding (Imperiali, 1997; O'Connor & Imperiali, 1998; Imperiali & O'Connor, 1999; Wormald & Dwek, 1999; O'Connor *et al.*, 2001). Indeed, when glycosylation sites are eliminated many glycoproteins misfold, aggregate, and/or are degraded within the ER. This interrelationship has been particularly well studied in the tyrosinase-related proteins (Branza-Nichita *et al.*, 2000).

In addition to these factors, it has recently been realized that the physicochemical environment of a cell may affect glycosylation (Goochee & Monica, 1990; Cumming, 1991; Goochee *et al.*, 1991, 1992; Goochee, 1992; Parekh, 1991; Rademacher, 1993, 1994; Andersen & Goochee, 1994; Jenkins &

Curling, 1994; O'Neill, 1994; Parekh, 1994a; Gawlitzek *et al.*, 1995a, 1995b; Jenkins, 1995; Jenkins *et al.*, 1996). Therefore, the glycoforms of recombinant glycoproteins may vary depending on the cell expression system used and the growth conditions in which they are expressed. It is the dynamic interplay of various genetic, biological, and environmental factors which accounts for cell-dependent, site-dependent, and physiologically-influenced glycosylation (Dinter & Berger, 1995; Varki *et al.*, 1998).

1.2.2.2 Threonine- and serine-linked oligosaccharides

The second important carbohydrate linkage is the O-glycosidic bond between a reducing terminal monosaccharide and the side chain hydroxyl oxygen of either a Thr or Ser residue. By far the most common Thr- or Ser-linked (O-linked) glycan attachment in mammals is the mucin-type glycan, which involves attachment of GalNAc to Thr/Ser via an α1,O-linkage. Elongation of this GalNAc generates different core structures; eight of which have been identified to date (Hounsell *et al.*, 1996; Van den Steen *et al.*, 1998; Varki *et al.*, 1999). In general, O-linked glycans are smaller than their N-linked counterparts. Other O-linked glycans, both α1,O- and β1,O-linked, are also observed. These include GlcNAc and core structures connected through GlcNAc, as well as other, less common, O-linked attachments (Varki *et al.*, 1999).

There is no established consensus sequence for O-linked glycoysylation. However, an increased frequency of Thr, Ser, valine, alanine, glycine, and especially proline, in the near vicinity of occupied Thr and Ser residues has been reported (Wilson *et al.*, 1991; Hansen *et al.*, 1998). Charged and large hydrophobic residues are disfavoured near the glycosylation site (Hansen *et al.*, 1998; Van den Steen *et al.*, 1998). The sequence context of glycosylated threonines is different from that of glycosylated serines, with threonines also more likely to be occupied than serines (Hansen *et al.*, 1998). Occupied sites tend to

cluster, and non-clustered sites have a sequence context different from that of clustered sites. O-glycosylation of Thr and Ser residues does not require Dol-P-linked intermediates. Attachment of the initial GalNAc occurs in the ER and *cis*-Golgi, while subsequent elongation occurs in the *trans*-Golgi (Schacter & Brockhausen, 1989; Hounsell *et al.*, 1996). Since O-glycosylation is mainly a post-translational and post-folding event, usually only surface accessible threonines and serines are further processed (Hansen *et al.*, 1998; Van den Steen, 1998).

The functional roles of O-linked glycans in glycoproteins include the conformational control of protein structure and stability, and in recognition and signalling events (Jentoft, 1990; Hounsell *et al.*, 1996; Van den Steen *et al.*, 1998). O-linked glycans serve to expand and stiffen the protein. This may be particularly true for proteins that contain domains of clustered O-linked sites.

1.2.3 Heterogeneity and glycoforms

The differential processing of glycoprotein glycans results in distinct oligosaccharide structures at different sites within a glycoprotein molecule. The same glycosylation site is also diversified by the association of more than one oligosaccharide structure, which is termed microheterogeneity. This leads to a restricted, defined, and reproducible collection of glycosylation variants for each site. In addition, each potential glycosylation site may be fully or partially occupied, or unoccupied. The consequence of microheterogeneity and differential occupancy of different sites is that a single glycoprotein is not isolated as a single structural entity, but rather as a set of glycosylation variants, also known as glycoforms (Parekh *et al.*, 1987; Rademacher *et al.*, 1988a; Yet & Wold, 1990; Parekh, 1994b; Rudd & Dwek, 1997). Glycoproteins are therefore populations of a single protein diversified into potentially hundreds of variants differing only in oligosaccharide structures; the glycoform profile or fingerprint.

While not each and every glycoform is expected to be in some sense functionally unique, particular glycoforms can clearly exhibit different physical and biochemical properties – and different biological activities. This may contribute to functional diversity and allow for 'fine-tuning' of biological processes. The effect of the glycoform profile on a specific biological property would be a weighted average of the component glycoforms.

Interesting questions with respect to glycoform biosynthesis arise. For example, does each cell within the population express all glycoforms, a unique subset, or just one? Should the glycosylation of one glycoprotein change under external influences, is there a similar and concomitant change in the glycosylation of all the other glycoproteins being expressed by the cell population in question? If not, how is such a change avoided? Perhaps there is simultaneous expression of all the glycoforms of a glycoprotein that are ever required, and the relative levels of each are controlled at any given time.

1.3 Functions of glycoprotein oligosaccharides

The essential pathways of biosynthesis of oligosaccharides are known and involve a large number of gene products, including many families of glycosyltransferases. Cell lines with mutations in a variety of specific steps in the biosynthesis of oligosaccharides have been obtained (Stanley, 1984, 1987, 1989, 1992; Stanley & Ioffe, 1995; Lee *et al.*, 2001; Oelmann *et al.*, 2001). In addition, wild-type cell lines can be grown in the presence of inhibitors of specific steps in the biosynthesis and processing of oligosaccharides (Elbein, 1987a, 1987b, 1991a, 1991b; Kaushal & Elbein, 1994). The functions of the oligosaccharides attached to glycoproteins may be probed by these and other methods.

The proposed biological roles of oligosaccharides include: a purely structural role; an aid in the conformation, solubility, and stability of proteins, and to prevent aggregation; the provision of target structures for microorganisms,

toxins, and antibodies; the masking of such target structures; control of the lifetime of glycoproteins and cells; direct or indirect influences on the specific activity of a glycoprotein; the modulation of protein functions; and the provision of ligands for specific binding events mediating protein targeting, cell-matrix interactions, or cell-cell interactions (Brockhausen, 1993; Lis & Sharon, 1993; Varki, 1993). Many contradictory observations exemplify a recurring theme: that while supporting evidence can be found for many theories regarding specific oligosaccharide function, exceptions to each can equally well be observed.

The expression of specific types of glycosylation on different glycoconjugates in different tissues at different times of development implies that these structures must have diverse and different roles in the same organism. Given that oligosaccharides are post-translational modifications, these observations should not be entirely surprising. Once it is expressed, the same oligosaccharide modification could have independently evolved several distinct usages in different tissues and at different times in development. If any one of these functions were vital to the survival, then the glycosyltransferase mediating the expression of the oligosaccharide would be conserved in evolution, thus perpetuating the less important situations where it is expressed as well. The expression of a particular structure on a particular glycoconjugate might be of no positive consequence whatsoever in that particular situation. However, the transferase responsible for this structure may have been selected because of its vital contribution to the function of an entirely different glycoconjugate. As long as there was no strongly negative consequence, its expression might persist in that situation.

Glycoproteins vary in carbohydrate content from about 2% (*e.g.* immunoglobulin G) to more than 40% (*e.g.* erythropoietin) by mass. Glycoprotein glycans are highly polar, bulky, and hydrophilic. They are also sometimes phosphorylated or sulfated, and are usually sialylated. As a result, most

glycoproteins have their oligosaccharides on their external surfaces. Oligosaccharides are hydrodynamically quite large: a typical tetraantennary glycan can cover 20-25 nm^2. For comparison, the typical surface area for an antigen in an antigen-antibody complex is 6-8 nm^2. So, for example, the serum glycoprotein α_1-acid glycoprotein (α_1-AGP), with a mass of 37 kD and five such glycans, could essentially be completely enshrouded by oligosaccharides. Incomplete or aberrant glycosylation may therefore result in exposure of antigenic sites on the underlying protein that were previously masked by the oligosaccharide. Oligosaccharides may protect the protein moiety of a glycoprotein against uncontrolled proteolysis, both inside and outside the cell. Some glycoproteins undergo proteolytic processing within the cell from a large primary translation product to smaller final products. This can be affected by the presence of glycans, which may serve to modulate this process. Some glycoproteins require proper glycosylation for their insertion into a membrane, for secretion, or for proper intracellular migration and sorting.

The many glycoforms of glycoproteins may be differentially targetted to distinct organs and cell types (Gross *et al.*, 1988, 1989; Chiu *et al.*, 1994; Wright *et al.*, 2000). There are two major oligosaccharide receptors involved in the clearance of glycoproteins (Morell *et al.*, 1968; Ashwell & Harford, 1982; Gross *et al.*, 1988, 1989; Chiu *et al.*, 1994; Wright *et al.*, 2000). The hepatic (liver) asialoglycoprotein receptor recognizes terminal Gal and GalNAc residues, and terminal GlcNAc to a lesser extent. Clearance is rapid, but the receptor is easily saturated. The mannose-binding lectin (MBL) and the hepatic mannose receptor (MR) recognize terminal Man and GlcNAc residues, and GalNAc to a lesser extent. Binding of MBLs can directly activate the complement innate immune system response via circulating forms of these receptors on immune cells such as macrophages, monocytes, natural killer (NK) cells, and some T cells – resulting in destruction of pathogens by phagocytosis or cell lysis. Cells expressing

the MR present the invaders to immune cells for the production of new antibodies directed against them. These networks are thought to be descendants of a primitive innate immune system which provided protection from both infection and tissue injury by making use of lectin domains. Abnormally glycosylated glycoproteins that escape clearance by these mechanisms are eventually cleared by renal (kidney) filtration.

The *in vivo* residence time of a given glycoprotein is often dependent on its glycosylation status. Selective glycosylation may have evolved as a means of controlling the persistence of glycoproteins in the circulation. That is, one function of the different glycoforms of a given glycoprotein is probably to allow for modulation of circulation time. Glycans with terminal Gal instead of Neu5Ac are rapidly removed from serum via the hepatic asialoglycoprotein receptor. Glycoproteins which are required to act for only a brief period, such as some hormones, contain sulfated oligosaccharides and are rapidly removed from circulation via a different hepatic receptor. In contrast, glycoproteins with sialylated oligosaccharides, rather than sulfated, have a markedly slower clearance rate. As previously discussed, human glycoprotein oligosaccharides are like those of yeast, bacteria, and mycobacteria (with terminal Man and/or GlcNAc) until they are converted from 'non-self' to 'self' by the addition of Gal and Neu5Ac. Glycosylation variants carrying terminal Man, GlcNAc, and GalNAc are removed from circulation by the aforementioned receptors. These receptors play key roles in the elimination of invaders (*i.e.* recognition of 'non-self' oligosaccharides), and for the normal turnover of circulating glycoproteins (*i.e.* recognition of degraded or incomplete 'self' oligosaccharides). However, few generalizations can be made about the clearance of a recombinant glycoprotein from a knowledge of its glycans alone, and each case must be tested individually.

Some glycoprotein oligosaccharides are immunogenic in some humans. Of these, the most common are the plant and food allergens Fucα1,3GlcNAc and Xylβ1,2Man (Feizi & Childs, 1987; Wilson *et al.*, 1998, 2001). There are also examples of oligosaccharides which result universally in an immune response in humans. The best examples are terminal Neu5Gc residues (Muchmore *et al.*, 1989, 1997; Varki, 1993; Chou *et al.*, 1998) and terminal Galα1,3Gal sequences (the αGal epitope) (Galili *et al.*, 1987, 1988; Galili, 1993). The αGal epitope is found on surface and secreted glycoproteins of most animals, including non-primate mammals, prosimians, and New World monkeys. The exceptions are humans, Old World monkeys, apes, and curiously, Chinese hamster ovary (CHO) cells (although some CHO cell lines express the epitope) and murine (mouse) lymphocytes and erythrocytes. Over 1% of human serum immunoglobulins (mostly immunoglobulin G) is directed against αGal. In the case of Neu5Gc, expression actually does occur in the normal fetus, and may be a required event, but is then suppressed postnatally. The oligosaccharides in question evidently must have no normal functions in the adult.

Glycosylation can substantially modulate the interaction of peptides with their cognate ligands or receptors. Some cell surface receptors for growth factors appear to acquire their binding functions in a glycosylation-dependent manner. Glycosylation of a ligand can also potentially mediate such an 'on-off' or 'switching' effect. In most cases, such effects of glycosylation are not 'all or nothing', but partial, or relative. In these 'tuning' functions, the biological activity of many glycosylated growth factors or hormones appears to be modulated over a significant range by the presence and extent of glycosylation. In other cases, the function of proteins can be tuned not by oligosaccharides on the receptors or ligands themselves, but by those on neighbouring structures. Since these tuning effects of oligosaccharides are usually partial and rarely absolute, their importance may be questioned. However, when taken together, such

partial effects could have a dramatic effect on the final biological outcome. Glycosylation can be a general mechanism for generating important functional diversity, while utilizing a limited set of receptor-ligand interactions. These arguments apply equally well to the interactions between enzymes and their substrates, as has been discussed with respect to proteolytic processing.

Many different theories have been advanced concerning the biological roles of the oligosaccharide units of individual classes of glycoconjugates. The biological roles of oligosaccharides appear to span the spectrum from those that are trivial, to those that are crucial for development, growth, function, or survival. It is difficult to predict the functions a given oligosaccharide on a given glycoconjugate might be mediating, and its relative importance. The same oligosaccharide sequence may mediate different functions at different locations, or at different times in the life cycle. In the final analysis, the only common features of the varied functions of oligosaccharides are that they either mediate 'specific recognition' events or that they provide 'modulation' of biological processes (Brockhausen, 1993; Lis & Sharon, 1993; Varki, 1993). In so doing, they generate much of the functional diversity required for the development and differentiation of complex organisms, and their interactions with other organisms in the environment.

1.4 Implications for glycoprotein production

Circulating glycoproteins may be exposed to many different environments and need to function at different pHs, ionic strengths, and osmolarities, or in the presence of activated proteases. This means that there will be environments where one glycoform may more effective and the others less so. While it is at present difficult to rationalize the physiological consequences of such a control mechanism, it is clear that the glycosylation state and heterogeneity of a glycoprotein contribute to its biological efficacy and

versatility. Therefore, a consistent degree of heterogeneity should be achieved. On the other hand, specific glycoforms of some glycoproteins have been demonstrated to have distinct biodistributions and biological activities. Increased clinical efficacy in these circumstances would be realized by the production of a glycoprotein with a single glycoform. While progress has been made in this regard, it is at present impossible to achieve. At best, a glycoprotein with a restricted glycosylation profile, enriched in certain glycoforms, can be produced.

As previously discussed, glycoforms that have exposed Man, GlcNAc, or GalNAc residues are targetted epitopes and will bind to many components of the innate immune system. These components, normally present in serum, may be increased in concentration in a number of disease states, in particular those accompanied by an acute phase response. In addition, hepatic receptors exist for the clearance of glycoproteins with exposed Gal, Man, GlcNAc, and GalNAc residues. Directed immune response can also be present in the blood, and significant levels of anti-Man (yeast) and anti-GlcNAc (bacteria) antibodies are present. In order for recombinant glycoproteins to survive they need to mimic the glycosylation of circulating glycoproteins, in which the oligosaccharides are capped with SA. Expression systems that do not mimic these processes will lead to the production of a glycoprotein susceptible to clearance by these networks.

Selection of a suitable cell system for recombinant glycoprotein production should include consideration of the glycosylation capabilities of the cell and whether the protein is intended to circulate or to be targeted to an organ. If the glycoprotein is to be targeted to a specific receptor on an organ or tissue then it may be important to ensure that inappropriate glycosylation does not interfere with this process. Just in physical size alone, there is a great difference between a biantennary complex sugar and a tetraantennary

oligosaccharide with repeating LacNAc units. If a long circulation time is required, the most important glycosylation characteristic is that all glycoforms should contain glycans that terminate with α2,6-SA. In contrast to human cells, the most widely used animal host, the CHO cell, is known to lack the functional enzyme α2,6-SAT, leading to exclusively α2,3-linked terminal SA residues. Murine cell lines possess both functional α2,3- and α2,6-SATs, as in humans. However unlike humans and some CHO cell lines, most murine cell lines (except those derived from lymphocytes and erythrocytes) express α1,3-galactosyltransferase (α1,3-GalT) which may result in oligosaccharides that terminate with the immunogenic αGal epitope. Other host cell lines have not been studied in sufficient detail to completely outline their glycosylation capabilities.

Species-specific glycosylation characteristics may not become evident until cells are subjected to various genetic engineering protocols. For example, normal murine IgG is glycosylated in a very similar way to human IgG. No terminal αGal residues are found on normal murine IgG despite the fact this species-specific glycan linkage is known to be present on other normal murine tissues. A number of monoclonal cells, however, produce IgG with αGal-containing oligosaccharides.

Only in the last decade has it been realized that perhaps the most difficult problem for the production of recombinant glycoproteins and monoclonal antibodies is that the culture environment itself can change the glycosylation profile. The effects of cell culture conditions on the glycosylation and function of glycosylated pharmaceuticals have been reported and reviewed extensively (Goochee & Monica, 1990; Cumming, 1991; Goochee *et al.*, 1991, 1992; Goochee, 1992; Parekh, 1991; Rademacher, 1993, 1994; Andersen & Goochee, 1994; Jenkins & Curling, 1994; O'Neill, 1994; Parekh, 1994a; Gawlitzek *et al.*, 1995a, 1995b; Jenkins, 1995; Jenkins *et al.*, 1996).

1.5 Polyclonal antibodies, hybridomas, and monoclonal antibodies

1.5.1 Polyclonal antibodies

Antibodies are glycoprotein products of B lymphocytes, although other white blood cells, such as T cells and macrophages, are involved in the complex regulation of antibody formation. B lymphocytes are found in abundance in the spleen, but upon activation by an antigen some of the B lymphocytes replicate and become plasma cells, which secrete a specific antibody to the antigen. The population of B lymphocytes is capable of producing a range of antibodies, the nature of which depend upon previous exposure to antigens. The usefulness of an antibody relates to its ability to bind a particular compound with high specificity. The nature of antigen-antibody binding is analogous to that of enzyme-substrate. The interactions are non-covalent and depend upon electrostatic, hydrogen bonding, and non-polar interactions to maintain a strong and specific binding.

The classical method for antibody production for clinical and diagnostic studies has been to repeatedly inoculate an animal (*e.g.* mouse, rat, goat) with a specific virus, bacterium, pharmacological agent, parasite, *etc.* The animal responds by producing antibodies. When the specific antibody titer in a blood sample is high enough, the animal is bled and the antibody molecules are isolated, purified, and concentrated. However, any attempt to isolate antibodies from an animal results in a heterogeneous antisera, the content of which depends upon the history of antigenic exposure. These antibody mixtures are termed polyclonal since they are derived from a population of B lymphocytes and contain a mixture of antibodies with specificities for different antigenic molecules and for different antigenic epitopes of the same molecule. Thus, some disadvantages of the classical method of producing antibody are: the quality and quantity of antibody varies between animals and even between bleedings using the same animal; even purified antisera may contain

antibodies of different affinities with different subspecificities and cross-reactivities; the antisera may contain antibodies of different classes and subclasses that vary in their ability to carry out effector functions such as to immunoprecipitate antigens, or to activate complement. It is this heterogeneity and lack of predictability inherent in the classical method that makes it virtually impossible to continually generate large amounts of antibody having constant properties. Although such polyclonal mixtures have been useful experimentally their widespread use has severe limitations because of the variability of each preparation.

The fundamental background to the development of hybridoma technology was the clonal selection theory which proposed that each mammalian B lymphocyte has a unique receptor specificity for antigen and is predetermined to synthesize only one type of antibody after the appropriate antigen stimulation. Thus, stimulation by an antigen causes a B lymphocyte cell having receptors for that particular antigen to expand into a population of plasma cells all secreting antibody of an identical type and specificity. It is possible to select a single lymphocyte capable of synthesizing one antibody type. However, such an isolated cell has too short a lifespan in culture to allow significant antibody production.

The natural fusion of somatic cells *in vivo* is a relatively rare event. One example is in the differentiation of myoblasts which fuse during the formation of multinucleated muscle cells. However, in certain malignancies continuous growth of lymphocytes results in overproduction of specific antibodies. In these cells, the two properties of antibody production and continuous growth are combined.

Somatic cell hybridization *in vitro* can be used to combine the genetic characteristics of two different cell types. The fusion of dissimilar cells to form hybrids is a useful research tool for transferring certain properties from specialized

non-dividing cells to dividing cells. The process of combining the two properties of antibody production and continuous growth by the fusion of two selected cell lines is the basis of the hybridoma technique.

1.5.2 Hybridomas and monoclonal antibodies

The hybridoma technique for monoclonal antibody (mAb) production was first developed by Georges Köhler and Cesar Milstein in 1975 (Köhler & Milstein, 1975, 1976; Shulman *et al.*, 1978). For this they were awarded the Nobel Prize for Physiology or Medicine in 1984.

The procedure for creation and selection of monoclonal antibody-producing hybridomas can be broken down into discrete steps: immunization, cell fusion/hybridization, hybridoma cell selection, and selection of high antibody-producing clones.

1.5.2.1 Immunization

The chosen antigen is injected into an animal; mice and rats have been commonly used for this purpose. The immunization procedure varies with the type of antigen selected but typically this will involve two or three injections of antigen over a three-week period. The effectiveness of immunization depends on the molecular size of the antigen. The antigenicity of smaller molecules may be improved by coupling to haptens or by administration with adjuvants which stimulate the antigenic response. After the immunization period the animal is killed and the spleen is removed. The spleen is macerated to a suspension of individual cells and the lymphocytes in this suspension are separated by gradient centrifugation.

1.5.2.2 Cell fusion/hybridization

A suitable fusion partner for the spleen cells is a transformed cell line capable of continuous growth and fusion with plasma cells. A range of suitable rodent myeloma cell lines have been developed for such fusions. The most commonly used fusion partners are murine myelomas of BALB/c origin. The naturally-occurring or chemically-induced myelomas are selected for their inability to secrete antibodies. This ensures that the hybridoma which is finally selected only secretes one type of antibody. While some rat myelomas also give high fusion frequencies, fusion of cells from species with wide evolutionary disparities is not recommended since such hybridomas are often unstable.

The lymphocytes isolated from the spleen of the immunized mouse are mixed with the selected myeloma cells in the fusion medium. Cell fusion occurs naturally with very low frequency in mixed populations of cells *in vitro*. The frequency of fusion can be artificially increased with many RNA viruses (particularly inactivated Sendai virus), with some DNA viruses (herpes group especially), and also with chemicals such as lysolecithin and polyethylene glycol. The technique of *in vitro* cell fusion was originally developed with the use of viruses, but has now been superseded by the use of other methods. Electrofusion is a more recent method of inducing cell fusion and involves passing an electric current through a chamber containing the two populations of cells. This causes them to orient themselves along the line of current. High voltage pulses of short duration cause cell fusion with high efficiency and a high percentage of viable hybridomas result. The process involves cell agglutination, membrane fusion, and eventually nuclei fusion.

The product of fusion is a cell with a tetraploid nucleus from the nuclei of both parent cells, a heterokaryon. If this cell proliferates, it forms a hybrid cell line. These fused cells, derived from spleen cells and myeloma cells, are called hybridomas (hybrid myeloma). The fusion of normal and malignant cells can

produce hybrids in which some of the genetic characteristics of the normal cells may be immortalized in the hybrid which is capable of continuous growth.

1.5.2.3 Hybridoma cell selection

The fusion treatment results in a mixed population of cells containing lymphocytes, lymphocyte-lymphocyte hybrids, myelomas, myeloma-myeloma hybrids, and hybridomas. The unfused spleen cells and lymphocyte-lymphocyte fusions die naturally in culture within a week or two, but some way of selecting for the hybridomas from myelomas is required. For this purpose, the myeloma cells chosen as fusion partners have a defective gene for the enzyme hypoxanthine guanine phosphoribosyltransferase (HGPRT) (Price, 1985; Butler, 1988; Harbour & Fletcher, 1991). This enzyme functions in the salvage mechanism of nucleotide synthesis whereby the purines, hypoxanthine and guanine, are converted to their corresponding nucleotides. Another popular option is a defective gene for the enzyme thymidine kinase (TK). This enzyme is similar to HGPRT, but it functions in the salvage pathway of nucleotide synthesis for the pyrimidine thymidine. The alternative *de novo* pathway for nucleotide synthesis can function by using simple precursors in the absence of HGPRT or TK. Non-mutant cells can use either of these two pathways for nucleotide synthesis. Thus the presence of the metabolic inhibitor, aminopterin, which blocks the *de novo* pathway of DNA synthesis by inhibiting dihydrofolate reductase, does not prevent growth of cells which are provided with a adequate supply of the nitrogen bases hypoxanthine and thymidine. However, aminopterin is growth inhibitory to cells having defective genes for HGPRT or TK. By choosing myelomas with the gene mutations HGPRT$^-$ or TK$^-$, aminopterin can be used as a basis for selection of hybridomas from the parental myelomas. HGPRT$^-$ myeloma cells can be selected from culture by treatment with 8-azaguanine or

6-thioguanine. TK- myeloma cells can be selected from culture by treatment with 5-bromodeoxyuridine.

The fusion mixture is transferred to a selective culture medium containing a combination of hypoxanthine, aminopterin, and thymidine (HAT). The unfused spleen cells and lymphocyte-lymphocyte fusions die naturally in culture within a week or two, and the myeloma cells and myeloma-myeloma fusions die in HAT as described above. The fused hybridoma cells survive because they have the immortality of the myeloma cells and the metabolic bypass of the spleen cells, which supply the HGPRT or TK enzyme.

1.5.2.4 Selection of high antibody-producing clones

During subsequent divisions of the selected hybridomas, chromosomes are randomly lost, resulting in aneuploid cells. Therefore the probability of generating hybrid cells with the required characteristic is quite low, and some sort of selection procedure for immortal clones capable of secreting the desired antibody has to be used. Hybridomas are randomly placed in culture wells at limiting dilutions. The wells are individually tested for production of the desired antibody. One method of screening, immunofluorescence, is an assay which involves the binding of a fluorescent label to the antigen which is allowed to attach to the hybridomas producing the appropriate antibody. Subsequent cell selection can be achieved using a fluorescence-activated cell sorter or simply isolating clones in separate wells and assaying for fluorescence. Some other techniques used are enzyme-linked immunosorbent assay (ELISA) and radioimmunoassay. Not all initial hybridomas will be genetically stable and re-cloning of the selected hybridomas ensures that the two desired characteristics of continuous growth and antibody production are stably maintained. By careful selection of the resulting hybridomas it is possible to isolate a single cell capable of continuous production of the desired antibody. Hybridomas cells

are not anchorage dependent and may be freely grown in continuous suspension culture. Since each hybridoma culture originated from a single myeloma cell and a single spleen cell, the antibody is called monoclonal.

1.5.2.5 Advantages and disadvantages of monoclonal antibodies

The major advantages and disadvantages of mAbs are described in the following lists (Price, 1985; Butler, 1988; Harbour & Fletcher, 1991).

Advantages of monoclonal antibodies:

- titer available from a hybridoma clone is 100-1000 times greater than that obtainable from the classical method
- nearly limitless supply of mAb can be produced because hybridoma cells can be grown in continuous culture
- high reproducibility over nearly unlimited time; low batch to batch variation since mAbs are produced from identical cells all derived from a single B cell clone; worldwide standardization possible
- reacts with single determinant; the mAb is a chemically defined analytical reagent with unique specificity; cell supernatants contain no unwanted antibodies, unlike polyclonal sera which contain a mixture of specificities
- any cross-reactions are consistent
- mAbs having desired effector functions, specificity, or affinity can be selected
- can be biologically modified or metabolically labelled; fusion proteins, bispecific, chimeric, and other mAb derivatives are possible

Disadvantages of monoclonal antibodies:

- affinity for their antigens is often low
- reacts with single determinant, so specificity may be more influenced by physicochemical conditions
- immunoprecipitation often impossible
- biological function may be limited by class of heavy chain
- high costs

1.5.2.6 Utilization of monoclonal antibodies

The high selectivity of mAbs to specific antigens has enabled a range of applications (James, 1990; Merten, 1990). They are particularly useful in medical diagnosis for identifying viruses, bacteria, and parasites associated with a range of diseases. Since mAbs are able to detect subtle antigenic differences, such as amino acid substitutions in a virus or bacterium, they can be used to monitor antigenic drift, decide the proper viral strains to be used in a vaccine, classify organisms by species, and probe the physical, biochemical, and antigenic characteristics of organisms.

Changes in enzyme levels and cellular antigens can be used as diagnostic probes for many medical conditions. Of particular significance is the development of targeted drug therapy whereby mAbs to the surface antigens of specific cancer cells are conjugated to toxins or chemotherapeutic agents. These 'magic bullets' allow targetting of the cancerous cells and a method of delivering a lethal dose of toxin to the cells, leading to their destruction.

Monoclonal antibodies can be utilized in organ, tissue, or blood typing. By improving the antigenic profile, the chance of rejection of an organ by the recipient, or the wrong blood being transfused, is greatly reduced. Specific anti-immunoglobulin mAbs may be also used to enhance the successful transplantation of a tissue or organ.

Monoclonal antibodies are also powerful in chromatography and the purification of compounds such as therapeutic biologicals.

Molecular engineering has allowed the creation of simple chimeric mAbs with mouse variable regions and human constant regions. These mAbs are preferred for therapy since they have proven less immunogenic and antigenic in humans. An even more sophisticated approach is to insert just the mouse complementarity-determining regions into the human framework.

1.6 Cell culture

1.6.1 Batch and fed-batch culture

Traditionally, animal cells have been cultivated in batch culture either as suspensions or monolayers. In batch cultivation, an inoculum of known cell density is seeded into a specified volume of medium in the bioreactor. Theoretically, nothing more is added or removed from the bioreactor during the course of the cultivation. However, in practice, additions of air (for oxygen), and carbon dioxide or acids and bases (for pH control), are made.

Batch cultures are closed systems; as cell multiplication proceeds nutrients are consumed and cell products and metabolites accumulate, thereby changing the environment of the culture. These changes in turn affect cell metabolism and lead ultimately to cessation of cell multiplication. A closed batch culture consists of a series of transient states difficult to define and even more difficult to control.

Numerous attempts have been made to improve the basic batch culture by the intermittent or continuous addition of medium. The periodic replacement of a constant fraction of cell suspension by fresh medium is termed solera culture, and is the most common means of subcultivating animal cells. Often described as semi-continuous culture, solera culture is really only a succession of batch cultures in which part of the old culture is used as an

inoculum. In fed-batch culture, the culture is fed continuously with medium with a corresponding increase in the volume of the culture. Since the medium flow rate is maintained constant and the culture volume increases progressively, the dilution rate and thus the growth rate of the culture will decrease progressively. If a portion of the culture is withdrawn at intervals, the culture can be maintained more or less continuously.

1.6.2 Continuous (perfusion and chemostat) culture

An alternative approach to batch cultivation is to continuously add fresh medium to the cells and to continuously remove either cell-free medium (perfusion culture) or medium mixed with cells (chemostat culture) from the bioreactor (Tovey, 1985; Griffiths, 1988). These techniques presumably best imitate the process by which cells *in vivo* are continuously supplied with blood, lymph, or other body fluids to keep them in a constant physiological environment. Continuous cultures greatly increase the ability for scale-up. The improvement in oxygenation allows for the reduction or elimination of head-space and the better utilization of bioreactor space. A continuous culture system should aim to maintain the cells in a viable state for prolonged periods, lasting up to several months. As in batch cultivation, pH, temperature, and dissolved oxygen (DO) concentration need to be monitored and controlled. In addition, automated pumps are required to control the addition of fresh nutrients and the removal of metabolites and the desired product and, in chemostat culture, cells. As mentioned, continuous culture can be classified into two divisions: those that remove only filtered cell medium, and those that remove cells in addition to cell medium.

Perfusion cultivation systems are becoming increasingly popular because they can achieve high cell densities and product concentrations, and require relatively less space and labour. Although perfusion systems undoubtedly allow

high cell densities to be attained, they still suffer from the same basic limitation of batch culture: they are closed systems. In perfusion culture, spent culture medium is continuously replenished but cells and cellular debris are retained in the bioreactor. Cell counts are not held constant, and the concentration of cell products and metabolites increases with increasing cell number. Thus, true steady state is never attained. Therefore, they consist of a series of transient states eventually culminating in the demise of the culture. Such difficulties can be overcome by the use of chemostat culture. In these open systems, fresh medium is continuously added and cells and cell products are continuously removed at the same rate from the bioreactor, minimizing inhibition of target product formation or cell multiplication. Such an open system allows a steady state to be obtained in which constant conditions can be maintained indefinitely.

Chemostat culture is based on the principle that at submaximal growth rates, the growth rate is determined by the concentration of a single growth-limiting substrate (Monod, 1950; Novick & Szilard, 1950). A fixed bioreactor volume is maintained and, if mixing is sufficient to approximate the ideal of perfect mixing, the effluent stream should have the same composition as the bioreactor contents. The culture is first started batchwise, and is then fed with fresh medium containing one (and sometimes two) growth-limiting nutrient(s); all other nutrients being supplied in excess. The concentration of the cells in the bioreactor is controlled by the concentration of the growth-limiting nutrient. A steady-state cell concentration is reached where the cell density and the substrate concentration are constant. Steady-state cultures become established after a period of adjustment ranging from about two days to two weeks of continuous operation of the chemostat. The cell growth rate is proportional to the dilution rate of the growth-limiting nutrient, and adjustment times are proportional to the dilution rate of the chemostat. Maximum cell

output is usually obtained at a dilution rate of about one to one-and-a-half volumes per day, but this is not necessarily the optimum range for production of cell products. The chemostat is a self-regulating system: a temporary increase or decrease in nutrient flow rate will cause a corresponding increase or decrease in cell growth rate, which acts to restore steady-state conditions. Steady state can be determined by a number of parameters including: constant cell number, intracellular concentrations of DNA, RNA, and protein, concentration of metabolites in culture supernatant, and rates of incorporation of radioactively-labelled nucleotides and amino acids.

The principal advantage of steady-state continuous (chemostat) cultures are that they enable production under precise physiological conditions. The chemostat offers a useful method of manipulating the culture environment for improved cell and/or product yields. A whole range of different environments can be established and maintained more or less indefinitely. Cells can be cultivated in a number of unique environments, under a variety of growth-limiting conditions, and at a wide range of growth rates. Chemostat cultures are a useful means of studying the effect of a single parameter such as DO by the perturbation and re-establishment of steady state.

There are some disadvantages of continuous cultures. They are not suitable for products produced during the stage of declining metabolic activity and decreasing viability. There is a great risk of genetic instability during the maintenance period which may last for months. The apparatus is relatively complicated and represents high capital costs and susceptibility to contamination and operation problems.

1.6.3 Serum versus serum-free media

Serum is an effective growth-promoting supplement for practically all types of cell because of its complexity and the multiplicity of growth-promoting, cell protection, and nutritional factors that it contains. In addition to the high cost and supply considerations, the inherent complexity and variability of serum hinder reproducibility, and therefore serum-free media have been developed for many cell cultures.

Each cell type is specific in its medium requirements for cell growth and proliferation. A certain serum-free formulation can only be applied to a limited number of cell lines, usually of the same cell type, but often from different species. Basal medium ingredients and supplements, and their optimum concentrations, are determined by trial and error. Increased concentrations are often detrimental due to feedback and other inhibition systems. Many culture constituents work either in concert or synergistically in their effects upon cell growth, proliferation, and differentiation. When establishing serum-free cultures, the serum component must be gradually reduced while concomitantly increasing the defined supplement. Weaning of the cells from serum is necessary because the cells must adapt to the new environment over the period of several passages.

The advantages and disadvantages of the use of serum-containing media (Table 1-3) and serum-free media (Table 1-4) for hybridoma culture are easily appreciated in tabular form (Glassy *et al.*, 1988; Shacter, 1989; Bjare, 1992).

Table 1-3. Advantages and disadvantages of serum.

Advantages of serum:

- provides essential nutrients and necessary trace elements
- provides favourable pH, osmolarity, and natural buffering ability
- stimulates growth via growth factors
- provides carrier proteins which facilitate the uptake of nutrients, vitamins, hormones, growth factors, lipids, and trace elements
- serum proteins help to stabilize the cell against mechanical stress
- provides factors which bind and neutralize toxins and heavy metals; furnishes protease inhibitors
- relatively small inoculations needed and high cell densities achieved
- comparative ease of preparation

Disadvantages of serum:

- biologically complex mixture of large number of constituents (>1000) with inherent batch to batch variability and ambiguity; lack of reproducibility
- undefined nutritional environment (may obscure studies of the effects of particular hormones, growth factors, trace elements, *etc.*)
- source of toxins and presence of growth inhibitors
- high cost and periodic scarcity of serum
- possibility of contamination of product (*i.e.* mycoplasmas, viruses)
- high protein content drastically complicates downstream processing and economically acceptable product purification

(From Glassy *et al.*, 1988; Shacter, 1989; Bjare, 1992.)

Table 1-4. Advantages and disadvantages of serum-free media.

Advantages of serum-free media:

- consistent and chemically defined composition; reduction of intangibles
- decreased variability of culture medium
- elimination of potential inhibitors; absence of known toxins
- reduced risk of contamination and infectious agents
- routine procedures more reliable; increased control over bioreactor conditions; improved reproducibility of cell culture growth and product yield
- can probe effects of specific compounds upon cell function
- experimental conclusions less speculative
- fewer variables for quality control and quality assurance
- more cost effective
- potential for increased antibody production
- ease of product purification due to increased initial purity and absence of contaminating immunoglobulins

Disadvantages of serum-free media:

- specific serum-free formulation is only applicable to a few (usually similar) cell lines; requires optimization for each hybridoma
- may require serum hormones and growth factors which are difficult to isolate and purify
- larger inoculations required; cells may not grow to as high densities
- cells may be more fragile than in serum
- cell growth rate, maximum cell density, and cell viability often lower
- media take longer to prepare

(From Glassy *et al.*, 1988; Shacter, 1989; Bjare, 1992.)

1.6.4 Carbon dioxide, oxygen, and culture aeration

1.6.4.1 Carbon dioxide

Culture media need to be buffered to compensate for the evolution of carbon dioxide (CO_2) and the production of lactic acid from the metabolism of glucose. Media have traditionally been buffered with bicarbonate buffer, which forms a buffering system with dissolved CO_2 produced by growing cells.

$$H^+ + HCO_3^- \text{ <===> } H_2CO_3 \text{ <===> } H_2O + CO_2(aq) \text{ <===> } CO_2(g)$$

In this system carbonic acid (H_2CO_3) is formed from dissolved CO_2 and H_2O in a reversible manner. The pH of the bicarbonate system is dependent on the concentration of carbonic acid and bicarbonate ion (HCO_3^-). Since carbonic acid concentration is dependent upon the amount of dissolved CO_2, the ultimate buffering capacity is dependent upon the amount of HCO_3^- and the partial pressure of CO_2 (pCO_2). Each basal medium has a recommended HCO_3^- concentration and pCO_2 to achieve and maintain correct pH and osmolality. Typically, cultures are grown in 24 mM $NaHCO_3$ and 5% pCO_2, or 44 mM $NaHCO_3$ and 10% pCO_2.

1.6.4.2 Oxygen

The primary function of oxygen in a cell culture environment is to serve as the terminal acceptor of electrons in the electron transport chain, a multienzyme complex located in the inner mitochondrial membrane. This enables cells to efficiently convert chemical energy derived from dehydrogenation reactions into high-energy phosphate bonds in the form of ATP by oxidative phosphorylation. An adequate DO concentration will be that concentration of extracelluar oxygen that provides a nonlimiting intramitochondrial oxygen concentration. Oxygen must diffuse through a polar intracelluar cytosolic

environment before it reaches the mitochondria, the site of oxidative phosphorylation. Since the solubility and diffusion of oxygen in water is low, this is no trivial matter. As oxygen is depleted within the cells, intracellular oxygen gradients are formed. These gradients may not be physiologically significant at elevated oxygen partial pressures (pO_2), but at low pO_2 intracellular concentration gradients may be substantial. Mitochondrial clustering and distribution within the cytosol are major factors in determining the magnitude and location of concentration gradients. Mitochondria may be localized in areas of high energy demand and associated microheterogeneity of metabolite concentrations can occur in cells which might determine the rates of high-flux processes. A constitutively produced recombinant protein or mAb would be an example of a high-flux process that would place heavy demands on cytosolic oxygen concentrations. Additionally, in oxygen-limited conditions, the less efficient production of energy by glycolysis might limit the ability of cells to maximally produce a recombinant protein or mAb, although cell growth rates may remain normal. Even if the level of production is unaffected, certain aspects of product quality that require additional energy, such as glycosylation, may be compromised.

While all animal cells probably require oxygen, the actual DO concentration which is optimum for growth seems to vary from one cell type to another. Hence, while some cell lines may be relatively unaffected over a wide range of DO concentrations, other cell lines show a distinctive optimum.

In small volume cell cultures, the surface area to volume ratio of the culture allows oxygen to be supplied by simple diffusion of oxygen from air in the headspace. At a constant temperature and pressure, the concentration of oxygen in the medium (*i.e.* % DO) in equilibrium with the headspace is proportional to the pO_2 in the gas phase. As mentioned, the solubility of oxygen in air-saturated medium is quite low. The oxygen utilization rate for most animal

cell lines is such that, without replenishment, a typical culture would exhaust the supply of oxygen within about one to two hours. The situation is exacerbated by the low rate of diffusion of oxygen in the medium. In addition, other solutes in the liquid medium influence the solubility of oxygen and the rate at which oxygen transfers to the liquid phase, so that DO must be monitored and aeration rate or composition of the gas mixture adjusted accordingly.

The DO concentration is measured directly using available DO electrodes. The most widely used is the polarographic probe (Harris & Spier, 1985). In a polarographic probe, a polarising voltage is applied and diffused oxygen is reduced at the cathode. The electrons circulate from anode to cathode in the external circuit and this current is measured. The ability to respond quickly to changes in the DO concentration is an essential property of any good DO electrode. The two principle properties of a probe which effect its response time are the thickness of the membrane and the diffusivity of oxygen through the membrane (Harris & Spier, 1985).

1.6.4.3 Culture aeration

Direct aeration by sparging of air bubbles into the bioreactor causes foaming in mammalian cell cultures. Excessive foaming may result in damage to the cells. There are two major mechanisms of bubble-induced damage to sensitive cells, one due to rapid oscillations caused by bursting bubbles in stable foams at the surface, and the other due to shear forces in draining films in unstable foams at the surface (Cherry & Papoutsakis, 1990; Handa-Corrigan, 1990; Murhammer & Goochee, 1990a, 1990b).

Since foaming is the direct result of dissolved serum proteins in the medium, particularly albumin, minimizing the amount of protein by lowering serum or protein supplementation reduces foaming. Ironically then, while serum components and proteins are directly responsible for foaming in bubble-aerated

cell cultures, they also help to physically stabilize and protect the delicate cell membranes from mechanical damage in a dose-dependent manner (Ozturk & Palsson, 1991a, 1991d). Addition of anti-foam surfactant agents, such as the nonionic surfactant Pluronic polyols, to the medium reduces foaming and allows the cells to disengage from the zone of bubble bursting before bubble rupture occurs. Pluronic F-68, a nonionic block copolymer consisting of a central block of polyoxypropylene with blocks of polyoxyethylene at both ends, is particularly effective in protecting cells from this type of damage and is now widely used in serum-free and low-protein medium as a protective agent against shear.

Cell damage increases with increasing gas flow rate (*i.e.* more bubbles of the same size) and, in low-protein media without shear protectants, decreasing bubble size (*i.e.* more bubbles to maintain constant flow rate). However, when sparging with very small micron-sized bubbles (*i.e.* microsparging) in media containing surfactants, such bubbles will behave as rigid spheres, will not coalesce, and will form more stable foams than larger bubbles.

Another approach which is widely used is to perform oxygenation in a compartment of the bioreactor which is physically separated from the cells in order to avoid contact between cells and bubbles. This involves housing the sparger in a fine mesh cage which traps the air bubbles and isolates the aeration process from the main cell population. This implies an efficient separation system and an adequate circulation system to ensure that oxygenated medium reaches all cells in the bioreactor.

1.7 Immunoglobulin G

The immune system is a major defence system of higher animals. As previously discussed, it can been divided into innate and adaptative arms. The adaptative system specifically recognizes and destroys foreign substances present in the body. The recognition is accomplished by antibodies or

immunoglobulins. An antigen stimulates the production of specific antibodies which bind the antigen and thus label antigens as targets for destruction by the effector systems of the immune response. Hence, the antibody molecule has two functions. The first is to combine specifically with a nearly unlimited range of antigenic structures, the second is to activate the effector systems.

Immunoglobulin G (IgG) is one of most examined glycoproteins. Of the five classes of immunoglobulins, it is the most abundant in serum, accounting for about 75% of total serum immunoglobulin and about 15% of all serum protein (Burton, 1987; Putnam, 1987). IgG is secreted by activated B lymphocytes and malignant myelomas. Each of these cells is committed to the production of one variant of IgG molecule with defined specificity (*i.e.* monoclonal antibody). IgG is present in the blood and interstitial fluids, and is the only immunoglobulin to cross the placental membrane. It is the main defense against bacteria, viruses, and malignant cells. It binds to these invaders and triggers their destruction by a variety of circulating and non-circulating effector mechanisms. The destruction is by means such as phagocytosis or antibody-dependent cell-mediated cytotoxicity (ADCC) in the adaptative immune system, or by the classical complement pathway in complement-mediated cell lysis (CMCL) in the innate immune system.

IgG can be divided structurally into two heavy chains (~50 kD) and two light chains (~25 kD) interconnected by disulfide bonds (Figure 1-12). It can also be divided into two functionally distinct parts (Burton, 1987; Putnam, 1987; Padlan, 1994). The Fab portion consists of the light chains and the N-terminal portion of the heavy chains. It contains hypervariable regions that recombine specifically to bind with a nearly unlimited range of antigenic structures. The Fc portion consists of the C-terminal portion of the heavy chains and is highly conserved. This is understandable since it functions in the targetted disposal of tagged antigens in the 'effector functions'.

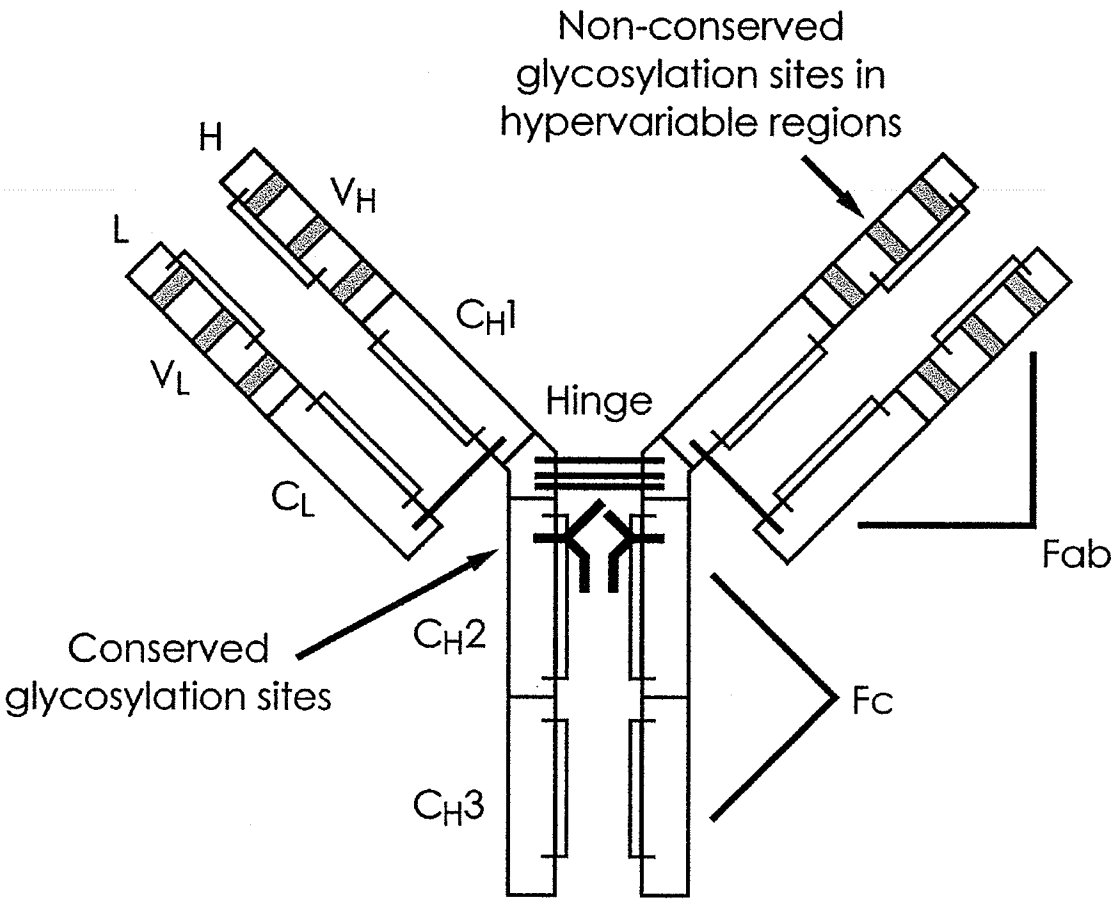

Figure 1-12. Schematic representation of IgG. The domain structure, intrachain and interchain disulfide bonds, and glycosylation sites are shown. The conserved N-linked oligosaccharides are attached to Asn-297 in the C_H2 domains of the Fc, and are generally asymmetric in order to establish the required tether between the two opposing heavy chains. Additional non-conserved N-linked sites may occur in the Fab hypervariable regions (shaded). While the diagram shows murine IgG_1, human IgG_1 is very similar, with only two inter-heavy chain disulfide bonds in the hinge region. H, heavy chain; L, light chain; V, variable domain; C, constant domain. (Adapted from Burton, 1987; Putnam, 1987; Padlan, 1994.)

IgG is the least glycosylated of the immunoglobulins, containing only about 2-3% carbohydrate by mass. In humans, IgG contains 2.8 N-linked biantennary oligosaccharides per molecule (Parekh *et al.*, 1985); 2.3 in mice (Mizuochi *et al.*, 1987; Patel *et al.*, 1992). Two of these represent the conserved glycosylation sites at Asn-297 in each of the two heavy chain CH2 domains of the Fc portion, and the remainder are found in the hypervariable regions of the Fab section with a frequency and position dependent on the chance occurrence of the N-glycosylation consensus sequence (Asn-X-Thr/Ser-Y) (Kobata, 1990) (Figure 1-12). The largest glycan is bisected core-fucosyl disialyl biantennary. Microheterogeneity is produced by the presence or absence of Gal, Fuc, SA, and bisecting GlcNAc (Figure 1-13). Over thirty variants based on at least sixteen neutral structures occur (Parekh *et al.*, 1985; Rademacher *et al.*, 1986; Takahashi *et al.*, 1987; Kobata, 1990). This may lead to an asymmetric distribution of oligosaccharides in the intact IgG since each of the two heavy chains may have a different glycan (Fujii *et al.*, 1990; Rademacher *et al.*, 1996; Masuda *et al.*, 2000). The possible permutations result in many different glycoforms of IgG. Despite this extremely high multiplicity, the ratios of each oligosaccharide in the sera of healthy individuals is quite constant (Kobata, 1990). Analyses of myeloma and monoclonal IgG show that although considerable similarity exists in their oligosaccharide profiles, each cell may express a restricted subset of these variant structures (Mizuochi *et al.*, 1982; Endo *et al.*, 1989; Rothman *et al.*, 1989; Jefferis *et al.*, 1990; Tandai *et al.*, 1991). This suggests that the B cell population is a mixture of clones with different sets and ratios of glycosyltransferases, and that the profile for polyclonal serum IgG is the sum of all the clones contributing to IgG production (Kobata, 1990; Jefferis, 1993).

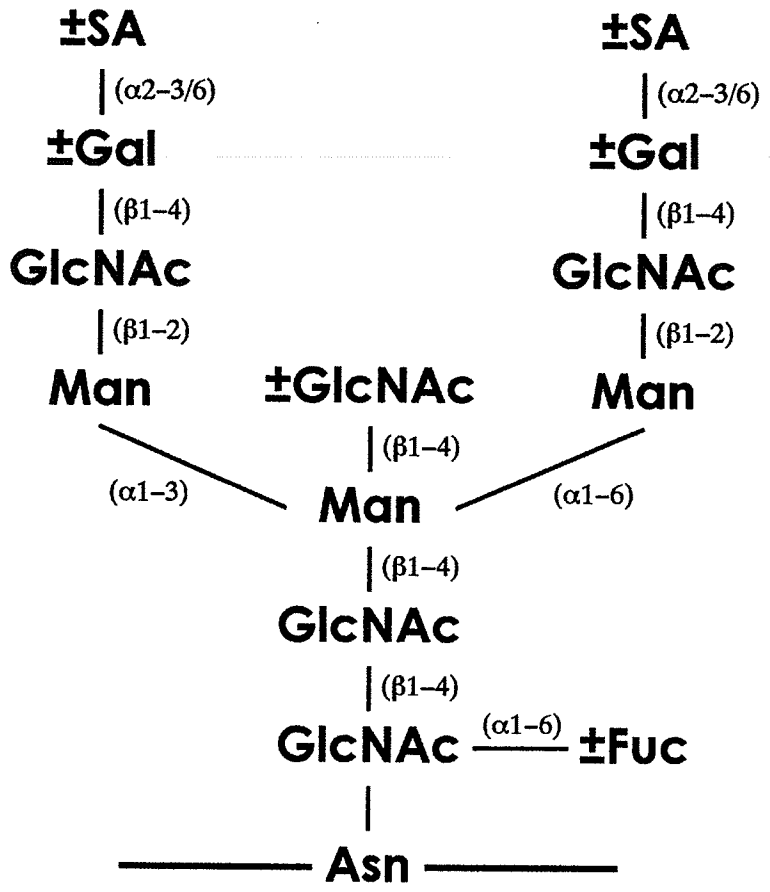

Figure 1-13. Composite structure of the N-linked oligosaccharides of IgG. The largest glycan is bisected core-fucosyl disialyl biantennary. Microheterogeneity is produced by the presence or absence of Gal, Fuc, SA, and bisecting GlcNAc. Over thirty variants based on at least sixteen neutral structures occur. Since each heavy chain may have any one of these structures at Asn-297, the possible permutations result in many different glycoforms of IgG. The terminal SAs, while infrequent in Fc glycans, are common in Fab glycans. (Adapted from Parekh *et al.*, 1985; Rademacher *et al.*, 1986; Takahashi *et al.*, 1987; Kobata, 1990.)

The majority of IgG N-linked oligosaccharides are core-fucosylated in both humans and mice (Mizuochi *et al.*, 1982, 1987; Parekh *et al.*, 1985; Takahashi *et al.*, 1987; Hamako *et al.*, 1993; Raju *et al.*, 2000). However, there are glycosylation differences between the Fc and Fab sites. Glycans of the Fc have varying degrees of galactosylation with none, one, or two terminal Gal. They have a low incidence of monosialylation, and no disialylation. Fab glycans are similar to that of the Fc, but are more completely galactosylated and characterized by a higher incidence of monosialylation and disialylation. In humans, Fc glycans have a low incidence of bisecting GlcNAc while those of the Fab have a high incidence (Dwek *et al.*, 1995; Wormald *et al.*, 1997). Bisecting GlcNAc in murine IgG is uncommon (Mizuochi *et al.*, 1987). To date, O-linked glycosylation of human or murine IgG_1 has not been reported, while that of other human and murine IgG subclasses is extremely rare. In general, O-linked glycans are rare in serum proteins.

The protein milieu near the conserved and potential glycosylation sites in IgG can affect the extent of oligosaccharide processing and lead to site-specific glycosylation (Savvidou *et al.*, 1981, 1984; Fujii *et al.*, 1990; Lee *et al.*, 1990; Wright *et al.*, 1991; Jefferis *et al.*, 1992; Endo *et al.*, 1995; Lund *et al.*, 1996, 2000; White *et al.*, 1997). The shielding of Fc glycans between the two C_H2 domains may limit their accessibility to processing enzymes resulting in the distinctions between Fc and Fab glycosylation. Peptide, disulfide, and glycosyl bond formation involved in the biosynthesis of IgG are not discrete events, but are temporally intertwined and influence the level of IgG-Fc oligosaccharide galactosylation (Rademacher *et al.*, 1995, 1996).

The Fc glycans of IgG are essential to the structural integrity of the antibody (Matsuda *et al.*, 1990; Dwek *et al.*, 1995; Malhotra *et al.*, 1995; Wormald *et al.*, 1997). Alterations of these oligosaccharides have been reported to affect susceptibility to proteolytic degradation, clearance rate, Fc receptor

binding, ADCC, monocyte binding, protein G binding, and C1q component binding and CMCL (Koide *et al.*, 1977; Nose & Wigzell, 1983; Leatherbarrow *et al.*, 1985; Tsuchiya *et al.*, 1989; Walker *et al.*, 1989; Lund *et al.*, 1990; Bond *et al.*, 1993; Pound *et al.*, 1993; Wright & Morrison, 1994, 1997, 1998; Adler *et al.*, 1995; Boyd *et al.*, 1995; Dwek *et al.*, 1995; Jefferis *et al.*, 1995, 1996, 1998; Lifely *et al.*, 1995; Lund *et al.*, 1996; Wright *et al.*, 2000). Interestingly, protein A binding is not affected by Fc glycosylation (Leatherbarrow & Dwek, 1983; Nose & Wigzell, 1983; Tao & Morrison, 1989; Tsuchiya *et al.*, 1989).

There are three classes of $Fc\gamma$ receptors (*i.e.* $Fc\gamma RI$, $Fc\gamma RII$, $Fc\gamma RIII$) for IgG (Winkelhake, 1978; Jefferis *et al.*, 1994; Anderson, 1989; Clark, 1997). They are found differentially on distinct effector constituents of the immune system such as monocytes, macrophages, NK cells, neutrophils, platelets, B cells, eosinophils, *etc.*, in overlapping but distinct combinations. They bind IgG in slightly different areas of the C_H2/hinge and C_H2/C_H3 regions in the Fc. The C1q serum component of complement also binds to the Fc portion of IgG. The structures of these areas, and the binding affinities to the Fc receptors, are variously affected by the state of glycosylation at Asn-297 (Jefferis, 1991, 1993; Jefferis *et al.*, 1995, 1996, 1998; Jefferis & Lund, 1997; Radaev & Sun, 2001).

There is absolute conservation of Asn-297, and the basic core structure of the Fc oligosaccharide throughout a variety of animals is identical. The Fc oligosaccharide must therefore play an important role. However, the relative incidences of glycoforms are different and each species displays a unique fingerprint (Rademacher *et al.*, 1986; Hamako *et al.*, 1993; Raju *et al.*, 2000). The species-specific sialylation and branch-specific galactosylation of the Fc glycans, and the implications for engineering recombinant glycoprotein therapeutics, have been explored (Raju *et al.*, 2000, 2001).

Fab N-linked glycosylation in the hypervariable regions, while occurring with much less frequency, has been reported to influence the binding affinity of

antigens (Hymes *et al.*, 1979; Wallick *et al.*, 1988; Wright *et al.*, 1991; Wright & Morrison, 1993; Tachibana *et al.*, 1994, 1996; Leibiger *et al.*, 1999). There is increasing evidence that IgG forms containing Fab oligosaccharides may be preferentially involved in IgG self-association, aggregation, and cryoprecipitation (Parekh *et al.*, 1988a).

Monoclonal antibodies, usually IgG, are finding increasing use as specific *in vitro* and *in vivo* diagnostic agents, as therapeutic agents, and as ligands for the affinity purification of both macromolecules and smaller molecules. The cell line, production conditions, and other culture factors have also been shown to affect mAb glycosylation (Patel *et al.*, 1992; Lund *et al.*, 1993a, 1993b; Kumpel *et al.*, 1994; Shah *et al.*, 1998; Hills *et al.*, 1999; Kloth *et al.*, 1999; Nahrgang *et al.*, 1999). The effects of different production methods on the glycosylation of CAMPATH-1H, a recombinant humanized murine monoclonal IgG_1, and the functional relevance of its glycans have been well documented (Ashton *et al.*, 1995a, 1995b; Boyd *et al.*, 1995; Lifely *et al.*, 1995; Lines, 1996; Sheeley *et al.*, 1997).

1.8 Purpose of this work

Monoclonal antibodies are becoming increasingly important as diagnostic reagents and pharmaceuticals. The majority of mAbs are of the IgG class and are produced in hybridoma or recombinant cell cultures. Many different aspects of cell culture have been shown to influence glycosylation of mAbs and recombinant glycoproteins. Because the glycosylation of mAbs can have major influences on their physicochemical and functional properties, it is imperative that they are generated in a consistent manner under carefully controlled production conditions. In the work presented in this report, the effect of varying the DO concentration on the structure of the N-linked oligosaccharides of a mAb was examined.

A murine B-lymphocyte hybridoma was grown in chemostat culture in various DO concentrations in two different bioreactors. The secreted mAb, an IgG_1, was subjected to both enzymatic deglycosylation by PNGase F digestion and chemical deglycosylation by hydrazinolysis. The released N-linked oligosaccharides were analyzed qualitatively and quantitatively by fluorophore-assisted carbohydrate electrophoresis (FACE) and high-pH anion-exchange chromatography with pulsed amperometric detection (HPAEC-PAD). Identification of the glycans was confirmed by matrix-assisted laser desorption/ionization tandem quadrupole time-of-flight mass spectrometry (MALDI-QqTOF-MS).

The level of DO affected the glycosylation of the mAb in both bioreactors. A definite shift towards decreased galactosylation of the glycans was observed in steady-state DO concentrations below and above 100% DO, establishing an optimum for maximum galactosylation. The DO effect was not a result of alterations in β1,4-galactosyltransferase (β1,4-GalT) activities, which were remarkably consistent. Other factors which may have been altered by varying the DO concentration, leading to the observed changes in glycosylation, are discussed.

Chapter 2 – Materials and methods

2.1 Experimental synopsis

The overall design of the experiments in this work can be concisely summarized (Figure 2-1). The experiments involve: serum-free continuous cell culture at different steady-state DO concentrations and in different bioreactors; purification of the mAbs from cell culture supernatant; deglycosylation of the mAbs by enzymatic and chemical methods; confirmation of quantitative and nonselective release of glycans by PNGase F digestion; analysis of the glycans by FACE, HPAEC-PAD, and MALDI-QqTOF-MS; GalT assays of the cell pellets.

In addition to the mAbs from cell cultures, bovine (cow) and human polyclonal IgGs were also removed by PNGase F digestion and analyzed by HPAEC-PAD and MALDI-QqTOF-MS.

Standard oligosaccharides were examined by all of the analytical methods, and the monoclonal and polyclonal IgG glycans were compared to these results. The glycan standards are listed elsewhere (Section 2.7.2).

Essentially, the synopsis describes four different pursuits.

1. Establish deglycosylation conditions for IgG and compare deglycosylation of the IgGs by enzymatic (PNGase F digestion) and chemical (hydrazinolysis) methods.
2. Establish glycan analysis protocols and compare the analyses by FACE, HPAEC-PAD, and MALDI-QqTOF-MS.
3. Compare the glycosylation of bovine and human IgGs, and the monoclonal IgGs (*i.e.* mAbs). Determine the effect of steady-state DO concentration in serum-free continuous culture on the glycosylation of the mAbs.
4. Establish GalT assay protocols and compare the GalT activities of the cells grown in different DO concentrations.

Figure 2-1. Experimental synopsis. A schematic representation of the experimental design including: serum-free continuous cell culture at different steady-state DO concentrations and in different bioreactors; purification of the mAbs from cell culture supernatant; deglycosylation of the mAbs by enzymatic and chemical methods; confirmation of quantitative and nonselective release of glycans by PNGase F digestion; analysis of the glycans by FACE, HPAEC-PAD, and MALDI-QqTOF-MS; GalT assays of the cell pellets.

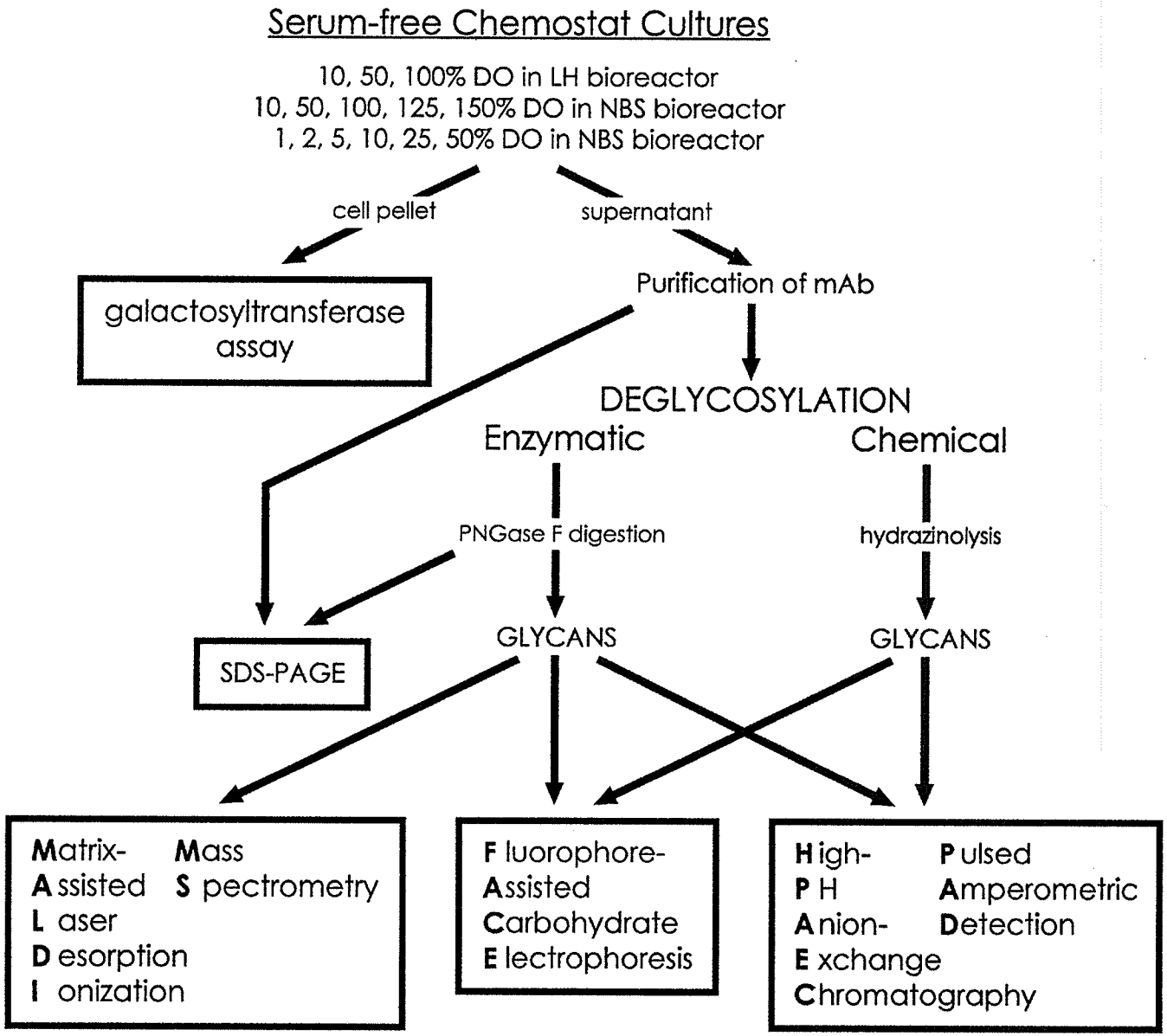
Serum-free Chemostat Cultures
10, 50, 100% DO in LH bioreactor
10, 50, 100, 125, 150% DO in NBS bioreactor
1, 2, 5, 10, 25, 50% DO in NBS bioreactor
cell pellet
supernatant
galactosyltransferase assay
Purification of mAb
DEGLYCOSYLATION
Enzymatic
Chemical
PNGase F digestion
hydrazinolysis
SDS-PAGE
GLYCANS
GLYCANS
Matrix-Assisted Laser Desorption Ionization
Mass Spectrometry
Fluorophore-Assisted Carbohydrate Electrophoresis
High-PH Anion-Exchange Chromatography
Pulsed Amperometric Detection

2.2 General

2.2.1 Water

Distilled-deionized water (DDW) with a background resistivity of not less than 17.0 MΩ was obtained from a Nanopure II system (Barnstead Thermolyne, Chicago, IL, USA) with a 0.2-μm final polishing filter using reverse-osmosis treated feedstock. Freshly-filtered DDW was acquired after a 2-min flush of the system, and not stored for longer than 1 day to minimize contamination.

2.2.2 Miscellaneous materials and equipment

Microcentrifuge tubes were 2-mL polypropylene screwcap tubes with O-rings (VWR, West Chester, PA, USA). Larger tubes were 50-mL disposable polypropylene centrifuge tubes (Fisher Scientific, Pittsburgh, PA, USA). All syringes (1-mL, 3-mL, 5-mL, 10-mL) were disposable polypropylene (Becton Dickinson, Franklin Lakes, NJ, USA) unless otherwise noted. Syringe filters were 0.2-μm nylon 25-mm polypropylene-housed (Nalge Nunc, Rochester, NY, USA) unless otherwise noted. All chemicals and reagents were obtained from one supplier (Sigma, St. Louis, MO, USA) unless otherwise specified.

2.2.3 Dialysis and lyophilization

Protein dialysis was in 12 000-D molecular weight cut-off (MWCO) cellulose dialysis tubing (Sigma) and oligosaccharide dialysis was in Spectra/Por 500-D MWCO cellulose ester dialysis tubing (Spectrum, Laguna Hills, CA, USA). The dialysis tubing was soaked and rinsed as advised by the manufacturers. Samples were loaded carefully with disposable glass pipettes. The cellulose tubing was double-knotted at each end, while the cellulose acetate tubing was doubled over and crimped using appropriate dialysis tubing closures (Spectrum). The samples were dialyzed against DDW (1:100, v/v) in covered Erlenmeyer flasks with gentle stirring for 4 days at 4 °C. The DDW was changed

every 24 h (3 changes total). When dialysis was complete the samples were carefully removed from the dialysis tubing to appropriately sized polypropylene tubes using disposable glass pipettes with rinsing of the inside walls of the tubing.

All samples were frozen using liquid nitrogen. Larger samples (*i.e.* greater than 10 mL) were frozen at approximately a 45° angle to maximize surface area. Tubes were covered with holed caps and lyophilized with the Freezemobile 5SL (Virtis, Gardiner, NY, USA) at -55 °C and less than 50 mTorr.

2.2.4 Mixing, microcentrifugation, and heating

Reconstitution of samples, complete dissolution of reagents, and mixing of tubes to produce homogeneous solutions are extremely important. These were accomplished with the use of the Vortex Genie 2 vortex mixer (Fisher) at full power. Microcentrifugation to settle tube contents after mixing, sediment precipitates, or separate immiscible phases was at 12 000 x *g* in a Model 235A benchtop microcentrifuge (Fisher). Enzymatic digestions and oligosaccharide-labelling reaction incubations were in thermostatted heating blocks (Fisher) at the appropriate temperature.

2.2.5 Weight, volume, pH, and molarity measurements and calculations

2.2.5.1 Weight, volume, and pH measurements

Weights of chemicals and reagents were determined by the tare method using AE50 (50-g) and AE240 (240-g) electronic top-loading balances (Mettler Toledo, Zurich, Switzerland). Both balances were periodically calibrated following manufacturer protocols.

Liquid volumes were determined using 0.5-10-, 10-100-, and 100-1000-μL Eppendorf Reference micropipettes and appropriate disposable polypropylene micropipette tips (Fisher Scientific). Larger volumes were measured using 10- and 25-mL disposable polystyrene pipettes (Fisher Scientific).

Measurements of pH were performed with an Accumet pH meter 915 (Fisher Scientific) fitted with a temperature probe. The pH meter was periodically calibrated by a three-point method following manufacturer protocols using standards of pH 4.0, 7.0, and 10.0.

2.2.5.2 Protein concentration measurement

Purified IgGs and cell lysate protein were quantitated by the bicinchoninic acid (BCA) protein assay. The BCA method is an adaptation of the classical biuret reaction (Smith *et al.*, 1985). It is simpler, more sensitive, and less susceptible to interference from many common detergents, buffer salts, and other compounds (Smith *et al.*, 1985; Stoscheck, 1990). Under alkaline conditions, proteins reduce Cu^{2+} to Cu^{+}. BCA reacts highly specifically with the resulting cuprous ion, forming a stable and intense purple-coloured complex with an absorbance maximum at 562 nm. The production of the chromophore is proportional to the protein concentration. There is excellent linearity in the range of 0-100 μg per 100 μL of sample, but it is best to work in the range of 10-50 μg/100 μL. There is low variability in the protein-to-protein response to the BCA assay, and bovine serum albumin (BSA) and IgG react nearly identically. Therefore, protein concentrations in samples are determined from a standard curve produced from a best-fit straight line of BSA standards.

The BCA assays were accomplished using the BCA-1 Kit (Sigma), which employs two reagents. The first reagent is 1% (w/v) sodium bicinchoninate solution in 0.1 M NaOH (containing sodium carbonate, sodium bicarbonate, sodium tartrate, pH 11.25). The second reagent is 4% (w/v) copper sulfate pentahydrate solution. The standard working reagent is prepared by mixing the first reagent with the second reagent (50:1, v/v). The protein standard solution is 1 mg/mL BSA in saline (0.15 M NaCl, 0.02% (w/v) sodium azide (NaN_3)).

For the determination of purified IgG, 50 μL of each dialyzed preparation

(Section 2.4.2) was mixed with 50 μL of DDW to give 100-μL solutions. For the determination of protein in cell lysates, 5 μL of each lysate, containing cellular protein from 10^6 cells (Section 2.4.4), was mixed with 95 μL of DDW to give 100-μL solutions. A protein calibration set, ranging in concentration from 12.5-100 μg/100 μL, was prepared by mixing appropriate volumes of the protein standard solution and DDW to give 100-μL solutions. The sample and standard solutions, each containing 0-100 μg protein, were mixed with 1.8 mL of standard working reagent and incubated at 37 °C for 30 min. The tubes were allowed to cool to ambient temperature. Absorbances were measured at 562 nm against a reagent blank in a Spectronic 3000 Array spectrophotometer (Milton Roy, USA) with a 1-mL quartz cuvette (Fisher). All determinations, for both samples and standards, were done in duplicate and the means calculated.

2.2.5.3 Molarity calculations for IgGs and oligosaccharides

The molar amounts of the monoclonal and polyclonal IgGs were calculated based on an average molecular weight of 156 kD.

The molar oligosaccharide contents of the IgGs were calculated based on a 2.5% (w/w) oligosaccharide content and a 1800 D average molecular weight for each oligosaccharide.

2.3 Cell line, cell culture, and bioreactor systems

2.3.1 Cell line

The murine B-lymphocyte hybridoma cell line, CC9C10, was obtained as HB-123 from the American Type Culture Collection (ATCC). The cell line is derived from the fusion of Sp2/0-Ag14 cells and B cells from splenic lymph nodes of a BALB/c mouse immunized with bovine insulin. Sp2/0-Ag14 is a hybridoma cell line itself derived from the fusion of BALB/c spleen cells and the P3X63Ag8 BALB/c myeloma, and does not synthesize or secrete any immunoglobulin chains.

Therefore, all fusion partners are initially derived from the same BALB/c mouse strain.

The CC9C10 hybridoma secretes a mAb of class $IgG_{1\kappa}$ against a variety of insulins and pro-insulins (Schroer *et al.*, 1983). The cells have a lymphoblast morphology and grow in suspension culture. The cells were shown to be mycoplasma-free by routine testing in an independent laboratory (Rh Pharmaceuticals/Cangene Corporation, Winnipeg, MB, Canada).

2.3.2 Cell culture medium

The cells were previously adapted for growth in serum-free medium based on an equal mixture (v/v) of reconstituted powdered basal Dulbecco's Modified Eagle's Medium (D-MEM) and reconstituted powdered Ham's F-12 medium (Gibco, Grand Island, NY, USA) (Barnabé & Butler, 1994; Jan *et al.*, 1997; Barnabé, 1998). The mixture was supplemented with glucose, glutamine, sodium bicarbonate ($NaHCO_3$), phenol red, insulin, transferrin, ethanolamine, phosphoethanolamine, sodium selenite (NaSe), and Pluronic F-68 such that the final concentrations were 17.5 mM glucose, 6 mM glutamine, 3.7 g/L (44 mM) $NaHCO_3$, 8.1 mg/L phenol red, 10 mg/L insulin, 10 mg/L transferrin, 10 μM ethanolamine, 100 μM phosphoethanolamine, 10 nM NaSe, and 0.1% (w/v) Pluronic F-68 (Jan *et al.*, 1997; Barnabé, 1998). The pH of the medium was adjusted to 7.1 and the osmolality was approximately 310-330 mOsm/kg. The medium was sterilized by peristaltic pumping through a syringe filter into sterile bottles.

2.3.3 Cell culture bioreactors and cell culture conditions

Continuous cultures were carried out in an LH Series 210 bioreactor (Inceltech, Toulouse, France) (LH) or a CelliGen bioreactor (New Brunswick Scientific, Edison, NJ, USA) (NBS). The working volumes were 1.5 L in the LH

bioreactor (the total reactor volume is 2 L) and 1.2 L in the NBS bioreactor (the total reactor volume is 1.5 L). The dilution rate was 1 reactor volume/day, the temperature was 37 °C, the pH was 7.1, the agitation rate was 100 rpm, and there was a 10% CO_2 (pCO_2) gas-phase overlay. Culture parameters in both bioreactors were therefore nominally identical.

The first set of chemostat cultures were established in DO concentrations of 10, 50, and 100% of air saturation in the LH bioreactor. The second set of chemostat cultures were in DO concentrations of 10, 50, 100, 125, and 150% of air saturation in the NBS bioreactor. The third set of chemostat cultures were in DO concentrations of 1, 2, 5, 10, 25, and 50% of air saturation in the NBS bioreactor. DO concentration was monitored using a polarographic DO sensor (Ingold Electrodes, Wilmington, MA, USA). Both DO and pH were controlled by the respective bioreactor controller(s). Adjustment of pH by dropwise addition of 0.5 M NaOH was required in 1 and 2% DO, when the CO_2 overlay and dissolved carbonate was insufficient to maintain pH. Eluted cell culture mixture was collected following the establishment of steady-state conditions, which was assumed after at least five reactor volume changes of culture mixture with constant viable cell concentration and nutrient levels over three days.

2.3.4 Cell enumeration

Viable cell concentrations were determined by the trypan blue exclusion method (Patterson, 1979). Samples of cell suspension (200 μL) were diluted with 200 μL of 0.2% (w/v) trypan blue in phosphate-buffered saline (PBS, 10 mM sodium phosphate, 30 mM NaCl, pH 7.1). The sample was loaded into both chambers of a Neubauer hæmocytometer slide and the number of cells present in the four large squares of each grid were counted by microscopy. The unstained cells were counted as viable. Cell counts were averaged from 8 squares, and multiplied by 2×10^4 to give viable cells/mL.

2.4 Monoclonal antibody collection and purification

2.4.1 Protein A-affinity chromatography

The monoclonal antibody product was collected and prepared once from each of the DO chemostat cultures. From each culture 1 L of eluted cell culture medium, containing about 1.5-2.5 x 10^9 viable cells/L and 40-50 mg/L of secreted mAb, was collected and chilled to 4 °C. For GalT assays, the collected cell culture suspension was first centrifuged at 300 x *g* for 5 min at 4 °C and the cell pellet treated as described (Section 2.4.4). Otherwise, the cell suspension (or supernatant) was (again) centrifuged at 10 000 x *g* for 15 min to remove cells (or residual cells), and filtered through a syringe filter to remove cellular debris. The mAb was purified by protein A-affinity chromatography (Ey *et al.*, 1978) with an alternate buffer system (van Sommeren *et al.*, 1992). Protein A was chosen over protein G because protein G may select for certain glycoforms (Bond *et al.*, 1993) and protein A does not (Nose & Wigzell, 1983; Leatherbarrow & Dwek, 1983; Boyd *et al.*, 1995). Three polypropylene Econo-Pac cartridges (Bio-Rad, Hercules, CA, USA), each packed with 5 mL of Affi-Prep protein A support (Bio-Rad), were connected in series. The eluate was monitored at 280 nm by connecting the cartridges to an Ultrospec II spectrophotometer (Pharmacia, Uppsala, Sweden) equipped with a flow cell (Fisher Scientific). The cartridges were loaded with buffer or samples by a peristaltic pump. The cartridges were first washed with DDW, elution buffer (0.1 M citric acid-sodium citrate, pH 5.0), and then binding buffer (0.1 M Tris, 1.5 M ammonium sulfate, pH 7.5 with HCl) at 4 mL/min for 10 min each to equilibrate the system. Each 1L of cell culture supernatant was diluted with 1 L of binding buffer and loaded onto the affinity cartridges at 1 mL/min. The cartridges were subsequently washed with approximately 100 mL of binding buffer at 4 mL/min to elute unbound contaminants until a stable absorbance was achieved. Monoclonal antibody was eluted at 1 mL/min with 20 mL of elution buffer and collected as a peak at

280 nm. The mAb fraction was neutralized with neutralization buffer (1 M Tris, pH 9.0 with HCl) and frozen at -20 °C. The cartridges were regenerated after each purification with 50 mL of 50% (v/v) methanol and reequilibrated with 50 mL of binding buffer at 4 mL/min. The cartridges were periodically cleaned with 25 ml of 0.1 M NaOH at 4 mL/min, followed by reequilibration with binding buffer. All buffers were filtered through syringe filters prior to use.

2.4.2 Preparation of aliquots of monoclonal and polyclonal IgGs

The mAb fractions, approximately 40-50 mL at roughly 1 mg/mL of prepared mAb from each of the DO chemostat cultures, were thawed and exhaustively dialyzed against DDW in 12 000-D MWCO dialysis tubing. Problems with mAb precipitation were not encountered.

Similarly, vials containing 10 mg each of bovine and human polyclonal IgGs (Sigma) were dissolved in 10 mL of DDW and exhaustively dialyzed against DDW in 12 000-D MWCO dialysis tubing. Again, solubility problems were not encountered.

The dialyzed preparations were filtered through syringe filters into tared large tubes. The IgGs were quantitated by the BCA protein assay (Section 2.2.5.2) and lyophilized. The large tubes containing the lyophilized IgGs were again weighed and the tared weight of IgGs compared against the results from the BCA assays. In all cases the two methods were in agreement to within 10%.

The lyophilized IgGs were dissolved in DDW to 5 mg/mL and aliquoted into 10-mg samples for analysis by size-exclusion chromatography, 1-mg samples (mAbs only) for deglycosylation for FACE, and 5-mg samples (mAbs and polyclonal IgGs) for deglycosylation for HPAEC-PAD and MALDI-QqTOF-MS. The aliquoted samples were lyophilized and frozen at -20 °C.

2.4.3 Size-exclusion chromatography

The purity of 10-mg samples of each mAb preparation from all three sets of chemostat cultures (and also the bovine polyclonal IgG) were confirmed by Bio-Gel P-300 (Bio-Rad) size-exclusion chromatography. The resin (50-100 wet mesh), with a fractionation range of approximately 10-400 kD, was first wetted with methanol for 6 h and then soaked in elution buffer (0.1 M pyridine, 0.02% (w/v) NaN_3, pH 5.1 with glacial acetic acid) for 24 h. In order to not damage the resin particles, the mixture was stirred, not shaken (with apologies to Ian Fleming). The slurry was allowed to settle briefly and the supernatant was discarded to remove fines. This step was repeated several times. The mixture was degassed under vacuum overnight. The slurry was poured into a 1.5-cm x 1.5-m glass column (Pharmacia) (approximately 250 mL) and allowed to settle under peristaltic pump pressure of 0.5 mL/min with elution buffer. When the column height was stable (approximately 6 h), excess eluent was removed from the top of the column and a 2-mL sample (5 mg/mL in the elution buffer) of IgG was allowed to settle into the column bed. Once the sample had settled, eluent was gently poured down the inside of the column to fill it (approximately 10 mL). The samples were eluted at 0.5 mL/min and monitored at 280 nm with the spectrophotometer and flow cell described (Section 2.4.1). The column was extensively washed with eluent between each sample until a stable absorbance was achieved.

2.4.4 Preparation of cell lysates for galactosyltransferase assay

The cell pellets from the third set of chemostat cultures obtained from gentle centrifugation (Section 2.4.1) were further prepared for analysis by the GalT assay (Section 2.8). Each cell pellet (approximately 1.5-2.5 x 10^9 viable cells) was enumerated and washed twice by resuspension at 2 x 10^8 cells/mL of ice-cold PBS (usually about 10 mL for 2 x 10^9 cells) and centrifugation at 300 x g

for 5 min at 4 °C. The third resuspension was aliquoted into 1-mL samples and frozen at -70 °C.

The 1-mL samples (2 x 10^8 cells) of washed and frozen cells were thawed and pelleted from the PBS by centrifugation at 300 x *g* for 5 min at 4 °C. Each sample was resuspended in 1 mL of ice-cold lysis buffer (10 mM Tris, 0.15 M NaCl, 2 mM phenylmethylsulfonyl fluoride (PMSF, a serine-protease inhibitor), 1% (w/v) Triton X-100, pH 7.4 with HCl). The resuspensions were homogenized with a Microson XL Ultrasonic Cell Disrupter (Misonix/Heat Systems, Farmingdale, NY, USA) fitted with the P-1 microprobe at full power (50 W, 23 kHz) three times for 30 s at 4 °C. The cell homogenates were centrifuged at 12000 x *g* for 15 min at 4 °C to remove cellular debris. Each supernatant (cell lysate) was aliquoted into 250-μL samples, containing cellular protein from 50 x 10^6 cells, and frozen at -70 °C.

2.5 Deglycosylation

2.5.1 PNGase F digestion

Peptide N-glycosidase F (PNGase F) may be used to release the N-linked oligosaccharides from glycoproteins. PNGase F is technically not an endoglycosidase, but an amidohydrolase that hydrolyzes the β-aspartylglycosylamine linkage between the proximal GlcNAc of the oligosaccharide and the side chain amide of asparagine (Tarentino *et al.*, 1985, 1989; Maley *et al.*, 1989). The hydrolysis generates an aspartic acid at the site of hydrolysis and liberates a 1-aminooligosaccharide (Tarentino & Plummer, Jr., 1994). The latter is slowly hydrolyzed by environmental water to ammonia and the oligosaccharide with a reducing terminal GlcNAc (Figure 2-2). This reaction can be facilitated by mildly acidic conditions or suspended by mildly basic conditions. However, in a typical 24-h incubation, the hydrolysis of the 1-aminooligosaccharide is essentially quantitative.

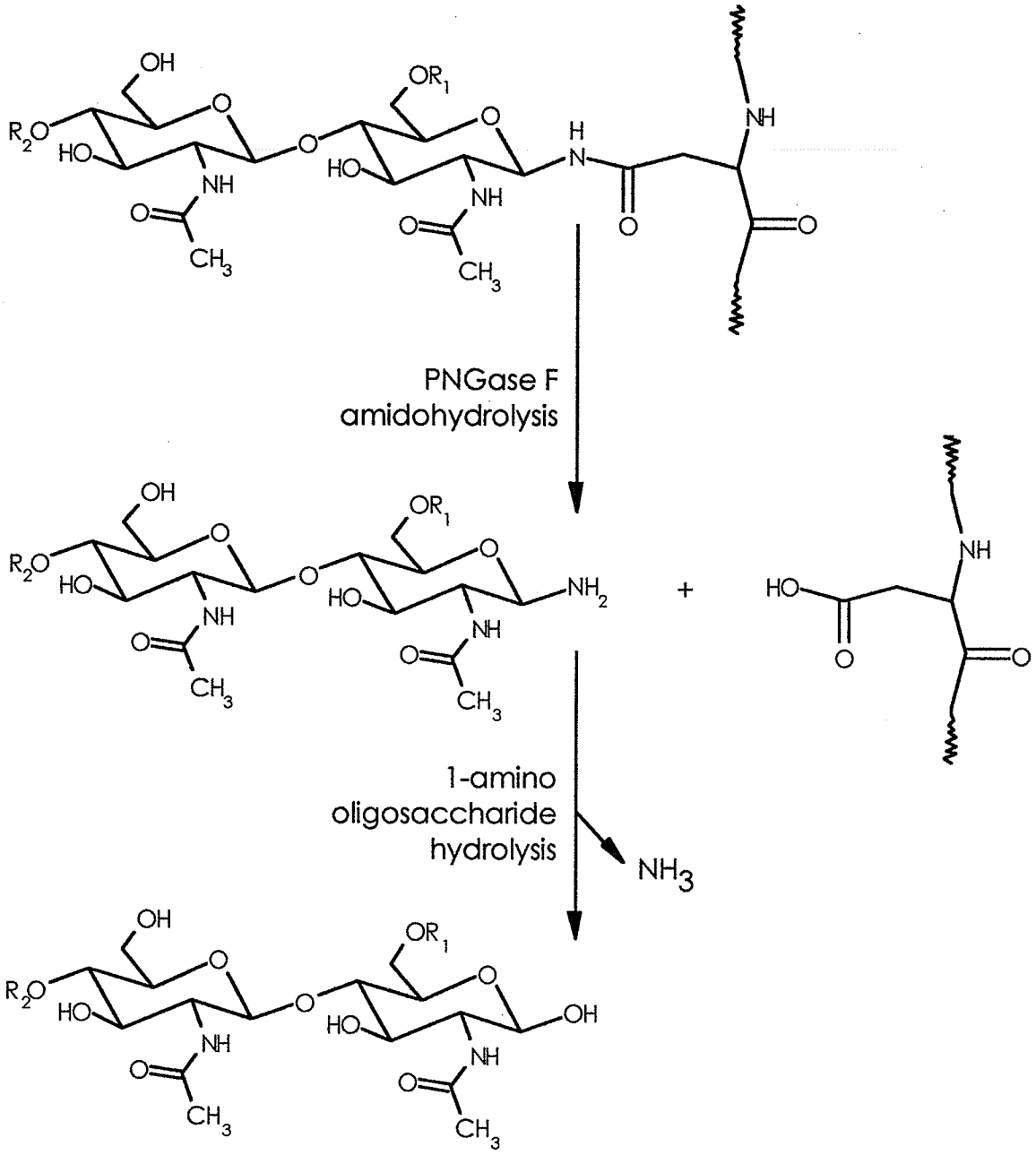

Figure 2-2. Deglycosylation of glycoproteins by PNGase F. R1 represents either hydrogen or α1,6-Fuc. R2 represents hydrogen or the rest of an oligosaccharide.

Unlike endoglycosidases, PNGase F is effective on most high-mannose, hybrid, and complex N-glycans (Maley *et al.*, 1989; Tarentino *et al.*, 1989; Hirani *et al.*, 1987; Tarentino & Plummer, Jr., 1987, 1994). The minimum glycan structural determinant is the $(GlcNAc)_2$ chitobiose core (Chu, 1986). The only known constraints to the activity of PNGase F are that the proximal GlcNAc must not have an attached α1,3-Fuc (Tretter *et al.*, 1991), which is common in plants but not observed in mammals, and that the Asn residue to which the oligosaccharide is attached may not be N- or C-terminal (Tarentino *et al.*, 1985; Tarentino & Plummer, Jr., 1987). Phosphate, sulfate, and sialic acid groups attached to the oligosaccharide do not affect cleavage (Maley *et al.*, 1989).

PNGase F will remove intact oligosaccharides from some native substrates, but not all. Denaturation of difficult substrates prior to the addition of enzyme and the use of detergents enhances the susceptibility and rate of hydrolytic cleavage of the glycans (Alexander & Elder, 1989; Nuck *et al.*, 1990). For a 'hypothetical standard glycoprotein' of 50 kD with four glycosylation sites, a substrate concentration of 1 mg/mL and an enzyme concentration of 500 mU/mL for native substrate or 100 mU/mL for denatured substrate is recommended. This yields an enzyme-to-substrate ratio of 500 mU/mg for native substrate or 100 mU/mg for denatured substrate.

2.5.1.1 PNGase F enzyme unit definitions

While there is an International Unit description for PNGase F, as defined by the International Union of Biochemistry (IUBMB), it has been the practice of PNGase F manufacturers to measure and supply the enzyme by their own definitions. This has led to considerable confusion, particularly since there are no reported differences in the intrinsic activity of these enzymes, whether they are native or recombinant. For the work reported here, recombinant PNGase F was obtained from two suppliers, Oxford GlycoSciences (Abingdon, UK) and Glyko

(Novato, CA, USA). Oxford GlycoSciences has since sold their 'Tools for Glycobiology' glycobiology product line to Glyko. The original unit definitions from Oxford GlycoSciences and Glyko differed from each other, and both from the IUBMB definition. However, Glyko has consolidated the way their products are named, supplied, and labelled. Glyko PNGase F unit definitions have changed to conform with the IUBMB definition. Accordingly, all PNGase F unit amounts reported in this work have been converted to IUBMB units.

One last word of caution. There remain manufacturers and suppliers of PNGase F who do not conform to IUBMB unit definitions for this enzyme. Product literature supplied with the enzyme from manufacturers other than Glyko should be closely scrutinized to obtain conversion factors and avoid misinterpretations.

2.5.1.2 Enzymatic deglycosylation protocol for FACE

For analysis by FACE, 1-mg samples of each mAb preparation from all three sets of chemostat cultures (but not the bovine and human polyclonal IgGs) were subjected to PNGase F digestion using the N-Linked Oligosaccharide Profiling Kit (Glyko) and accompanying protocol. The samples were dissolved in 50 μL of incubation buffer (20 mM sodium phosphate, 50 mM ethylenediamine-tetraacetic acid (EDTA), 0.02% (w/v) NaN_3, pH 7.5) in microcentrifuge tubes. To each tube 5 IUBMB milliunits (mU) of recombinant PNGase F was added. The tubes were mixed and briefly centrifuged after the addition of enzyme to ensure homogeneity. These solutions, with an enzyme concentration of 100 mU/mL, a substrate concentration of 20 mg/mL, and an enzyme-to-mAb ratio of 5 mU/mg, were incubated at 37 °C for 24 h. No attempt was made to first denature the mAbs before the addition of enzyme. After incubation, the tubes were cooled on ice and three volumes (150 μL) of ice-cold absolute ethanol were added. After 10 min on ice, the tubes were centrifuged at 12 000 x *g* for 10 min. The supernatants were set aside and the remaining proteinaceous pellets were

washed with 50 μL of DDW. A second precipitation with three volumes of ethanol, cooling, and centrifugation followed. The pooled N-linked oligosaccharide-containing supernatants (approximately 400 μL total) for each mAb sample were not dialyzed or filtered prior to lyophilization. After lyophilization the samples were frozen at -20 °C.

2.5.1.3 Enzymatic deglycosylation protocol for HPAEC-PAD

For analysis by HPAEC-PAD, 5-mg samples of each mAb preparation from all three sets of chemostat cultures (and also the bovine and human polyclonal IgGs) were dissolved in 250 μL of incubation buffer (20 mM sodium phosphate, 50 mM EDTA, 0.02% (w/v) NaN_3, pH 7.5) in microcentrifuge tubes. To each tube 10 IUBMB mU of recombinant PNGase F (Oxford GlycoSciences) was added. The tubes were mixed and briefly centrifuged after the addition of enzyme to ensure homogeneity. These solutions, with an enzyme concentration of 40 mU/mL, a substrate concentration of 20 mg/mL, and an enzyme-to-mAb ratio of 2 mU/mg, were incubated at 37 °C for 24 h. Again, no attempt was made to first denature the mAbs before the addition of enzyme. After incubation, the tubes were cooled on ice and three volumes (750 mL) of ice-cold absolute ethanol were added. After 10 min on ice, the tubes were centrifuged at 12 000 x *g* for 10 min. The supernatants were set aside and the remaining proteinaceous pellets were washed with 250 mL of DDW. A second precipitation with three volumes ethanol, cooling, and centrifugation followed. Finally, the pooled N-linked oligosaccharide-containing supernatants (approximately 2 mL total) for each mAb sample were exhaustively dialyzed against DDW in 500-D MWCO dialysis tubing, filtered through syringe filters, and lyophilized. After lyophilization the samples were frozen at -20 °C.

2.5.1.4 Enzymatic deglycosylation protocol for MALDI-QqTOF-MS

For analysis by MALDI-QqTOF-MS, the PNGase F deglycosylation of mAb samples of preparations from the first set of chemostat cultures (but also the bovine and human polyclonal IgGs) was identical to that for HPAEC-PAD analysis.

2.5.2 Hydrazinolysis

Hydrazinolysis may be used to release the O- and N-linked oligosaccharides from glycoproteins (Takasaki *et al.*, 1982; Patel *et al.*, 1993; Patel & Parekh, 1994). The main benefit of hydrazinolysis is the inherent nonspecificity of chemical deglycosylation methods compared to enzymatic methods. The reaction mechanisms by which hydrazinolysis leads to the release of O- and N-linked oligosaccharides from glycoproteins have not been fully elucidated. Reaction conditions have therefore been established empirically (Patel *et al.*, 1993). Despite the structural diversity of the oligosaccharides and protein moieties of a range of glycoprotein standards, similar reaction conditions were found to allow essentially complete release of unreduced O- and N-linked oligosaccharides. Hydrazinolysis of O-linked glycans can be achieved under milder conditions than for that of N-linked glycans. Therefore, the method may be used to remove both O- and N-linked glycans at once, or O-linked glycans separately from N-linked glycans. Hydrazinolysis is the only chemical deglycosylation method that releases glycans with an intact reducing terminal GlcNAc, well-suited for glycan labelling. However, hydrazinolysis has several disadvantages. It requires careful preparation of the hydrazine and sample, which must be free of the water, salts, most detergents, and dyes that interfere with the reaction. Hydrazinolysis also results in the destruction of the protein component and the deacetylation of any acetamido groups (*i.e.* GlcNAc, Neu5Ac, GalNAc), which must be re-acetylated. Hydrazine is also both toxic

and volatile.

Hydrazinolysis involves the use of anhydrous hydrazine to cleave O- and N-glycosidic bonds, chromatographic separation of glycan hydrazides from unreacted hydrazine and peptide/amino acid hydrazides, re-*N*-acetylation of any de-*N*-acetylated amino groups, cleavage of the terminal acetohydrazide group, and chromatographic recovery of O- and N-glycans in an unreduced form.

All hydrazinolysis reagents must be analytical grade or better. All glass must be acid washed to remove surface-bound metals and mineral impurities. Hydrazine must be less than 1% water and metal ion-free (double vacuum distilled at ambient temperature in the presence of phosphorus pentoxide and sealed into acid-washed and lyophilized glass ampoules).

Hydrazinolysis at 60 °C for 5 h removes greater than 90% of O-linked glycans and less than 10% of N-linked oligosaccharides. Incubation at 95 °C for 5 h removes greater than 90% of both O- and N-linked glycans, but may result in some degradation of the O-linked chains. The glycans are released as partially de-*N*-acetylated hydrazide derivatives; linked to hydrazine by a glycosylamine bond (Figure 2-3). Purification of the released glycans is often by paper chromatography, or by column chromatography using microgranular (microcrystalline) or fibrous cellulose. However, the procedure in this work employs column chromatography with acid-washed glass beads. When equilibrated in 1-butanol, glycan hydrazides bind to the surface by hydrophilic interaction (*i.e.* hydrogen bonding) with the silanol groups of the glass and the peptide-hydrazides are eluted. The glycan hydrazides are then eluted with water. During the re-*N*-acetylation reaction with acetic anhydride, the hydrazide is converted to the acetohydrazide. The acetohydrazide bond is extremely acid labile and the glycans are converted to the reducing form by the addition of copper (II) acetate in acetic acid. The reducing

oligosaccharides are desalted by cation-exchange chromatography.

The losses of glycan in manipulations during execution of these procedures are neglible. There is less than 10% recovery of peptide derivatives, and greater than 90% recovery of trisaccharide glycans and larger. Most acidic (*i.e.* phosphorylated, sulfated, or sialylated) oligosaccharides are stable to the process, but sialic acids may be converted to the *N*-acetyl derivative.

2.5.2.1 Chemical deglycosylation protocols for FACE and HPAEC-PAD

For analysis by FACE and HPAEC-PAD, 5-mg samples of each mAb preparation from the first set of chemostat cultures (and not the bovine and human polyclonal IgGs) were subjected to deglycosylation by hydrazinolysis using the N-Glycan Recovery Kit (Oxford GlycoSciences) and accompanying protocol.

The salt-free mAb samples were each dissolved in 1 mL of DDW and transferred into 1-mL glass reaction vessels (Fisher). The samples were exhaustively lyophilized and held on the lyophilizer until immediately before the addition of hydrazine.

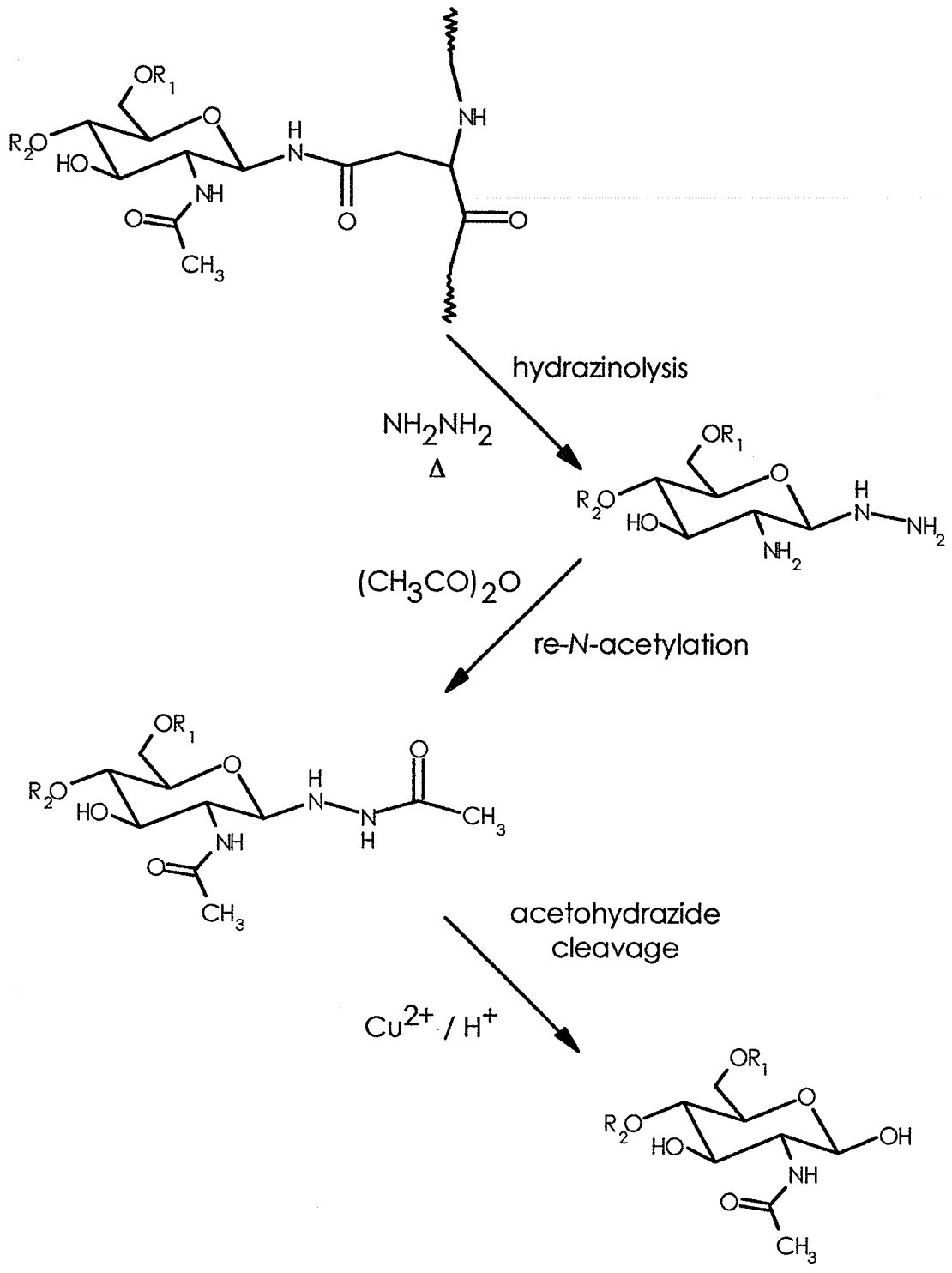

Figure 2-3. Deglycosylation of glycoproteins by hydrazinolysis.

For each sample, a sealed glass ampoule containing 500 μL of anhydrous hydrazine was carefully opened and the contents transferred to the reaction vessel with a disposable glass pipette. The vessel was sealed with a Teflon-lidded screwcap (Fisher). These steps were done as quickly as possible to prevent significant water uptake. The glass reaction vessels and glass pipettes were previously acid washed by soaking for 10 min in 2 M nitric acid followed by extensive soaking and rinsing with DDW, and dried first at ambient temperature and then under vacuum. Each sample was therefore dissolved to 10 mg/mL in anhydrous hydrazine with gentle mixing. Since the IgGs were not expected to be O-glycosylated, the reaction vessels were incubated at 95 °C for 5 h. During the incubation time, the samples were periodically mixed to ensure the samples were completely dissolved. After the incubation the reaction vessels were allowed to cool to ambient temperature.

Glycan-binding columns were prepared by packing disposable polypropylene Poly-Prep columns (Bio-Rad) with 2 mL of 75-μm (200-mesh) acid-washed glass beads (Supelco, Bellefonte, PA, USA) which had been acid washed a second time with nitric acid as above. The columns were washed four times with 1 mL of DDW, once with 0.5 mL of absolute ethanol as the transition solvent, and four times with 1 mL of 1-butanol. The columns were plugged and an additional 2 mL of 1-butanol was added. To each cooled reaction vessel 1 mL of 1-butanol was added and thoroughly mixed with the sample solution. The contents of each reaction vessel were transferred onto the glycan-binding column and carefully mixed with the liquid above the column bed, without disturbing more than the top 0.2 mL of the bed. The column was unplugged. The reaction vessel was washed twice with 1 mL of 1-butanol, and the washes added to the column after allowing the solution above the bed to enter the column each time. The 1-butanol washes removed the unreacted hydrazine and some of the peptide hydrazides from the column. The column

was then eluted four times with 2 mL of 1-butanol/absolute ethanol/DDW (4:1:1, v/v/v). These washes removed the remaining peptide hydrazides. Column flow with the 1-butanol-containing eluents was assisted by applying gentle pressure from a disposable 10-mL syringe. The last wash was once with 0.5 mL of absolute ethanol as the transition solvent. The column was then allowed to run dry. All of the above washes were discarded. Finally, the glycan hydrazides were eluted with four 0.5-mL additions of 0.2 M sodium acetate. The eluates from each column (approximately 2 mL total) were collected into a 20-mL acid-washed (as above) glass vials (Fisher Scientific).

To each vial was added 200 μL of acetic anhydride/absolute ethanol (2:5, v/v). The vials were capped, gently shaken, and incubated at ambient temperature for 30 min. Then 100 μL of 0.1 M copper (II) acetate was added to each vial and the vials mixed and incubated at ambient temperature for another 30 min.

Mixed-bed cation-exchange columns were prepared by packing disposable polypropylene Poly-Prep columns (Bio-Rad) with 0.6 mL of Chelex 100 resin (Bio-Rad) (200-400 mesh, Na^+ form) and 1.4 mL of AG 50W-X12 resin (Bio-Rad) (200-400 mesh, H^+ form). The columns were washed twice with 4 mL of DDW with gentle shaking to thoroughly mix the resins. The columns were plugged until needed. The Chelex 100 and AG 50W resins desalt the samples by removing the copper and sodium ions, and also remove the monoacetyl hydrazine that has been released from the glycans.

When ready, the glycan solutions were transferred onto the unplugged mixed-bed cation-exchange columns and the eluates collected into 20-mL translucent polyethylene scintillation vials (Fisher Scientific). The vials were washed three times with 0.5 mL of DDW, and the washes added to the respective columns after allowing the solution above the bed to enter the column each time. The washes were also collected in the appropriate vials.

The reducing oligosaccharides were recovered in dilute acetic acid and ethanol solutions (approximately 3.8 mL total), which were filtered through 0.2-μm nylon 4-mm polypropylene-housed syringe filters (Nalge Nunc). Aliquots equivalent to the glycans released from 1 mg of each mAb were set aside for analysis by FACE, and the remaining portions equivalent to the glycans released from 4 mg of each mAb were analyzed by HPAEC-PAD. All samples were lyophilized and frozen at -20 °C. Samples were not dialyzed prior to lyophilization.

2.6 SDS-PAGE

Sodium dodecyl sulfate polyacrylamide gel electrophoresis (SDS-PAGE) was used to confirm the quantitative deglycosylation of the mAbs by PNGase F digestion. Prior to PNGase F digestion (Section 2.5.1), 20-μL aliquots from samples of each of the mAb preparations from the first set of chemostat cultures were set aside. These were compared with 20-μL aliquots of each sample after the digestions were completed. SDS-PAGE was carried out essentially by the use of a discontinuous buffer system (Laemmli, 1970; Shi & Jackowski, 1998), except that SDS was omitted from the running buffer and stacking and resolving gels (but was included in the loading buffer).

The 20-μL aliquots before and after PNGase F digestion were diluted to 100 μL with DDW to bring their mAb concentrations to 1 mg/mL. For non-reducing conditions, 25-μL portions containing 25 μg of mAb were removed and diluted in 25 μL of 2x loading buffer (0.125 M Tris, 20% (v/v) glycerol, 4% (w/v) SDS, 0.1% (w/v) bromophenol blue, pH 6.8 with HCl). For reducing conditions, the samples were diluted in the loading buffer as above, except that the buffer also contained 10% (v/v) 2-mercaptoethanol. Tubes were heated at 95 °C for 5 min and centrifuged at 12 000 x *g* for 10 min.

PAGE was performed in slab gels. The resolving gels were 6% (w/v) total

acrylamide for non-reduced samples and 10% (w/v) total acrylamide for reduced samples. The resolving gels were cast in resolving gel buffer (0.375 M Tris, pH 8.8 with HCl). For both resolving gels, a 4% (w/v) total acrylamide stacking gel was employed. The stacking gels were cast in stacking gel buffer (0.125 M Tris, pH 6.8 with HCl). The gels contained 2.7% *bis*-acrylamide of the total acrylamide content for crosslinking. The 8 x 8-cm gels were cast and run using the Mini-Protean II Electrophoresis Cell (Bio-Rad) with 0.75-mm spacers and a 8-well comb to yield 48-μL well volumes.

Prior to loading, sample wells were rinsed with running buffer (25 mM Tris, 0.2 M glycine, pH 8.3). This buffer was discarded and fresh running buffer was added. Wells were loaded with a blunt-point narrow-bore Hamilton 25-μL Microliter syringe which was thoroughly rinsed with DDW between samples. From the samples diluted in the loading buffers, 10 μg (20 μL) of each non-reduced mAb, and 20 μg (40 μL) of each reduced mAb, were loaded onto the 6 and 10% gels, respectively. For calibration, 10 μL of high- and low-range molecular weight standards (Bio-Rad) were loaded and run concurrently with the non-reduced and reduced samples, respectively. To prevent possible lane distortions, any empty lanes were loaded with 20 or 40 μL of 1x loading buffer.

Both non-reducing and reducing gels were resolved at ambient temperature with a run of 5 min at a constant current of 200 mA to load, followed by 55 min at 150 mA to separate, using a programmable power supply.

The gels were removed from their cassettes and stained and fixed by bathing the gels in a solution of 0.1% Coomassie blue G-250 (Pierce, Rockford, IL, USA) in 40% methanol/10% acetic acid (v/v) for 1 h, followed by destaining in 40% methanol/10% acetic acid (v/v) for a similar time and rinsing with DDW.

The gels were photographed on Polaroid Type 667 black-and-white instant pack film (Eastman Kodak, Rochester, NY, USA) using a Polaroid DS-34 direct screen instant camera fitted with an EP H-5 electrophoresis hood and a

#58 green lens filter (Polaroid Corporation, Cambridge, MA, USA). With this equipment, a 1/125-s exposure at an aperture of *f* 11 provided the best reproduction. Polaroid photographs of the SDS-PAGE gels were quantitated as described (Section 2.7.3.3).

2.7 Glycosylation analysis

2.7.1 N-glycan nomenclature

The N-glycan nomenclature used in this work is based on nomenclature adapted from the Oxford GlycoSciences system (Hermentin *et al.*, 1992a, 1992b) (Figure 2-4). Prefixes M, H, and C indicate the class of high-mannose, hybrid, or complex structures, respectively. The designations C2-, C3-, C4-, and C5- indicate the antennarity of the complex structure. The next four digits following the hyphen, from left to right, describe the number of residues of Neu5Ac, Gal, non-bisecting GlcNAc, and Man, respectively. The fifth digit following the hyphen indicates the absence (0) or presence (1) of bisecting GlcNAc. The sixth and final digit indicates the absence (0) or presence (1) of Fuc at the proximal GlcNAc.

2.7.2 Glycan standards

Eight standard complex N-linked oligosaccharides (Oxford GlycoSciences and Glyko) were examined by all of the analytical methods (Figure 2-5). The monoclonal and polyclonal IgG glycans were compared to these results.

The eight standard glycans were dissolved in DDW to 0.1 μg/μL. These solutions were mixed in various combinations and volumes to give different equimolar sets of standards for FACE, HPAEC-PAD, and MALDI-QqTOF-MS.

AB-CDEFGH

A - high-mannose (M), hybrid (H), complex (C),
or subcomponent of trimannosyl core (R)
B - number of antenna
C - number of sialic acid residues
D - number of galactose residues
E - number of (non-bisecting) *N*-acetylglucosamine residues
F - number of mannose residues
G - bisecting *N*-acetylglucosamine residue (0 or 1)
H - core-fucose residue (0 or 1)

C2-224301

C - complex
2 - biantennary
2 - number of sialic acid residues
2 - number of galactose residues
4 - number of (non-bisecting) *N*-acetylglucosamine residues
3 - number of mannose residues
0 - no bisecting *N*-acetylglucosamine residue
1 - core-fucose residue

non-bisected, core-fucosyl biantennary complex glycan

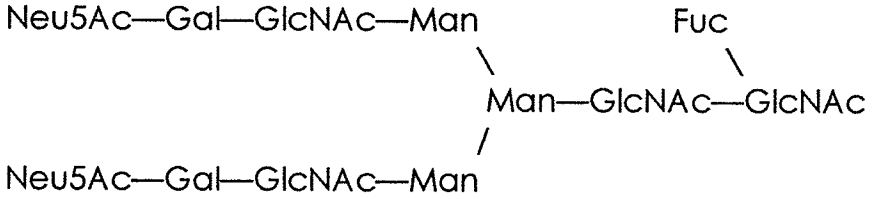

Figure 2-4. Nomenclature for N-linked oligosaccharides. The general system (top) and an example (bottom).

Figure 2-5. Eight N-linked oligosaccharide standards. These standards were examined by FACE, HPAEC-PAD, and MS, and utilized for the identification of unknown sample glycans.

C2-004300 asialyl agalactosyl biantennary

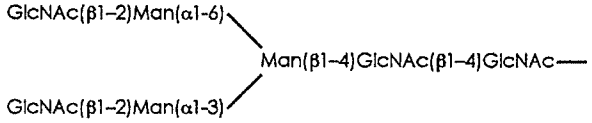

C2-004301 core-fucosyl asialyl agalactosyl biantennary

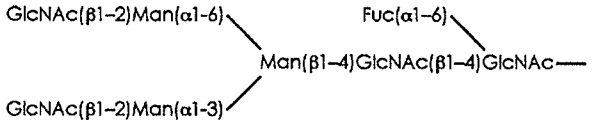

C2-024300 asialyl digalactosyl biantennary

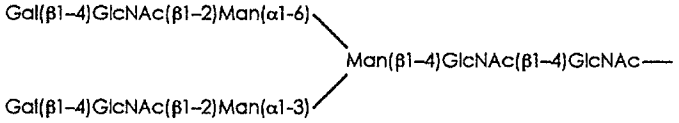

C2-024301 core-fucosyl asialyl digalactosyl biantennary

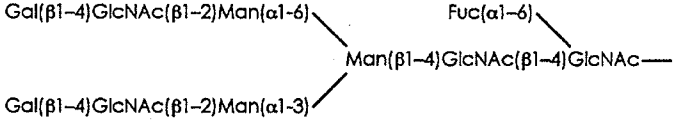

C2-124300 monosialyl biantennary

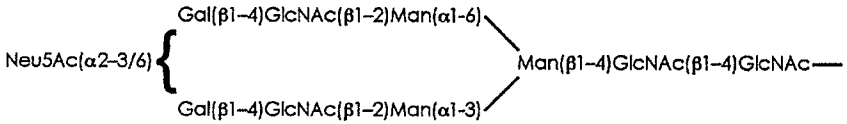

C2-124301 core-fucosyl monosialyl biantennary

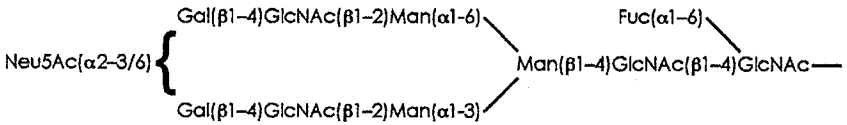

C2-224300 disialyl biantennary

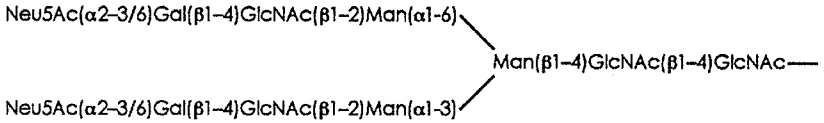

C2-224301 core-fucosyl disialyl biantennary

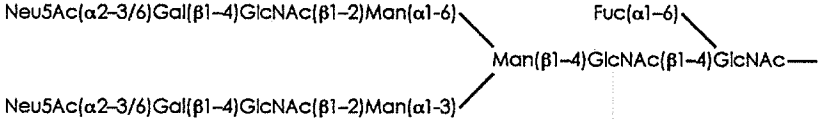

2.7.2.1 Glycan standard solutions for FACE

Standard glycan sets for FACE were:

Set 1: 1 nmol each of the neutral biantennary glycans C2-004300, C2-004301, C2-024300, C2-024301 (4 nmol or 6.2 μg total); Set 2: 1 nmol each of the (mono- and di-) sialyl biantennary glycans C2-124300, C2-124301, C2-224300, C2-224301 (4 nmol or 8.6 μg total).

These standards were lyophilized and frozen at -20 °C in preparation for ANTS-labelling.

2.7.2.2 Glycan standard solutions for HPAEC-PAD

Standard glycan sets for HPAEC-PAD were:

Set 1: 2.5 nmol each of the afucosyl biantennary glycans C2-004300, C2-024300, C2-124300, C2-224300 (10 nmol or 17.8 μg total); Set 2: 2.5 nmol each of the core-fucosyl biantennary glycans C2-004301, C2-024301, C2-124301, C2-224301 (10 nmol or 19.3 μg total); Set 3: Sets 1 and 2 combined (20 nmol or 37.1 μg total).

Each set was diluted to 500 μL with DDW such that the 50-μL HPAEC-PAD injections contained 250 pmol of each standard glycan. These standards were frozen at -20 °C.

2.7.2.3 Glycan standard solutions for MALDI-QqTOF-MS

Standard glycan sets for MALDI-QqTOF-MS were:

Set 1: 1 nmol each of the neutral biantennary glycans C2-004300, C2-004301, C2-024300, C2-024301 (4 nmol or 6.2 μg total); Set 2: 1 nmol each of the (mono- and di-) sialyl biantennary glycans C2-124300, C2-124301, C2-224300, C2-224301 (4 nmol or 8.6 μg total); Set 3: Sets 1 and 2 combined (8 nmol or 14.8 μg total).

These standard sets were lyophilized and frozen at -20 °C in preparation for PMP-labelling.

2.7.3 FACE

2.7.3.1 Essentials of FACE

Fluorophore-assisted carbohydrate electrophoresis (FACE) combines the high resolution and simplicity of polyacrylamide gel electrophoresis with the sensitivity of fluorescence (Jackson, 1990, 1993, 1994a, 1994b, 1996, 1997, 1998; Jackson & Williams, 1991; Stack & Sullivan, 1992; Hu, 1995; Starr *et al.*, 1996; Klock & Starr, 1998; Quintero *et al.*, 1998). The general fundamentals of FACE analysis of oligosaccharides can be divided into three categories: labelling, separation, and detection.

2.7.3.1.1 Labelling

The release of N-linked oligosaccharides from glycoproteins, accomplished either enzymatically or chemically, has been described (Section 2.5). The only strict requirement is the presence of a reducing end for incorporation of the fluorophore label.

Because reducing oligosaccharides possess an aldehyde functional group, reductive amination with a suitable amino compound is a common method for selective derivatization of carbohydrates (Schwartz & Gray, 1977). In reductive amination, the reducing terminus of a carbohydrate reacts with an amine-containing derivatization agent to form a Schiff base (Figure 2-6). Selective and mild reduction of the Schiff base with sodium cyanoborohydride ($NaBH_3CN$) pulls the amination equilibrium forward and forms the stable secondary amine derivative. The use of arylamines permits the derivatization reaction to be done at mild pH and most also have the advantage of being strong chromophores and/or fluorophores. In addition, the aromatic character of the reductive amination products prepared from arylamines increases the retention of derivatized carbohydrates on many commonly used liquid chromatography columns.

In the FACE method, the derivatization agent is the charged fluorophore 8-aminonaphthalene-1,3,6-trisulfonic acid (ANTS, excitation 365 nm, emission 515 nm). ANTS possesses a single arylamine for stoichiometric (1:1) labelling and three sulfonic acids for strong negative charge (Figure 2-6). It is soluble in aqueous solutions and has a large Stokes shift to facilitate discrimination between excitation and emission radiation.

2.7.3.1.2 Separation

FACE is an effective method for separating all classes of oligosaccharides including O-linked glycans and high-mannose, hybrid, and complex N-glycans. The method of separation is based on those used for PAGE of proteins with two important modifications: relatively high concentration gels are used in the range of 20-40% acrylamide – higher percentages for smaller oligosaccharides; and detergents and thiol reagents are omitted throughout. The higher percentage gels in the FACE method require higher current to obtain relative rapid movement so it is important to maintain good cooling of the gels during the electrophoresis. This is best achieved by surrounding the gels by a well-stirred cooled running buffer. The liquid flowrate over each side of the gel cassette should be the same. If cooling is uneven between opposite sides of the gel cassette then resolution will be lost and some bands may even appear as artifactual doublets.

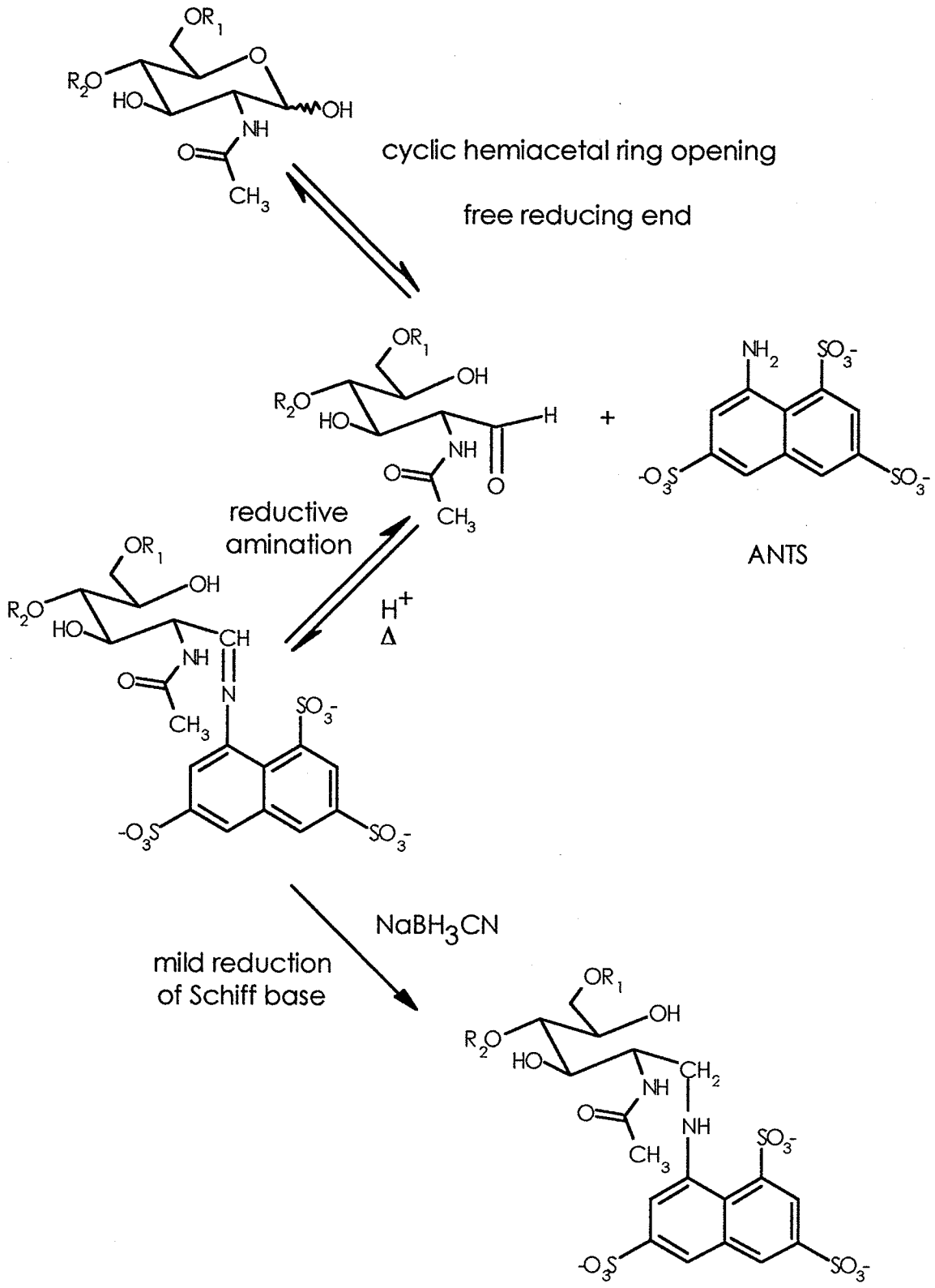

Figure 2-6. Structure of ANTS and ANTS-labelling scheme.

The electrophoretic mobilities of ANTS-labelled oligosaccharides in FACE are related largely to their hydrodynamic volumes and charge-to-mass ratios, which are characteristically influenced by the individual structures of the component monosaccharides and their number, connectivity, conformation, and charge (Jackson, 1990, 1994; Hu, 1995). There may also be some interaction of the oligosaccharides with the gel matrix providing a partial affinity electrophoresis effect (Jackson, 1993, 1994a, 1996). Positional isomers, epimers, and anomers can be resolved.

The migration of glycans is gauged relative to a ladder of partially hydrolyzed dextran (a linear polymer of α1,4-Glc), and is measured in glucose units (GU) or degree of polymerization (DP). This work uses GU as the designator. The separation of oligosaccharides by electrophoresis is largely empirical, and it is not always possible to predict their relative mobilities. However, the average contributions to oligosaccharide mobility of the constituent monosaccharide residues have been determined (Hu, 1995; Starr *et al.*, 1996; Quintero *et al.*, 1998) (Table 2-1).

Table 2-1. Relative monosaccharide contribution to N-glycan migration in FACE.

	Mobility shift in GU		
Monosaccharide residue	Hu, 1995	Starr *et al.*, 1996	Quintero *et al.*, 1998
Fuc	+ 0.60	+ 0.50	+ 0.50
bisecting GlcNAc	–	+ 0.50	–
GlcNAc	+ 0.75	+ 0.75	+ 0.70
Man	+ 0.75	+ 0.75	+ 0.70
Gal	+ 1.00	+ 1.00	+ 1.00
Neu5Ac	- 1.00	- 1.00	- 0.70

2.7.3.1.3 Detection

The ANTS-labelled oligosaccharides may be detected when the gels (electrofluorograms) are illuminated at the appropriate wavelength and imaged on photographic film or by a digital charge-coupled device (CCD) camera. Photography can show as little as 1 pmol per band, while 10 pmol gives a bright band. Quantitation in the range of 10-500 pmol is possible. Polyacrylamide gels are well suited for achieving high sensitivity because they have low intrinsic fluorescence. Photographic film has greater sensitivity and resolution than digital imaging. If there is a signal to detect, no matter how weak, it will eventually appear on film given enough exposure time. However, electronic digital cameras have a much broader dynamic range. In practical terms, the greater dynamic range of digital systems means that it is possible to obtain more information before being limited by blackout. With digital systems, it is possible to read the high-density and low-density bands on a single image. Digital cameras are quite expensive, compared to conventional photography, but allow for easier image storage and retrieval. These last disadvantages of film may be mitigated by scanning and saving photographs of appropriate gels and analyzing them with publically available or commerical software. The narrower dynamic range of film can be alleviated by adjusting the exposure times such that the heaviest bands are not saturated to the point of blackout and that quantitation of the faintest bands is not attempted. It must be stressed that in this work the intensities of bands were quantitated relative to other bands in the same lane. For absolute quantitation, calibrated standards of different concentrations must be run in different lanes of the same gel. This is not only costly in terms of standards, but occupies lanes that would otherwise contain samples.

2.7.3.2 FACE protocols

N-linked glycans from 1-mg samples of each of the mAb preparations from all three sets of chemostat cultures (but not the bovine and human polyclonal IgGs) were analyzed by FACE using the N-Linked Oligosaccharide Profiling Kit (Glyko) and accompanying protocol. For the first set of chemostat cultures, glycans were released from mAb preparations by both PNGase F digestion and hydrazinolysis; for the second and third sets only PNGase F digestion was used for deglycosylation.

Complete protocols for the preparation of the glucose ladder standard, ANTS-labelling of glycans, and preparation, running, viewing, and imaging of FACE gels have been reviewed (Jackson, 1994, 1997, 1998; Klock & Starr, 1998).

The N-linked oligosaccharides were stoichiometrically labelled with ANTS by reductive amination. Each tube of lyophilized oligosaccharides (approximately 15 nmol) was first dissolved in 5 μL of labelling reagent (0.15 M ANTS in 15% (v/v) acetic acid). Next, 5 μL of reducing reagent (1 M $NaBH_3CN$ in dimethyl sulfoxide (DMSO)) was added. The tubes were mixed, briefly centrifuged, and incubated at 45 °C for 4 h. After lyophilization to a viscid gel, the samples were frozen at -20 °C.

Two sets of N-linked oligosaccharide standards (Section 2.7.2.1) were also derivatized with ANTS as described. The two sets contained equimolar mixtures of 4 neutral biantennary glycans (4 nmol or 6.2 μg total) and 4 sialyl biantennary glycans (4 nmol or 8.6 μg total), respectively.

FACE was performed in slab gels essentially by the use of a discontinuous system (Laemmli, 1970; Jackson, 1994, 1997, 1998), except that SDS and thiol reagent were omitted throughout, and a special stacking gel buffer was not required. The resolving gels were 20% (w/v) total acrylamide. The stacking gels were 4% (w/v) total acrylamide and 5% (w/v) polyethylene glycol (8000 MW). The polyethylene glycol equalizes the osmolarity between the high and low

density gels, and, due to the opacity imparted to the stacking gel, aids in visualizing the well for loading. The resolving gels and stacking gels were cast in gel buffer (0.112 M Tris, pH 7.0 with glacial acetic acid). The gels contained 2.6% *bis*-acrylamide of the total acrylamide content for crosslinking. The 8 x 10-cm gels were cast with 0.5-mm spacers and an 8-well comb to yield 32-μL well volumes.

The samples were thawed and diluted with equal volumes of DDW and 2x sample loading solution (20% (v/v) glycerol, 0.1% (w/v) thorin 1 dye). Prior to loading, sample wells were rinsed with running buffer (50 mM Tris, 50 mM tricine, pH 8.2). This buffer was discarded and fresh running buffer was added. Wells were loaded with a blunt-point narrow-bore Hamilton 10-μL Microliter syringe which was thoroughly rinsed with DDW between samples. From the diluted samples, 4-μL of ANTS-labelled glycans (approximately 4 nmol) from 288 μg of mAb were loaded into the wells of the FACE gel. Standard glycan sets for FACE were dissolved in DDW and diluted with an equal volume of loading solution such that standard wells were loaded with 4 μL containing 300 pmol of each ANTS-labelled glycan. At least one lane of each gel was loaded with 4 μL of a pre-labelled standard glucose ladder solution. To prevent possible lane distortions, the same volumes were added to each lane, and any empty lanes were loaded with 4 μL of 1x loading solution.

The gels were resolved with a run of approximately 1 h 45 min at a constant current of 15 mA using a programmable power supply and cooling to 5 °C using chilled 5% (v/v) ethanol via a circulating refrigerated water bath (Haake, Berlin, Germany). The electrophoretic runs were terminated shortly after the orange thorin 1 band eluted from the gel (approximately 15 min). Thorin 1 has a similar mobility to unreacted ANTS which appeared as the strongest fluorescent band moving through the gel ahead of the labelled oligosaccharides.

The resolved FACE gels were documented by fluorescence on a lab-built long-wave UV illuminator. This consisted of four 18"-long F15T8-BLB fluorescent 15-watt 1"-diameter black light bulbs (General Electric, Cleveland, OH, USA) and a UV-transmitting visible-absorbing U-235C glass filter (Hoya, San Jose, CA, USA). The black light bulbs have peak emissions in the long-wave UV (350-400 nm, maximum 365 nm) and the glass filter allows 80% transmittance at 365 nm and 0% transmittance at 430-655 nm. The gels were photographed using the same camera equipment as described (Section 2.6) except for the substitution of a #8 yellow lens filter (Kodak). The lens filter allowed 0% transmittance of 365 nm and 80% transmittance of 515 nm. The FACE gels were not removed from their cassettes, but the cassette glass allowed 90% transmittance of long-wave UV and visible light and possessed low intrinsic fluorescence. With this equipment, a 1-s exposure at an aperture of *f* 4.5 provided the best reproduction.

Oligosaccharide bands in the samples were identified by comparison of their electrophoretic mobility in GU with those from the glycan standard solutions, and by comparison with previous reports for standard oligosaccharides (Stack & Sullivan, 1992; Hu, 1995; Starr *et al.*, 1996; Quintero *et al.*, 1998) and for glycans released from IgG (MacGillivray *et al.*, 1995; Frears & Axford, 1997; Frears *et al.*, 1999; Martin *et al.*, 2001).

2.7.3.3 Quantitation of SDS-PAGE and FACE gels

Polaroid photographs of the SDS-PAGE and FACE gels were scanned in grayscale into Photoshop v5.5 (Adobe Systems, San Jose, CA, USA) at 360 dpi and 150% size using a SuperVista S-12 flatbed scanner (UMAX Technologies, Fremont, CA, USA) and VistaScan v2.4.3. The files were converted to TIFF format at 250-300 dpi and imported into the public-domain software NIH Image v1.62 (U.S. National Institutes of Health, Bethesda, MD, USA), available at http://rsb.info.nih.gov/nih-image/ for Macintosh only. The bands in each lane

were quantitated relative to other bands in the same lane using the gel-plotting macro; absolute quantitation was not performed. The integration data were statistically analyzed as described (Section 2.9).

2.7.4 Analysis by HPAEC-PAD

2.7.4.1 Essentials of HPAEC-PAD

The general fundamentals of high-pH anion-exchange chromatography with pulsed amperometric detection (HPAEC-PAD) analysis of oligosaccharides can be divided into four categories: column resin, eluents, separation, and detection.

2.7.4.1.1 Column resin

The CarboPac PA-100 column is packed with a pellicular resin – a resin with a solid, nonporous core coated with a thin layer of more porous material (Figure 2-7). The exchange sites of this resin are located only on the surface layer of the bead. The resin has a low ion-exchange capacity but is more resistant to pressure-induced mechanical stresses.

The core substrate of the PA-100 resin is a 8.5-μm bead of ethylvinylbenzene with 55% divinylbenzene crosslinking. The bead is surface-sulfonated for electrostatic attachment of the surface resin. The surface resin is a pellicular coating of agglomerated 275-nm MicroBeads of polyacrylate alkyl quaternary amine-derivatized latex with 6% crosslinking. The CarboPac PA-100 resin is therefore a strongly basic anion exchanger.

The pellicular resin can withstand operating pressures of up to 4000 psi (28 MPa), operating temperatures of 4-90 °C, pH 0-14, and is compatible with up to a 90% solution of most common organic HPLC solvents. The latex has a medium-high hydrophobicity and an ion-exchange capacity of 90 μeq for the 4 x 250-mm analytical column.

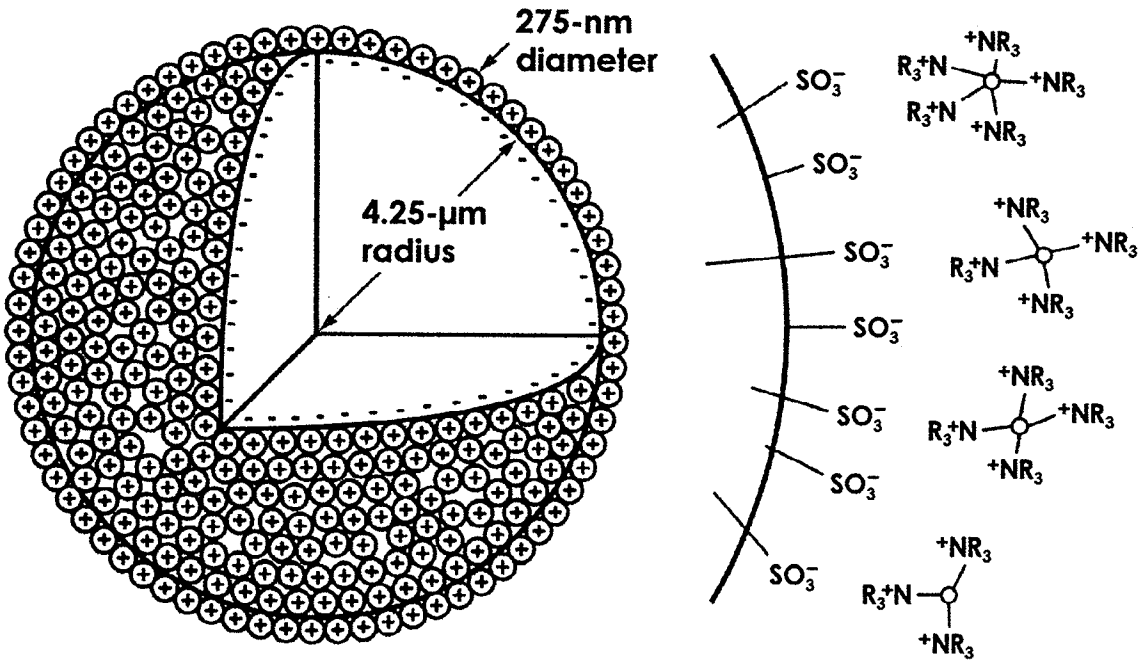

Figure 2-7. CarboPac PA-100 pellicular anion-exchange resin.

2.7.4.1.2 Eluents

For oligosaccharide separations, the most useful conditions involve the use of sodium acetate gradients at constant high pH. Sodium hydroxide acts as the supporting electrolyte and increases the conductivity and pH of the solution. The hydroxide concentration must be high enough to ionize the carbohydrate hydroxyl groups (pH > pKa) in order to form oxyanions which will exchange on the column resin. However, eluent concentrations that are too high may cause the sample to overload the column even though only a very small amount of the analyte of interest is present in the sample. At high concentrations, the sodium ion may also form bridges between vicinal oxyanions in solution and interfere with chromatography. For similar reasons, samples with very high salt concentrations should be avoided. This is especially true of strong anions (*e.g.* chloride, carbonate, phosphate, *etc.*). The presence of anionic detergents (*e.g.* SDS) in samples should be entirely avoided. Nonionic or cationic detergents are acceptable but should be minimized. The application of an acetate gradient accelerates the elution of acidic (*i.e.* phosphorylated, sulfated, or sialylated) oligosaccharides by acting competitively as a pusher anion.

Only filtered deionized water with a minimum background resistivity of 16.7 MΩ should be used – 18 MΩ is preferred. Only high quality reagents should be used, and all eluents should be filtered and degassed well with helium. Helium has a very low solubility in water and forces gasses such as carbon dioxide and oxygen out of solution. This eliminates later outgassing and the formation of bubbles in eluent selector valves and the detector cell. More critically, high-pH eluents tend to absorb carbon dioxide from the atmosphere, resulting in carbonate formation, which is divalent at pH greater than 12 and binds strongly to the column. This interferes with carbohydrate binding and causes a drastic loss in column selectivity, and a loss of resolution and efficiency.

The change of eluent pH and composition also results in baseline shifts during gradients and reduced retention time reproducibility, increased background conductivity, and increased detection limits for target analytes. In addition, dissolved oxygen is PAD-active and produces negative peaks when reduced to hydrogen peroxide. Reabsorption of carbon dioxide and oxygen can be minimized by storage of the degassed eluents in helium-pressurized containers.

2.7.4.1.3 Separation

HPAEC is an effective method for separating all classes of oligosaccharides including O-linked glycans and high-mannose, hybrid, and complex N-glycans (Hardy & Townsend, 1994).

Carbohydrates are in fact weak acids with pKa values commonly in the range of 12-14. The pKa values for the individual hydroxyls of a particular monosaccharide are dependent on the identity of the monosaccharide itself and the position of the hydroxyl within the monosaccharide (Rendleman, Jr., 1971; Neuberger & Wilson, 1971; Hardy & Townsend, 1994). Because of activation by the hemiacetal functional group, the acidity of reducing monosaccharides is largely from ionization of the anomeric hydroxyl (Rendleman, Jr., 1971). For oligosaccharides, the anomeric hydroxyl groups of the constituent monosaccharides are, except for the reducing terminus, involved in glycosidic bonds. Polar, steric, and hydrogen-bonding effects produce a hierarchy of acidity for the other ring hydroxyls (2-OH >> 6-OH > 3-OH > 4-OH) (Rendleman, Jr., 1971). For *N*-acetylated monosaccharides, the 3-OH is considerably more acidic than the 3-OH of neutral sugars (Neuberger & Wilson, 1971). The pKa values for neutral reduced sugar alcohols (*i.e.* alditols) are higher than those of their respective neutral reducing monosaccharides.

The separation of oligosaccharides using a strong anion-exchange stationary phase is based on the relative ionization and acidities of the

constituent monosaccharide hydroxyl groups under alkaline conditions (Rocklin & Pohl, 1983; Hardy & Townsend, 1988, 1989, 1994; Townsend *et al.*, 1988, 1989a, 1989b; Lee, 1990; Basa & Spellman, 1990; Pfeiffer *et al.*, 1990; Spellman, 1990; Townsend & Hardy, 1991). No sample derivatization is required. Factors affecting separation include hydrodynamic volume (*i.e.* size and conformation), monosaccharide composition and sequence, linkage and positional connectivity, degree of branching, and degree of sialylation. Acidic oligosaccharides (*i.e.* phosphorylated, sulfated, or sialylated) are predictably more retained, but separation attributable to the neutral portion of the oligosaccharide is not lost.

While predicting elution order of oligosaccharides is largely empirical, thirteen well-established relationships between oligosaccharide structure and chromatographic retention have been documented (Hardy & Townsend, 1994; Rohrer, 1995; Strang, 1998) (Table 2-2).

Lastly, carbohydrates undergo a number of well documented reactions (*e.g.* epimerization, keto-enol tautomerism) at high pH that can potentially interfere with chromatography. However, in most cases these reactions are slow at ambient temperature and do not appear to occur to any noticeable extent over the time course of the chromatography.

Table 2-2. Relationships of N-linked glycan structure to PA-100 retention.

- oligosaccharides with a greater number of residues or a higher degree of branching have increased retention
- reduction of the reducing terminal GlcNAc decreases retention
- oligosaccharides with the chitobiose core intact have decreased retention compared to their analogues with half the chitobiose core
- addition of Fuc to the chitobiose core decreases retention
- addition of bisecting GlcNAc to the trimannosyl core increases retention
- oligosaccharides with a greater proportion of Galβ1,3GlcNAc to Galβ1,4GlcNAc have increased retention
- addition of a LacNAc (Galβ1,4GlcNAc) repeat to an antenna of a neutral oligosaccharide increases retention
- the triantennary isomer with a disubstituted α1,3Man antenna has less retention than the isomer with a disubstituted α1,6Man antenna
- addition of each formal negative charge to an oligosaccharide increases retention
- sialylated oligosaccharides with a greater proportion of α2,3-linked sialic acids to α2,6-linked sialic acids have increased retention
- sialylated oligosaccharides with only α2,3-linked sialic acids are better resolved at pH 5
- sialylated oligosaccharides with a greater proportion of Neu5Gc to Neu5Ac have increased retention
- addition of a LacNAc repeat to a sialylated oligosaccharide decreases retention

2.7.4.1.4 Detection

Detection and direct quantitation of carbohydrates at low picomole levels with excellent signal-to-noise ratios has been optimized using PAD. No sample derivatization is required and only a small fraction of the total sample is oxidized in the electrochemical cell.

Pulsed amperometry detects only those compounds that contain functional groups that are oxidizable at the detection voltage employed. Careful selection of the applied potential allows selective oxidation of the carbohydrates without also oxidizing the eluent and other species in the sample. High concentrations of PAD-active compounds (*e.g.* Tris, alcohols, and other hydroxylated compounds) should be avoided. However, under typical HPAEC-PAD conditions, the sensitivity for carbohydrates is orders of magnitude greater than for other interfering species.

Electrons are transferred from the oxyanions of the deprotonated carbohydrate hydroxyl groups to the working electrode, resulting in positive or anodic current. The current resulting from the oxidation of the carbohydrates is plotted as a function of time. When a flow-through electrochemical cell is used the current versus time plot is a chromatogram. The use of a single potential results in poor reproducibility and a rapid loss of sensitivity because the reaction products from the oxidation of the carbohydrates or other interfering species react with and poison the working electrode surface. A triple-pulse sequence sets up a repeating sequence of potentials which electrochemically clean the electrode.

The PAD supplies up to three potentials for specified time intervals. In pulsed amperometry, the current is measured at the end of the first pulse, which allows the charging current to decay (Figure 2-8). The optimum pulse potentials (E) and time intervals (t) are determined empirically. For oxidations, E1 is set to a small positive value. E2 is generally used as a positive cleaning potential and is

set near the positive potential limit of the working electrode in the eluent to oxidize the gold surface and cause desorption of the carbohydrate oxidation products. The positive potential limit is the applied potential at which the solution, the supporting electrolyte, or the electrode itself can be oxidized. E2 must be high enough and long enough to oxidize the electrode and clean the surface fully but not cause excessive gold oxidation and wear the electrode too rapidly. E3 is a negative cleaning potential and is usually set at an intermediate negative potential to reduce the electrode surface back to gold. At the negative potential limit the solution or the supporting electrolyte are reduced. E3 must be low enough to reduce the oxidized surface fully but not so low that chemical reductions occur. The results of these reactions may cause baseline disturbances during subsequent measurement at E1.

The potential limits are strongly affected by the pH of the eluent. In general, positive potential limits are greater in acid and smaller in base; conversely, negative potential limits are greater in base and smaller in acid. A gold working electrode possesses an excellent combination of both positive and negative potential limits. For a gold working electrode in 0.1 M NaOH solution, the positive potential limit is approximately +0.75 V and the negative potential limit is approximately -1.25 V.

Because the gold working electrode is slowly fouled and pitted even when a triple-pulse sequence is employed it should be physically polished and reequilibrated periodically to maintain maximum sensitivity and reproducibility. This should be done whenever a degradation in performance is noticed, such as a decrease in sensitivity, increase in background current, noisy baseline or tailing peaks are observed, or when the surface is visably discoloured.

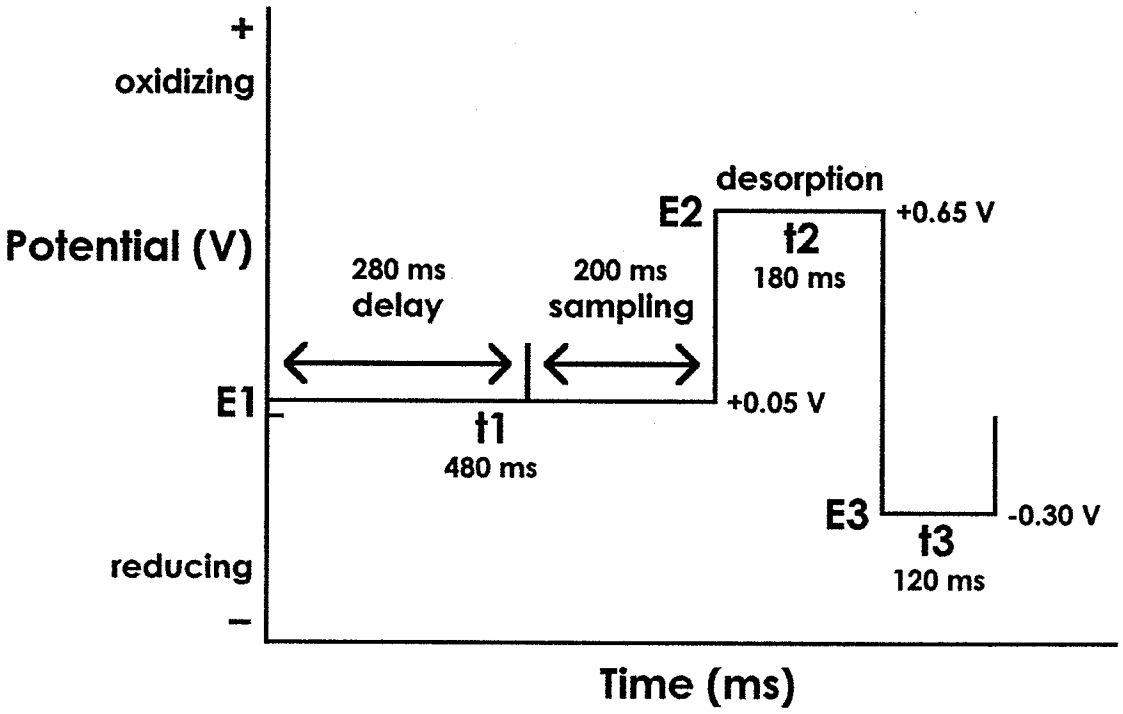

Figure 2-8. Triple-pulse PAD waveform used in this work.

2.7.4.2 HPAEC-PAD protocols

N-linked oligosaccharides from 5-mg samples of each of the mAb preparations from all three sets of chemostat cultures (and also the bovine and human polyclonal IgGs) were analyzed by HPAEC-PAD using a DX-300 system (Dionex, Sunnyvale, CA, USA). For the first set of chemostat cultures, glycans were released from mAb preparations by both PNGase F digestion and hydrazinolysis; for the second and third sets only PNGase F digestion was used for deglycosylation. For the polyclonal IgGs, glycans were removed only by PNGase F digestion.

Sample or standard glycans were separated by HPAEC at ambient temperature using 4 x 50-mm guard and 4 x 250-mm analytical CarboPac PA-100 columns at a flow rate of 1 mL/min. The operating pressure typically was 2300-2500 psi. The elution scheme employed was as follows: isocratic at 0.1 M NaOH for 0.5 min; a linear gradient to 0.04 M sodium acetate (in 0.1 M NaOH) in 49.5 min; a linear gradient to 0.2 M sodium acetate (in 0.1 M NaOH) in 30 min; a 15-min hold with this eluent to wash the columns; a return to the initial eluent by a linear gradient to 0.1 M NaOH in 5 min; a 15-min hold with the initial eluent to reequilibrate the columns. Post-column pre-detector addition of NaOH is not necessary for PAD baseline stability at constant 0.1 M NaOH, and was not exercised. Eluents were prepared with DDW, 50% NaOH solution (Mallinckrodt, Paris, KY, USA) and sodium acetate trihydrate (Mallinckrodt). Sodium acetate solutions were filtered through 0.2-μm nylon 47-mm membrane filters (Nalge Nunc). Sodium acetate solutions were again degassed prior to the addition of NaOH to prevent carbonate formation from dissolved carbon dioxide introduced during filtration.

Electrochemical detection was with the PAD-2 using the basic PAD cell, a 1.4-mm gold working electrode, a replenishable silver (Ag/AgCl) reference electrode, and a 0.014-in thick cell gasket at 300 mA full-scale. The triple-pulse

PAD sequence was set at 0.05 V for 480 ms, 0.65 V for 180 ms, and -0.30 V for 120 ms (Figure 2-8), with a response time of 1 s and a 0.20 s sampling rate (5 scans/s).

N-linked glycan samples diluted to contain approximately 2 nmol total oligosaccharides from 144 μg of each mAb or polyclonal IgG were injected automatically from a 50-μL sample loop. Injections of samples into the sample loop were first filtered through 0.2-μm nylon 4-mm polypropylene-housed syringe filters (Nalge Nunc). Prior to the injection of a new sample, the sample loop was flushed with at least ten loop volumes (500 μL) of DDW and then at least ten loop volumes of the sample. Subsequent repetitive injections of the same sample required only five loop volumes (250 μL) of sample. Each glycan sample was typically run five or six times in the case of oligosaccharides released by PNGase F digestion (except for three times for the polyclonal IgGs), but only three times in the case of oligosaccharides released by hydrazinolysis. Each of the replicate analyses for the different sets of mAb and IgG samples were arranged so that they were performed on different days over several 6-month periods.

Data were collected using the Advanced Computer Interface Model II (full-control) and manually integrated using AI-450 Chromatography Software (v3.30). The peaks in each chromatogram were quantitated relative to the other peaks; absolute quantitation was not performed. The integration data were statistically analyzed as described (Section 2.9).

Oligosaccharide peaks in samples were identified by comparison of their retention times with those from glycan standard solutions, and by comparison with previous reports (Weitzhandler *et al.*, 1994; Rohrer *et al.*, 1995; McGuire *et al.*, 1996). The N-linked oligosaccharide standard sets for HPAEC-PAD (Section 2.7.2.2) were thawed. The three sets contained equimolar mixtures of 4 afucosyl biantennary glycans (10 nmol or 17.8 μg total), 4 core-fucosyl biantennary glycans (10 nmol or 19.3 μg total), and the former two sets combined (20 nmol or

37.1 μg total), respectively. Each 50-μL injection of a standard set contained 250 pmol of each standard glycan.

2.7.5 Analysis by MALDI-QqTOF-MS

2.7.5.1 Essentials of MALDI-TOF-MS

The two most successful methods for the production of large molecular ions are electrospray ionization (ESI) and matrix-assisted laser desorption/ ionization (MALDI). Both are 'soft' ionization modes which produce fairly stable molecular ion species and few fragment ions. The MALDI technique is particularly simple and quick (Karas & Hillenkamp, 1988; Hillenkamp *et al.*, 1991). Sample consumption in MALDI is minimal, but amounts in the femtomole to low picomole range are currently required for successful sample handling. The technique is reasonably tolerant of the presence of buffer salts and other additives, although excessive amounts may cause signal suppression.

To obtain a spectrum, the sample is first mixed in solution with a large excess of a suitable UV-absorbing matrix. One of the most effective matrix materials for neutral underivatized oligosaccharides is 2,5-dihydroxybenzoic acid (DHB), particularly when used as the dominant constituent of a mixed matrix (Mohr *et al.*, 1995; Harvey, 1996; Papac *et al.*, 1997; Harvey *et al.*, 1998). For oligosaccharides that contain sialic acid, or are otherwise charged due to the presence of phosphate or sulfate, 2',4',6'-trihydroxyacetophenone (THAP) with negative-ion detection is extremely effective (Papac *et al.*, 1996, 1997). The sample/matrix mixture is allowed to co-crystallize, and the dried target is irradiated with 10-30 pulses of laser light; a nitrogen laser operating at 337 nm (UV) is frequently used. Mass separation usually employs a time-of-flight (TOF) system. In a TOF mass analyzer, ions are separated by their mass-to-charge (m/z) ratio. A group of ions is accelerated to a fixed kinetic energy by an electrical potential of up to 30 kV. The velocity of the ions is characteristic of the

m/z of each particular ion species. The ions are then permitted to pass through a field-free region where they separate into a series of spatially discrete individual ion packets. Each ion packet travels with a velocity inversely proportional to its m/z, and arrives at the detector at the end of the field-free region with less massive ion packets arriving faster than more massive ion packets. The detector generates a signal as each ion packet arrives. The spectra from the multiple laser pulses are averaged. Mass accuracies for oligosaccharides using a TOF-MS can be as high as 0.1% (0.01% with internal standards). The application of an ion mirror analyzer, rather than linear TOF, increases resolution and mass accuracy to 0.01% or better, even without an internal standard (Costello *et al.*, 1996; Harvey *et al.*, 1998).

While glycoproteins generally give abundant $[M+H]^+$ ions accompanied by lower amounts of doubly-charged ions, oligosaccharides give peaks mainly due to both singly-charged $[M+H]^+$ and $[M+Na]^+$ ions (Harvey, 1996; Harvey *et al.*, 1998). While sodiated $[M+Na]^+$ molecular ions predominate in positive-ion mode, deprotonated $[M-H]^-$ molecular ions are most abundant in negative-ion mode. Often positive- and negative-ion modes are compared to determine the presence of phosphorylated, sulfated, or sialylated oligosaccharides (Costello *et al.*, 1996). However, derivatization with PMP (Section 2.7.5.3) enhances the ionization efficiences of neutral glycans and augments positive-ion production of sialylated species (Saba *et al.*, 1999).

Sodiated molecular ions are preferable to protonated molecular ions in the determination of the molecular masses of oligosaccharides. Sodiated ions require more internal energy to fragment than protonated ions, and remain intact while protonated ions are dissociated, complicating the spectra with fragments. However, the oligosaccharide molecular ions still tell us little more about the their specific structures than their masses. Also, the type of hexose (Man or Gal) or hexosamine (GlcNAc or GalNAc) can only be assumed based

on knowledge of N-linked glycan structure, and cannot be determined solely by this method (Costello *et al.*, 1996). However, due to the fact that only a limited subset of all the oligosaccharide structures possible are actually used by cells, molecular mass allows for some assumptions regarding these structures.

2.7.5.2 MALDI-QqTOF-MS system

The MALDI-TOF system used in this work is a tandem quadrupole-TOF instrument using orthogonal ion-injection techniques, and was developed in the TOF Lab of the Department of Physics at the University of Manitoba (Loboda *et al.*, 2000). The MALDI-QqTOF-MS is equipped with an electrostatic ion mirror for state-of-the-art mass resolution (Figure 2-9). Mass accuracy in the range of 10 ppm (0.001%) and femtomole sensitivity are attainable.

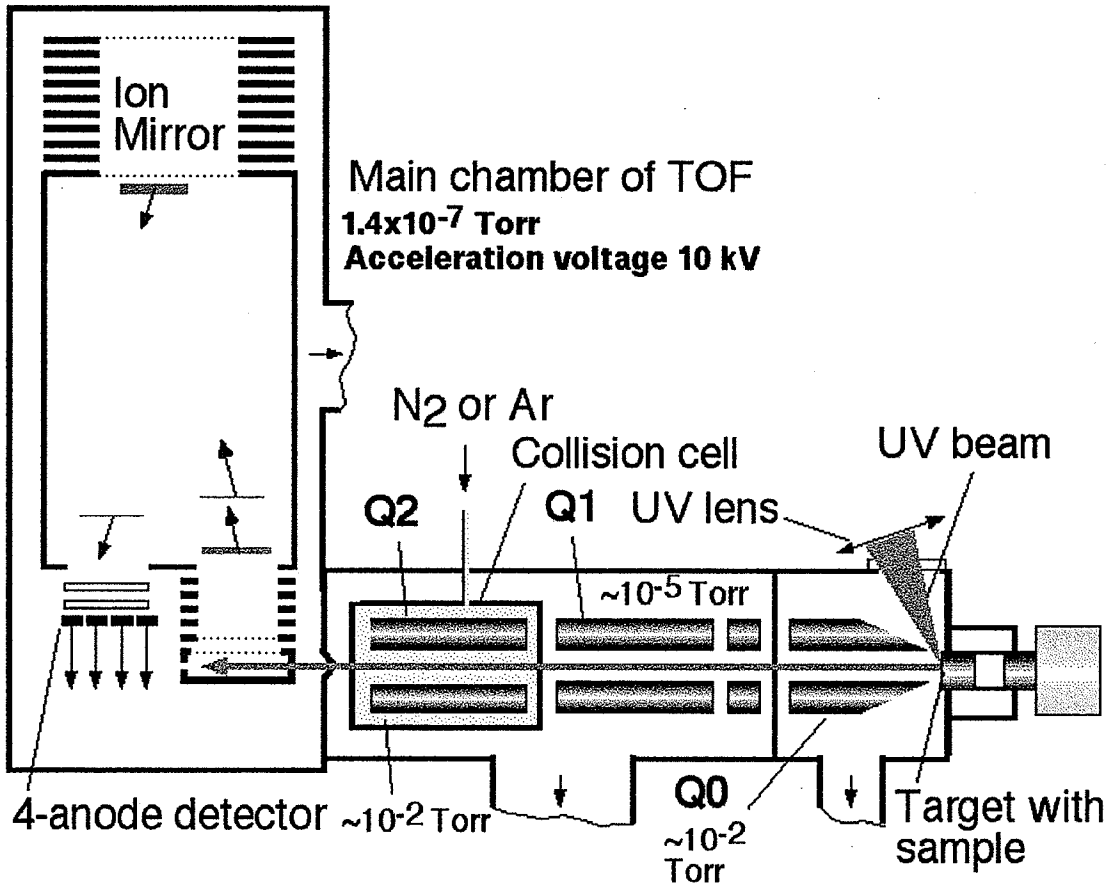

Figure 2-9. Schematic representation of MALDI-QqTOF-MS.

2.7.5.3 Labelling

It is most practical to conduct the analysis of all glycans under investigation in the same polarity. This is particulary true for the mixed populations of neutral and acidic oligosaccharides removed from glycoproteins. While negative-ion mode logically offers better sensitivity than positive-ion mode for native sialyl oligosaccharides, asialyl oligosaccharides remain more sensitive under positive-ion mode conditions owing to the presence of *N*-acetylated residues. For this reason, the oligosaccharides were labelled with 1-phenyl-3-methyl-5-pyrazolone (PMP) (Figure 2-10). The PMP-labelling reaction is rapid with quantitative yields and simple cleanup (Honda *et al.*, 1989, 1991; Fu & O'Neill, 1995; Shen & Perreault, 1998). It safely prevents desialylation of sialylated glycans, which is not always the case with other labelling reactions. The labelling is stoichiometric (2:1), and the *bis*-PMP-labelled glycans yield enhanced positive-ion mode sensitivity relative to unlabelled glycans, particularly of sialylated species (Shen & Perreault, 1998, 1999; Saba *et al.*, 1999, 2001). The derivatives also produce more predictable cleavage fragment patterns.

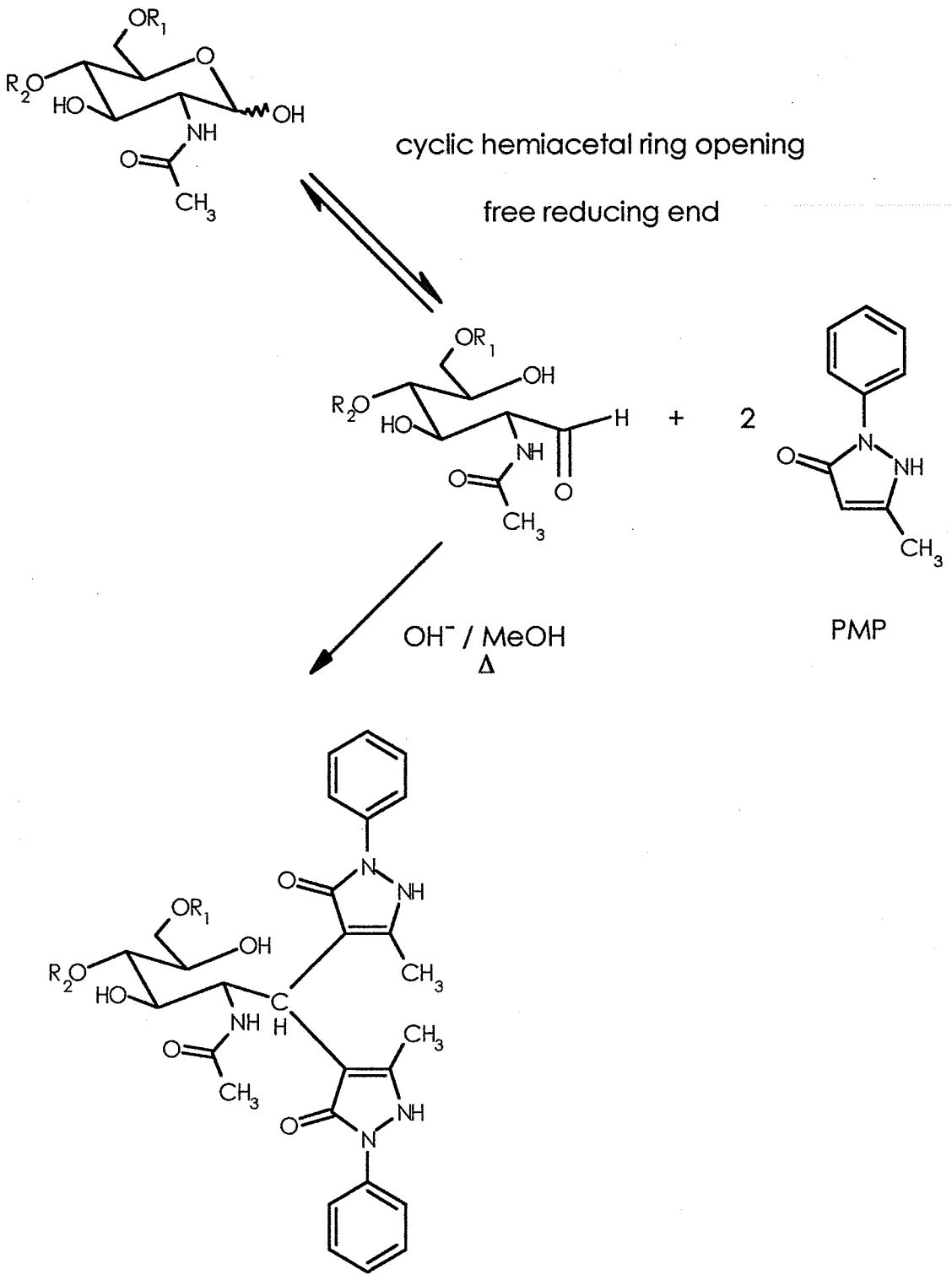

Figure 2-10. Structure of PMP and PMP-labelling scheme.

2.7.5.4 Monoisotopic masses of the monosaccharides and PMP label

The monoisotopic molecular masses of the PMP-labelled standard and sample N-linked oligosaccharides are calculated by considering the mass contribution of each constituent monosaccharide residue and the *bis*-PMP label (Table 2-3).

Table 2-3. Monosaccharide and PMP mass contribution to N-linked glycans.

General description	Specific description	Monoisotopic molecular mass	Monoisotopic residue mass
deoxyhexose	Fuc	164.0681	146.0576
hexose	Man, Gal	180.0630	162.0525
N-acetylhexosamine	GlcNAc	221.0895	203.0790
sialic acid	Neu5Ac	309.1054	291.0949
sialic acid	Neu5Gc	325.1003	307.0898
PMP x 2	*bis*-PMP	348.1582	330.1477

The monoisotopic masses are based on the following atomic masses of the most abundant isotope of the elements:

C=12.0000 (98.90%), H=1.0078 (99.99%), O=15.9949 (99.76%), N=14.0031 (99.63%), H_2O=18.0105, Na=22.9898 (100%)

Oligosaccharide molecular masses are calculated by adding the appropriate residue masses together with the mass of water for a free reducing end. Protonated $[M+H]^+$ molecular ion masses are obtained by further adding the mass of hydrogen. Sodiated $[M+Na^+]^+$ molecular ion masses are obtained by adding the mass of sodium instead of hydrogen.

2.7.5.5 MALDI-QqTOF-MS protocol

2.7.5.5.1 PMP-labelling

N-linked glycans removed by PNGase F digestion from 5-mg samples of each of the mAb preparations from the first set of chemostat cultures (and also the bovine and human polyclonal IgGs) were derivatized with PMP. Tubes containing mixed glycans (70 nmol or 125 μg total) from each mAb or polyclonal IgG sample were dissolved in 10 μL of 0.3 M NaOH in microcentrifuge tubes. To each tube 10 μL of 0.5 M PMP in methanol was added. The tubes were mixed and briefly centrifuged to ensure homogeneity. The solutions were incubated at 70 °C for 30 min. After being allowed to cool to ambient temperature, the solutions were neutralized by the addition of 10 μL of 0.3 M HCl. The solutions were diluted with 500 μL of DDW, and 1 mL of chloroform was added to extract the unreacted PMP. The tubes were mixed and briefly centrifuged to enhance phase separation. The upper organic phase was discarded and the lower aqueous phase was retained. Two more extractions with 1 mL of chloroform were performed. The lower aqueous phases (approximately 530 μL total) were not dialyzed or filtered prior to lyophilization. After lyophilization to a viscid gel, the samples were frozen at -20 °C.

Three sets of N-linked oligosaccharide standards (Section 2.7.2.3) were derivatized with PMP and analyzed by MALDI-QqTOF-MS. The three sets contained equimolar mixtures of 4 neutral biantennary glycans (4 nmol or 6.2 μg total), 4 sialyl biantennary glycans (4 nmol or 8.6 μg total), and the former two sets combined (8 nmol or 14.8 μg total), respectively. Each of the three sets was dissolved in 10 μL of 0.3 M NaOH in microcentrifuge tubes and derivatized as described.

2.7.5.5.2 MALDI-QqTOF-MS experimental

The PMP-labelled oligosaccharides from samples or standards were dissolved in 50% (v/v) acetonitrile to 10^{-4} M. A 0.5-μL drop of sample solution containing approximately 50 pmol of total oligosaccharides was spotted onto a polished stainless steel target and allowed to dry at ambient temperature. A 0.5-μL drop of matrix solution (0.5 M DHB, 50% (v/v) acetonitrile, 0.1% (v/v) formic acid) was added and the solvent allowed to evaporate. The addition of a small amount of formic acid facilitates protonation of the molecular ions. Finally, the crystals were redissolved in a 1-μL drop of absolute ethanol and allowed to dry.

The spectra were acquired by MALDI-QqTOF-MS operating in positive-ion mode. The samples were irradiated with a nitrogen laser (337 nm) at a laser power just above that needed to obtain a signal. Each analysis represents a total of approximately 10 shots. An accelerating potential of 10 kV was used. The mass analyzer was externally calibrated using a mixture of peptide standards. The target was rinsed well with DDW and dried at ambient temperature between samples.

The acquired spectra were mass-analyzed using Tofma 99.6 (2k.01.05) proprietary software developed in the TOF Lab of the Department of Physics at the University of Manitoba.

2.8 Galactosyltransferase assay

2.8.1 Essentials of galactosyltransferase assays

UDP-galactose: *N*-acetylglucosaminyl β1,4-galactosyltransferase (β1,4-GalT) catalyzes the transfer of Gal from UDP-Gal, the nucleotide sugar donor, to GlcNAc in a glycoprotein acceptor sugar, or to free GlcNAc (Figure 2-11).

The β1,4-GalT activity of cellular protein from the supernatant of a cell homogenate (*i.e.* a cell lysate) can be determined by measuring the

radioactivity transferred from the tritiated UDP-^{3}H-Gal sugar donor to the acceptor GlcNAc (Brew *et al.*, 1968; Khatra *et al.*, 1974; Sichel *et al.*, 1990; Furukawa *et al.*, 1990). Separation of the unreacted and negatively-charged UDP-^{3}H-Gal substrate from the ^{3}H-labelled LacNAc neutral reaction product is accomplished by simply passing the reaction mixture over an anion-exchange resin. The eluate obtained by washing the column with water is collected directly in a scintillation vial. The radioactivity in the vial is proportional to the amount of ^{3}H-Gal transferred, and thus the enzyme activity. The radioactive β-decay results in excitation of the scintillation fluid and proportional photon emission, which is detected by a spectrophotometer. The major advantages of this technique compared to other β1,4-GalT assays are that it is simple, quick, and inexpensive.

The β1,4-GalT enzyme has an absolute requirement for the Mn^{2+} ion (Fraser & Mookerjea, 1976), which facilitates the reaction as a cofactor by complexing with the diphosphate in free and β1,4-GalT-bound UDP-Gal (Khatra *et al.*, 1974). It assists the release of UDP as MnUDP. Both UDP-Gal and MnUDP-Gal are bound by β1,4-GalT, but only MnUDP is released – not UDP itself. Ethylenediaminetetraacetic acid (EDTA) chelates Mn^{2+} and can be used to effectively halt the reaction by disabling the recycling of β1,4-GalT.

It has been found that 0.5% (w/v) Triton X-100 (a nonionic detergent) and 0.2 mg/mL BSA in the reaction solution each activated β1,4-GalT by up to 500% (Khatra *et al.*, 1974). Both effects are not fully understood but are likely due to increased solubilization from membranes, and protection from denaturation or aggregation (Khatra *et al.*, 1974; Fraser & Mookerjea, 1976). BSA may also protect against non-serine proteases and serine-proteases that escape inhibition by PMSF.

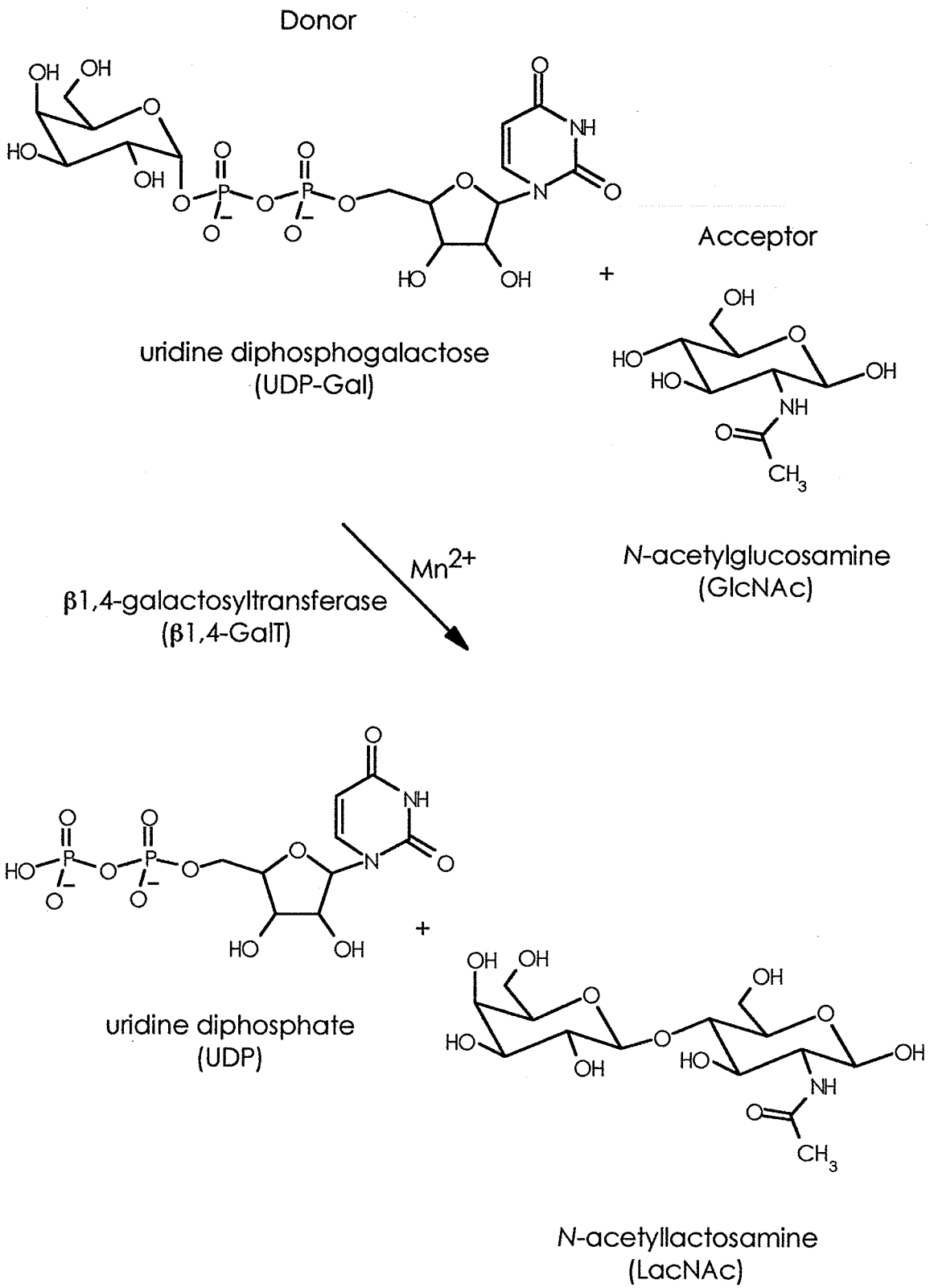

Figure 2-11. Transfer of Gal to GlcNAc by β1,4-GalT.

2.8.2 Galactosyltransferase assay protocol

The β1,4-GalT activities of CC9C10 cellular protein from the third set of chemostat cultures were determined. The nucleotide sugar donor was 50 mCi/μmol UDP-[4,5-^{3}H(N)-Gal] (500 μL at 0.1mCi/mL) (NEN, Boston, MA, USA). The reaction solution consisted of 20 μL of 100 mM $MnCl_2$, 40 μL of 100 mM GlcNAc, 10 μL of 2 μM (0.1mCi/mL) UDP-^{3}H-Gal, and 4 μL of 10 mg/mL BSA. The reaction solution was not incubated prior to addition of cellular protein. Protein from cell lysates (Section 2.4.4) was determined by the BCA assay (Section 2.2.5.2) and a volume (approximately 10-20 μL) of cell lysate equivalent to 200 μg of cellular protein was added. The required volume (approximately 105-115 μL) of lysis buffer (Section 2.4.4) was added to bring the total volume to 200 μL. Final concentrations in the reaction solution were 10 mM $MnCl_2$, 20 mM GlcNAc, 0.1 μM (1μCi) UDP-^{3}H-Gal, 0.2 mg/mL BSA, and 1 mg/mL (200 μg) protein-equivalent CC9C10 cell lysate in approximately 6.25 mM Tris, 93.75 mM NaCl, 1.25 mM PMSF, 0.625% (w/v) Triton X-100, pH 7.4 with HCl.

All tubes were kept on ice until the addition of the lysis buffer and cell lysate, at which point they were mixed and briefly centrifuged to ensure homogeneity, then transferred to 37 °C. The β1,4-GalT assays were incubated for 20 min.

For the assays, conditions were established such that the product formation was linear with respect to both time and the amount of enzyme protein (*i.e.* cell lysate) used. Enzyme activities resulting from endogenous acceptors (bound or free GlcNAc, and to a lesser extent, free Glc) were determined using controls where exogenous acceptor was omitted. These values were subtracted from the total values. These same controls also corrected for background radiation and the production of ^{3}H-Gal from nonspecific hydrolysis of UDP-^{3}H-Gal. For each sample, two assay tubes and one control tube without exogenous acceptor were used.

At time intervals (0, 5, 10, 15, and 20 min), two 10-μL samples of each reaction solution and the respective control were removed immediately and placed into tubes containing 30 μL of ice-cold 100 mM EDTA, stopping the reaction. Ice-cold DDW (0.5 mL) was added to each of the collected samples, which were kept on ice until all samples were obtained.

Anion-exchange columns were prepared by packing disposable polypropylene Poly-Prep columns (Bio-Rad) with 2 mL of AG 1-X8 resin (Bio-Rad) (50-100 mesh, Cl^- form). The columns were washed twice with 4 mL of DDW and plugged until needed. When ready, the terminated reaction solutions were transferred onto the unplugged anion-exchange columns. The sample tubes were washed twice with 0.5 mL of DDW, and the washes added to the respective columns, allowing the solution above the bed to enter the column each time. The eluate from each column (approximately 1.54 mL total) was collected into a 20-mL translucent polyethylene scintillation vial (Fisher Scientific) and capped.

To each vial was added 15 mL of EcoLume scintillation fluid (ICN Biomedicals, Costa Mesa, CA, USA). The vials were counted on a RackBeta II Model 1215 liquid scintillation spectrophotometer (LKB-Wallac, Turku, Finland) with the channel gate set to 8-130 for ^3H. The corrected radioactivity was obtained by subtracting the value of the respective controls from the mean of those of the assay tubes. The counts-per-minute (cpm) was converted to disintegrations-per-minute (dpm). The efficiency of scintillation counting with these methods was determined by counting 5 μL of 0.1 mCi/mL of the UDP-^3H-Gal (in duplicate). With an average 6.39% count efficiency, a measured radioactivity of 1000 cpm corresponded to 15,650 dpm.

The specific β1,4-GalT activity of the cellular protein in each cell lysate was determined from the slope of a best-line plot of the corrected cpm versus time. These values were converted into specific activities using the cpm-dpm

count efficiency (6.39%) and the specific radioactivity of the UDP-^{3}H-Gal donor (50 mCi/μmol).

2.9 Statistical analyses

The quantitative data for the FACE, HPAEC-PAD, and β1,4-GalT experiments were treated statistically. The means of the samples were calculated using the equation for sample mean:

$$\bar{x} = \sum \frac{x_i}{n}$$

The standard deviations of the sample means were determined using the equation for sample standard deviation:

$$s = \sqrt{\sum \frac{(x_i - \bar{x})^2}{n-1}}$$

The slopes and standard errors of the best-fit straight lines for the β1,4-GalT data were determined using the sum of least squares method by regression analysis.

Chapter 3 – Results

3.1 Size-exclusion chromatography

The purities of the mAb preparations purified by Protein A-affinity chromatography were confirmed by running a sample of each mAb on a BioGel P-300 size-exclusion column. Each mAb chromatogram indicated a single peak of approximately 156 kD immediately following the void volume (Figure 3-1). The absence of further prominences showed there were no contaminating proteins and verified the purity of the mAb preparations. A similar result was obtained from the chromatogram of the bovine polyclonal IgG standard, which showed a single peak of approximately 158 kD immediately following the void volume.

3.2 SDS-PAGE

The location of N-linked glycans and the extent of enzymatic deglycosylation were examined by SDS-PAGE under non-reducing and reducing conditions. Under non-reducing conditions (Figure 3-2a) a single band of approximately 156 kD, representing the intact mAb, was observed for each DO concentration. The absence of multiple bands at approximately this weight due to possible mAb glycoforms is not surprising, since the difference in weight caused by the presence or absence of one or two monosaccharide residues is negligible compared to the total weight of the mAb. Deglycosylation of the mAb resulted in a slight molecular weight reduction to a single band of approximately 152 kD in all cases.

Figure 3-1. Size-exclusion chromatography of bovine IgG and murine mAb. Bio-Gel P-300 elution profiles for bovine polyclonal IgG and the murine mAb. Each of the chromatogram represents 10 mg of sample.

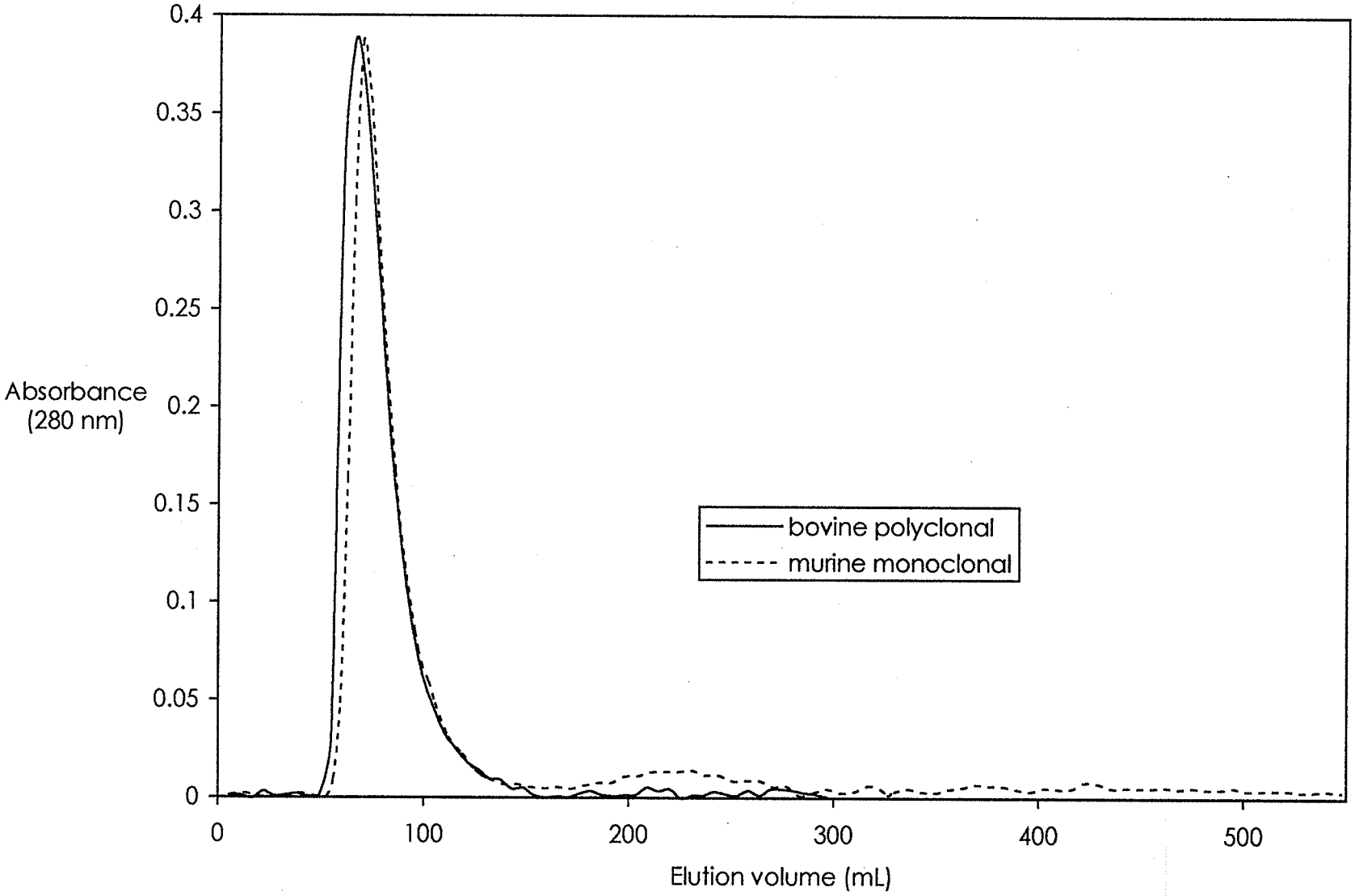
0.4
0.35
0.3
0.25
0.2
0.15
0.1
0.05
0
Absorbance
(280 nm)
0
100
200
300
400
500
Elution volume (mL)
bovine polyclonal
murine monoclonal

Under reducing conditions (Figure 3-2b), two bands of approximately 52 kD and 26 kD with unequal intensities were observed, corresponding to the heavy (γ) and light (κ) chains of the mAb, respectively. Molecular weight reduction due to deglycosylation was observed only with the heavy chains (50 kD), indicating that the glycan resides on these chains, and that there is very little or no N-linked oligosaccharides associated with the light chains.

The highly hydrophilic glycans of glycoproteins extend over the protein surface and result in reduced electrostatic binding of SDS. This lowers the protein mobility during electrophoresis disproportionally, yielding artifactually high molecular weights (Hames, 1990; Shi & Jackowski, 1998). Therefore, SDS-PAGE may often be used to quantify the occupancy of N-glycosylation sites. Glycoproteins can in some cases be fractionated into distinct bands on the basis of differences in the number of N-linked oligosaccharides associated with each band (Arvieux *et al.*, 1986; Alexander & Elder, 1989). The absence of multiple bands before PNGase F digestion implied that an equal number of N-glycosylation sites were occupied in all mAbs; the absence of multiple bands after PNGase F digestion confirmed the complete removal of N-linked oligosaccharides. The absence of other bands in the gels corroborated the results of size-exclusion chromatography and the purity of the preparations.

Figure 3-2. SDS-PAGE analysis of the first set of mAbs. Coomassie blue-stained samples of mAbs produced in 10, 50, and 100% DO in the LH bioreactor (first set) before (–) and after (+) PNGase F digestion. (a) 6% non-reducing gel. Each lane was loaded with 10 μg of mAb. Note the small decreases in molecular weight of the mAb after digestion. (b) 10% reducing gel. Each lane was loaded with 20 μg of mAb. Note the small but discernable decreases in molecular weight after PNGase F digestion of the heavy chain but not the light chain.

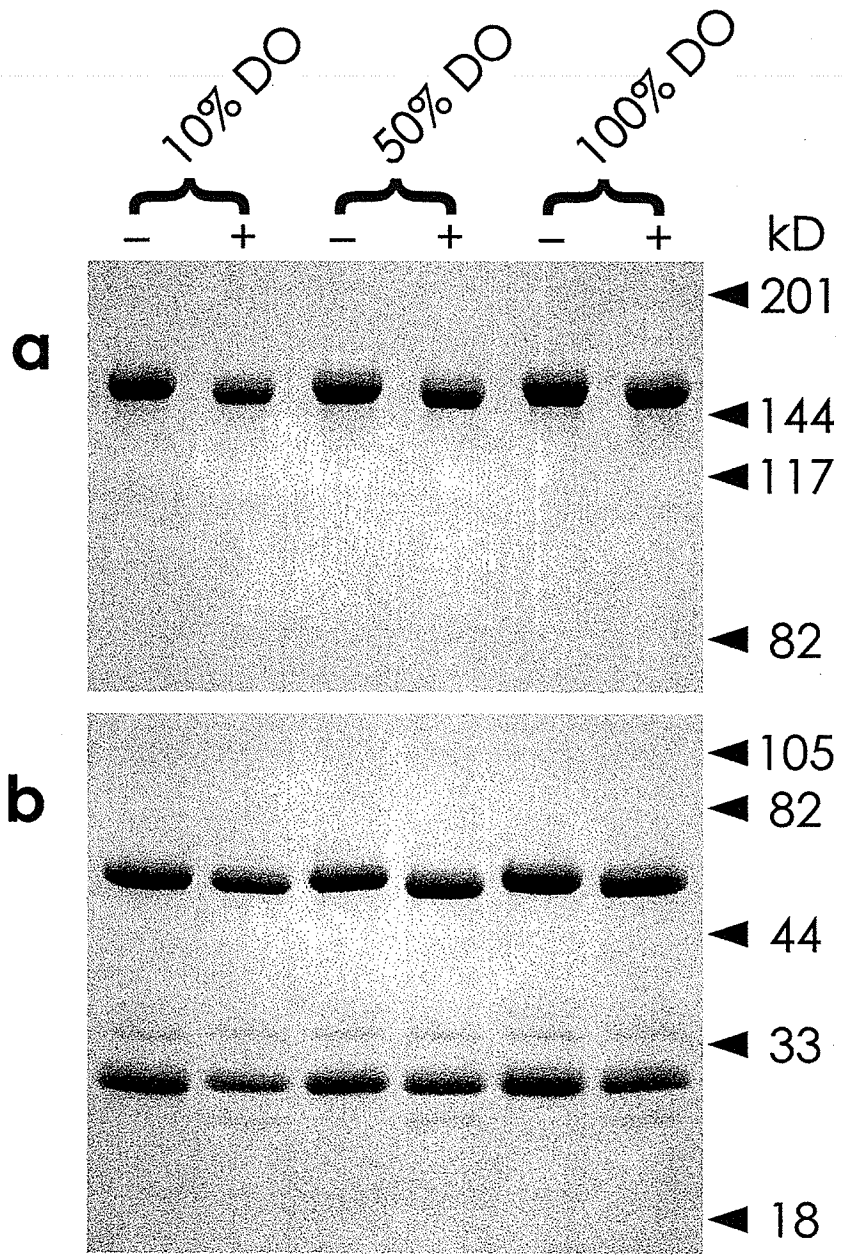
10% DO
50% DO
100% DO
– + – + – +
kD
a
201
144
117
82
b
105
82
44
33
18

It has been previously shown that no carbohydrate (O- or N-linked) is associated with the light chains of this antibody (Barnabé & Butler, 1998; Barnabé, 1998). Unstained mAb was transferred by (Western) electroblotting of reducing polyacrylamide gels onto nitrocelluose sheets (Towbin *et al.*, 1979). The carbohydrate was specifically stained by mild periodate oxidation of vicinal hydroxyl groups to yield aldehyde groups, biotinylation of the aldehydes with biotin-hydrazide, ligation to streptavidin-alkaline phosphatase, and visualization with a substrate that is chromogenic and precipitates upon dephosphorylation (Bayer *et al.*, 1990a, 1990b). Because the light chains were not glycosylated, and to minimize the potential for degradation of the heavy chain oligosaccharides in the necessary purification steps, it was decided not to separate the heavy and light chains of the mAbs prior to the enzymatic and chemical deglycosylation procedures.

Most of the heavy chain glycosylation was expected to be at Asn-297 in the C_H2 domain of the Fc, although heavy chain glycosylation in the Fab region could not be excluded from consideration.

Since the Coomassie stain is quantitative and linear to 20 μg for non-reduced IgG and 10 μg for reduced IgG, their relative quantitation is achievable (Hames, 1990; Birch *et al.*, 1995). Quantitative analysis was performed on the reducing SDS-PAGE gel as described (Section 2.7.3.3). The relative band intensities of the mAbs from 10, 50, and 100% DO before and after deglycosylation with PNGase F on denaturing SDS-PAGE were compared. Different proteins bind Coomassie blue to different extents, however the relative staining of IgG heavy and light chains is proportional to their weights (Birch *et al.*, 1995). The glycosylation of proteins interferes with the electrostatic and hydrophobic binding of the Coomassie stain in a manner similar to the inhibition of SDS-binding such that glycosylated variants are relatively less stained – and are underestimated compared to their non-glycosylated counterparts. Since

the Coomassie blue stain is non-stoichiometric to the number of molecules, it was expected that the larger heavy chains would be stained to a greater degree than the smaller light chains. The heavy chain is approximately twice as large as the light chain, thus the heavy-chain bands were predicted to be stained about twice as intensely as the light-chain bands. Image processing showed relative intensities of 55.5% for the heavy-chain bands and 45.5% for the light-chain bands before deglycosylation (Figure 3-3; Table 3-1), which is nearly a 1:1 staining ratio. After deglycosylation, the heavy-chain bands showed greater relative intensity (61.5%) compared to the light-chain bands (38.5%). This is closer to the assumed staining ratio of 2:1, and indicates that the presence of attached N-linked oligosaccharides inhibits staining of the heavy chains.

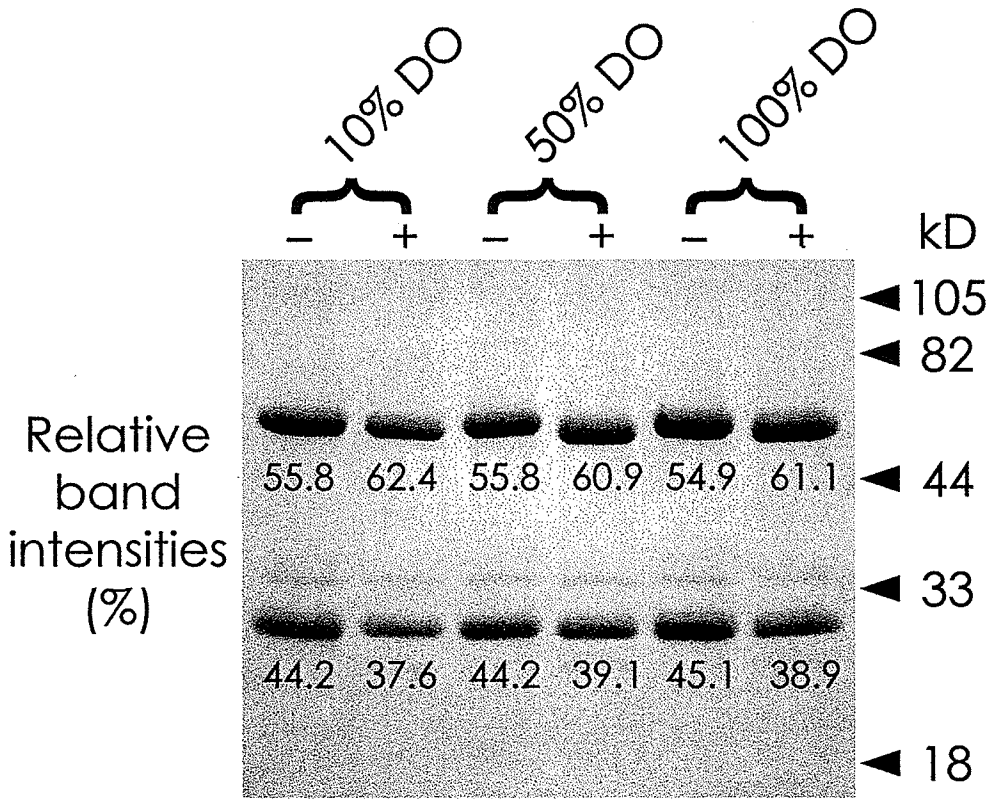

Figure 3-3. Relative band intensities from reducing SDS-PAGE.

Table 3-1. Relative band intensities from reducing SDS-PAGE. Intensities of the heavy- and light-chain bands before and after PNGase F digestion.

mAb preparation (*n*)[a]	Chain	Before	After
10% DO (2)	Heavy	55.8 ± 0.1	62.4 ± 0.1
	Light	44.2 ± 0.1	37.6 ± 0.1
50% DO (2)	Heavy	55.8 ± 0.3	60.9 ± 0.2
	Light	44.2 ± 0.3	39.1 ± 0.2
100% DO (2)	Heavy	54.9 ± 0.1	61.1 ± 0.1
	Light	45.1 ± 0.1	38.9 ± 0.1
Average	Heavy	55.5 ± 0.5	61.5 ± 0.8
	Light	45.5 ± 0.5	38.5 ± 0.8

Data are presented as the average relative band intensities (%) and standard deviation with (*n* -1) degrees of freedom.

[a] Denotes the number of quantitation measurements of a single SDS-PAGE experiment.

3.3 Glycosylation analysis

3.3.1 Bovine and human polyclonal IgG

3.3.1.1 HPAEC-PAD

Bovine and human polyclonal IgG were first examined to establish and verify the protocols and methods used for PNGase F deglycosylation and HPAEC-PAD analysis of released N-glycans. The results indicated that both polyclonal IgGs gave three main peaks of varying relative areas eluting at approximately 18.5, 21.0, and 23.5 min (Figure 3-4). These peaks were identified by the use of the standard glycan sets for HPAEC-PAD (Section 2.7.2.2) to correspond to structures 1-3 (Figure 3-5). They were core-fucosyl asialyl agalactosyl biantennary, core-fucosyl asialyl monogalactosyl biantennary, and core-fucosyl asialyl digalactosyl biantennary, respectively. The trace peaks eluting after peak 3 in the range of 25-30 min may have included structures resulting from the presence of a bisecting GlcNAc, or the lack of core-Fuc, in one or more of structures 1-3. Due to the comparative paucity of these peaks, their ultimate identification was not pursued by HPAEC-PAD.

There were also three groups of minor peaks eluting at about 47-51, 53-57, and 62-66 min. These peaks owed their delayed elution to their relative acidity as a result of monosialylation of the core-fucosyl biantennary chains. Two of the groups of peaks were a consequence of their different SA content; either Neu5Ac (47-51 min) or Neu5Gc (62-66 min), in α2,6-linkages and perhaps α2,3-linkages, to either one or the other, but not both, of the antennae of the core-fucosyl biantennary structures (Figure 3-5, structures 4a & 4b). These variations in monosialylation could yield up to four different monosialylated structures for each of the two sialic acids with minor differences in retention times in this HPAEC gradient. Compared to Neu5Ac, Neu5Gc has one additional hydroxyl group available for deprotonation to the oxonium ion, resulting in later elution. The sialic acids of glycoproteins are usually Neu5Ac and, less commonly Neu5Gc.

However, upwards of 30 neuraminic acid derivatives are known, and it is likely that traces of these sialic acids also exist in glycoproteins. Note that bovine IgG showed no sialylation with Neu5Ac, and that human IgG sialylation was almost entirely Neu5Ac with just a very small contribution from Neu5Gc. Additional structures in these regions may have resulted from a lack of core fucosylation, or if the antenna not containing a SA were also devoid of Gal. The third group of peaks (53-57 min) may have been variants of structure 4a containing a bisecting GlcNAc. Again, because these peaks represented only a small measure of the total oligosaccharide content, their definite assignment was not endeavored.

The identification of the major neutral oligosaccharides and the sialylated derivatives from polyclonal IgG (Table 3-2), were in excellent agreement with results previously reported (Weitzhandler *et al.*, 1994), which used the same approaches of PNGase F deglycosylation and HPAEC-PAD analysis. There was remarkable agreement in the quantitative HPAEC-PAD results for the relative peak areas of the major neutral oligosaccharides with those of the previous report. In this work and the previous one, the human IgG was derived from different batches of pooled sera from different years and the results substantiate that while differences between individuals may occur, the ratio of IgG glycoforms varies little in the general human population. The protocols and methods used in this work for the PNGase F deglycosylation and HPAEC-PAD analysis of N-glycans were thus validated.

Figure 3-4. HPAEC-PAD analysis of bovine and human IgG. Representative chromatograms of the PNGase F-released N-linked oligosaccharides (2 nmol total) from 144 μg of bovine and human polyclonal IgG. Three major peaks are evident with several minor peaks. Peaks were identified by the use of three sets of standards containing 250 pmol each of four afucosyl (Set 1), four core-fucosyl (Set 2), and eight mixed afucosyl and core-fucosyl (Set 3) N-linked oligosaccharides (not shown). Peak 1 is core-fucosyl asialyl agalactosyl biantennary (C2-004301) and peak 3 is core-fucosyl asialyl digalactosyl biantennary (C2-024301). Peak 2 is inferred to be core-fucosyl asialyl monogalactosyl biantennary (C2-014301). Peaks 4a and 4b are core-fucosyl monosialyl biantennary (C2-124301) with the SA being either Neu5Ac or Neu5Gc, respectively. Note that the bovine IgG has no Neu5Ac-sialylation and that the human IgG sialylation is almost entirely Neu5Ac with just a very small contribution from Neu5Gc. Peaks 4a and 4b may include a small contribution of the respective afucosyl monosialyl biantennary species (C2-124300). There may be some contribution to peak 2 by asialyl agalactosyl biantennary (C2-004300) and to peak 3 by asialyl monogalactosyl biantennary (C2-014300). The small peaks eluting immediately after peak 3 may include asialyl digalactosyl biantennary (C2-024300). Structures for the identified peaks are shown in Figure 3-5.

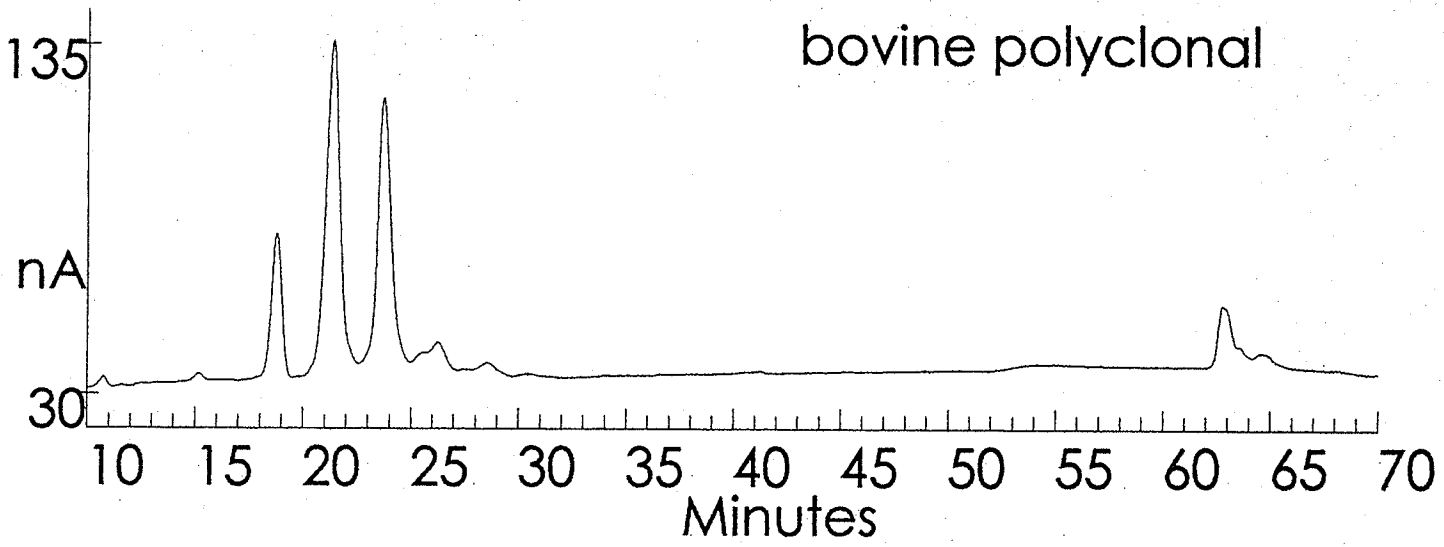
bovine polyclonal
135
nA
30
10 15 20 25 30 35 40 45 50 55 60 65 70
Minutes

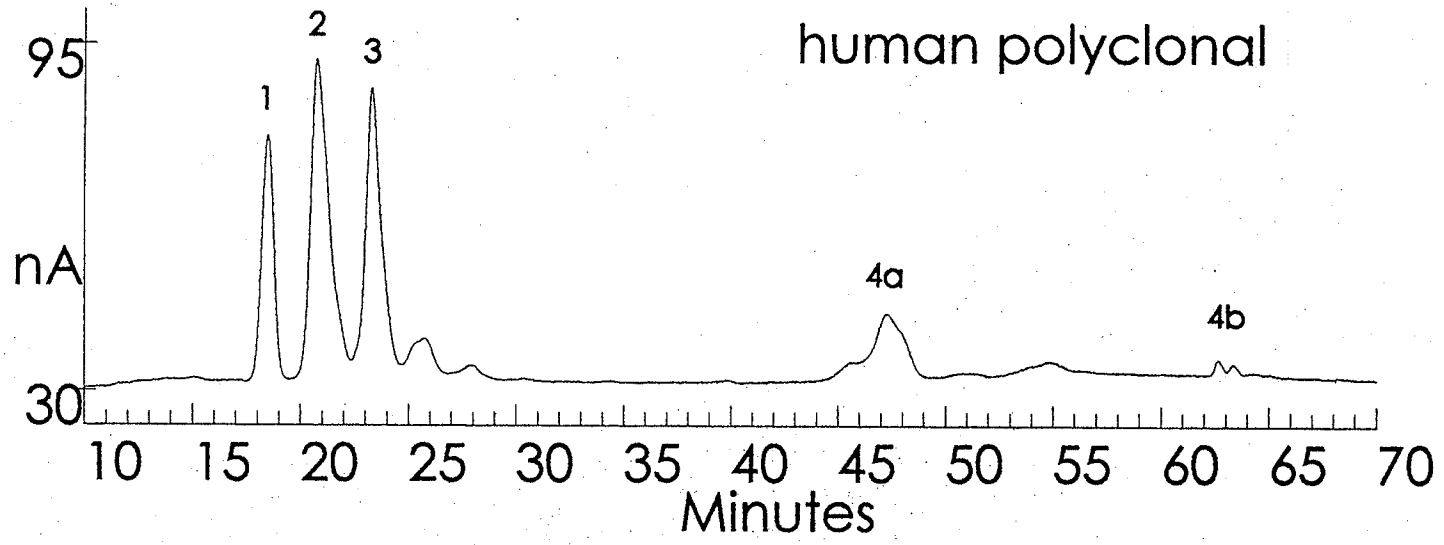
human polyclonal
95
nA
30
1
2
3
4a
4b
10 15 20 25 30 35 40 45 50 55 60 65 70
Minutes

Figure 3-5. Identified polyclonal IgG and mAb N-linked glycans. The structure numbering corresponds to the peak numbering in HPAEC-PAD chromatograms (Figures 3-4, 3-7, 3-10, 3-11, & 3-15), the band numbering in FACE electrofluorograms (Figures 3-6, 3-9, & 3-14), and in the respective tables (Tables 3-2, 3-4, 3-5, 3-6, & 3-7) and graphs (Figures 3-8, 3-12, 3-13, & 3-16). Structures 1, 3, and 4a were determined by the use of standards; structures 2 and 4b by inference and comparison with previous reports (Weitzhandler *et al.*, 1994; Ashton *et al.*, 1995b; Lifely *et al.*, 1995; Rohrer *et al.*, 1995; Lines, 1996; McGuire *et al.*, 1996; Frears & Axford, 1997; Routier *et al.*, 1997; Sheeley *et al.*, 1997; Frears *et al.*, 1999) and the MALDI-QqTOF-MS results (Section 3.3.5). Structure 1, core-fucosyl asialyl agalactosyl biantennary (C2-004301); structure 2, core-fucosyl asialyl monogalactosyl biantennary (C2-014301); structure 3, core-fucosyl asialyl digalactosyl biantennary (C2-024301); structure 4a, core-fucosyl monosialyl (Neu5Ac) biantennary (C2-124301); structure 4b, core-fucosyl monosialyl (Neu5Gc) biantennary (C2-124301).

1

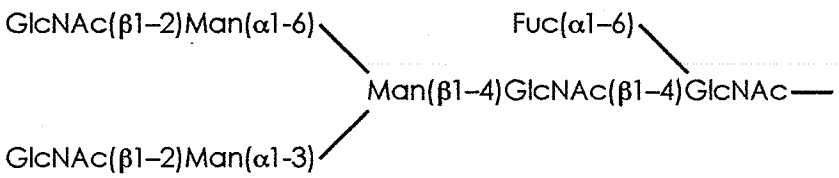
GlcNAc(β1–2)Man(α1-6)
Fuc(α1–6)
Man(β1–4)GlcNAc(β1–4)GlcNAc
GlcNAc(β1–2)Man(α1-3)

2

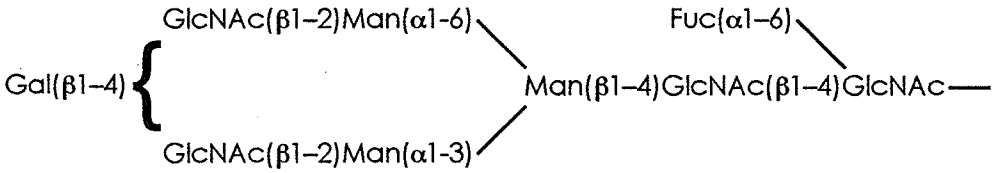
GlcNAc(β1–2)Man(α1-6)
Fuc(α1–6)
Gal(β1–4)
Man(β1–4)GlcNAc(β1–4)GlcNAc
GlcNAc(β1–2)Man(α1-3)

3

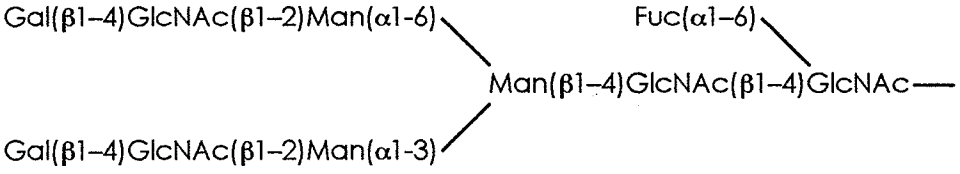
Gal(β1–4)GlcNAc(β1–2)Man(α1-6)
Fuc(α1–6)
Man(β1–4)GlcNAc(β1–4)GlcNAc
Gal(β1–4)GlcNAc(β1–2)Man(α1-3)

4a

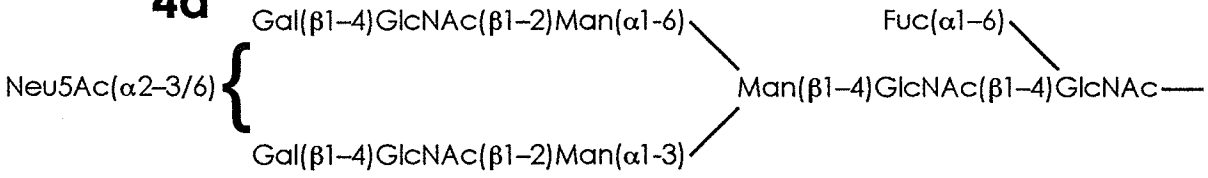
Gal(β1–4)GlcNAc(β1–2)Man(α1-6)
Fuc(α1–6)
Neu5Ac(α2–3/6)
Man(β1–4)GlcNAc(β1–4)GlcNAc
Gal(β1–4)GlcNAc(β1–2)Man(α1-3)

4b

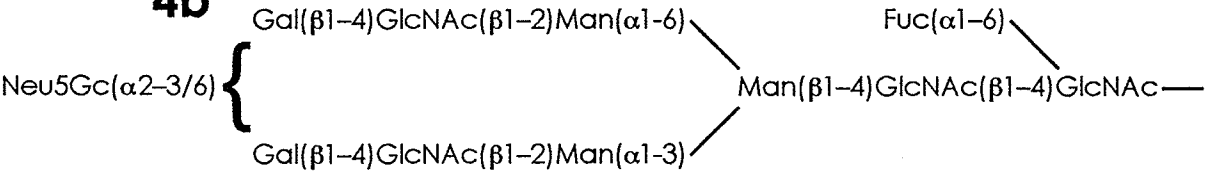
Gal(β1–4)GlcNAc(β1–2)Man(α1-6)
Fuc(α1–6)
Neu5Gc(α2–3/6)
Man(β1–4)GlcNAc(β1–4)GlcNAc
Gal(β1–4)GlcNAc(β1–2)Man(α1-3)

Table 3-2. Quantitative results for bovine and human polyclonal IgG. Relative peak areas of the major neutral oligosaccharides.

IgG preparation (*n*)[a]	Peak 1 C2-004301 core-fucosyl asialyl agalactosyl biantennary	Peak 2 C2-014301 core-fucosyl asialyl monogalactosyl biantennary	Peak 3 C2-024301 core-fucosyl asialyl digalactosyl biantennary
Polyclonal bovine (2)	14.6 ± 0.4	47.0 ± 0.3	38.4 ± 0.8
Polyclonal human (2)	21.3 ± 0.1	43.8 ± 0.2	34.9 ± 0.1
Polyclonal human (3)[b]	22.6 ± 0.6	42.7 ± 0.6	34.7 ± 1.2

Data are presented as the average relative peak areas (%) and standard deviation with (*n* -1) degrees of freedom.

[a] Denotes the number of separate HPAEC-PAD experiments.

[b] Calculated from Weitzhandler et al., 1994.

Comparison of the HPAEC-PAD results for bovine and human polyclonal IgG underscored the fact that there are interspecies variations in glycosylation of IgG. Not only does the glycoform ratio of the major neutral oligosaccharides vary between the two species, but so also does the predominant form of SA. Sialylation of bovine IgG was solely with Neu5Gc, while human sialylation was primarily with Neu5Ac and just traces of Neu5Gc. These results are in general agreement with the literature (Hamako *et al.*, 1993; Raju *et al.*, 2000). However, the Neu5Gc in human IgG is surprising since it is conventionally held that humans do not produce Neu5Gc. The nucleotide sugar donor CMP-Neu5Gc is formed biosynthetically from CMP-Neu5Ac (Muchmore *et al.*, 1989, 1997, 1998). Similar to α1,3-GalT, which is expressed in New World primates and many non-primate mammals, but not humans and Old World primates (Galili *et al.*, 1987, 1988; Galili, 1993), it appears that the hydroxylase responsible for the conversion of CMP-Neu5Ac to CMP-Neu5Gc is expressed in Old World primates but contains a deletion mutation in humans and is therefore inactive (Chou *et al.*, 1998; Irie *et al.*, 1998). Indeed, it has been stressed that evolutionary pressures must be considered in relating the diversity of oligosaccharide structures to biological function (Galili, 1993; Muchmore *et al.*, 1997, 1998; Chou *et al.*, 1998; Gagneux & Varki, 1999). Therefore, all Neu5Gc in human glycoproteins must come from 'leakage' through a related hydroxylase reaction, or from diet. In addition, the αGal and Neu5Gc epitopes are immunogenic in humans (Galili, 1989, 1993; Muchmore *et al.*, 1989, 1997; Varki, 1993; Chou *et al.*, 1998), and this must be considered in the production of glycosylated biological pharmaceuticals (Jenkins & Curling, 1994; Noguchi *et al.*, 1995).

3.3.2 Chemostat culture first set mAbs

Analyses of the glycans from the mAb produced in 10, 50, and 100% DO in the LH bioreactor was undertaken to determine the effect of DO concentration on the glycosylation of this mAb.

3.3.2.1 FACE

FACE was applied to separate and characterize the oligosaccharides released by PNGase F digestion and hydrazinolysis from the mAb preparations from the first set of cultures. The results illustrated a notable trend (Figure 3-6). The mAb produced in 10% DO (lanes b & c) displayed only two major bands with mobilities of approximately 6 and 7 GU (bands 1 & 2, respectively), with a third very faint band (band 3) of approximately 8 GU. Band 2 appeared to be a doublet. However, in 50% DO (lanes d & e) and 100% DO (lanes f & g), there were three major bands: bands 1 and 2, with band 2 again being a doublet, and band 3, which had increased significantly in intensity.

Based on the use of the standard glycan sets for FACE (Section 2.7.2.1), one of which was run in parallel in this gel (lane h), band 1 was identified as core-fucosyl asialyl agalactosyl biantennary, band 3 was core-fucosyl asialyl digalactosyl biantennary, and band 2 was intermediate between these two structures as core-fucosyl asialyl monogalactosyl biantennary (Figure 3-5). The doublets of band 2 were a result of galactosylation of either one or the other, but not both, of the antennae of the biantennary structure.

The band migrating at approximately 6.25 GU in 50 and 100% DO, but not 10% DO, was determined to be monosialyl core-fucosyl digalactosyl biantennary. The increase in intensity of this band in 50 and 100% DO cultures is consistent with the greater intensity of bands 2 (core-fucosyl asialyl monogalactosyl biantennary) and 3 (core-fucosyl asialyl digalactosyl biantennary). Similarly, this band is greatly diminished in intensity along with the

decrease of intensity of bands 2 and 3 in the 10% DO culture. This is to be expected, since Gal is required for the attachment of terminal SA.

The enzymatic (PNGase F) and chemical (hydrazinolysis) deglycosylation methods resulted in similar glycan profiles in FACE (Figure 3-6, compare lanes b & c, d & e, f & g). This indicated equivalent and quantitative deglycosylation employing the protocols in this report.

It was possible to resolve agalactosyl, monogalactosyl, and digalactosyl biantennary standard glycans with and without core-fucosylation, but it was more difficult to resolve these structures from some of their sialylated variants. There was little evidence for the presence of afucosyl versions of any of the identified structures in the sample glycans.

Our assignment of N-linked oligosaccharides, based on their relative mobility in FACE and co-migration with standards, is accordant with the monosaccharide residue contribution to oligosaccharide mobility (Hu, 1995; Starr *et al.*, 1996; Quintero *et al.*, 1998) and results previously found for these structures (Stack & Sullivan, 1992; Hu, 1995; Starr *et al.*, 1996; Quintero *et al.*, 1998) (Table 3-3).

The FACE profiles for mAb glycosylation in this work (Figures 3-6, 3-9, & 3-14) are congruent with published reports for polyclonal IgG glycosylation (MacGillivray *et al.*, 1995; Frears & Axford, 1997; Frears *et al.*, 1999; Martin *et al.*, 2001).

The bands in the FACE electrofluorogram were quantitated and compared to the HPAEC-PAD results (Section 3.3.2.3).

Figure 3-6. FACE analysis of the first set of mAbs. Electrofluorogram of the N-linked oligosaccharides (4 nmol total) released by PNGase F digestion (P) and hydrazinolysis (H) from 288 μg of mAb produced in 10, 50, and 100% DO in the LH bioreactor (first set). Lane a contains the glucose ladder with an arrow designating maltotetraose (GU=4). Three major bands (bands 1, 2, & 3) with mobilities of approximately 6, 7, and 8 GU, respectively, are evident in the samples with a minor band of about 6.25 GU. Note the enrichment of band 1 and depletion of band 3 in 10% DO, and the increase in intensity of the minor band in 50 and 100% DO. Lane h contains 300 pmol each of four neutral glycan standards (Set 1, from top to bottom): core-fucosyl asialyl digalactosyl biantennary (C2-024301), asialyl digalactosyl biantennary (C2-024300), core-fucosyl asialyl agalactosyl biantennary (C2-004301), and asialyl agalactosyl biantennary (C2-004300) chains. Therefore, band 1 is core-fucosyl asialyl agalactosyl biantennary and band 3 is core-fucosyl asialyl digalactosyl biantennary. Band 2 is inferred to be core-fucosyl asialyl monogalactosyl biantennary (C2-014301). The minor band was tentatively designated as core-fucosyl monosialyl biantennary (C2-124301), which was confirmed in subsequent FACE experiments. Structures for the identified bands are shown in Figure 3-5.

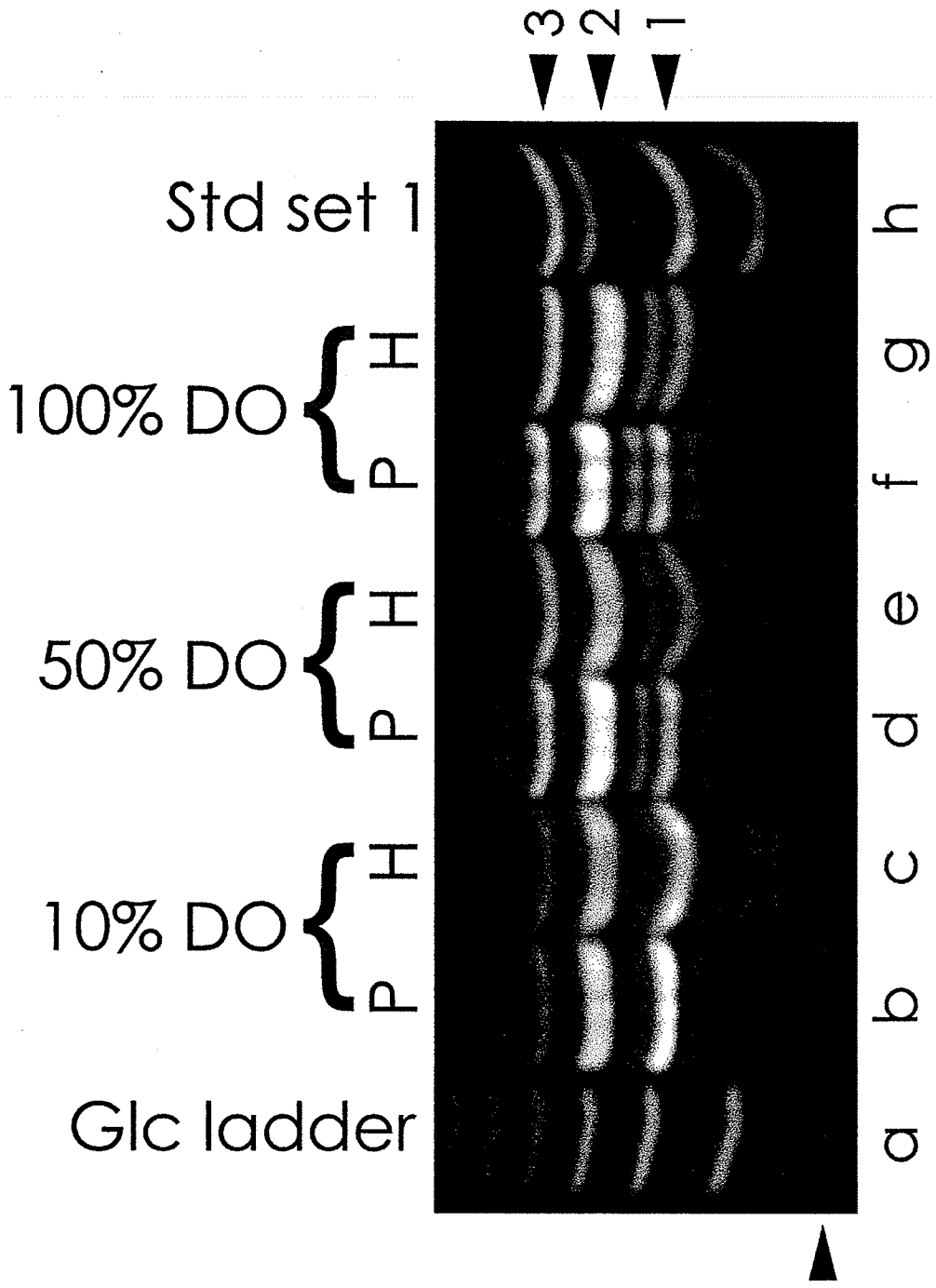
3
2
1
Std set 1
100% DO
H
P
50% DO
H
P
10% DO
H
P
Glc ladder
a
b
c
d
e
f
g
h

Table 3-3. Relative migration of ANTS-labelled N-glycans in FACE.

	Mobility in GU				
	Literature			This work	
Glycan code	Stack & Sullivan, 1992	Hu, 1995	Starr *et al.*, 1996	Standard N-glycans	Sample N-glycans
C2-004300	5.4	5.6	5.6 ± 0.5	5.25	5.25
C2-004301	6.1	6.2	6.2 ± 0.2	6.00	6.00
C2-014300	–	–	–	–	6.00
C2-014301	–	–	–	–	7.00
C2-024300	7.4	7.8	7.8 ± 0.2	7.50	7.50
C2-024301	8.1	8.5	8.5 ± 0.3	8.00	8.00
C2-124300	–	–	–	6.00	6.00
C2-124301	–	–	–	6.25	6.25
C2-224300	5.5	5.4	5.4 ± 0.3	4.75	4.75
C2-224301	5.8	5.7	5.7 ± 0.2	5.50	5.50

Structures for these oligosaccharides are shown in Figures 2-5 and 3-5.

Differences in oligosaccharide mobilities reflect small variations in the makeup of the PAGE gels employed – in terms of the exact percentages of acrylamide content, crosslinking, and other additives such as ethylene glycol; as well as other factors such as the precise composition and pH of buffers, *etc.*

3.3.2.2 HPAEC-PAD

The oligosaccharides released enzymatically and chemically from the mAb preparations from the first set of cultures were also examined by HPAEC-PAD.

The results of the HPAEC-PAD analyses of these mAb glycans were similar for those for bovine and human polyclonal IgG glycans and indicated three main peaks of varying relative areas eluting at approximately 18.5, 21.0, and 23.5 min (Figure 3-7). These peaks were identified by the use of the standard glycan sets for HPAEC-PAD (Section 2.7.2.2) to correspond to structures 1-3 (Figure 3-5) and to the bands 1-3 from FACE (Figure 3-6). They were core-fucosyl asialyl agalactosyl biantennary, core-fucosyl asialyl monogalactosyl biantennary, and core-fucosyl asialyl digalactosyl biantennary, respectively. The trace peaks at 25-30 min may have resulted from a lack of core fucosylation, the presence of a bisecting GlcNAc, which is unlikely in murine IgG Fc glycans (Mizuochi *et al.*, 1987; Hamako *et al.*, 1993; Raju *et al.*, 2000), or terminal α1,3Gal residues. The two groups of minor peaks eluting at about 47-51 and 62-66 min were monosialylated core-fucosyl biantennary chains. Again, the two groups of peaks were a consequence of their different sialic acid content; either Neu5Ac (47-51 min) or Neu5Gc (62-66 min), to either one or the other, but not both, of the antennae (Figure 3-5, structures 4a & 4b). The sialylation was predominantly Neu5Ac with a small contribution from Neu5Gc. The structures at 53-57 min may have been variants of structure 4a resulting from the presence of a bisecting GlcNAc. Again, due to the relatively small contribution by these minor peaks, their decisive identification was not pursued by HPAEC-PAD.

Figure 3-7. HPAEC-PAD analysis of the first set of mAbs. Representative chromatograms of the N-linked oligosaccharides (2 nmol total) released by (a) PNGase F digestion and (b) hydrazinolysis from 144 μg of mAb produced in 10, 50, and 100% DO in the LH bioreactor (first set). There were three major peaks (peaks 1, 2, & 3) with respective elution times of approximately 18.5, 21.0, and 23.5 min – and several minor peaks. Note the enrichment of peak 1 and depletion of peak 3 in 10% DO and the increase in peaks 4a and 4b with increases in peaks 2 and 3 in 50 and 100% DO. Peaks were identified by the use of three sets of standards containing 250 pmol each of four afucosyl (Set 1), four core-fucosyl (Set 2), and eight mixed (Set 3) N-linked oligosaccharides (not shown). Peak 1 is core-fucosyl asialyl agalactosyl biantennary (C2-004301) and peak 3 is core-fucosyl asialyl digalactosyl biantennary (C2-024301). Peak 2 is inferred to be core-fucosyl asialyl monogalactosyl biantennary (C2-014301). Peaks 4a and 4b are core-fucosyl monosialyl biantennary (C2-124301) with the SA being either Neu5Ac or Neu5Gc, respectively. Peaks 4a and 4b may include a small contribution of the respective afucosyl monosialyl biantennary species (C2-124300). There may be some contribution to peak 2 by asialyl agalactosyl biantennary (C2-004300) and to peak 3 by asialyl monogalactosyl biantennary (C2-014300). The small peaks eluting immediately after peak 3 may include asialyl digalactosyl biantennary (C2-024300). Structures for the identified peaks are shown in Figure 3-5.

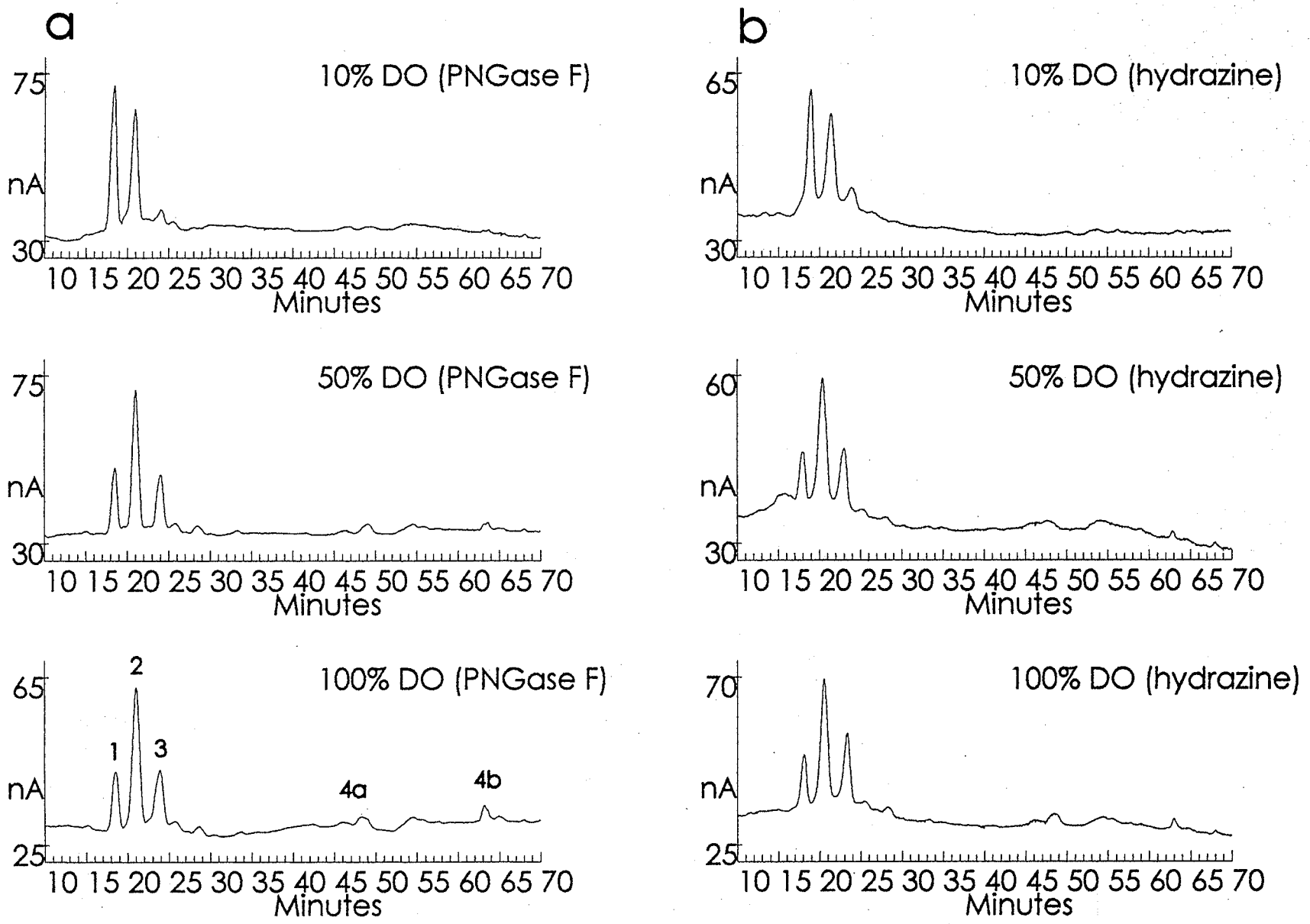
a
b
10% DO (PNGase F)
10% DO (hydrazine)
50% DO (PNGase F)
50% DO (hydrazine)
100% DO (PNGase F)
100% DO (hydrazine)
nA
Minutes
10 15 20 25 30 35 40 45 50 55 60 65 70
1
2
3
4a
4b

The results of analyses with HPAEC-PAD separation and detection of N-linked oligosaccharides removed by PNGase F digestion (Figure 3-7a) and hydrazinolysis (Figure 3-7b) from mAb preparations from 10, 50, and 100% DO presented a salient trend. In 10% DO only two main peaks were obtained, corresponding to core-fucosyl asialyl agalactosyl biantennary (peak 1) and core-fucosyl asialyl monogalactosyl biantennary (peak 2) chains. Peak 3, the core-fucosyl asialyl digalactosyl biantennary chain, was only a minor component, in agreement with the qualitative results obtained with FACE. The oligosaccharides from mAb produced in 50 and 100% DO showed a shift towards increased amounts of the core-fucosyl asialyl digalactosyl biantennary chain (peak 3) and a reduction in the amount of the core-fucosyl asialyl agalactosyl biantennary chain (peak 1). The effect of DO on peaks 4a and 4b, which are sialylated structures, was observed to mirror that of peak 3. Again, this is expected since Gal is required for the attachment of terminal SA.

The HPAEC-PAD chromatograms of the N-linked oligosaccharides cleaved by either PNGase F digestion or hydrazinolysis were essentially identical (Figure 3-7, compare a & b). Again, this indicated equivalent and quantitative deglycosylation employing the protocols in this report.

Chromatograms of deglycosylation controls (not shown) indicated that the peaks eluting at less than 10 min to be constituents of the enzyme and oligosaccharide preparations, or artifacts from the workup procedures from the PNGase F digestions and hydrazinolysis, not oligosaccharides.

If any of the mAbs were O-glycosylated we would have expected to find some recovery of O-linked oligosaccharides in the glycan pools derived by chemical deglycosylation since hydrazinolysis, using the protocol employed, removes both O- and N-linked glycans. In contrast, enzymatic deglycosylation by PNGase F digestion removes only the N-linked structures. Comparison of the HPAEC-PAD results for the enzymatically- and chemically-released N-glycans

exhibited no discernible differences (Figure 3-7, compare a & b). The conclusion is that the mAbs were not O-glycosylated. To date, O-linked glycosylation of human or murine IgG_1 has not been reported, while that of other human and murine IgG subclasses is extremely rare. In general, O-linked glycans are rare in serum proteins.

In contrast to FACE, it was possible with HPAEC-PAD to resolve agalactosyl, monogalactosyl, and digalactosyl biantennary standard glycans from their sialylated variants, but it was more difficult to resolve these structures with and without core-fucosylation. However, the FACE results depicted little evidence for the presence of afucosylated variants in the sample glycans and this was later confirmed by MALDI-QqTOF-MS (Section 3.3.5). The two methods were therefore complementary and corroborating.

The HPAEC-PAD profiles for polyclonal IgG and mAb glycosylation in this work (Figures 3-4, 3-7, 3-10, 3-11, & 3-15) are congruent with published reports for polyclonal and monoclonal IgG glycosylation (Weitzhandler *et al.*, 1994; Ashton *et al.*, 1995b; Lifely *et al.*, 1995; Rohrer *et al.*, 1995; Lines, 1996; McGuire *et al.*, 1996; Routier *et al.*, 1997; Sheeley *et al.*, 1997) and the MALDI-QqTOF-MS results.

The peaks in the HPAEC-PAD chromatograms were quantitated and compared to the FACE results.

3.3.2.3 FACE and HPAEC-PAD quantitation

Since the labelling of reducing oligosaccharides with ANTS in FACE is stoichiometric, glycan abundance is directly proportional to band intensity. However, peak areas from PAD integration are not directly commensurate to the quantity of each oligosaccharide, since it is well established that the PAD response varies from glycan to glycan (Lee, 1990). However, if glycans of similar size and composition are considered, as they are here for the three major neutral oligosaccharides, it is reasonable to postulate that their peak areas

approximate their relative quantity (Townsend *et al.*, 1988; Hardy & Townsend, 1988).

The relative band intensities from FACE and the relative peak areas from HPAEC-PAD of the three major neutral oligosaccharides were calculated (Table 3-4). Repeated PNGase F digestions of different samples of the same mAb preparations, and analysis by HPAEC-PAD on different dates, generated extremely consistent data as indicated by the small standard deviations in relative peak areas. Results from PNGase F digestion also gave essentially identical ratios to those obtained from hydrazinolysis. The relative band intensities from FACE were strikingly similar to the relative peak areas from HPAEC-PAD. This is especially remarkable considering the orthogonality of separation and detection procedures in these disparate methods.

The qualitative and quantitative results from FACE and HPAEC-PAD indicate that the level of galactosylation of the mAb N-glycans decreased as the steady-state DO concentration in chemostat culture was reduced from 100-10% DO. This trend is most easily appreciated by inspection of a bar graph of the relative peak area data from HPAEC-PAD (Figure 3-8). While the drop in galactosylation from 100-50% DO is marginal, there was a remarkable drop in galactosylation from 50-10% DO.

Table 3-4. Quantitative results for the first set of mAbs. Relative band intensities and peak areas of the major neutral oligosaccharides from the LH bioreactor (first set).

			Peak 1	Peak 2	Peak 3
			C2-004301	C2-014301	C2-024301
	mAb preparation (*n*)[a]	Deglycosylation method	core-fucosyl asialyl agalactosyl biantennary	core-fucosyl asialyl monogalactosyl biantennary	core-fucosyl asialyl digalactosyl biantennary
FACE	10% DO (2)	PNGase F	44.9 ± 0.2	46.5 ± 0.1	8.6 ± 0.2
	50% DO (2)	PNGase F	23.4 ± 0.3	52.1 ± 0.2	24.5 ± 0.1
	100% DO (2)	PNGase F	21.5 ± 0.1	51.6 ± 0.1	26.9 ± 0.1
	10% DO (2)	hydrazinolysis	45.5 ± 0.2	45.8 ± 0.2	8.7 ± 0.1
	50% DO (2)	hydrazinolysis	20.8 ± 0.1	54.7 ± 0.1	24.5 ± 0.1
	100% DO (2)	hydrazinolysis	19.0 ± 0.1	53.1 ± 0.6	27.9 ± 0.6
HPAEC–PAD	10% DO (6)	PNGase F	45.1 ± 0.1	46.1 ± 0.1	8.8 ± 0.2
	50% DO (6)	PNGase F	21.1 ± 0.2	54.0 ± 0.1	24.9 ± 0.2
	100% DO (6)	PNGase F	17.6 ± 0.4	52.6 ± 0.2	29.8 ± 0.5
	10% DO (3)	hydrazinolysis	45.1 ± 0.1	45.9 ± 0.1	9.0 ± 0.2
	50% DO (3)	hydrazinolysis	21.0 ± 0.2	54.5 ± 0.9	24.5 ± 0.8
	100% DO (3)	hydrazinolysis	18.0 ± 0.4	52.0 ± 0.8	30.0 ± 0.7

Data are presented as the average relative band intensities or peak areas (%) and standard deviation with (*n* -1) degrees of freedom.

[a] Denotes the number of quantitation measurements of a single FACE experiment, or the number of separate HPAEC-PAD experiments.

Figure 3-8. Glycosylation of the first set of mAbs. Chemostat cultures in three different steady-state DO concentrations in the LH bioreactor (first set). Deglycosylation by PNGase F digestion (P) and hydrazinolysis (H). Separation and quantitation by HPAEC-PAD.

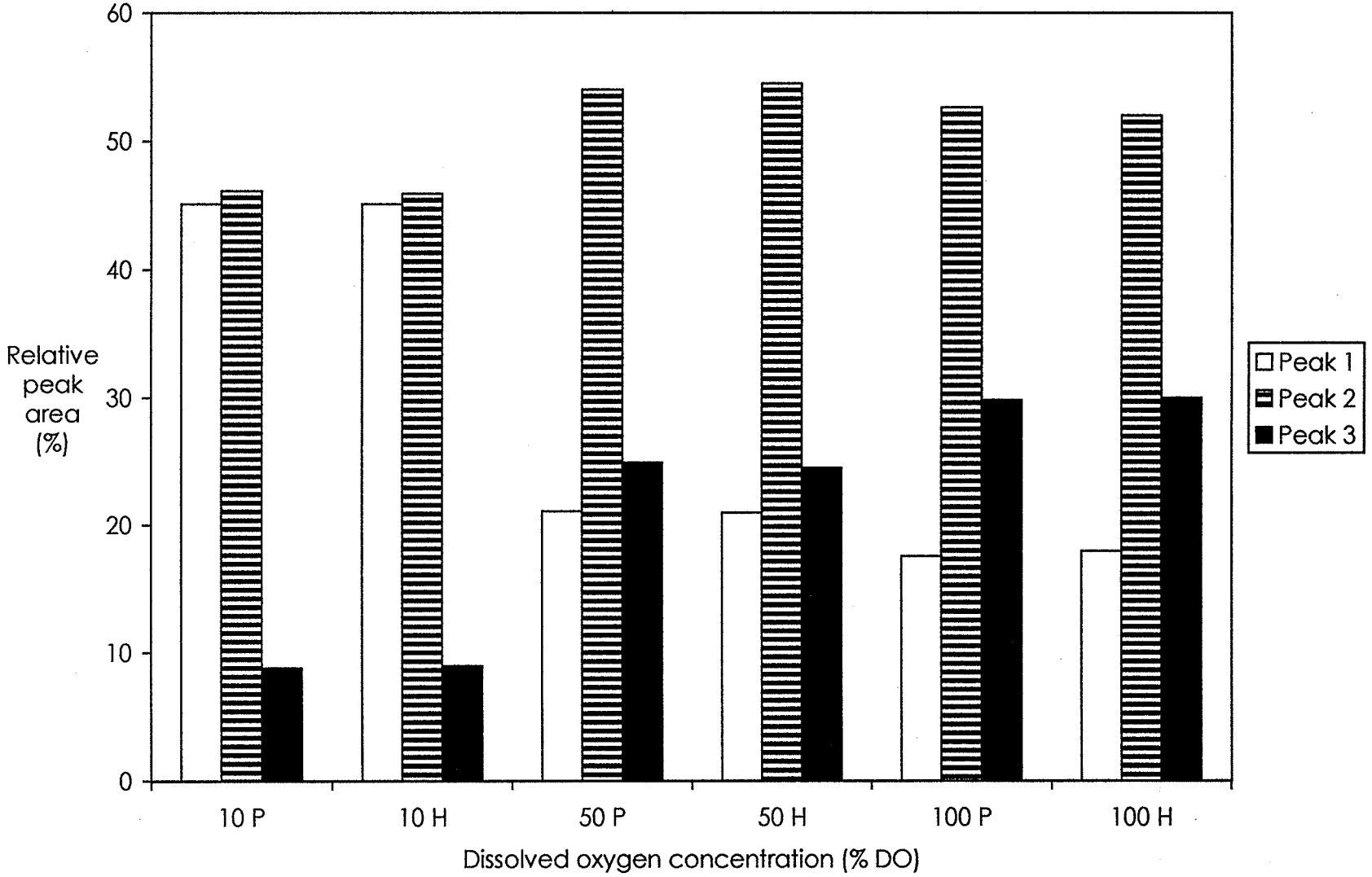
60
50
40
30
20
10
0
Relative peak area (%)
10 P
10 H
50 P
50 H
100 P
100 H
Dissolved oxygen concentration (% DO)
Peak 1
Peak 2
Peak 3

3.3.3 Chemostat culture second set mAbs

Analyses of the glycans from the mAb produced in 10, 50, and 100% DO in the NBS bioreactor was undertaken to determine whether the effect of DO concentration on the glycosylation of this mAb was general or bioreactor specific. The examination was also extended to the higher concentrations of 125 and 150% DO in the NBS bioreactor.

3.3.3.1 FACE

The oligosaccharides released by PNGase F digestion from the mAb preparations from the second set of cultures were analyzed by FACE (Figure 3-9). The results illustrated a trend consistent with the previous FACE data for the same DO concentrations in the LH bioreactor (first set), and showed an interesting change above 100% DO.

The mAb produced in 10 and 150% DO (lanes b & g, respectively) displayed two major bands with mobilities of approximately 6 and 7 GU (bands 1 & 2, respectively), with a minor band (band 3) of approximately 8 GU. Band 2 appeared to be a doublet. However, in 50, 100, and 125% DO (lane c, d, & h, respectively), there were three major bands: bands 1 and 2, with band 2 again being a doublet, and band 3, which had increased in intensity.

Band 1 was identified as core-fucosyl asialyl agalactosyl biantennary, band 3 was core-fucosyl asialyl digalactosyl biantennary, and band 2 was intermediate between these two structures as core-fucosyl asialyl monogalactosyl biantennary (Figure 3-5). Again, the doublets of band 2 were a result of galactosylation of either one or the other, but not both, of the antennae of the biantennary structure.

Figure 3-9. FACE analysis of the second set of mAbs. Electrofluorogram of the N-linked oligosaccharides (4 nmol total) released by PNGase F digestion from 288 μg of mAb produced in 10, 50, 100, 125, and 150% DO in the NBS bioreactor (second set). Lane a contains the glucose ladder with an arrow designating maltotetraose (GU=4). As before, three major bands (bands 1, 2, & 3) of approximately 6, 7, and 8 GU, respectively, are evident in the samples with a minor band of about 6.25 GU. Note the enrichment of band 1 and depletion of band 3 in 10 and 150% DO. Lane e contains 300 pmol each of four neutral glycan standards (Set 1) previously identified (Figure 3-6). Lane f contains 300 pmol of each of four sialylated glycan standards (Set 2, from top to bottom): core-fucosyl monosialyl biantennary (C2-124301), monosialyl biantennary (C2-124300), core-fucosyl disialyl biantennary (C2-224301), and disialyl biantennary (C2-224300) chains. Bands 1-3 were previously identified (Figure 3-6). The minor band was confirmed to be core-fucosyl monosialyl biantennary (C2-124301). There may be some contribution to band 2 by asialyl digalactosyl biantennary (C2-024300), and to band 1 by asialyl monogalactosyl biantennary (C2-014300) and monosialyl biantennary (C2-124300). The faint bands immediately below band 1 may be, in descending order, core-fucosyl disialyl biantennary (C2-224301) and asialyl agalactosyl biantennary (C2-004300).

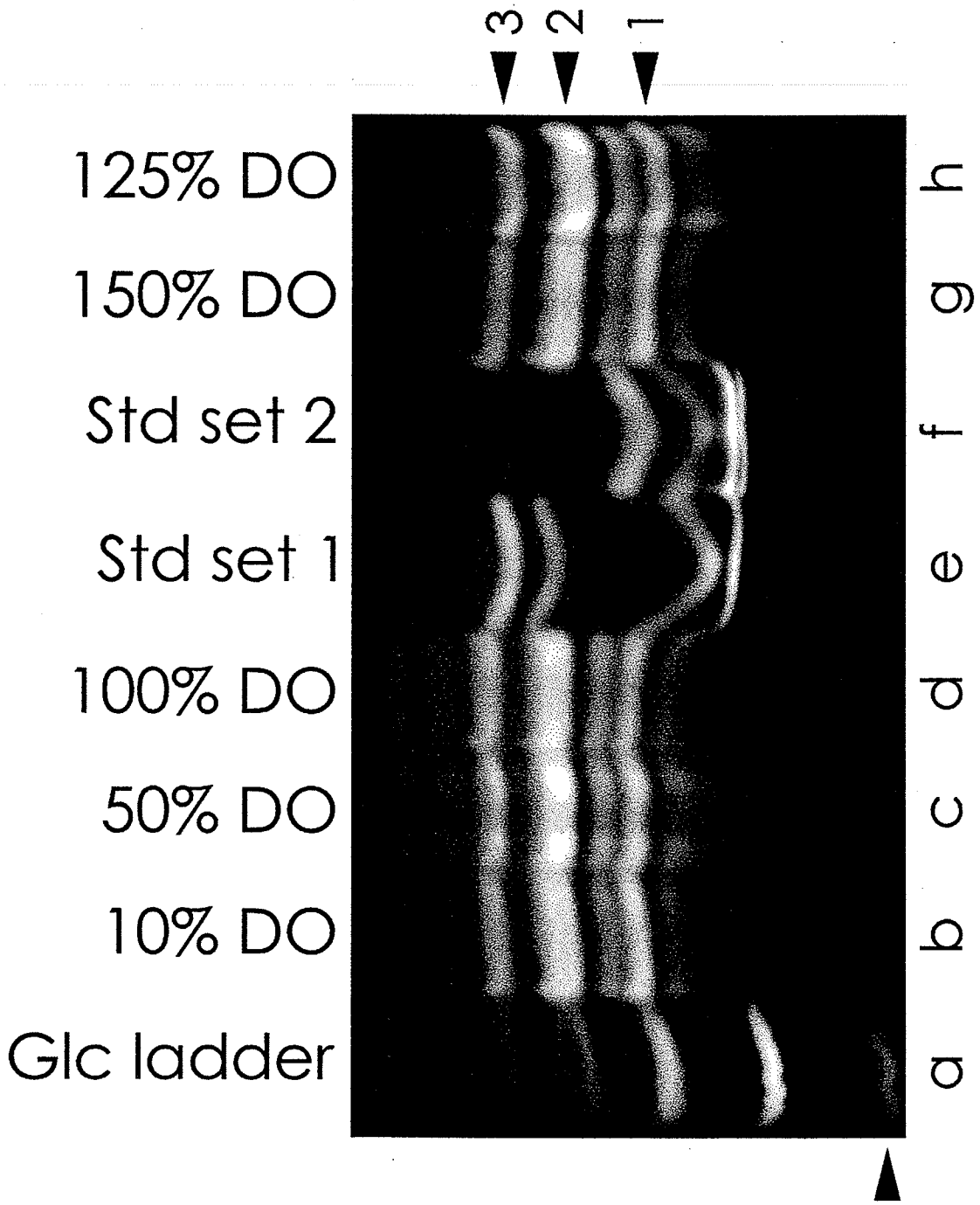
3
2
1
125% DO
150% DO
Std set 2
Std set 1
100% DO
50% DO
10% DO
Glc ladder
h
g
f
e
d
c
b
a

The minor band migrating at approximately 6.25 GU was monosialyl core-fucosyl digalactosyl biantennary. There was also evidence for the afucosyl variants of the asialyl structures and presence of monosialyl structures (Figure 3-9).

The bands in the FACE electrofluorograms were quantitated and compared to the HPAEC-PAD results (Section 3.3.3.3).

3.3.3.2 HPAEC-PAD

The oligosaccharides released enzymatically from the mAb preparations from the second set of cultures were separated and detected by HPAEC-PAD. As before for mAbs from the LH bioreactor (first set), the chromatograms for mAbs from the NBS bioreactor indicated three main peaks of varying relative areas eluting at approximately 18.5, 21.0, and 23.5 min (Figure 3-10). Again, these peaks were identified to correspond to structures 1-3 (Figure 3-5) and to the bands 1-3 from FACE (Figure 3-9). They were core-fucosyl asialyl agalactosyl biantennary, core-fucosyl asialyl monogalactosyl biantennary, and core-fucosyl asialyl digalactosyl biantennary, respectively. The trace peaks eluting after peak 3 in the range of 25-30 min may have included structures resulting from the presence of a bisecting GlcNAc, or the lack of core-Fuc, in one or more of structures 1-3. The same three groups of minor peaks eluting at about 47-51, 53-57, and 62-66 min were also evident. Peaks 4a and 4b were monosialylated core-fucosyl biantennary chains with Neu5Ac (47-51 min) or Neu5Gc (62-66 min), respectively. The structures at 53-57 min may have been variants of structure 4a resulting from the presence of a bisecting GlcNAc.

The HPAEC-PAD results for 10, 50, and 100% DO cultures in the NBS bioreactor (Figure 3-10) presented the same conspicuous trend observed with the previous HPAEC-PAD data for the LH bioreactor (first set) and the previous FACE data for the LH and NBS bioreactors (first and second sets). In both the LH

and NBS bioreactors, only two prominent peaks were obtained in 10% DO, corresponding to core-fucosyl asialyl agalactosyl biantennary (peak 1) and core-fucosyl asialyl monogalactosyl biantennary chains (peak 2). The core-fucosyl asialyl digalactosyl biantennary chain (peak 3) was less pronounced. The oligosaccharides from mAb produced in 50 and 100% DO in both bioreactors showed a shift towards increased amounts of the core-fucosyl asialyl digalactosyl biantennary chain (peak 3) and a reduction in the amount of the core-fucosyl asialyl agalactosyl biantennary chain (peak 1). Most of the increase in peak 3 appeared to be at the expense of peak 1, as peak 2 appeared largely unaffected. As before, the effect of DO on peaks 4a and 4b, which are sialylated structures, was observed to mirror that of peak 3. However, the NBS bioreactor showed a more constant and slightly greater level of sialylation of mAb glycans (peaks 4a & 4b) than the LH bioreactor at all three DO setpoints, especially in 10% DO. This indicates that a greater proportion of monogalactosyl and digalactosyl structures were sialylated in the NBS bioreactor.

The mAb glycans showed an interesting reversal in galactosylation above 100% DO (Figure 3-11). As the DO concentration was increased to 125 and 150% there was a concomitant shift towards increased amounts of the core-fucosyl asialyl agalactosyl biantennary chain (peak 1) and a reduction in the amount of the core-fucosyl asialyl digalactosyl biantennary chain (peak 3). Most of the increase in peak 1 again appeared to be mainly at the detriment of peak 3.

The peaks in the HPAEC-PAD chromatograms were quantitated and compared to the FACE results (Section 3.3.3.3).

Figure 3-10. HPAEC-PAD comparison of the first and second sets of mAbs. Representative chromatograms of the PNGase F-released N-linked oligosaccharides from 144 μg of the mAb produced in 10, 50, and 100% DO in the (a) LH (first set) and (b) NBS (second set) bioreactors. As before, there were three major peaks (peaks 1, 2, & 3) with respective elution times of approximately 18.5, 21.0, and 23.5 min – and several minor peaks. Note the enrichment of peak 1 and depletion of peak 3 in 10% DO and the increase in peaks 4a and 4b with increases in peaks 2 and 3 in 50 and 100% DO. Peaks were previously identified by the use of three sets of standards (Figure 3-7).

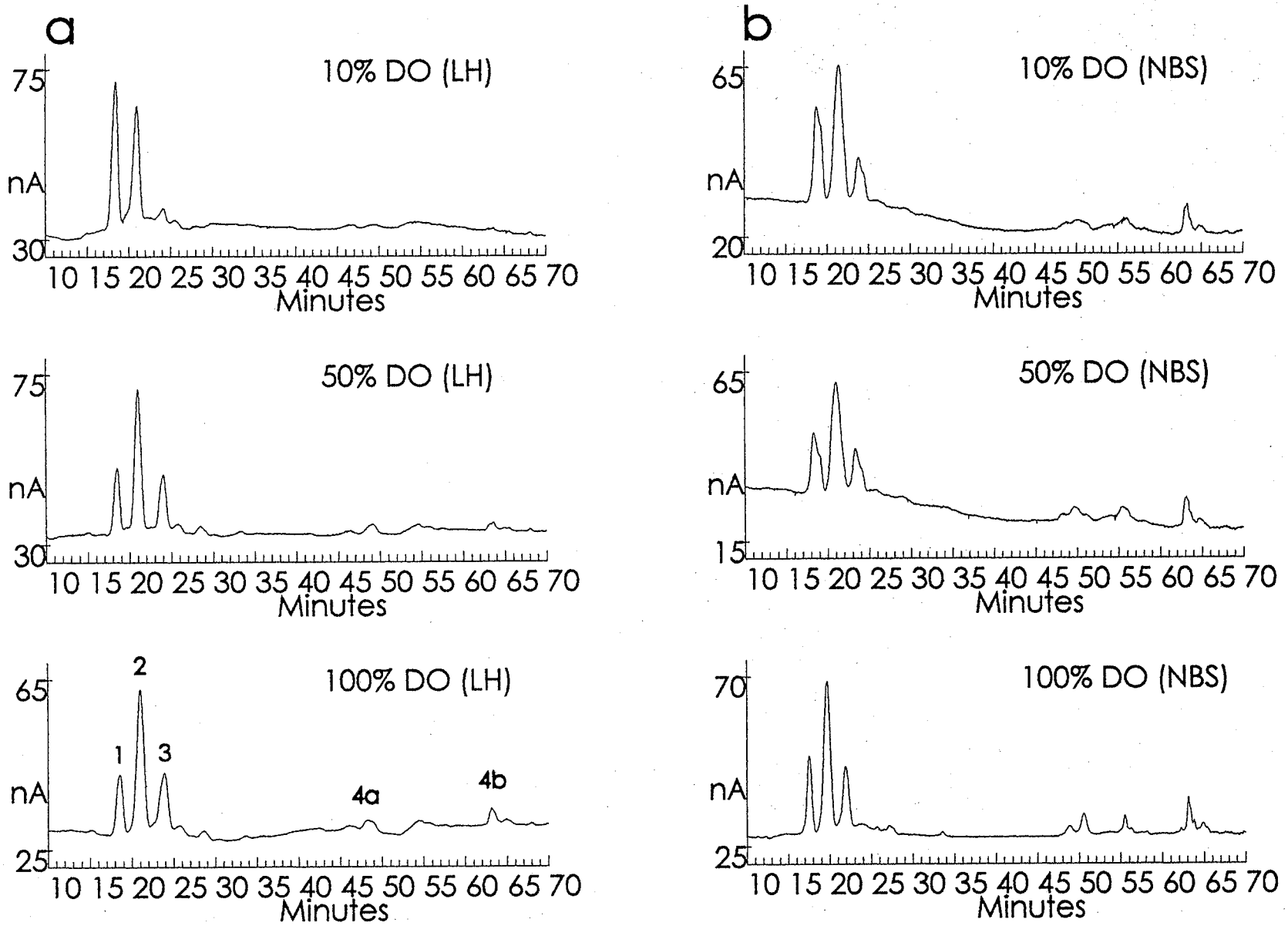
a
10% DO (LH)
75
nA
30
10 15 20 25 30 35 40 45 50 55 60 65 70
Minutes
50% DO (LH)
75
nA
30
10 15 20 25 30 35 40 45 50 55 60 65 70
Minutes
100% DO (LH)
65
nA
25
1
2
3
4a
4b
10 15 20 25 30 35 40 45 50 55 60 65 70
Minutes
b
10% DO (NBS)
65
nA
20
10 15 20 25 30 35 40 45 50 55 60 65 70
Minutes
50% DO (NBS)
65
nA
15
10 15 20 25 30 35 40 45 50 55 60 65 70
Minutes
100% DO (NBS)
70
nA
25
10 15 20 25 30 35 40 45 50 55 60 65 70
Minutes

Figure 3-11. HPAEC-PAD analysis of the second set of mAbs. Representative chromatograms of PNGase F-released N-linked oligosaccharides from 144 μg of the mAb produced in 10, 50, 100, 125, and 150% DO in the NBS bioreactor (second set). Again, there were three major peaks (peaks 1, 2, & 3) with respective elution times of approximately 18.5, 21.0, and 23.5 min – and several minor peaks. Note the enrichment of peak 1 and depletion of peak 3 in 10 and 150% DO. Peaks were previously identified by the use of three sets of standards (Figure 3-7).

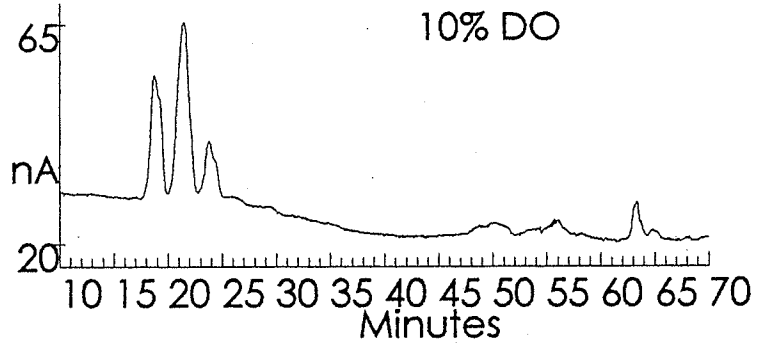
10% DO
65
nA
20
10 15 20 25 30 35 40 45 50 55 60 65 70
Minutes

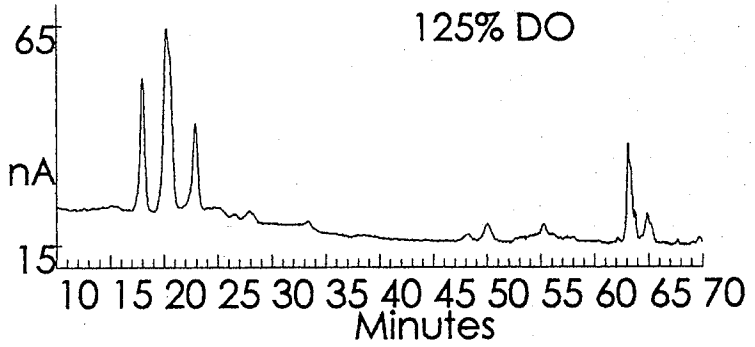
125% DO
65
nA
15
10 15 20 25 30 35 40 45 50 55 60 65 70
Minutes

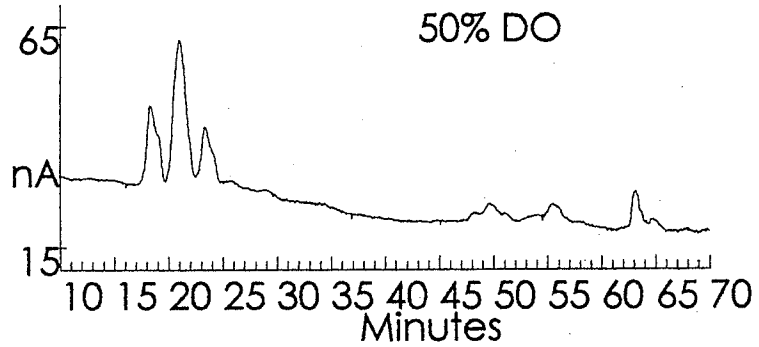
50% DO
65
nA
15
10 15 20 25 30 35 40 45 50 55 60 65 70
Minutes

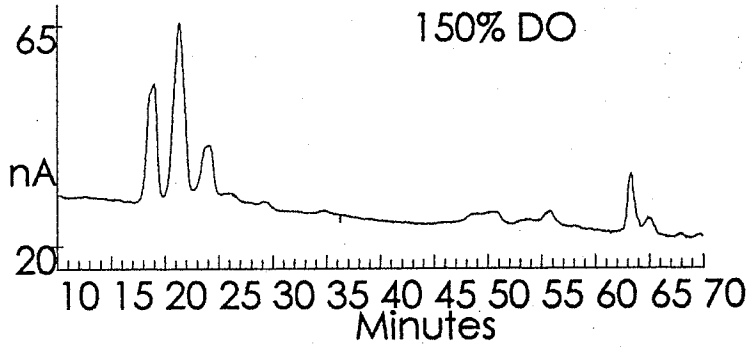
150% DO
65
nA
20
10 15 20 25 30 35 40 45 50 55 60 65 70
Minutes

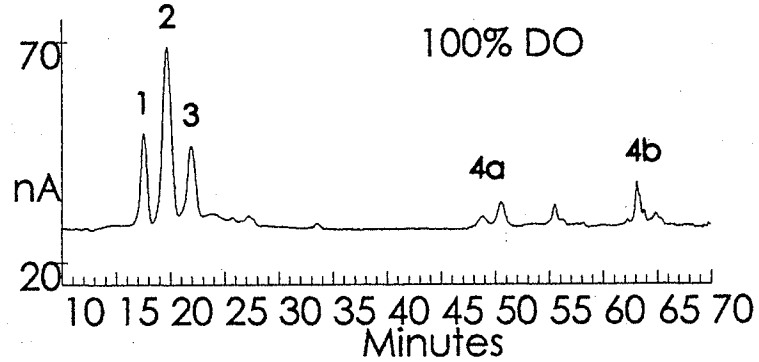
100% DO
2
70
1
3
4a
4b
nA
20
10 15 20 25 30 35 40 45 50 55 60 65 70
Minutes

3.3.3.3 FACE and HPAEC-PAD quantitation

The relative peak areas from HPAEC-PAD of the three major neutral oligosaccharides from 10, 50, and 100% DO from the LH and NBS bioreactors were calculated and compared (Table 3-5). As is indicated by the standard deviation in relative peak areas, repeated PNGase F digestions and analyses by HPAEC-PAD were again remarkably consistent. However, while the tendency for decreased galactosylation of the mAb glycans with lower DO was common to both LH and NBS bioreactors, there were quantitative differences between the two bioreactors. The effect of DO on galactosylation was less pronounced in the NBS bioreactor than in the LH bioreactor. The general trend observed in the LH and NBS bioreactors is most easily appreciated by inspection of a bar graph of the relative peak area data from HPAEC-PAD (Figure 3-12).

The relative band intensities from FACE and the relative peak areas from HPAEC-PAD of the three major neutral oligosaccharides from 10, 50, 100, 125, and 150% DO from NBS bioreactor were calculated (Table 3-6). Again, the relative amounts of each oligosaccharide determined by FACE and HPAEC-PAD were in extremely close agreement.

The qualitative and quantitative results from FACE and HPAEC-PAD indicate that the level of galactosylation of the mAb N-linked oligosaccharides decreased as the steady-state DO concentration in chemostat culture was reduced from 100-10%. However, as the DO concentration was increased from 100-150% the correlation reversed. There appeared to be an optimum DO concentration of 100% for maximum galactosylation of the mAb glycans. This is most easily appreciated by inspection of a bar graph of the relative peak area data from HPAEC-PAD (Figure 3-13).

Table 3-5. Comparison of the results for the first and second sets of mAbs. Relative peak areas of the major neutral oligosaccharides from the LH and NBS bioreactors (first & second sets).

		Peak 1	Peak 2	Peak 3
		C2-004301	C2-014301	C2-024301
		core-fucosyl asialyl agalactosyl biantennary	core-fucosyl asialyl monogalactosyl biantennary	core-fucosyl asialyl digalactosyl biantennary
Bioreactor	mAb preparation (*n*)[a]			
LH	10% DO (6)	45.1 ± 0.1	46.1 ± 0.1	8.8 ± 0.2
	50% DO (6)	21.1 ± 0.2	54.0 ± 0.1	24.9 ± 0.2
	100% DO (6)	17.6 ± 0.4	52.6 ± 0.2	29.8 ± 0.5
NBS	10% DO (5)	32.4 ± 0.2	52.9 ± 0.1	14.7 ± 0.2
	50% DO (5)	25.6 ± 0.1	54.9 ± 0.3	19.5 ± 0.2
	100% DO (5)	20.6 ± 0.1	56.2 ± 0.2	23.2 ± 0.1

Data are presented as the average relative peak areas (%) and standard deviation with (*n* -1) degrees of freedom.

[a] Denotes the number of separate HPAEC-PAD experiments.

Figure 3-12. Glycosylation of the first and second sets of mAbs. Chemostat cultures in three different steady-state DO concentrations in the LH (first set) and NBS (second set) bioreactors. Deglycosylation by PNGase F digestion. Separation and quantitation by HPAEC-PAD.

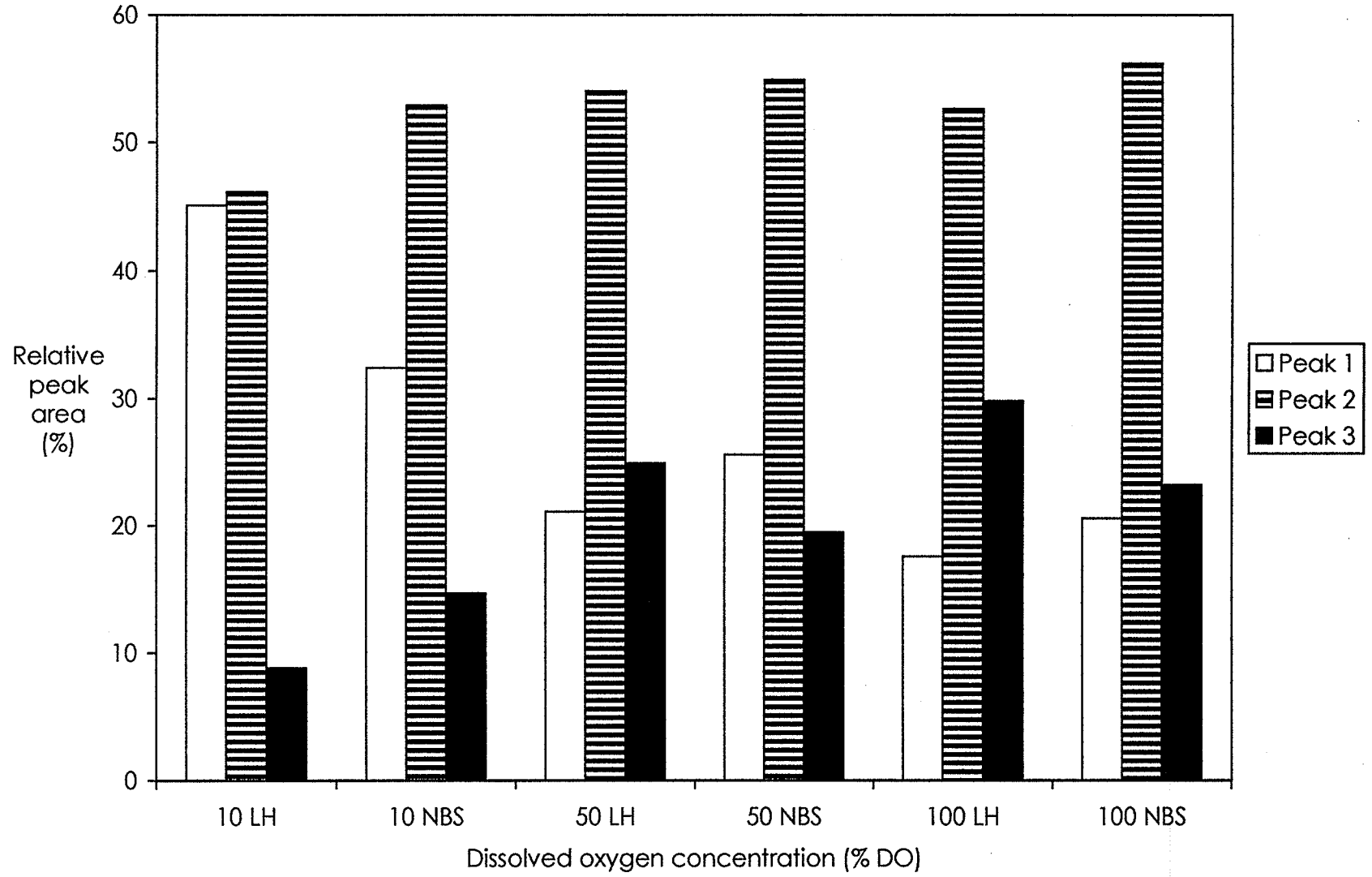
60
50
40
30
20
10
0
Relative peak area (%)
10 LH
10 NBS
50 LH
50 NBS
100 LH
100 NBS
Dissolved oxygen concentration (% DO)
Peak 1
Peak 2
Peak 3

Table 3-6. Quantitative results for the second set of mAbs. Relative band intensities and peak areas of the major neutral oligosaccharides from the NBS bioreactor (second set).

		Peak 1	Peak 2	Peak 3
		C2-004301	C2-014301	C2-024301
	mAb preparation (*n*)[a]	core-fucosyl asialyl agalactosyl biantennary	core-fucosyl asialyl monogalactosyl biantennary	core-fucosyl asialyl digalactosyl biantennary
FACE	10% DO (2)	32.9 ± 0.3	51.7 ± 0.3	15.4 ± 0.6
	50% DO (2)	25.7 ± 0.2	53.6 ± 0.4	20.6 ± 0.3
	100% DO (2)	21.0 ± 0.2	55.3 ± 0.3	23.7 ± 0.2
	125% DO (2)	24.7 ± 0.1	54.9 ± 0.4	20.4 ± 0.6
	150% DO (2)	31.1 ± 0.3	51.7 ± 0.2	17.2 ± 0.1
HPAEC–PAD	10% DO (5)	32.4 ± 0.2	52.9 ± 0.1	14.7 ± 0.2
	50% DO (5)	25.6 ± 0.1	54.9 ± 0.3	19.5 ± 0.2
	100% DO (5)	20.6 ± 0.1	56.2 ± 0.2	23.2 ± 0.1
	125% DO (5)	24.3 ± 0.1	56.7 ± 0.1	19.0 ± 0.1
	150% DO (5)	30.7 ± 0.2	52.9 ± 0.4	16.4 ± 0.4

Data are presented as the average relative band intensities or peak areas (%) and standard deviation with (*n* -1) degrees of freedom.

[a] Denotes the number of quantitation measurements of a single FACE experiment, or the number of separate HPAEC-PAD experiments.

Figure 3-13. Glycosylation of the second set of mAbs. Chemostat cultures in five different steady-state DO concentrations in the NBS (second set) bioreactor. Deglycosylation by PNGase F digestion. Separation and quantitation by HPAEC-PAD.

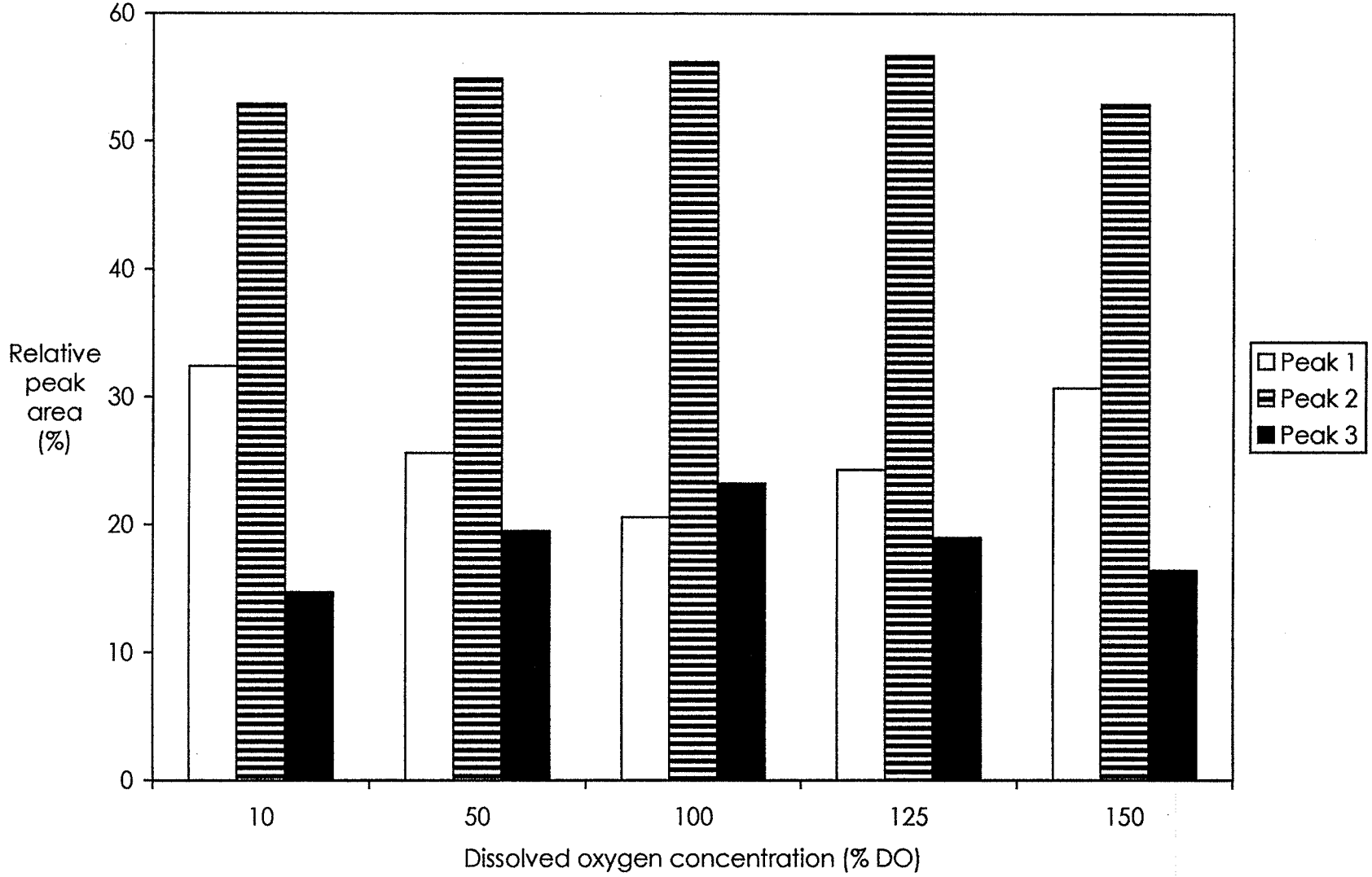
60
50
40
30
20
10
0
Relative peak area (%)
10
50
100
125
150
Dissolved oxygen concentration (% DO)
Peak 1
Peak 2
Peak 3

3.3.4 Chemostat culture third set mAbs

Analyses of the glycans from the mAb produced in 1, 2, 5, 10, 25, and 50% DO in the NBS bioreactor was undertaken to examine the effect of DO concentration on the glycosylation of this mAb at lower concentrations.

3.3.4.1 FACE

The oligosaccharides released by PNGase F digestion from the mAb preparations from the third set of cultures were analyzed by FACE (Figure 3-14). As in the previous FACE electrofluorograms, there were three main bands of 6, 7, and 8 GU. The relative intensity of band 1 (core-fucosyl asialyl agalactosyl biantennary) increased, and the relative intensity of band 3 (core-fucosyl asialyl digalactosyl biantennary) decreased, as the DO concentration was decreased from 50-1% (lanes b to g).

The bands in the FACE electrofluorogram were quantitated and compared to the HPAEC-PAD results (Section 3.3.4.3).

3.3.4.2 HPAEC-PAD

The oligosaccharides released enzymatically from the mAb preparations from the third set of cultures were analyzed by HPAEC-PAD (Figure 3-15). As in the previous HPAEC-PAD chromatograms, there were three main peaks with retention times of 18.5, 21.0, and 23.5 min. The relative area of peak 1 (core-fucosyl asialyl agalactosyl biantennary) increased, and the relative area of peak 3 (core-fucosyl asialyl digalactosyl biantennary) decreased, as the DO concentration was decreased from 50-1%.

The peaks in the HPAEC-PAD chromatograms were quantitated and compared to the FACE results.

Figure 3-14. FACE analysis of the third set of mAbs. Electrofluorogram of the N-linked oligosaccharides (4 nmol total) released by PNGase F digestion from 288 μg of mAb produced in 1, 2, 5, 10, 25, and 50% DO in the NBS bioreactor (third set). Lanes a and h contain the glucose ladder. Again, three major bands (bands 1, 2, & 3) of approximately 6, 7, and 8 GU, respectively, are evident in the samples with a minor band of about 6.25 GU. No glycan standards were run on this gel due to lane availability constraints. Bands were previously identified (Figures 3-6 & 3-9).

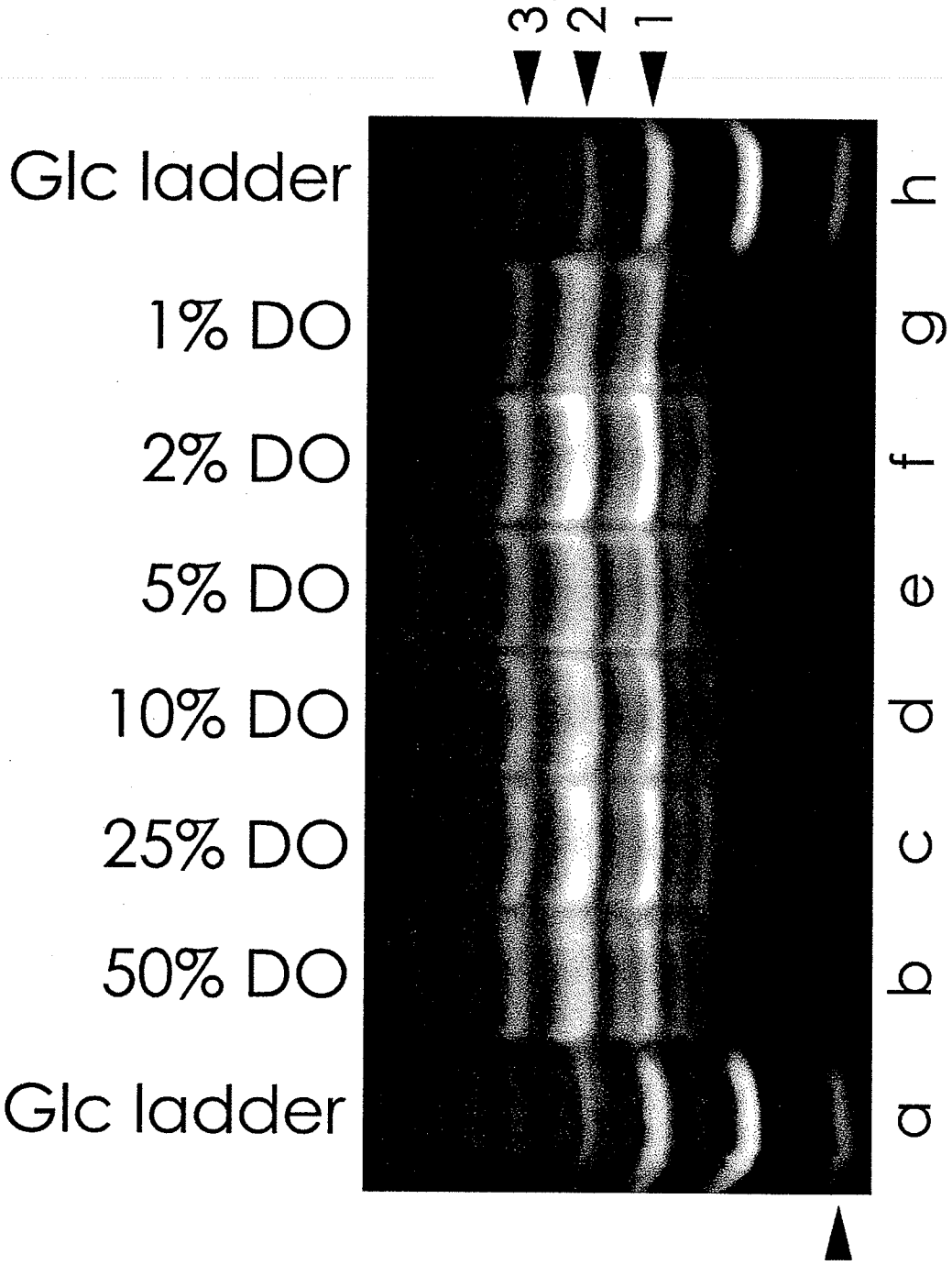
3
2
1
Glc ladder
1% DO
2% DO
5% DO
10% DO
25% DO
50% DO
Glc ladder
h
g
f
e
d
c
b
a

Figure 3-15. HPAEC-PAD analysis of the third set of mAbs. Representative chromatograms of PNGase F-released N-linked oligosaccharides from 144 μg of the mAb produced in 1, 2, 5, 10, 25, and 50% DO in the NBS bioreactor (third set). Again, there were three major peaks (peaks 1, 2, & 3) with respective elution times of approximately 18.5, 21.0, and 23.5 min – and several minor peaks. Note the enrichment of peak 1 and depletion of peak 3 as the DO concentration is decreased from 50-1%. Peaks were previously identified by the use of three sets of standards (Figure 3-7).

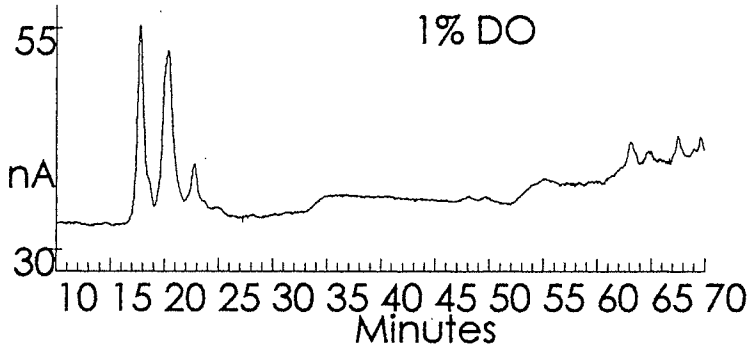
1% DO
55
nA
30
10 15 20 25 30 35 40 45 50 55 60 65 70
Minutes

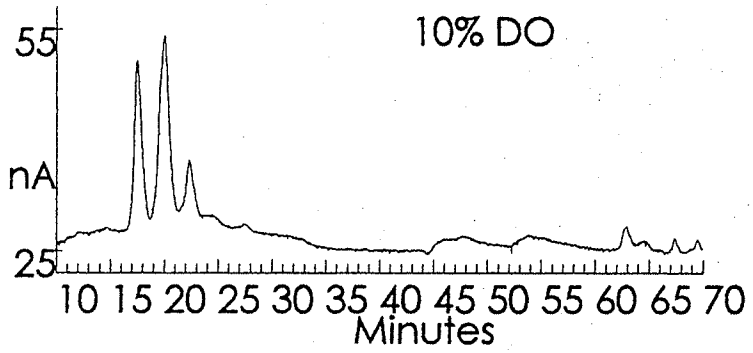
10% DO
55
nA
25
10 15 20 25 30 35 40 45 50 55 60 65 70
Minutes

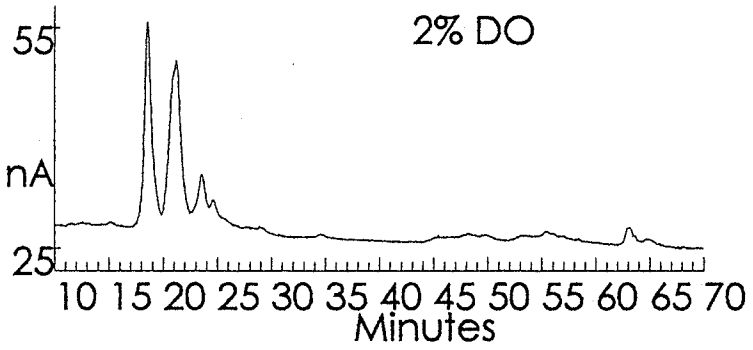
2% DO
55
nA
25
10 15 20 25 30 35 40 45 50 55 60 65 70
Minutes

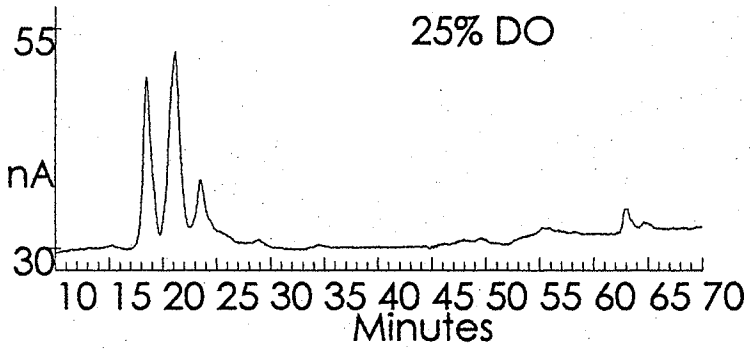
25% DO
55
nA
30
10 15 20 25 30 35 40 45 50 55 60 65 70
Minutes

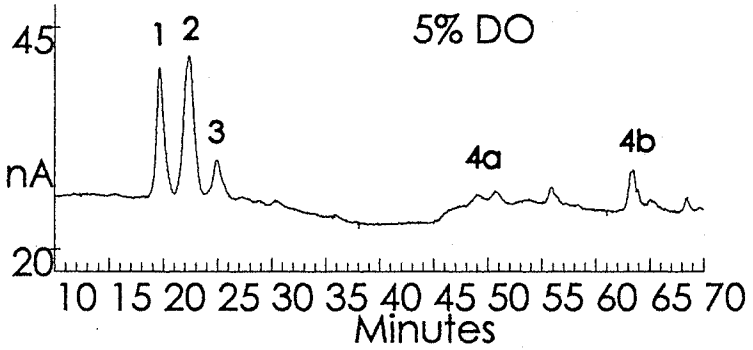
5% DO
1
2
3
4a
4b
45
nA
20
10 15 20 25 30 35 40 45 50 55 60 65 70
Minutes

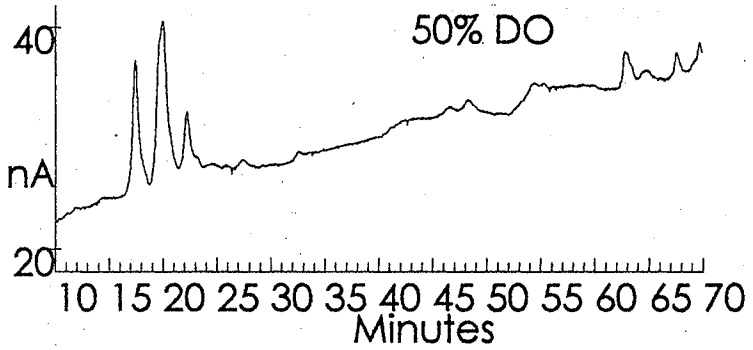
50% DO
40
nA
20
10 15 20 25 30 35 40 45 50 55 60 65 70
Minutes

3.3.4.3 FACE and HPAEC-PAD quantitation

The relative band intensities from FACE and the relative peak areas from HPAEC-PAD of the three major neutral oligosaccharides from 1, 2, 5, 10, 25, and 50% DO in the NBS bioreactor were calculated (Table 3-7).

The qualitative and quantitative results from FACE and HPAEC-PAD indicate that the level of galactosylation of the mAb N-linked oligosaccharides decreased as the steady-state DO concentration in chemostat culture was reduced from 50-1%. There appeared to be a threshold DO concentration of 25% DO and below for minimum galactosylation of the mAb glycans. This is most easily appreciated by inspection of a bar graph of the relative peak area data from HPAEC-PAD (Figure 3-16).

Table 3-7. Quantitative results for the third set of mAbs. Relative band intensities and peak areas of the major neutral oligosaccharides from the NBS bioreactor (third set).

		Peak 1	Peak 2	Peak 3
		C2-004301	C2-014301	C2-024301
	mAb preparation (*n*)[a]	core-fucosyl asialyl agalactosyl biantennary	core-fucosyl asialyl monogalactosyl biantennary	core-fucosyl asialyl digalactosyl biantennary
FACE	1% DO (2)	39.0 ± 0.1	48.5 ± 0.3	12.5 ± 0.4
	2% DO (2)	37.9 ± 0.5	49.1 ± 0.5	13.0 ± 0.1
	5% DO (2)	35.7 ± 0.5	50.0 ± 1.0	14.3 ± 0.5
	10% DO (2)	33.7 ± 0.7	51.2 ± 0.7	15.1 ± 0.1
	25% DO (2)	33.0 ± 0.1	51.5 ± 0.5	15.5 ± 0.6
	50% DO (2)	26.5 ± 0.1	55.0 ± 0.1	18.5 ± 0.1
HPAEC–PAD	1% DO (6)	39.6 ± 0.2	48.7 ± 0.2	11.7 ± 0.3
	2% DO (6)	38.5 ± 0.3	49.3 ± 0.2	12.2 ± 0.2
	5% DO (6)	36.1 ± 0.2	50.5 ± 0.3	13.4 ± 0.2
	10% DO (6)	34.3 ± 0.1	51.7 ± 0.2	14.0 ± 0.2
	25% DO (6)	33.4 ± 0.2	52.0 ± 0.2	14.6 ± 0.1
	50% DO (6)	26.2 ± 0.2	55.9 ± 0.1	17.9 ± 0.3

Data are presented as the average relative band intensities or peak areas (%) and standard deviation with (*n* -1) degrees of freedom.

[a] Denotes the number of quantitation measurements of a single FACE experiment, or the number of separate HPAEC-PAD experiments.

Figure 3-16. Glycosylation of the third set of mAbs. Chemostat cultures in six different steady-state DO concentrations in the NBS (third set) bioreactor. Deglycosylation by PNGase F digestion. Separation and quantitation by HPAEC-PAD.

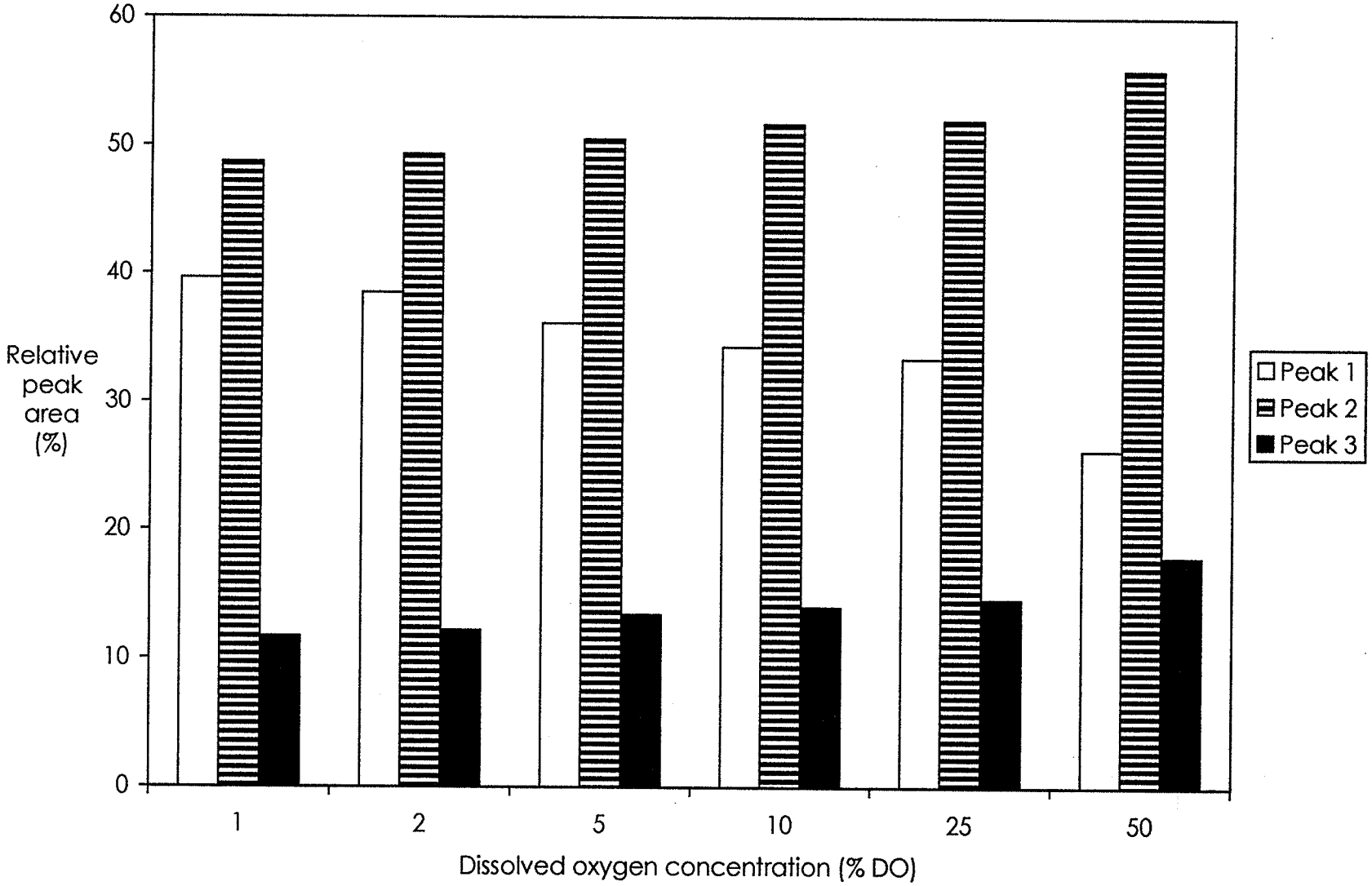
60
50
40
30
20
10
0
Relative peak area (%)
1
2
5
10
25
50
Dissolved oxygen concentration (% DO)
Peak 1
Peak 2
Peak 3

3.3.5 MALDI-QqTOF-MS

The N-linked glycans removed by PNGase F digestion from the bovine and human polyclonal IgGs, and each of the mAb preparations from the first set of cultures, were derivatized with PMP and analyzed by MALDI-QqTOF-MS. However, prior to this the standard glycan sets for MALDI-QqTOF-MS (Section 2.7.2.3) were examined.

The PMP-labelled oligosaccharides in all three sets of glycan standards were observed as mixtures of protonated $[M+H]^+$ and sodiated $[M+Na]^+$ molecular ions. The derivatization with PMP was essentially quantitative; no unlabelled glycans were observed. Thus, the neutral and sialylated standards (Sets 1 & 2, respectively) each exhibited 4 major peaks and 4 minor peaks (Figures 3-17 & 3-18), while the mixed standards (Set 3) exhibited 8 major peaks and 8 minor peaks (Figure 3-19). The extent of ionization by either protonation or addition of a sodium ion partly depends on which region of the sample spot is irradiated (Lemoine *et al.*, 1996). Irradiation of the crystalline region at the edges of the sample spot tends to produce $[M+H]^+$ species, whereas desorption/ionization from the centre of the spot, which is less crystalline and sometime amorphous, yields more $[M+Na]^+$ ions. The theoretical and observed monoisotopic masses of the standard protonated and sodiated molecular ions were remarkably accurate (Table 3-8).

Figures 3-17 – 3-19. MALDI-QqTOF-MS analysis of the standard glycan sets. Mass spectra of the neutral (Set 1), sialylated (Set 2), and mixed (Set 3) standards, respectively. Monosaccharide symbols are defined in Table 1-1.

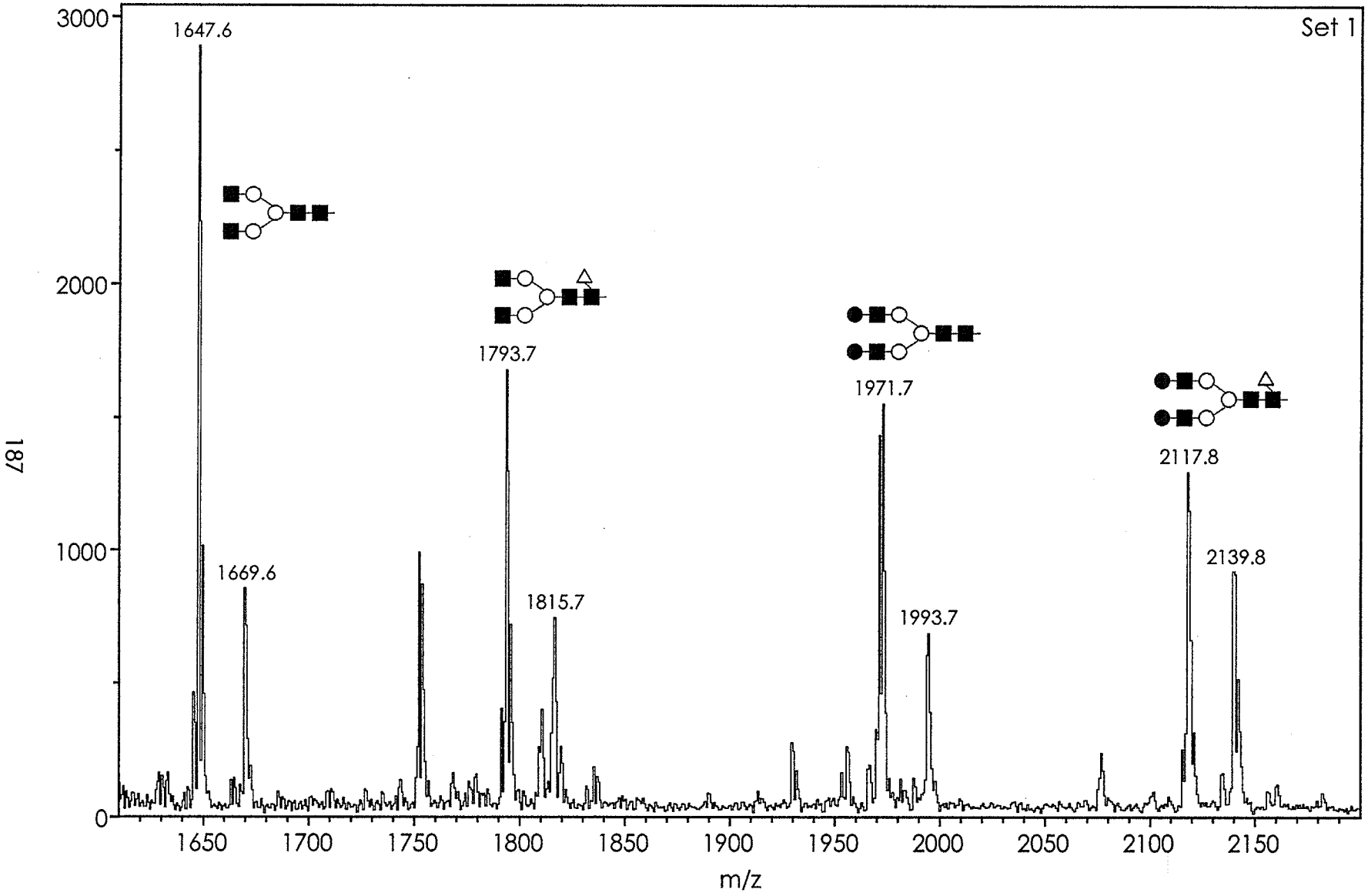
Set 1
3000
2000
1000
0
187
1647.6
1669.6
1793.7
1815.7
1971.7
1993.7
2117.8
2139.8
1650
1700
1750
1800
1850
1900
1950
2000
2050
2100
2150
m/z

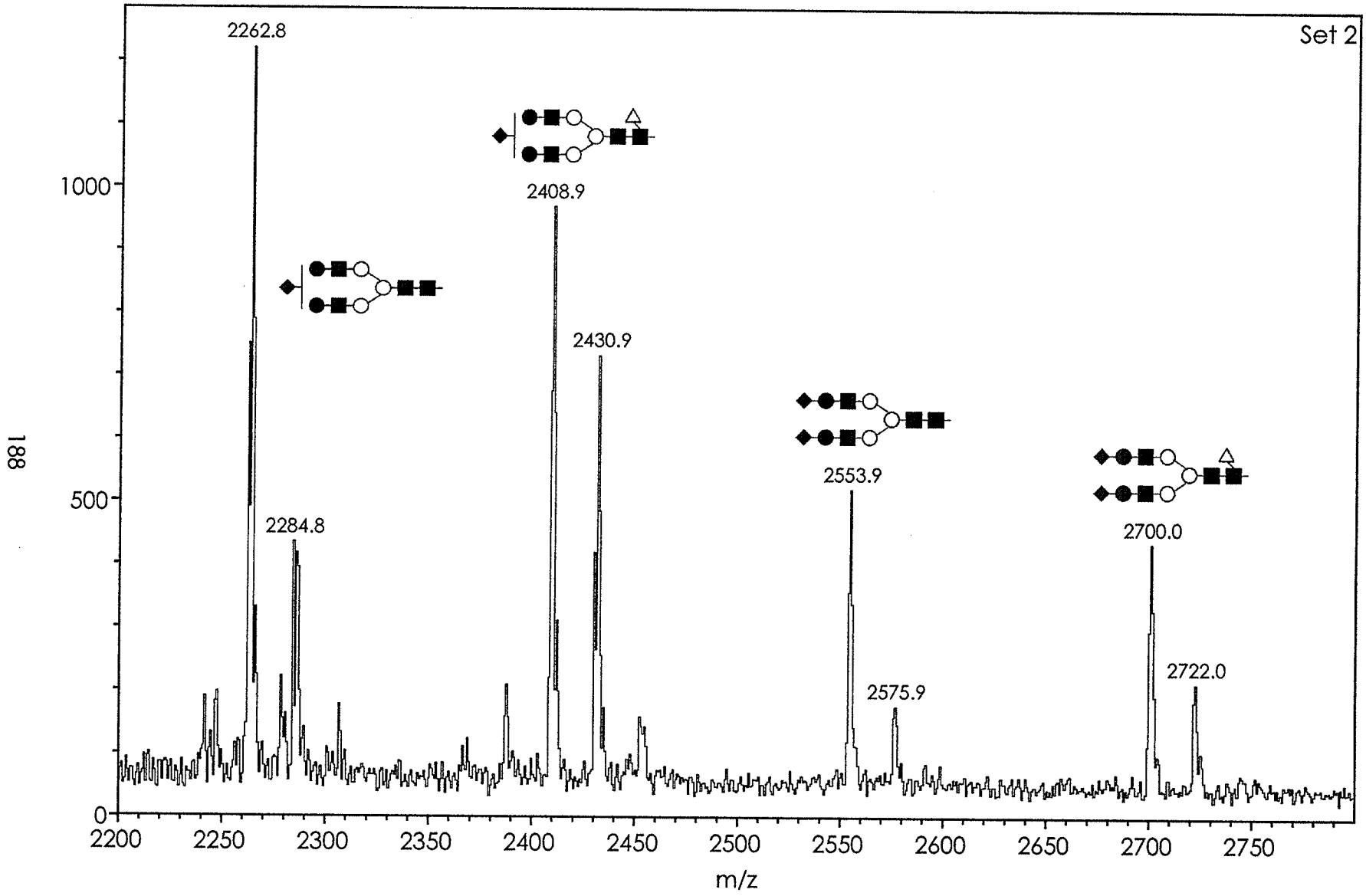
Set 2
2262.8
2408.9
2430.9
2284.8
2553.9
2700.0
2722.0
2575.9
1000
500
0
2200
2250
2300
2350
2400
2450
2500
2550
2600
2650
2700
2750
m/z
188

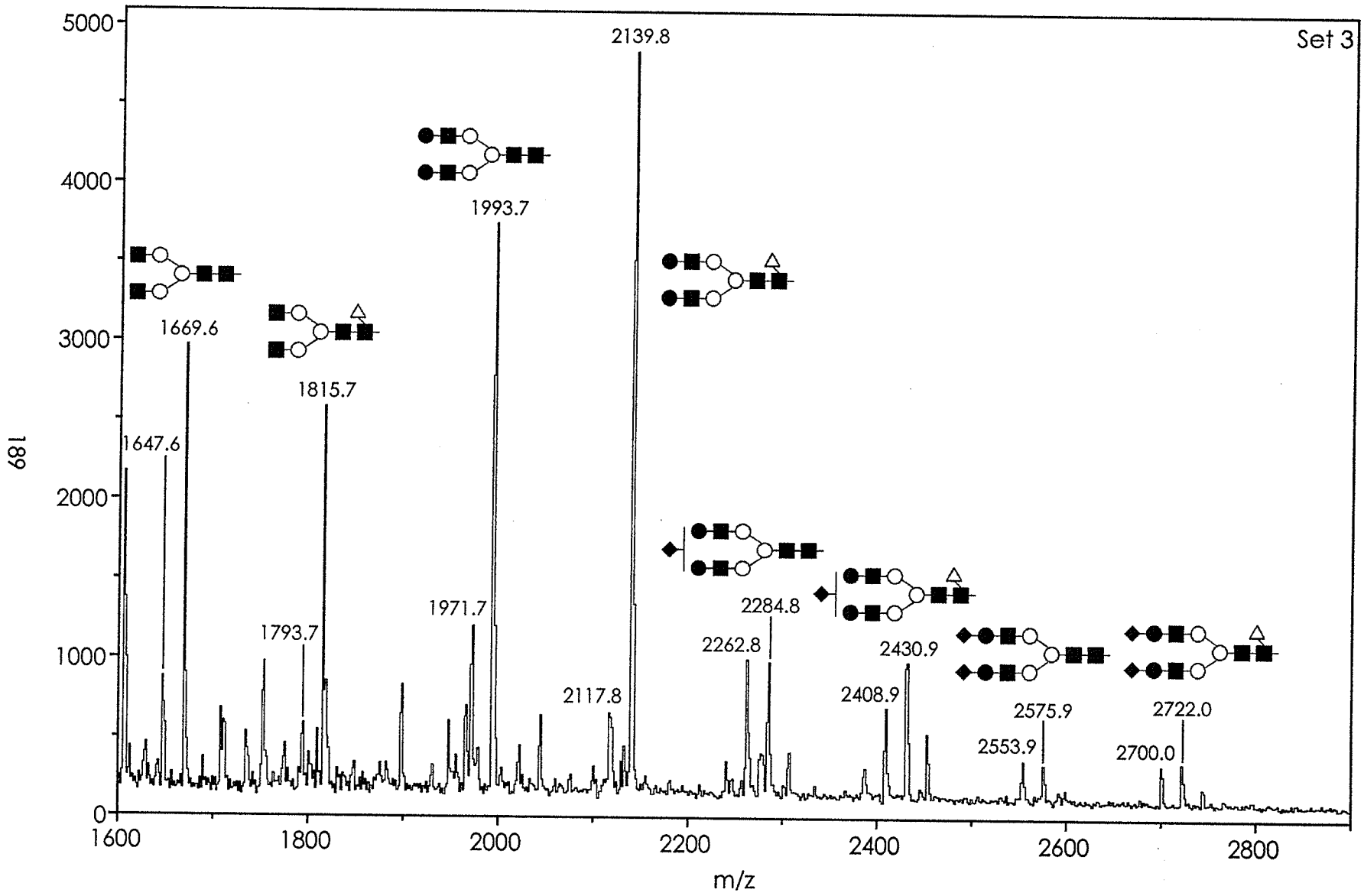
Set 3
5000
4000
3000
2000
1000
0
189
1600
1800
2000
2200
2400
2600
2800
m/z
2139.8
1993.7
1669.6
1815.7
1647.6
1793.7
1971.7
2117.8
2284.8
2262.8
2430.9
2408.9
2575.9
2553.9
2722.0
2700.0

Table 3-8. Monoisotopic masses of the eight PMP-labelled N-glycan standards.

Glycan code	Mono-isotopic molecular mass	PMP-labelled $[M+H]^+$ $[M+Na]^+$ ions	Observed $[M+H]^+$ $[M+Na]^+$ ions
C2-004300	1316.5	1647.6 1669.6	1647.6 1669.6
C2-004301	1462.5	1793.7 1815.7	1793.7 1815.7
C2-024300	1640.6	1971.7 1993.7	1971.7 1993.7
C2-024301	1786.6	2117.8 2139.8	2117.8 2139.8
C2-124300	1931.7	2262.8 2284.8	2262.8 2284.8
C2-124301	2077.7	2408.9 2430.9	2408.9 2430.9
C2-224300	2222.8	2553.9 2575.9	2553.9 2575.9
C2-224301	2368.8	2700.0 2722.0	2700.0 2722.0

For an explanation of how these values were calculated see Table 2-3.

Structures for these oligosaccharides are shown in Figures 2-5 and 3-5.

While PMP-labelling allowed the detection of sialylated oligosaccharides in positive-ion mode, it was apparent from the spectra of the three sets of equimolar standards that the ionization efficiency of the oligosaccharides decreased with increased SA content. The intensity of the monosialyl oligosaccharides was approximately one-third of that of the neutral glycans, and that of the disialyl oligosaccharides approximately one-third that of the monosialyl oligosaccharides.

The PMP-labelled N-linked glycans from the polyclonal IgGs and mAbs were then analyzed by MALDI-QqTOF-MS. The oligosaccharides were observed as protonated $[M+H]^+$ and sodiated $[M+Na]^+$ molecular ions (Figures 3-20 – 3-24). The mass accuracies in the complex sample glycan mixtures were as striking as with the glycan standard sets (Table 3-9); approximately 5 ppm (0.0005%).

Lastly, unlike peptides which show large variations in peak height as a function of structure and proton affinity, the relative abundances of related oligosaccharides can be related to their peak heights/areas in the mass spectra since the ionization efficiencies for each structure are essentially proportional (Kroon *et al.*, 1995; Harvey *et al.*, 1998). Therefore, similar to the results from FACE and HPAEC-PAD analyses, the contributions to mass spectra from structures lacking core-Fuc or those containing bisecting GlcNAc were relatively quite minor. The three main oligosaccharides for both polyclonal and monoclonal IgG were the three variants of the core-fucosyl biantennary chain with none, one, or two Gal. These results are entirely consistent with previous MALDI-TOF-MS profiles of oligosaccharides from polyclonal (Küster *et al.*, 1997; Raju *et al.*, 2000) and monoclonal (Ashton *et al.*, 1995a, 1995b; Kroon *et al.*, 1995) IgG.

Figures 3-20 – 3-21. MALDI-QqTOF-MS analysis of the polyclonal IgGs. Mass spectra of the PNGase F-released N-linked oligosaccharides from bovine and human polyclonal IgG, respectively. Monosaccharide symbols are defined in Table 1-1.

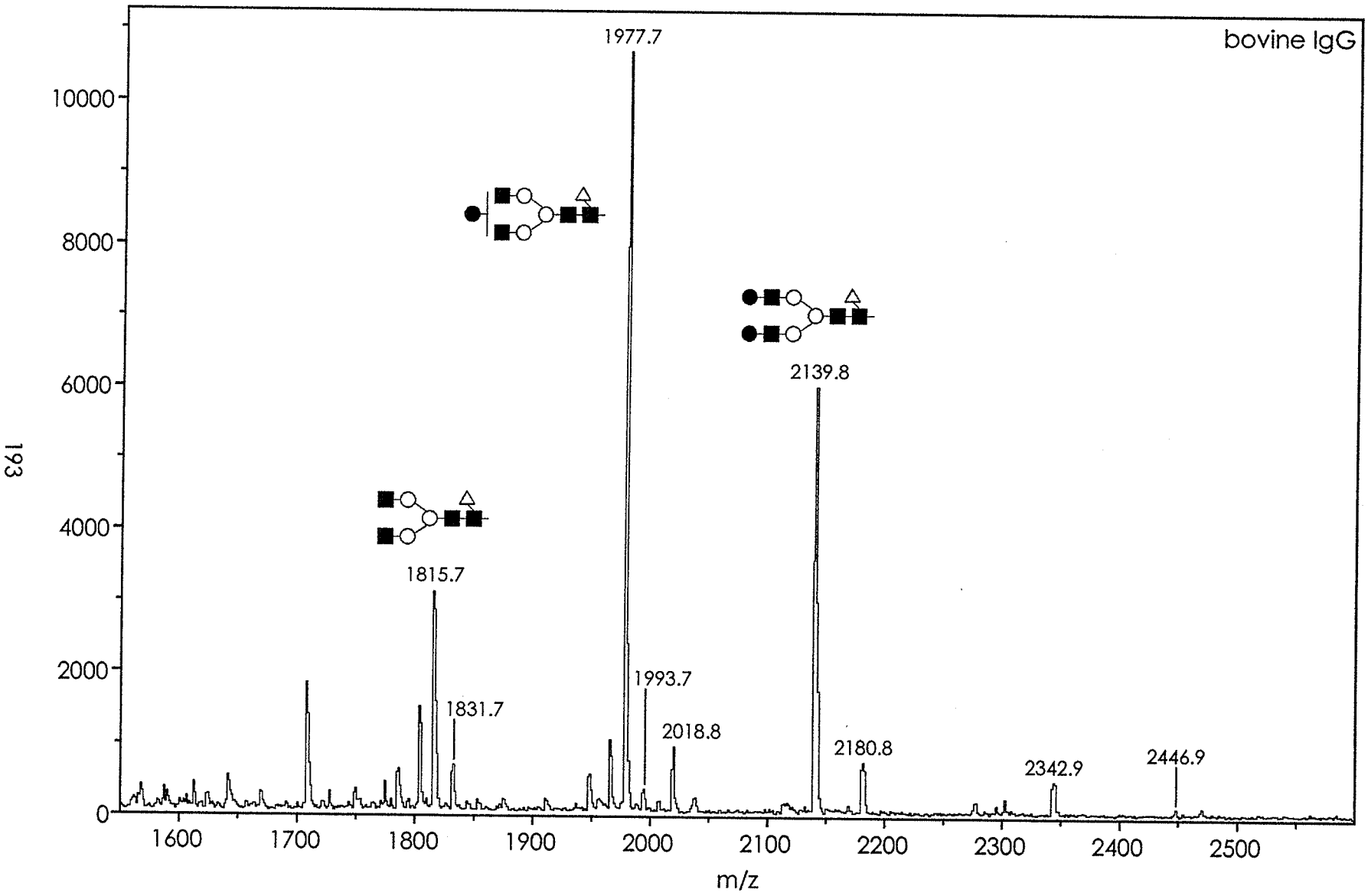
bovine IgG
1977.7
2139.8
1815.7
1831.7
1993.7
2018.8
2180.8
2342.9
2446.9
10000
8000
6000
4000
2000
0
1600
1700
1800
1900
2000
2100
2200
2300
2400
2500
m/z
193

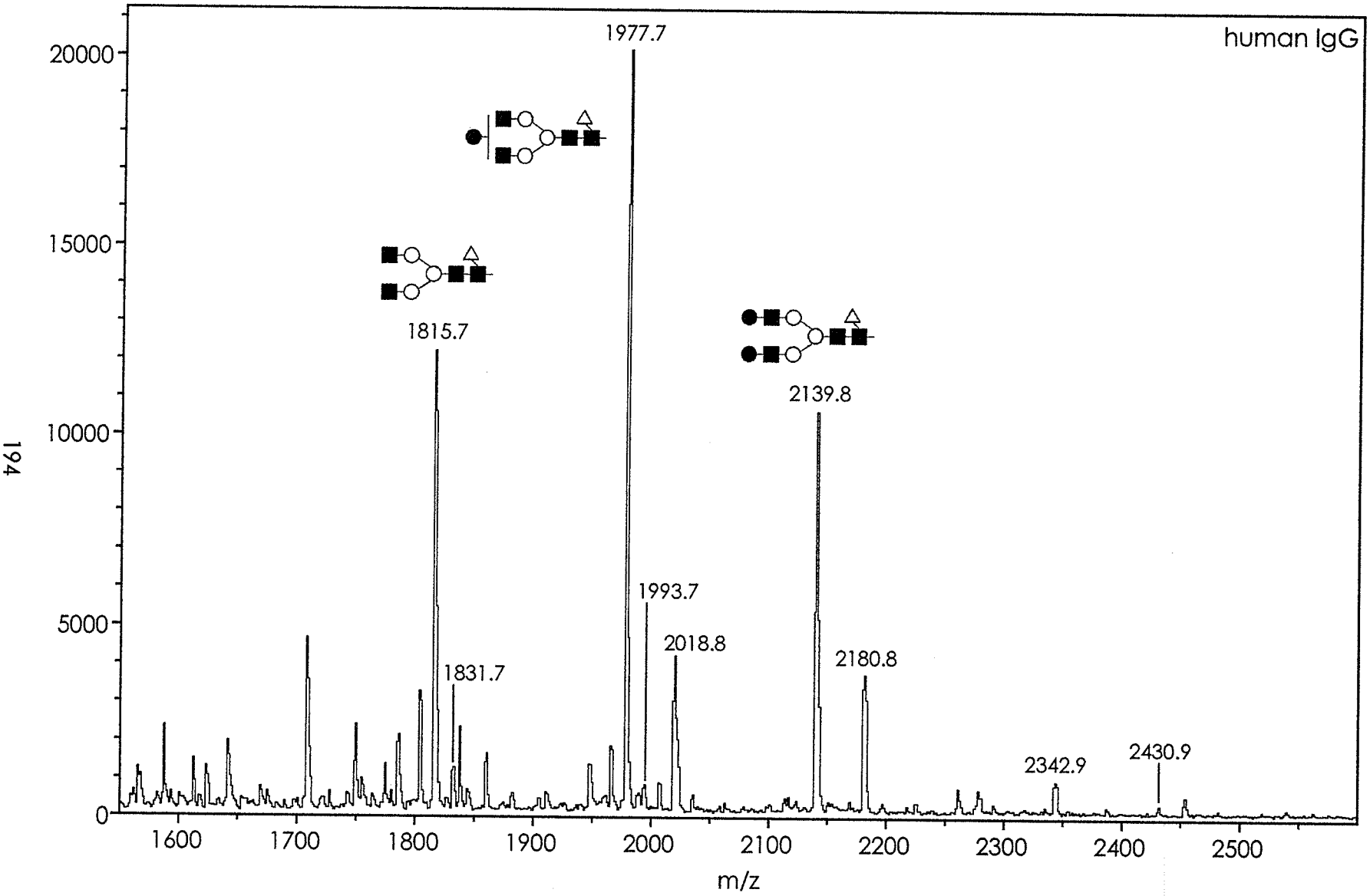
human IgG
1977.7
1815.7
2139.8
1993.7
2018.8
1831.7
2180.8
2342.9
2430.9
20000
15000
10000
5000
0
1600
1700
1800
1900
2000
2100
2200
2300
2400
2500
m/z
194

Figures 3-22 – 3-24. MALDI-QqTOF-MS analysis of the first set of mAbs. Mass spectra of the PNGase F-released N-linked oligosaccharides from the mAbs from the LH bioreactor (first set) in 10% DO, 50% DO, and 100% DO, respectively. Monosaccharide symbols are defined in Table 1-1.

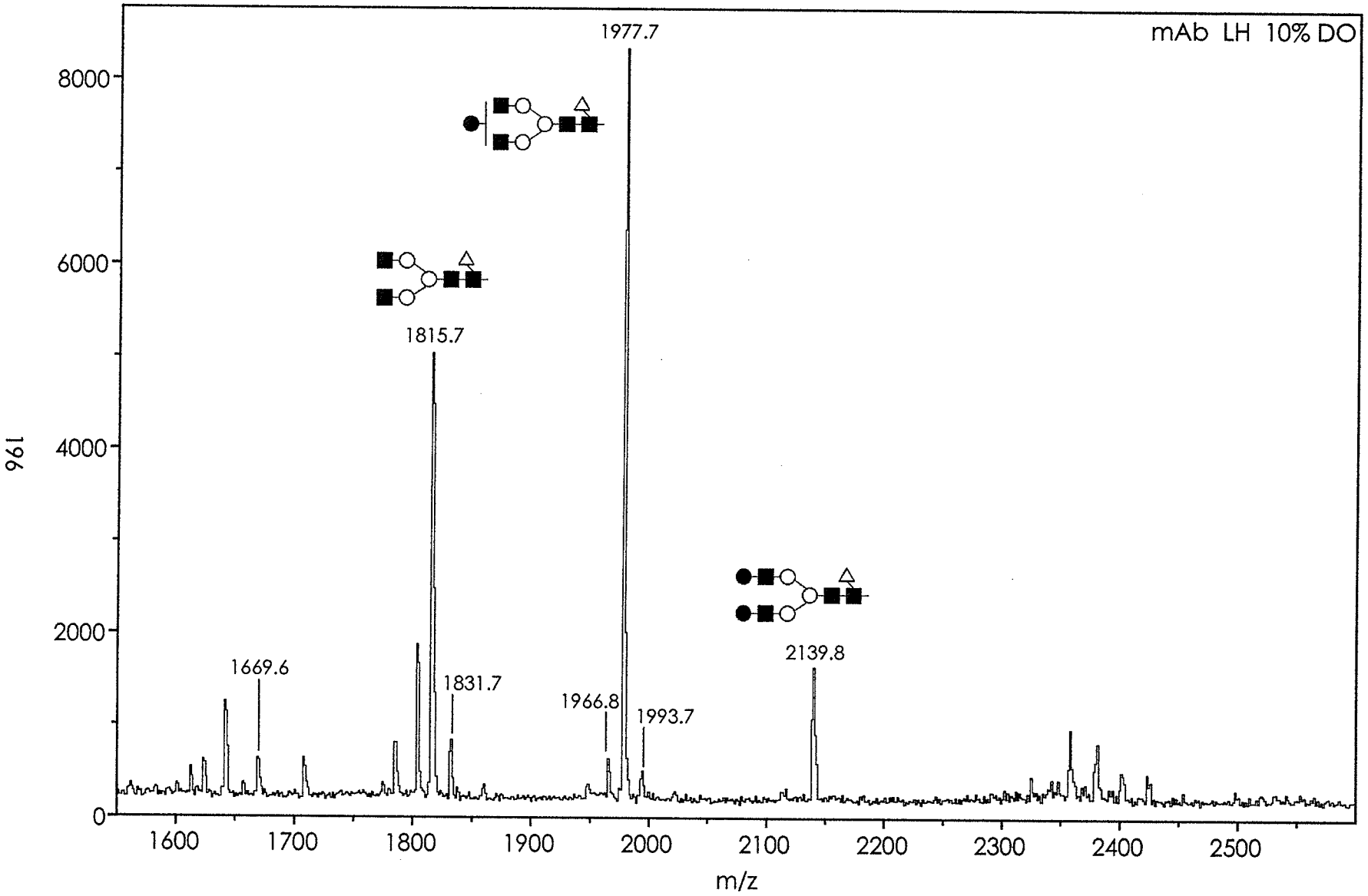
mAb LH 10% DO
1977.7
8000
6000
4000
2000
0
1815.7
1669.6
1831.7
1966.8
1993.7
2139.8
196
1600
1700
1800
1900
2000
2100
2200
2300
2400
2500
m/z

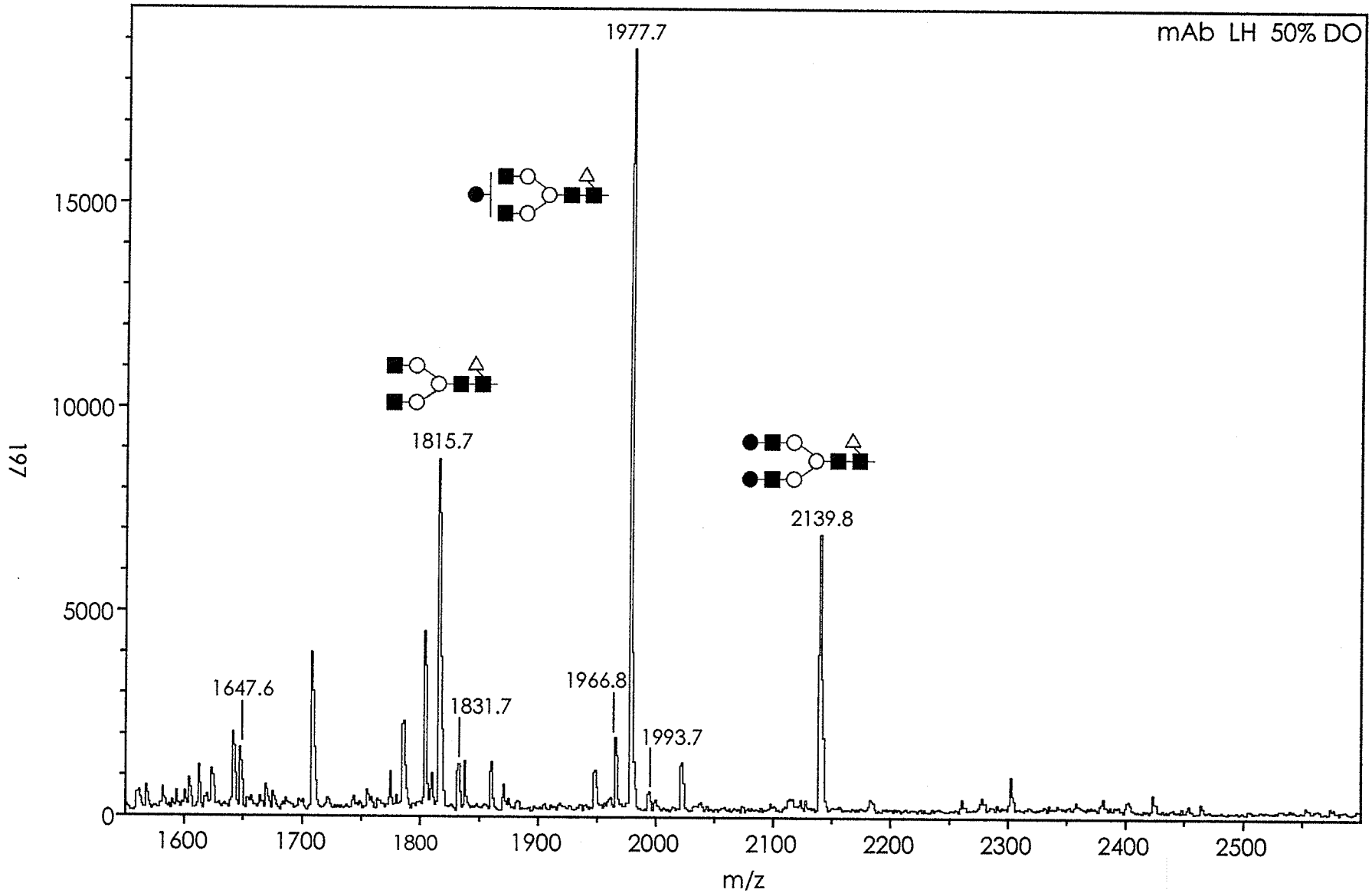
mAb LH 50% DO
1977.7
15000
10000
5000
0
197
1815.7
2139.8
1647.6
1831.7
1966.8
1993.7
1600
1700
1800
1900
2000
2100
2200
2300
2400
2500
m/z

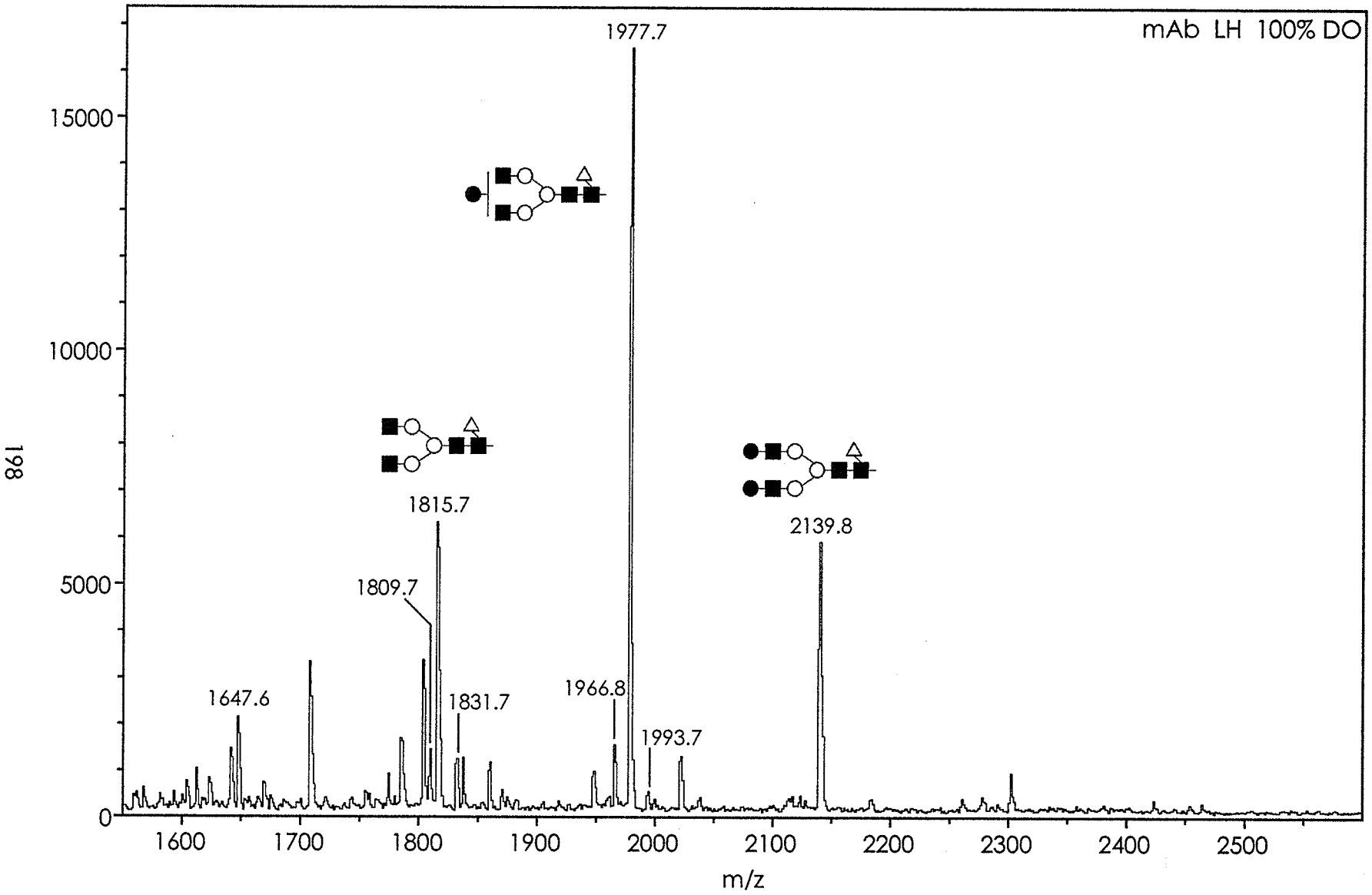
mAb LH 100% DO
1977.7
15000
10000
5000
0
198
1815.7
1809.7
2139.8
1647.6
1831.7
1966.8
1993.7
1600
1700
1800
1900
2000
2100
2200
2300
2400
2500
m/z

Table 3-9. Monoisotopic masses of the IgG and mAb PMP-labelled N-glycans.

Glycan code	Mono-isotopic molecular mass	PMP-labelled $[M+H]^+$ $[M+Na]^+$ ions	Observed bovine IgG ions	Observed human IgG ions	Observed mAb 10% DO ions	Observed mAb 50% DO ions	Observed mAb 100% DO ions
C2-004300	1316.5	1647.6 1669.6	– –	– –	– 1669.6	1647.6 –	1647.6 –
C2-004301	1462.5	1793.7 1815.7	– 1815.7	– 1815.7	– 1815.7	– 1815.7	– 1815.7
C2-004311	1666.6	1966.8 2018.8	– 2018.8	– 2018.8	1966.8 –	1966.8 –	1966.8 –
C2-014300	1478.5	1809.7 1831.7	– 1831.7	– 1831.7	– 1831.7	– 1831.7	1809.7 1831.7
C2-014301	1624.6	1955.7 1977.7	– 1977.7	– 1977.7	– 1977.7	– 1977.7	– 1977.7
C2-014311	1828.7	2158.8 2180.8	– 2180.8	– 2180.8	– –	– –	– –
C2-024300	1640.6	1971.7 1993.7	– 1993.7	– 1993.7	– 1993.7	– 1993.7	– 1993.7
C2-024301	1786.6	2117.8 2139.8	– 2139.8	– 2139.8	– 2139.8	– 2139.8	– 2139.8
C2-024311	1990.7	2320.9 2342.9	– 2342.9	– 2342.9	– –	– –	– –
C2-124300 (Neu5Ac)	1931.7	2262.8 2284.8	– –	– –	– –	– –	– –
C2-124300 (Neu5Gc)	1948.7	2278.8 2300.8	– –	– –	– –	– –	– –
C2-124301 (Neu5Ac)	2077.7	2408.9 2430.9	– –	– 2430.9	– –	– –	– –
C2-124301 (Neu5Gc)	2094.7	2424.9 2446.9	– 2446.9	– –	– –	– –	– –
C2-124311 (Neu5Ac)	2281.8	2612.0 2634.0	– –	– –	– –	– –	– –
C2-124311 (Neu5Gc)	2297.8	2628.0 2650.0	– –	– –	– –	– –	– –

For an explanation of how these values were calculated see Table 2-3.

Structures for these oligosaccharides are shown in Figures 2-5 and 3-5.

3.3.6 Glycosylation analysis summary

Approximately ten to twelve N-linked oligosaccharides were observed by HPAEC-PAD in the polyclonal IgGs and the mAbs, with a few less observed by FACE and about the same number by MALDI-QqTOF-MS. In HPAEC-PAD and FACE, the ultimate identification of several glycans was made tenuous due to a lack of resolution caused by the co-elution/co-migration of other candidate glycans. Only MALDI-QqTOF-MS had the sensitivity and resolution needed to identify the oligosaccharides. Unfortunately, because of the low levels of sialylated glyans in the mAb samples, and their decreased ionizabilities in positive-ion mode, they were not well observed in the spectra. However, the molecular masses from MS alone can not unequivocably distinguish between structures. It is the comparison and corroboration of results from HPAEC-PAD, FACE, and MALDI-QqTOF-MS for the standard and sample glycans that provide confidence in the assignment of these oligosaccharides. Further experiments using the power of collision-induced dissociation and selectivity of the MS/MS quadrupole were performed, but are beyond the scope of this work.

N-linked oligosaccharides obtained from bovine and human IgG had approximately the same incidence of core-Fuc (85-90%) and bisecting GlcNAc (5-15%), and the presence of at least one terminal Gal (75-85%). The incidence of sialylation was low and consisted solely of Neu5Gc in bovine IgG and almost entirely of Neu5Ac in human IgG. The results agree well with previous reports for bovine and human polyclonal IgGs (Parekh *et al.*, 1985; Hamako *et al.*, 1993; Küster *et al.*, 1997; Raju *et al.*, 2000).

N-linked oligosaccharides obtained from the murine mAbs had approximately the same incidence of core-Fuc (~95%) and bisecting GlcNAc (~5%) as polyclonal murine IgG (Mizuochi *et al.*, 1987; Hamako *et al.*, 1993; Raju *et al.*, 2000). The main effect of DO concentration on glycosylation of the mAb was a shift in the level of galactosylation of the chains. In this work, the optimum

DO concentration for maximum galactosylation of the mAb glycans was 100% DO, while the optimum for minimum galactosylation was less than 25% DO. In 25% DO and below, the chains were mainly agalactosyl (35-45%) or monogalactosyl (45-55%), with very little digalactosyl (10-15%) chains. In 50-125% DO there was a significant reduction in the amount of agalactosyl chains (15-25%), with a corresponding increase in the amount of monogalactosyl (50-55%) and digalactosyl (20-30%) chains, particularly the latter. In 150% DO galactosylation declined, with an increase in agalactosyl (25-30%) chains and a decrease in digalactosyl (15-20%) chains. Compared to the incidence of glycans with at least one terminal Gal in polyclonal murine IgG (~45%), the incidence in mAb from culture in 150% DO and less than 25% DO was considerably greater (55-70%), while from cultures in 50-125% DO was substantially greater (70-85%) (Mizuochi *et al.*, 1987; Hamako *et al.*, 1993; Raju *et al.*, 2000).

The incidence of sialylation was low, but increased slightly with the increase in galactosylation. This is reasonable since most SA attaches to Gal in N-glycans. The sialylation consisted mainly of Neu5Ac with a moderate contribution from Neu5Gc, unlike in polyclonal murine IgG, where Neu5Ac is the principal SA (Raju *et al.*, 2000).

3.4 Galactosyltransferase assays

The β1,4-GalT activities of the hybridoma cellular protein from the third set of cultures were determined. The cellular protein levels were measured at 50-85 $\mu g/10^6$ cells utilizing the BCA assay (Smith *et al.*, 1985). Previous work with the CC9C10 cell line (Petch, 1994) found cellular protein in the range of 50-200 $\mu g/10^6$ cells employing the Bradford assay (Bradford, 1976). The BCA assay has less protein-to-protein variability and is linear over a wider range of protein concentration than the Bradford assay (Stoschek, 1990). In addition, the

Bradford assay greatly overestimates (nearly doubles) the amount of IgG against BSA standards, while the BCA assay tends to only very slightly underestimate the amount of IgG against BSA standards (Stoschek, 1990). Consideration of the combination of these two effects brings the two cellular protein estimates closer together and gives more weight to the BCA assay results in this report.

The β1,4-GalT activities of CC9C10 cellular protein from the third set of cultures (1, 2, 5, 10, 25, & 50% DO in the NBS bioreactor) were remarkably similar in all six cultures (Figure 3-25). The difference between the duplicate experiments for each cell lysate at each timepoint was less than 10-15%. Since the β1,4-GalT activities were clearly unaffected by the DO concentration of the cultures, the mean activity was determined by averaging the data for all six cultures at each timepoint (Figure 3-26).

The β1,4-GalT activities showed a loss of linearity after 20 min of incubation (not shown). At the specific activities calculated in this work, approximately 75% of the UDP-^{3}H-Gal substrate was consumed after 20 min. The total consumption of substrate should be less than 25% to conform to the condition of constant substrate concentration assumed for Michaelis-Menten kinetics (Khatra *et al.*, 1974). However, linearity was excellent up to 20 min in all plots and there was exceptional agreement in the specific β1,4-GalT activity between plots.

Figure 3-25. β1,4-GalT activities from the third set of chemostat cultures. Hybridoma cellular protein from the third set of chemostat cultures (1, 2, 5, 10, 25, & 50% DO).

50% DO: filled squares

25% DO: open squares

10% DO: filled circles

5% DO: filled triangles

2% DO: open diamonds

1% DO: open circles

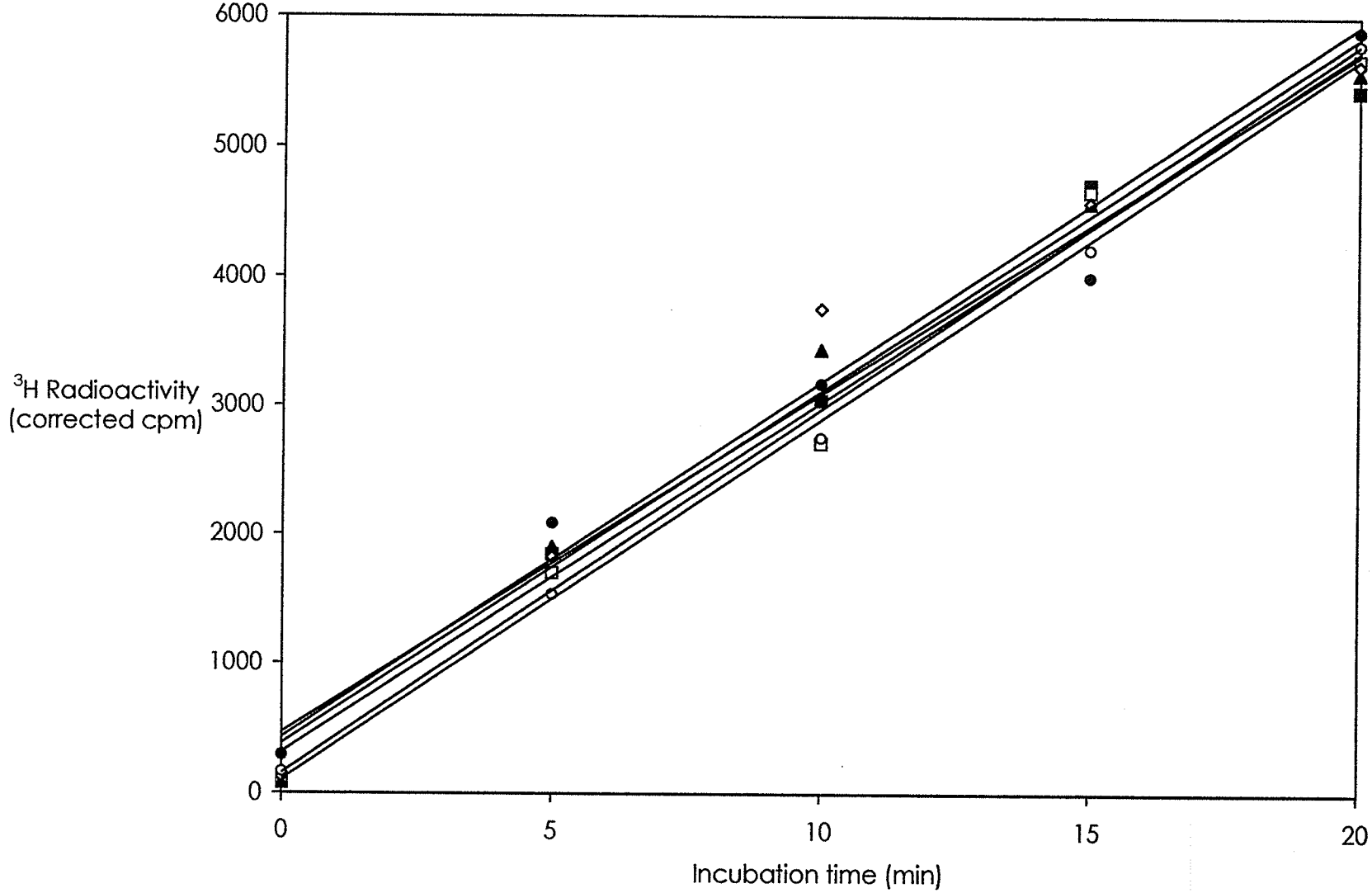
6000
5000
4000
3000
2000
1000
0
^{3}H Radioactivity (corrected cpm)
0
5
10
15
20
Incubation time (min)

Figure 3-26. Average β1,4-GalT activities from the third set of chemostat cultures.

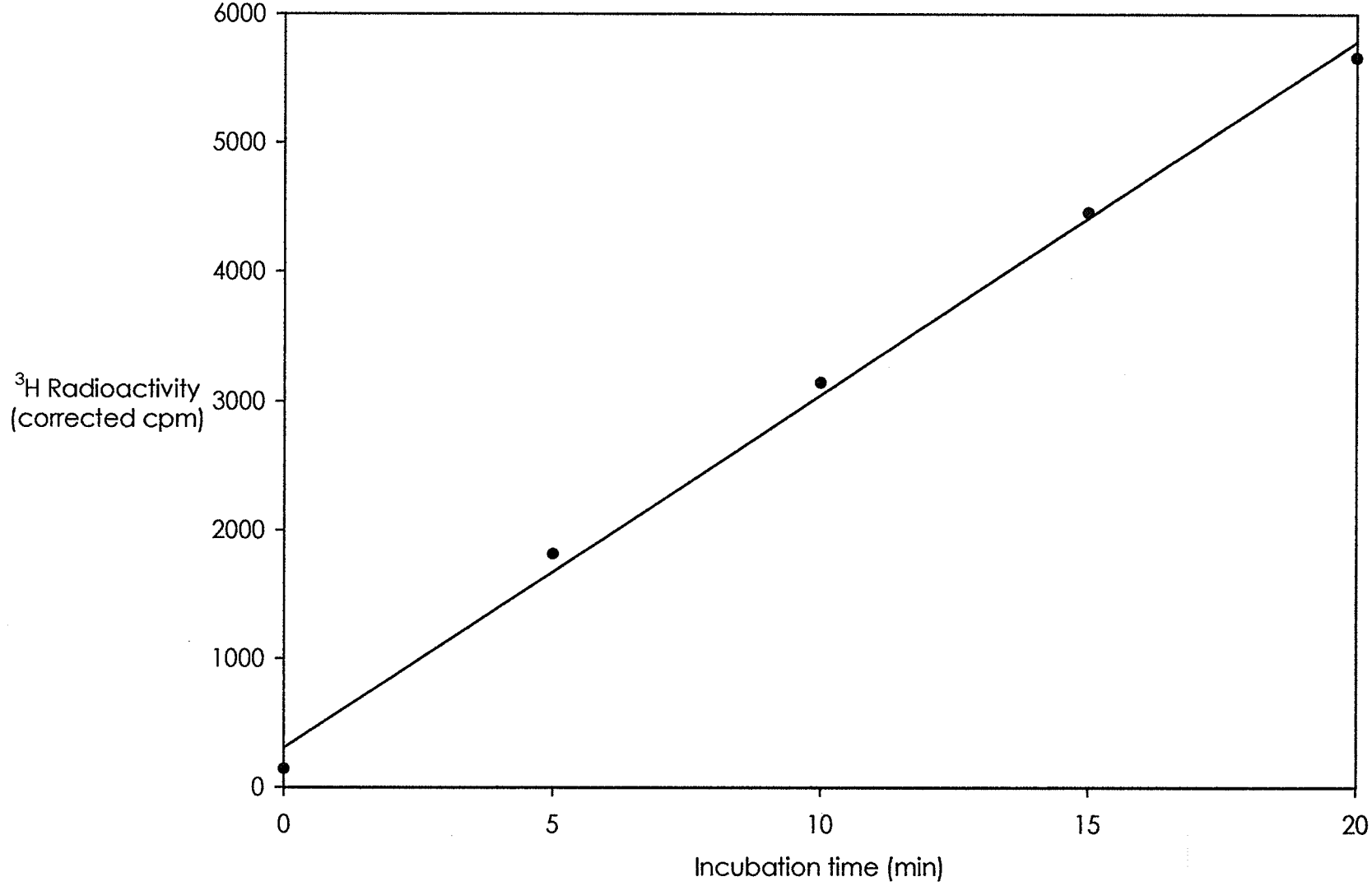
6000
5000
4000
3000
2000
1000
0
^{3}H Radioactivity
(corrected cpm)
0
5
10
15
20
Incubation time (min)

The specific β1,4-GalT activities for each of the six cultures were calculated as described (Section 2.8). The specific activities were exceptionally consistent, ranging from 222-238 pmol/mg/h, and were independent of the steady-state DO concentration of the cultures (Table 3-10). The average specific β1,4-GalT activity was 232 ± 8 pmol/mg/h. The average specific activity determined in this work for the CC9C10 lymphocytic B-cell hybridoma compares well with the specific β1,4-GalT activity of cultures of a human leukemic B-cell line, which was found to be 100-700 pmol/mg/h with macromolecular acceptors (Furukawa *et al.*, 1990). It should be noted that the cited study used the Lowry assay to determine cellular protein (Lowry *et al.*, 1951), which has greater protein-to-protein variability, is linear over a narrower range of protein concentration (especially lower concentrations), and is more sensitive to interfering buffer components than the BCA assay used in this work (Stoschek, 1990). This leads to greater error in the final values reported for β1,4-GalT activity. However, it should also be noted that β1,4-GalT incubations in Tris buffers, such as the one in this work, yield only about 80% the activity as incubations in an equal concentration of sodium cacodylate buffer (Sichel *et al.*, 1990).

Table 3-10. Specific β1,4-GalT activities from the third set of chemostat cultures.

Steady-state DO concentration (% of air saturation)	Specific activity (pmol/mg/h)
50	229 ± 16
25	238 ± 13
10	222 ± 18
5	231 ± 17
2	233 ± 22
1	236 ± 6
Average	232 ± 8

Chapter 4 – Discussion

4.1 Immunoglobulin G oligosaccharide structure and function

4.1.1 IgG and glycan structure

X-ray crystallographic studies of IgG-Fc fragments (Deisenhofer *et al.*, 1976; Huber *et al.*, 1976; Deisenhofer, 1981; Sutton & Phillips, 1983) and intact IgG (Silverton *et al.*, 1977; Harris *et al.*, 1998) have shown that, in contrast to other immunoglobulin domains, the two C_H2 domains do not form extensive associations. Instead,the N-linked biantennary oligosaccharides attached to Asn-297 of each heavy chain fill the resulting interstitial space, making contacts with each other and their respective C_H2 domains (Figure 4-1).

As with most glycoproteins, the glycosylation profiles (glycoforms) of polyclonal IgG are species-specific (Hamako *et al.*, 1993; Raju *et al.*, 2000). For example, galactosylation of the α1,6Man antennae in Fc glycans in the human and mouse species is more prevalent than that of the α1,3Man antennae (Fujii *et al.*, 1990; Mizuochi *et al.*, 1990; Masuda *et al.*, 2000; Raju *et al.*, 2000; Wright *et al.*, 2000). This is opposite to the β1,4-GalT specificity, which preferentially adds Gal to the α1,3Man antenna before the α1,6Man antenna in both bisected and non-bisected biantennary oligosaccharides (Pâquet *et al.*, 1984; Narasimhan *et al.*, 1985; Raju *et al.*, 2000). Interestingly, β1,4-GalT galactosylates the α1,6Man antennae preferentially in native human IgG_1, but the α1,3Man antennae in the denatured antibody (Fujii *et al.*, 1990; Wilson *et al.*, 1993). In another study, a series of truncated IgG peptide-deletion mutants were constructed such that the Asn-297 glycosylation sites were more exposed. Increased accessibility correlated with increased levels of galactosylation and sialylation of the oligosaccharides (Lund *et al.*, 2000). These results suggest steric interference in the activity of the glycosyltransferase by the protein portion of the antibody. This is supported by the increased galactosylation and sialylation of

Fc glycans of immunoglobulin A (IgA), where these glycosylation sites are surface accessible, over those of IgG-Fc, where they normally are not (Mattu *et al.*, 1998).

The ratio of the two N-glycan chains of the Fc are different from what would be expected from random pairing. Crystallographic experiments and oligosaccharide sequence studies have shown that there is a restriction in pairing of the two glycans across the domains (Rademacher *et al.*, 1986, 1996). The pairing of Fc oligosaccharides results in at least 50% of the α1,3Man antennae being devoid of Gal. This leads to there being different α1,3Man antennae for the oligosaccharide of each CH2 in some Fc. One α1,3Man antenna is devoid of Gal and the terminal GlcNAc interacts with the core of the opposing oligosaccharide; the other α1,3Man antenna extends outward between the domains with no apparent restrictions (Figure 4-2). The α1,6Man antennae interact with hydrophobic and polar amino acids in lectin-like pockets on the domain surfaces of their respective heavy chains (Axford *et al.*, 1987; Parekh *et al.*, 1989; Furukawa & Kobata, 1991; Rudd *et al.*, 1991; Wormald *et al.*, 1997). The restriction in glycan pairing highlights the importance of the terminal GlcNAc in the α1,3Man antennae and the terminal Gal in the α1,6Man antennae in establishing the specific carbohydrate-carbohydrate and carbohydrate-protein contacts, respectively. These associations effectively form a tether between the CH2 domains of the two heavy chains necessary to maintain the proper conformational arrangement of the Fc, as well as the hinge region, and shield the α1,3Man antennae from galactosylation (Lund *et al.*, 1996; Wormald *et al.*, 1997). These constraints also result in loss of flexibility of the α1,6 Man antennae.

Figure 4-1. Detail of the X-ray crystal structure of IgG_1. The internal nature of the Fc N-linked oligosaccharides is shown. The C_H2 domains are in wireframe (dark blue) and the oligosaccharides in spacefill (GlcNAc, light blue; Fuc, orange; Man, red; Gal, yellow). Note how the glycans fill the interstitial space between the two C_H2 domains. Compare this representation with the schematic for C_H2-domain tethering (Figure 4-2).

Created using the public-domain software RasMac v2.6 (copyright 1993-1996 by R. Sayle) (Sayle & Milner-White, 1995) and a composite IgG_1 crystal structure (Clark, 1997).

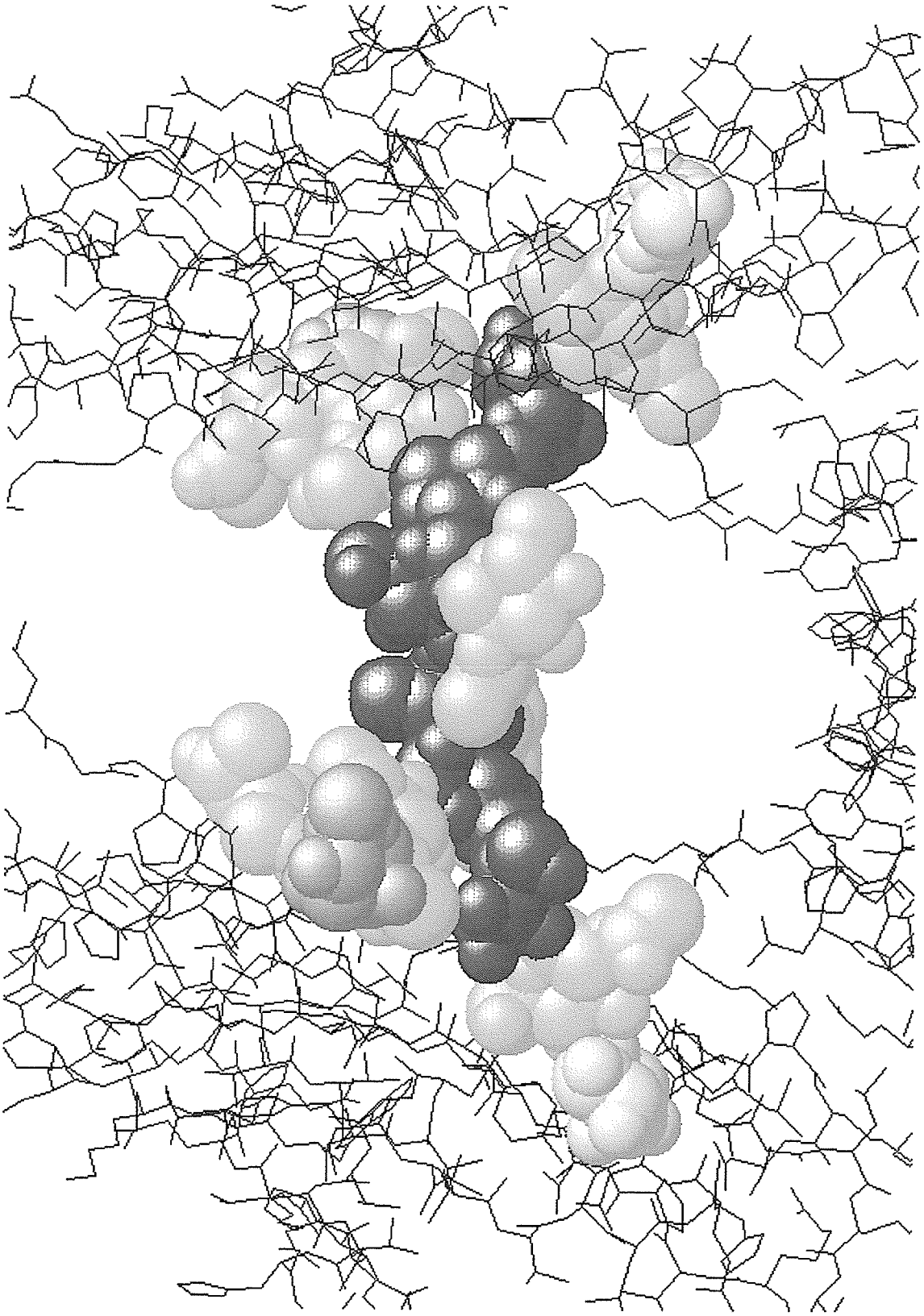

Figure 4-2. Tethering of the two CH2 domains by the Fc N-glycans. An increase in protein and glycan mobility is a result of hypogalactosylation. The arrow on the left shows the location of glycan-glycan interaction. Note that at least half of the glycans associated with the Fc must be not be galactosylated on the α1,3Man antennae, and that galactosylation of the α1,6Man antennae is critical for glycan-protein interaction. (Adapted from Parekh *et al.*, 1989.)

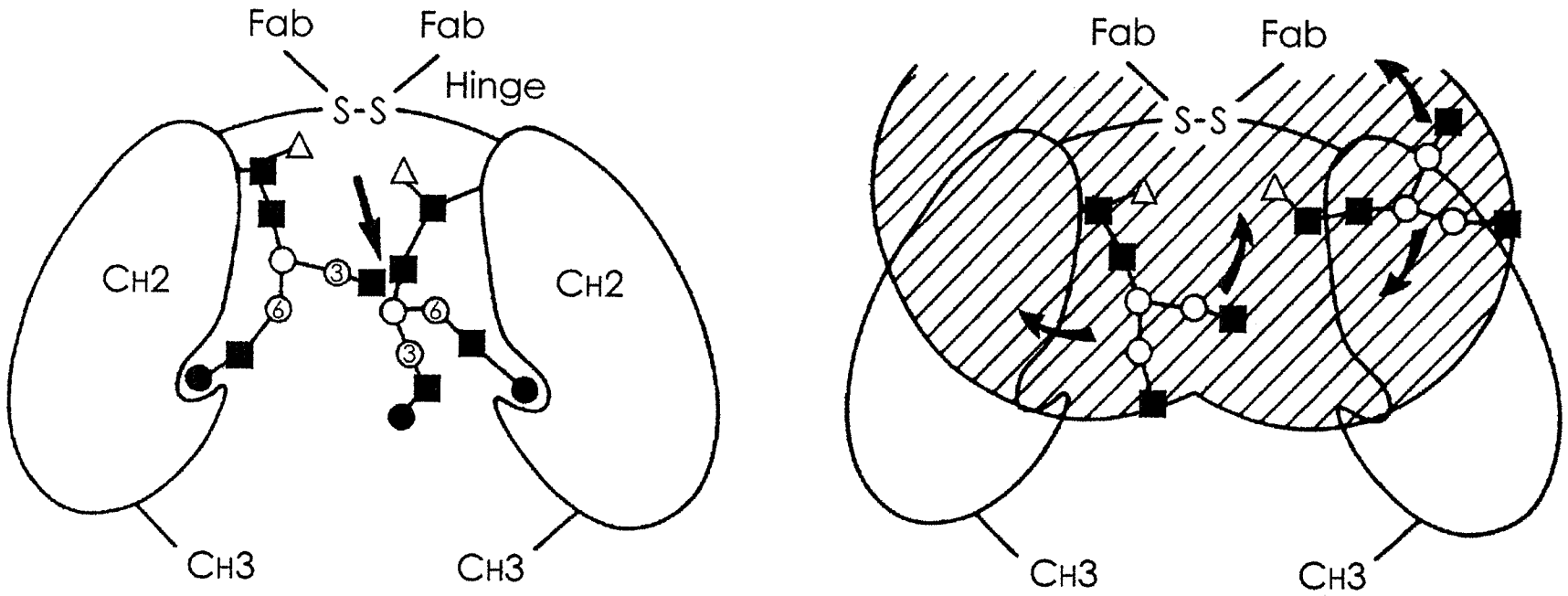
Fab
Fab
Hinge
S-S
CH2
CH2
CH3
CH3
Fab
Fab
S-S
CH3
CH3
Man
GlcNAc
Gal
Fuc

Therefore, one role of Fc glycans is to maintain the conformational arrangements of the C_H2 domains as well as the hinge regions (Dwek *et al.*, 1995). The differences in structure between normally glycosylated and non-glycosylated Fc fragments and whole IgG have been compared (Lund *et al.*, 1990; Matsuda *et al.*, 1990). Despite having quite similar structures overall, there is considerable disparity in structure between normally glycosylated and non-glycosylated Fc near the Asn-297 glycosylation site, which is reflected by differences in their effector functions (Walker *et al.*, 1989; Tao & Morrison, 1989; Lund *et al.*, 1990, 1996). The absence of Fc glycans abolishes the association of the C_H2 domains, mediated by the N-linked oligosaccharides, resulting in a lateral movement of the C_H2/hinge and C_H2/C_H3 regions relative to the normally glycosylated IgG. Agalactosyl oligosaccharides at Asn-297 have considerable dynamic freedom when compared to their galactosylated counterparts and the rest of the protein (Malhotra *et al.*, 1995; Wormald *et al.*, 1997) (Figure 4-2). Indeed, glycan mobility was reported to increase by thirty times when the Gal on the α1,6Man antenna was absent (Wormald *et al.*, 1997). A subsequent report failed to observe such a marked alteration, but still observed significant structural changes in the oligosaccharides and surrounding protein (Yamaguchi *et al.*, 1998).

Glycoprotein glycans are generally not rigid, as in crystal structures, but are flexible to varying degrees, with some residues or oligosaccharides possessing greater mobility than others (Homans, 1993; Qasba *et al.*, 1997). The flexibility of oligosaccharides has functional significance, although the most favoured conformation of the glycoprotein glycan free in solution may not be that of the oligosaccharide in its functional state (Pérez *et al.*, 1993; Rice *et al.*, 1993). Therefore, any interpretation of the effects of oligosaccharide conformation upon function must take dynamics into account (Rice *et al.*, 1993; Qasba *et al.*, 1997).

Molecular modelling and dynamics calculations of the core-fucosyl biantennary glycan typical of IgG has indicated considerable dynamic freedom in the α1,6Man antenna of the isolated Fc glycan as compared to the α1,3Man antenna (Mazurier *et al.*, 1991; Dauchez *et al.*, 1992). This appears to be the case in general for the α1,6Man antennae in an exhaustive survey of available crystallographic data for glycoproteins (Petrescu *et al.*, 1999). However, the conformational space of the α1,6Man antenna of the Fc glycan is restricted in the glycopeptide (Stuike-Prill & Meyer, 1990). In fact, the lectin-like interactions between each C_H2 domain and its own N-linked glycan result in severe distortion of the α1,6Man antenna, indicating the strong interactions that must be present between the Gal residue and the protein surface (Petrescu *et al.*, 1999). Again this emphasizes the role of the terminal Gal residues in the α1,6Man antennae in establishing the proper C_H2/hinge and C_H2/C_H3 conformations. It is becoming apparent that N-glycosylation of a folded protein can have a significant stabilizing effect on large regions of the backbone structure (Wormald & Dwek, 1999).

4.1.2 Functional relevance of IgG glycosylation

Unlike most glycoproteins, the oligosaccharides of IgG are sequestered internally between the two C_H2 domains. One consequence of this is that unlike other serum glycoproteins lacking sialylation, normal IgG is not rapidly cleared. The terminal Gal residues of the Fc N-glycans are hidden from recognition by the hepatic asialoglycoprotein receptor. However, the absence of Gal on the α1,6Man antennae abolishes specific associations between the C_H2 domains mediated by the N-linked oligosaccharides. The loss of this tether, and the resultant increase in oligosaccharide mobility, lead to conformational changes in the C_H2/hinge and C_H2/C_H3 regions, which result in the observed biological and clinical effects attributed to agalactosyl IgG.

The absence of Gal and the alterations in protein conformation and oligosaccharide mobility lead to exposure of the underlying GlcNAc residues, which become accessible to endogenous lectins such as the circulating mannose-binding lectin (MBL) and the hepatic mannose receptor (MR) (Rademacher, 1993, 1994; Wormald *et al.*, 1997). These lectins recognize GlcNAc in addition to Man, and activate the complement cascade. This may contribute to the pathogenesis of RA (Section 4.2.2) by providing mechanisms for activation of the classical complement immune system response by IgG binding to circulating MBL (Malhotra *et al.*, 1995). The main function of hepatic Kupffer cells is to bind invaders to their MR and present pieces of the invaders (*i.e.* haptens) to immune cells for the production of new antibodies directed against them. So, in addition to the activation of the humoral immune system (*i.e.* complement), capture of agalactosyl IgG by MR may result in a directed autoimmune response against IgG (Dong *et al.*, 1999).

Alterations in the level of galactosylation of Fc glycans have been shown to impact the immunological functions of IgG. For example, the functional activities of a monoclonal IgG after the sequential removal of SA, Gal, and total glycan have been examined (Boyd *et al.*, 1995). It was found that the complete removal of total glycan abolished complement-mediated cell lysis (CMCL) and antibody-dependent cell-mediated cytotoxicity (ADCC), while removing only SA had no effect. By contrast, the removal of Gal in addition to SA reduced CMCL but did not affect ADCC. Similar results were obtained for monoclonal IgGs expressed in several biosynthetically-defective CHO cell lines (Wright & Morrison, 1998). This indicates a differential requirement for Gal in these activities, and a potential avenue for the 'decoupling' of these functions (Jefferis & Lund, 1997; Jefferis *et al.*, 1998). Indeed, the level and branch specificity of IgG-Fc galactosylation has become a primary analytical consideration in the

production of therapeutic mAbs (Ma & Nashabeh, 1999; Raju *et al.*, 1999, 2000, 2001).

Protein engineering studies have also shown that the Fc oligosaccharide core structure influences FcγR and C1q binding, whereas the terminal residues influence interaction with circulating MBL and hepatic MR (Jefferis, 1993, Abadeh *et al.*, 1997; Jefferis & Lund, 1997; Jefferis *et al.*, 1998; Mimura *et al.*, 2000, 2001).

Experiments with site directed mutagenesis of the amino acids in the Fc portions of human, murine, and chimeric IgG that make contact with Asn-297 glycans show that the outer antennae Gal and GlcNAc residues do not affect recognition of the Fc by all Fc receptors (Lund *et al.*, 1995, 1996; Jassal *et al.*, 2001). However, the presence of the trimannosylchitobiose core structure appears to be important in the recognition of IgG by all Fc receptors. The emerging understanding of the influence of oligosaccharide-protein interactions on the protein conformation and biological function of IgG suggests a potential to generate novel protein sequences or glycoforms of IgG having unique or customized profiles of effector functions (Jefferis, 1991; Jefferis *et al.*, 1994, 1995, 1998). For example, in a series of truncated IgG peptide-deletion mutants, increased accessibility of the Asn-297 glycosylation site correlated with increased levels of galactosylation and sialylation of the oligosaccharides (Lund *et al.*, 2000). These changes influenced the thermal stabilities and effector functions of the constructs (Lund *et al.*, 2000; Mimura *et al.*, 2000).

The potential for glycosylation machinery remodelling by the use of certain mutant cell lines or by the expression of endogenous glycosyltransfersases has been explored (Stanley 1992; Stanley & Ioffe, 1995; Umaña & Bailey, 1997; Wright & Morrison, 1997, 1998; Jassal & Jenkins, 1998; Grabenhorst *et al.*, 1999; Weikert *et al.*, 1999; Lee *et al.*, 2001; Raju *et al.*, 2001). This includes protein and glycosylation engineering of IgG to modulate and optimize particular functions

(Abadeh *et al.*, 1997; Wright & Morrison, 1997, 1998; Umaña *et al.*, 1999; Weikert *et al.*, 1999; Mimura *et al.*, 2000; Wright *et al.*, 2000; Jassal *et al.*, 2001).

4.2 Physiological changes in galactosylation of IgG-Fc glycans

4.2.1 IgG galactosylation fluctuates with age and pregnancy

The overall level of galactosylation of serum IgG is parabolic with age, with a maximum at about 40-45 years, declining rapidly thereafter (Parekh *et al.*, 1988b; Sumar *et al.*, 1990; Bodman *et al.*, 1992; Yamada *et al.*, 1997; Shikata *et al.*, 1998). Increases in agalactosyl IgG correlate with a weakened immune system. Interestingly, the amount of monogalactosyl glycans is remarkably constant and does not vary with age (Bodman *et al.*, 1992; Rademacher *et al.*, 1996). The increase in the level of agalactosyl glycans is largely a result of a proportional decrease in the level of digalactosyl glycans. This is strikingly comparable to the results reported in this work. The level of monogalactosyl oligosaccharides was relatively consistent in all DO concentrations, and the observed increases in agalactosyl glycans were chiefly at the expense digalactosyl glycans (Section 4.4.2).

Galactosylation of IgG glycans also increases during pregnancy (Rook *et al.*, 1991; Williams *et al.*, 1995; Alavi *et al.*, 2000). In addition, in paired samples of fetal and maternal IgG, a higher level of galactosylation was observed in the fetal IgG, indicating selective placental transport of galactosylated IgG (Williams *et al.*, 1995; Kimura *et al.*, 2000). This suggests that the increased galactosylation in placental IgG and pregnant females enhances neonatal immunity (Kimura *et al.*, 2000).

Alterations in IgG galactosylation in both normal and disease states provide strong evidence that the IgG glycoform ratio is not static and is a highly regulated event (Rademacher, 1991). Indeed, during the immune response to an antigen in a mouse model, the galactosylation of the specific monoclonal

IgG changed, while the galactosylation of total serum IgG showed little variation (Lastra *et al.*, 1998).

4.2.2 IgG galactosylation decreases in rheumatoid arthritis

Serum IgG from patients with rheumatoid arthritis (RA) contains the same set of N-linked biantennary oligosaccharides found in normal individuals, although in very different and characteristic proportions (Mullinax & Mullinax, 1975; Mullinax *et al.*, 1976; Parekh *et al.*, 1985, 1988c; Rademacher *et al.*, 1986; Furukawa & Kobata, 1991; Rudd *et al.*, 1991; Rahman & Isenberg, 1996). In RA, the incidence of structures lacking Gal is dramatically increased. The decreased galactosylation is almost entirely due to changes in the Fc glycans. Further, these changes are restricted only to RA and a limited number of other rheumatological disorders, and are not found in other disorders with an acute or chronic inflammatory process (Rademacher *et al.*, 1988b; Tomana *et al.*, 1988; Parekh *et al.*, 1989; Pilkington *et al.*, 1996; Axford, 1999; Watson *et al.*, 1999).

Decreased glycosylation of IgG in RA is not a generalized disorder, since the N-linked oligosaccharides of other serum glycoproteins are normally galactosylated (Rademacher *et al.*, 1986). For example, the N-linked glycans of IgA, the second most abundant immunoglobulin in serum, accounting for about 15% of total serum immunoglobulin (Burton, 1987; Putnam, 1987), are normally more completely processed than those of IgG and show no evidence of RA-associated changes (Field *et al.*, 1994; Mattu *et al.*, 1998). It has been suggested that the reason that IgA is not hypogalactosylated in RA is because the defect in RA is restricted to IgG-producing cells (Field *et al.*, 1994), or because of structural differences in the antibodies resulting in increased accessibility of the IgA glycans compared to IgG glycans (Mattu *et al.*, 1998). Increased levels of agalactosyl IgG are therefore diagnostic for RA and can predict rheumatic episodes for those not already presenting clinical symptoms (Tomana *et al.*,

1994). An increased proportion of agalactosyl IgG correlates with increased disease activity and poor prognosis (Parekh *et al.*, 1988c; Van Zeben *et al.*, 1994; Bodman-Smith *et al.*, 1996).

It has been previously mentioned that galactosylation of IgG glycans increases during pregnancy. Interestingly, in women with RA and with elevated agalactosyl IgG glycoforms, the increase in galactosylation during gestation is correlated with remission of the disease (Rook *et al.*, 1991; Williams *et al.*, 1995; Alavi *et al.*, 2000). This is followed by a return to elevated agalactosyl IgG levels commensurate with post-partum recurrence of RA.

Comparative FACE studies of the IgG oligosaccharides from normal subjects and RA patients (MacGillivray *et al.*, 1995; Frears & Axford, 1997; Martin *et al.*, 2001) show remarkable similarities to the results reported here. They describe three main bands of approximately equal intensity in both pooled human IgG and in the IgG from normal subjects, resembling the FACE results for both 50 and 100% DO reported in this work. However, the IgG from RA patients display banding patterns similar to the results for 10% DO reported here, with increased intensity of the band corresponding to the smallest glycan and decreased intensity of the band corresponding to the largest. They attribute these changes to the decrease in galactosylation of the core-fucosyl biantennary glycan known to occur in RA. This work has shown that the FACE glycosylation profile of the mAb at typical DO concentrations (*e.g.* 50% DO) is similar to control serum IgG, and that the profile at lower DO concentrations is similar to the glycan profile of serum IgG in RA (MacGillivray *et al.*, 1995; Frears & Axford, 1997; Martin *et al.*, 2001).

4.2.2.1 Pathogenesis of rheumatoid arthritis

As discussed earlier, agalactosyl oligosaccharides have considerable dynamic freedom compared to monogalactosyl and digalactosyl

oligosaccharides. This, and the loss of the tether between CH2 domains, alters the CH2/hinge and CH2/CH3 region structures. This not only affects Fc receptor binding, but may also contribute to RA by the exposure of critical antigenic sites on the protein, as well as the lectin-like pocket, which would be free to interact with other carbohydrate ligands (Parekh *et al.*, 1985, 1988c; Rademacher, 1991; Leader *et al.*, 1995).

Rheumatoid factors (RFs) are IgM, IgG, and IgA autoantibodies that bind preferentially to the Fc portion of agalactosyl IgG to form RF-IgG complexes (Soltys *et al.*, 1994, 1995; Newkirk, 1996; Sutton *et al.*, 1998). Therefore, agalactosyl IgG is itself antigenic. Indeed, agalactosyl IgG can passively transmit disease in mouse models of RA (Rademacher *et al.*, 1994; Thompson *et al.*, 1996). The terminating GlcNAcs of agalactosyl IgG also become exposed to circulating MBL, activating complement directly in the joint where autoantibody is bound to collagen (Leader *et al.*, 1995; Malhotra *et al.*, 1995; Rudd *et al.*, 1995). Interestingly, the glycans of IgG-RFs in patients with RA have significantly reduced galactosylation even compared to the already hypogalactosylated RA IgG (Matsumoto *et al.*, 2000).

Reductions in galactosylated IgG have been attributed to a decrease in the β1,4-GalT activities in circulating peripheral, but not splenic, B cells (and to a less significant extent, T cells) from RA patients compared to age-matched controls (Axford *et al.*, 1987, 1992; Axford, 1988; Furukawa *et al.*, 1990; Wilson *et al.*, 1993; Alavi & Axford, 1995a, 1995b, 1996). Congruently, cultures of peripheral B cells from RA patients produce higher proportions of agalactosyl IgG than controls (Bodman *et al.*, 1992). Transfection of human B cells with the classical β1,4-GalT1 was shown to be enough to increase the galactosylation of IgG (Keusch *et al.*, 1998a). However, in RA, levels of both B-cell β1,4-GalT mRNA and protein remain consistent while β1,4-GalT activity decreases (Jeddi *et al.*, 1996; Keusch *et al.*, 1998b). While no change was observed in the binding of

agalactosyl substrates, a decreased affinity for UDP-Gal has been reported (Furukawa *et al.*, 1990). This suggests that the activity of β1,4Gal-T may be regulated post-translationally by reversible serine phosphorylation, altered glycosylation, disulfide bond formation, or protein folding.

It has also been recently established that the β1,4-GalT activity in the serum from RA patients is increased compared to controls, and is correlated to the extent of clinical activity of the disease (Alavi & Axford, 1997). The increase in serum β1,4-GalT activity is converse to the decrease in B-cell intracellular activity. This appears to indicate an increase in release of the enzyme as a consequence of synovial inflammation. The proteolytic cleavage and release of other Golgi membrane glycosyltransferases such as SATs in response to inflammation is well established (Lammers & Jamieson, 1988, 1990; McCaffrey & Jamieson, 1993; Richardson & Jamieson, 1995).

However, compared to the galactosylation of free agalactosyl oligosaccharides with β1,4-GalT, the glycans of denatured IgG are galactosylated very slowly, while those of native IgG is minimal even after extended reaction times (Fujii *et al.*, 1990; Wilson *et al.*, 1993). These observations suggest that changes in the levels of β1,4-GalT may have little effect on changing the extent of IgG galactosylation (Rademacher *et al.*, 1995, 1996). Another mechanism for the hypogalactosylation of IgG in RA has been proposed (Section 4.6.1).

Rheumatoid arthritis has been studied in several mouse models. The degree of pathology in these models is also correlated with the level of agalactosyl IgG (Mizuochi *et al.*, 1990; Bond *et al.*, 1990; Thompson *et al.*, 1992, 1996; Bodman *et al.*, 1994) and B-lymphocyte β1,4-GalT activity (Axford *et al.*, 1994; Jeddi *et al.*, 1996; Alavi *et al.*, 1998). Mouse models have shown that pregnancy affects the incidence and severity of arthritis (Thompson *et al.*, 1992). However, unlike in humans, both the level of splenic β1,4-GalT mRNA and β1,4-

GalT activity were unaffected by pregnancy, indicating some other regulatory mechanism (Jeddi *et al.*, 1997). This gives further credence to the postulate that the observed decrease in β1,4-GalT activity in human RA is not the primary cause of decreased IgG galactosylation (Rademacher *et al.*, 1995, 1996).

4.3 Cell culture and glycosylation

The glycosylation of secreted glycoproteins can be affected by changes in the physicochemical environment of the producing cells. As mentioned above, the IgG glycoform distribution has been shown to change with age, pregnancy, and rheumatic disease. Since IgG glycosylation is responsive to normal physiological changes and certain disease states, it is not surprising that different cell culture systems and conditions may affect the glycosylation of mAbs and other recombinant proteins (Goochee & Monica, 1990; Cumming, 1991; Goochee *et al.*, 1991, 1992; Goochee, 1992; Parekh, 1991; Rademacher, 1993, 1994; Andersen & Goochee, 1994; Jenkins & Curling, 1994; O'Neill, 1994; Parekh, 1994a; Gawlitzek *et al.*, 1995a, 1995b; Jenkins, 1995; Jenkins *et al.*, 1996).

4.3.1 Cell culture and monoclonal antibody glycosylation

The pursuit for optimal cell culture conditions and process control parameters for production of mAbs is a continuous enterprise (Lavery *et al.*, 1985; Reuveny *et al.*, 1986, 1987; Bibila & Robinson, 1995; Moran *et al.*, 2000). For example, a monoclonal IgG_1 produced from NS0 cells in fed-batch culture contained more high-mannose and truncated-complex glycans with increasing age of the culture (Robinson *et al.*, 1994). Monoclonal IgG_1 produced in perfusion cultures in a high-density hollow-fibre bioreactor showed higher amounts of truncated-complex oligosaccharides in serum-free versus serum-containing culture (Kloth *et al.*, 1999). These experiments also demonstrated an increase in truncated-complex glycans with an increase in culture duration.

Lower dilution rates in continuous culture of a murine hybridoma resulted in compromised mAb integrity due to increased sialylation of heavy chains and varied lectin affinity (Mohan *et al.*, 1993). Higher dilution rates produced mAbs of consistent oligosaccharide heterogeneity. Increases in N-linked oligosaccharide size and variability also increased with culture duration (Mohan *et al.*, 1993).

Monoclonal antibodies are glycosylated differently when produced in ascites or by a variety of cell culture techniques with serum-free and serum-supplemented media (Patel *et al.*, 1992; Maiorella *et al.*, 1993; Monica *et al.*, 1993; Black *et al.*, 1995; Marino *et al.*, 1997). Stepwise adaptation from serum-containing to serum-free media of batch cultures of a mAb-producing NS0 cell line resulted in progressive increases in agalactosyl Fc N-glycans (Hills *et al.*, 1999).

The Fc N-glycans of murine monoclonal IgG_{2b} and various chimeric murine-human antibodies expressed in a murine cell line were more highly galactosylated in static batch cultures than in hollow fibre bioreactors or ascites (Lund *et al.*, 1993a, 1993b). Various human monoclonal IgG antibodies, produced by Epstein-Barr virus (EBV)-transformed B-cell lines in serum-free media, were more highly galactosylated in low-density batch culture than in high-density hollow fibre bioreactors (Kumpel *et al.*, 1994). Decreased galactosylation correlated with decreased activity of some effector functions (Kumpel *et al.*, 1994). Similarly, the heavy chain glycosylation of a murine mAb exhibited marked decreases in complexity as culture intensity was increased from continuous stirred tank bioreactor to fluidized bed bioreactor to hollow fibre bioreactor (Schweikart *et al.*, 1999). The glycoform profile of another mAb was also dependent on whether the murine hybridoma was grown in perfusion culture in a stirred tank bioreactor or a hollow fibre bioreactor (Marino *et al.*, 1997).

Further physiological influences on recombinant IgG glycosylation have been reported (Shah *et al.*, 1998; Nahrgang *et al.*, 1999). In addition, it is well established that glycosylation is affected by clonal variation and that transformation and transfection events themselves may be sufficient to activate cryptic glycosyltransferase genes and alter glycosylation machinery (Rothman *et al.*, 1989; Jefferis *et al.*, 1990; Tandai *et al.*, 1991; Vandamme *et al.*, 1992; Cole *et al.*, 1993; Cant *et al.*, 1994; Jenkins & Curling, 1994; Kumpel *et al.*, 1994; Rademacher, 1994; Bergwerff *et al.*, 1995; Nahrgang *et al.*, 1999).

The fact that cell selection and cell culture conditions can affect glycosylation has obvious implications for the development and production of glycoproteins for diagnostic and therapeutic use. Changes in the biological activities of mAbs as a consequence of altered glycosylation have been observed when they are expressed in different cell lines (Lifely *et al.*, 1995; Sheeley *et al.*, 1997) and under different culture conditions (Gauny *et al.*, 1991; Maiorella *et al.*, 1993; Tachibana *et al.*, 1994, 1996; Black *et al.*, 1995; Lifely *et al.*, 1995; Sheeley *et al.*, 1997).

4.4 DO effect on monoclonal antibody glycosylation

4.4.1 DO in mammalian cell cultures

Mammalian cell cultures in controlled bioreactors are typically supplied with 30-60% DO in order to maintain optimal growth, although some cell lines may be adapted to grow at much lower (Miller *et al.*, 1987; Ozturk & Palsson, 1990) and much higher (van der Valk *et al.*, 1985; Oller *et al.*, 1989) DO concentrations. To date, surprisingly very little of the effects of DO on glycosylation of proteins have been studied. For instance, in the production of human follicle stimulating hormone (FSH) from CHO cells in perfusion culture, the DO concentration was varied from 10-90% (Chotigeat *et al.*, 1994). Sialyltransferase activity, SA content, and specific productivity all increased with

greater DO. By contrast, there was little change in the N-glycosylation of tissue-type plasminogen activator (t-PA) from CHO cells in microcarrier perfusion culture under normal, mildly hypoxic, severely hypoxic, and anoxic conditions (Lin *et al.*, 1993). Another study also found that anoxic conditions in perfusion culture for short time periods did not alter the N-glycosylation of an interleukin-2 variant from baby hamster kidney (BHK) cells (Gawlitzek *et al.*, 1995a, 1995b).

A major limitation of the experiments reported above is that they were not performed at metabolic steady states. Chemostat cultures at steady state are a useful means of studying the metabolism of cells because they are held in an equilibrium under constant and defined physiological conditions, where no variations in culture parameters or cell metabolism occur. The effect of a single parameter, such as the DO concentration, can be distinctly studied by the perturbation and re-establishment of steady state. The variability and uncertainty of serum content is also avoided if serum-free medium is used. However, hybridoma cells undergo physiological and metabolic changes during the adaptation from serum-containing to low serum and serum-free media, and this must be considered (Ozturk & Palsson, 1991a, 1991c).

4.4.2 Galactosylation of the mAb glycans was affected by DO

In this work, glycosylation analysis of the monoclonal IgG_1 samples by FACE, HPAEC-PAD, and MALDI-QqTOF-MS indicated the predominant N-linked structures were core-fucosyl asialyl biantennary glycans with varying galactosylation. There were also minor amounts of monosialyl oligosaccharides and trace amounts of afucosyl oligosaccharides. Integration and statistical analysis of the data indicated obvious shifts in the of level of galactosylation of the biantennary glycans as the DO concentration was adjusted.

Alterations of the steady-state DO concentration in serum-free chemostat culture of the CC9C10 hybridoma dramatically affected galactosylation of the

secreted mAb. The level of galactosylation of the Fc N-linked glycans peaked in 100% DO, with decreases in galactosylation in higher and lower DO (Table 4-1; Figures 4-3 & 4-4). These changes were evidenced principally by fluctuations in the proportions of agalactosyl and digalactosyl glycans. The level of monogalactosylation remained relatively constant. The effect of DO was more markedly observed at low DO concentrations.

The effect of low DO on galactosylation of the mAb N-glycans appears to be a general result, but is evidently less pronounced in the NBS bioreactor than in the LH bioreactor (Table 4-1; Figure 4-3). These results indicated that the DO effect is not bioreactor-specific, but that nominally identical steady-state conditions in different chemostat bioreactors may still lead to some incongruities in glycosylation.

Clearly, not only is DO an important factor for energy metabolism and metabolic flux of the CC9C10 cell line, but it has now been shown to be critical in determining the final structures of the N-linked oligosaccharides of the mAb produced by these cells.

Table 4-1. Quantitative results for all three sets of mAbs. Relative peak areas of the major neutral oligosaccharides from the LH and NBS bioreactors (all three sets).

	Peak 1			Peak 2			Peak 3		
	C2-004301			C2-014301			C2-024301		
	core-fucosyl asialyl agalactosyl biantennary			core-fucosyl asialyl monogalactosyl biantennary			core-fucosyl asialyl digalactosyl biantennary		
	Chemostat set			Chemostat set			Chemostat set		
mAb preparation	1st (LH) (6)[a]	2nd (NBS) (5)	3rd (NBS) (6)	1st (LH) (6)	2nd (NBS) (5)	3rd (NBS) (6)	1st (LH) (6)	2nd (NBS) (5)	3rd (NBS) (6)
1% DO	–	–	39.6 ± 0.2	–	–	48.7 ± 0.2	–	–	11.7 ± 0.3
2% DO	–	–	38.5 ± 0.3	–	–	49.3 ± 0.2	–	–	12.2 ± 0.2
5% DO	–	–	36.1 ± 0.2	–	–	50.5 ± 0.3	–	–	13.4 ± 0.2
10% DO	45.1 ± 0.1	32.4 ± 0.2	34.3 ± 0.1	46.1 ± 0.1	52.9 ± 0.1	51.7 ± 0.2	8.8 ± 0.2	14.7 ± 0.2	14.0 ± 0.2
25% DO	–	–	33.4 ± 0.2	–	–	52.0 ± 0.2	–	–	14.6 ± 0.1
50% DO	21.1 ± 0.2	25.6 ± 0.1	26.2 ± 0.2	54.0 ± 0.1	54.9 ± 0.3	55.9 ± 0.1	24.9 ± 0.2	19.5 ± 0.2	17.9 ± 0.3
100% DO	17.6 ± 0.4	20.6 ± 0.1	–	52.6 ± 0.2	56.2 ± 0.2	–	29.8 ± 0.5	23.2 ± 0.1	–
125% DO	–	24.3 ± 0.1	–	–	56.7 ± 0.1	–	–	19.0 ± 0.1	–
150% DO	–	30.7 ± 0.2	–	–	52.9 ± 0.4	–	–	16.4 ± 0.4	–

Data are presented as the average relative peak areas (%) and standard deviation with (n -1) degrees of freedom.

[a] Denotes the number of separate HPAEC-PAD experiments.

Figure 4-3. Glycosylation of the first and second sets of mAbs. Chemostat cultures in different steady-state DO concentrations in the LH (first set) and the NBS (second set) bioreactors. Deglycosylation by PNGase F digestion. Separation and quantitation by HPAEC-PAD.

Dashed lines and open symbols: first set, LH bioreactor

Solid lines and filled symbols: second set, NBS bioreactor

Peak 1, core-fucosyl asialyl agalactosyl biantennary (C2-004301): diamonds

Peak 2, core-fucosyl asialyl monogalactosyl biantennary (C2-014301): squares

Peak 3, core-fucosyl asialyl digalactosyl biantennary (C2-024301): triangles

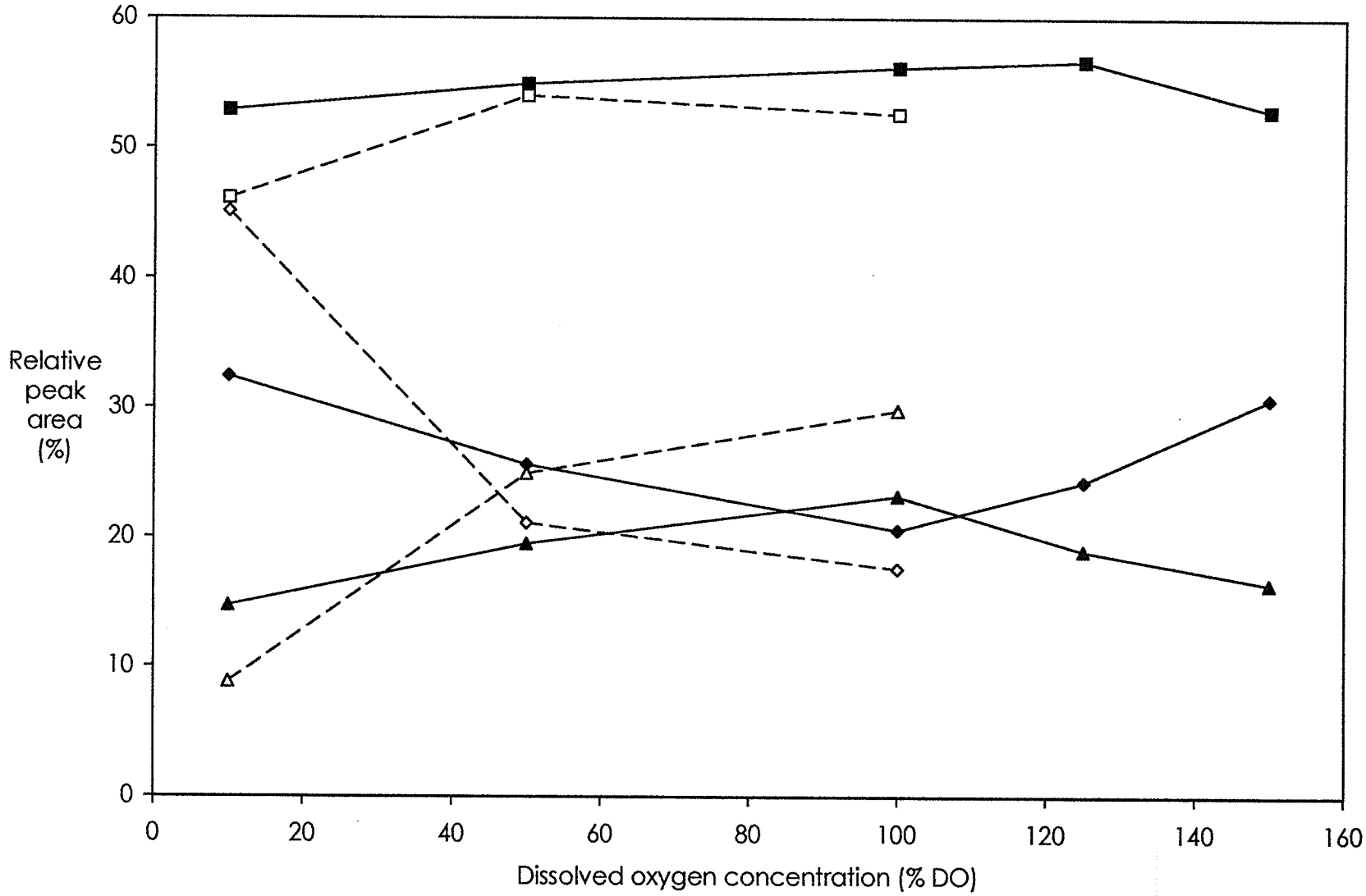
60
50
40
30
20
10
0
Relative peak area (%)
0
20
40
60
80
100
120
140
160
Dissolved oxygen concentration (% DO)

Figure 4-4. Glycosylation of the second and third sets of mAbs. Chemostat culture in different steady-state DO concentrations in the NBS (second and third sets) bioreactor. Deglycosylation by PNGase F digestion. Separation and quantitation by HPAEC-PAD.

Solid lines and filled symbols: second set, NBS bioreactor

Dashed lines and open symbols: third set, NBS bioreactor

Peak 1, core-fucosyl asialyl agalactosyl biantennary (C2-004301): diamonds

Peak 2, core-fucosyl asialyl monogalactosyl biantennary (C2-014301): squares

Peak 3, core-fucosyl asialyl digalactosyl biantennary (C2-024301): triangles

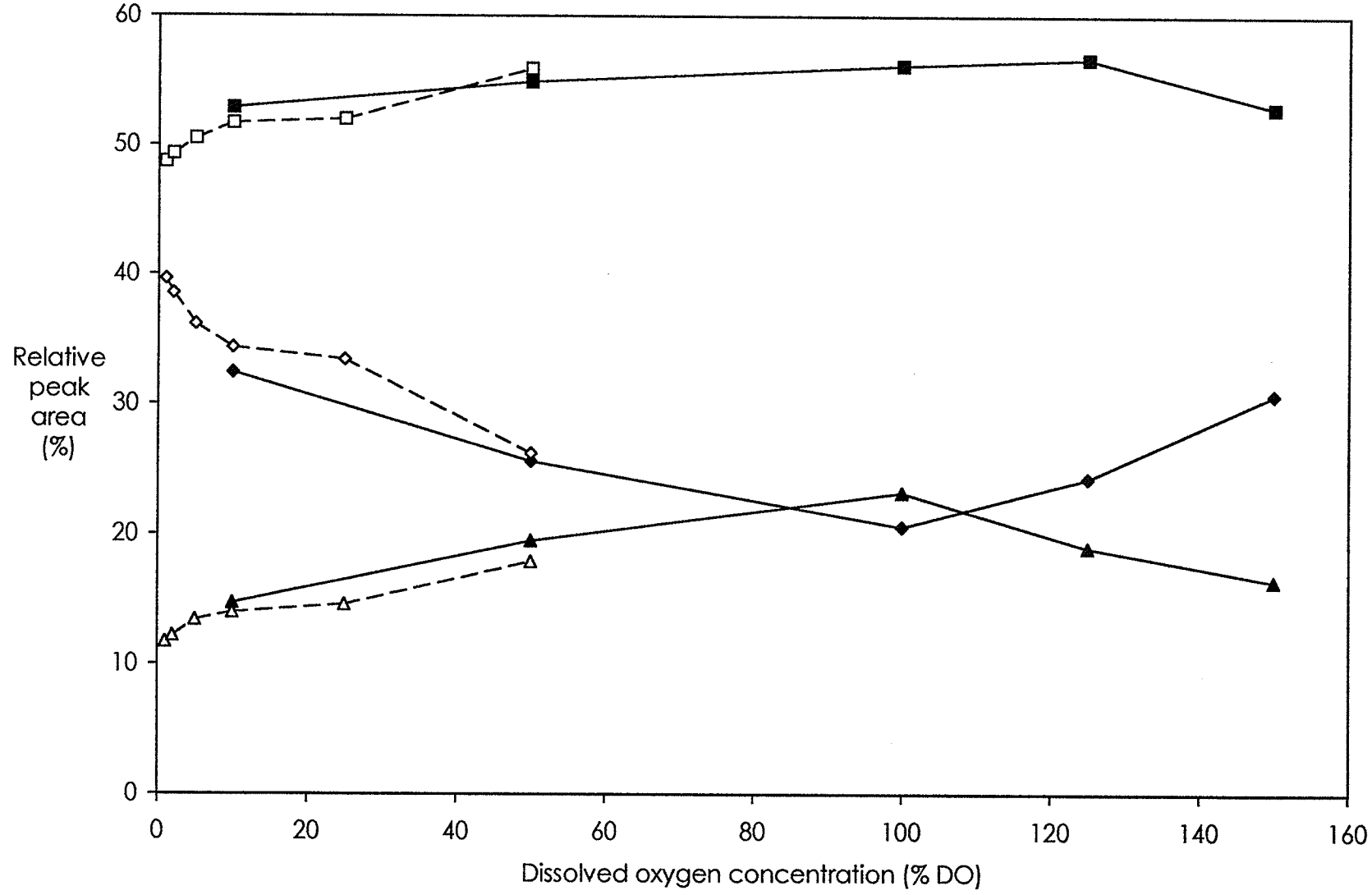
60
50
40
30
20
10
0
Relative peak area (%)
0
20
40
60
80
100
120
140
160
Dissolved oxygen concentration (% DO)

4.4.3 Galactosylation levels were not correlated to cell metabolism

Unlike the differences in the level of galactosylation of the Fc glycans observed in this work, previous work with serum-free continuous cultures of the CC9C10 murine hybridoma showed that steady-state viable cell concentration, cell viability, and the specific rate of mAb production did not significantly change in DO concentrations from 10-100% in either the LH or NBS bioreactor (Petch, 1994; Jan *et al.*, 1997). Also largely unchanged were the specific rate of glutamine utilization and the specific rate of ammonia production. The specific rate of glucose utilization and the specific rate of lactate production increased marginally from 10-100% DO. The results are basically concordant with other reports examining hybridoma metabolism in this DO range, which also calculated that the specific ATP production rate for a hybridoma is essentially constant from 10-100% DO (Miller *et al.*, 1987; Ozturk & Palsson, 1990, 1991c). The effects of DO on cell metabolism in the production of other glycoproteins in different expression systems appear to be more variable (Lin *et al.*, 1993; Wang *et al.*, 1994, 1995).

Above 100% DO, the specific rate of glucose utilization and the specific rate of lactate production increased dramatically, while those of glutamine and ammonia increased only marginally (Petch, 1994; Jan *et al.*, 1997). The specific mAb production rate was relatively constant from 10-100% DO, but rose sharply above 100% DO. This was in contrast to the viable cell concentration, which was relatively constant from 10-100% DO, but dropped above 100% DO. As in another report (Miller *et al.*, 1987), this suggested a differential effect of DO on the growth of the hybridoma and specific mAb production rates.

It was also found that the flux of glucose through the glycolysis and pentose phosphate pathways increased considerably with increasing DO concentration, whereas the flux through the tricarboxylic acid cycle decreased substantially at high DO (Petch, 1994; Jan *et al.*, 1997). Thus, the increase in

specific glucose utilization at higher DO could be explained almost entirely by an increase in anaerobic metabolism. The degree of aerobic metabolism in these cultures was highly sensitive to the glucose concentration. The cultures did not appear to be limited by glucose, although it was not possible to establish conclusively a single limiting substrate (Jan *et al.*, 1997).

Increases in DO were also associated with the induction of the intracellular antioxidant enzymes glutathione S-transferase and glutathione peroxidase, which serve to reduce the cytotoxic effect of reactive oxygen species, but not the extracellular antioxidant enzyme superoxide dismutase – which continued to be increasingly secreted by the hybridoma cells with increasing DO (Jan *et al.*, 1997).

In all cases, there were no correlations between the various measurements of cell metabolism and the observed changes in glycosylation of the mAb product. Unfortunately, neither the levels of ATP or the adenylate energy charge [(ATP+0.5ADP)/ATP+ADP+AMP] were determined in these cultures. Not all changes in culture parameters which affect metabolism and lead to altered metabolic states affect glycosylation. Metabolic flux may be altered, but glycosylation may not be influenced if the intracellular energy state (*i.e.* ATP level and/or adenylate energy charge) is unperturbed.

Metabolic studies were performed on batch and chemostat cultures of BHK cells producing a recombinant IgG fusion protein in large variations of glucose and glutamine concentrations (Cruz *et al.*, 1999b, 1999c). At very low glucose concentrations, the glucose-to-lactate yield decreased markedly, showing a metabolic shift towards lower lactate production. At very low glutamine concentrations, the glutamine-to-ammonia yields increased, showing a more efficient glutamine metabolism. Metabolic flux analysis revealed metabolic shifts to more energetically efficient pathways at these low nutrient concentrations. The intracellular ATP levels were unaffected under the different

metabolic states, but the adenylate energy charge was not calculated (Cruz *et al.*, 2000a). In all cultures, the N-linked glycans of the IgG fusion protein were the typical biantennary oligosaccharides with varying galactosylation, but with only about two-thirds of the glycans core-fucosylated (Cruz *et al.*, 1999a, 2000a). The ratios of the different oligosaccharides were relatively insensitive to the levels of glucose or glutamine in the culture media, and no correlation was observed between the metabolic state and the glycosylation state of the IgG fusion protein (Cruz *et al.*, 1999a, 2000a).

Not all alterations in cell culture conditions that affect the level of ATP affect the energy status of the cell. For example, while the absolute concentration of ATP increased in batch cultures of the CC9C10 hybridoma as the culture temperature was raised from 33-39 °C, the relative concentration of ATP decreased (Barnabé & Butler, 1994; Barnabé, 1998). Despite the decrease in relative ATP, no significant differences in the adenylate energy charge were found. Unfortunately, the effect of culture temperature on the glycosylation of the secreted mAb was not determined, and any correlation that may exist in this system between glycosylation state and the absolute and relative ATP concentrations, and the energy charge, were not elucidated. The adenylate energy charge is a good indicator of the energy status of the cell (Atkinson, 1968, 1969, 1977). However, other nucleotide ratios may be more reflective of intracelluar energy metabolism (Ryll & Wagner, 1992).

4.4.4 DO effect influenced by bioreactor but not bioreactor-specific

The observed differences in glycosylation of the mAb between the LH and NBS bioreactors may be explained by differences in the gassing regimes between the two bioreactors. Temperature, pH, agitation rate, dilution rate, and DO were monitored and controlled at specific setpoints, and were nominally equivalent at steady state in the two bioreactors. Identical DO

sensors were used in both the LH and NBS bioreactors capable of DO control within ±1% DO at each setpoint. Although steady-state cultures were established at identical DO setpoints in the two bioreactors, it is possible that distinctions in oxygen monitoring and control contributed to the observed differences in mAb glycosylation.

The LH bioreactor provides a base level of culture aeration by constant headspace gassing. Additionally, the culture is intermittently sparged with oxygen as required via a ring sparger. The sparging is directed by an independent DO module with proportional-integral-differential (PID) control activated by the DO sensor. The NBS bioreactor uses an alternative system for oxygenation based on a combined four-gas interactive pH and DO controller with proportional-integral (PI) control activated by pH and DO sensors. Proportionally-measured gases are sparged continuously and sequentially (air, oxygen, nitrogen, carbon dioxide) into a stainless-steel mesh aeration cage separated from the bulk culture. The four-gas control system maintains the pH and DO simultaneously by employing any single gas or a combination of the four gases. The aeration cage prevents bubble formation directly in the culture in an attempt to reduce cell damage.

For optimal growth, cells grown in serum-free suspension culture with low protein supplementation require protection from shear stress from agitation due to gas sparging and stirring. Shear damage is reduced most widely by the use of Pluronic F-68. Pluronic F-68 has been demonstrated to have a significant effect in protecting animal cells grown in suspension in sparged or stirred bioreactors. The protective effect is thought to be exerted through the formation of an interfacial structure of adsorbed molecules on the cell surface. It is thought that the hydrophobic portion of the molecule interacts with the cell membrane, while the polyoxyethylene oxygen may form hydrogen bonds with water molecules to generate a hydration sheath, which provides the protection from laminar shear

stress and cell-bubble interactions (Murhammer & Goochee, 1990a, 1990b). Although Pluronic F-68 was included in the culture media, it has been shown that differences in gas supply can radically affect the level of protection in bioreactors of otherwise similar design (Murhammer & Goochee, 1990a, 1990b).

The absence of serum and low protein content in these cultures reduced the protective effects attributed to them, and rendered the cells more susceptible to any potential toxic or stress effects from the culture media and bioreactor architecture. Mammalian cells grown in low-serum or serum-free media have shown enhanced sensitivity to DO levels resulting in altered metabolic patterns compared to those grown in serum-based media (Kilburn & Webb, 1968; Kilburn *et al.*, 1969; Ogawa *et al.*, 1992; Wang *et al.*, 1994, 1995).

4.5 Parameters influential to glycoprotein glycosylation in cell culture

4.5.1 Carbon dioxide, pH, and osmolality

Carbon dioxide can accumulate in poorly ventilated cultures, particularly batch and fed-batch cultures, causing an increase in the partial pressure of CO_2 (pCO_2) and a concomitant increase in osmolality due to an increase in dissolved bicarbonate ion (HCO_3^-). The increase in osmolality is exacerbated by pH control with $NaHCO_3$ or NaOH. The ideal osmolality is usually in the range of 280-300 mOsmol/kg, that of plasma *in vivo*. Most cells are quite tolerant of deviations from their optimal osmolality and will grow in a range from 260-320 mOsmol/kg. However, greater extremes in osmolality have been found to variably affect cell growth, energy metabolism, and glycoprotein production (Ozturk & Palsson, 1991b; Ozturk *et al.*, 1992; Oh *et al.*, 1993; Gray *et al.*, 1996; Kimura & Miller, 1996; deZengotita *et al.*, 1998). It has also been shown that an increase in osmolality can affect glycoprotein glycosylation to varying degrees in a pH-dependent manner (Kimura & Miller, 1997; Zanghi *et al.*, 1999).

The pCO_2 and osmolality were not monitored in the work reported here, and may have been slightly different at steady state in the two bioreactors as a result of the differences in gassing regimes. However, since the changes in glycosylation that are reported in the literature are from batch or perfusion cultures, and over relatively large variations in pCO_2 or pH, the constant influx of fresh medium in the chemostat cultures would largely mitigate their effects. As mentioned earlier, steady-state viable cell concentration, cell viability, and the specific rate of mAb production did not significantly change in DO concentrations from 10-100% in either the LH or NBS bioreactor (Petch, 1994; Jan *et al.*, 1997). Also largely unchanged in this range were the specific rate of glutamine utilization and the specific rate of ammonia production, while the specific rate of glucose utilization and the specific rate of lactate production increased only marginally. These data support the assertion that pCO_2 and osmolality were not factors in the observed DO and bioreactor effects on glycosylation.

Further support comes from work with fed-batch cultures of a NS0 cell line producing a mAb, where the pCO_2 typically varied from 20-140 mmHg (2.5-18.5% pCO_2) and the osmolality from 300-400 mOsmol/kg. These ranges were not considered likely to affect product quality (Moran *et al.*, 2000). In the same report, large differences in cell viability, cell growth rate, specific rate of mAb production, and mAb titre at harvest were observed between two different sets of culture parameters. However, the glycosylation and function of the mAb were not significantly affected.

4.5.2 Ammonium, intracellular pH, and nucleotide sugar pools

Ammonium has been found to variably affect cell growth, energy metabolism, and glycoprotein production (McQueen & Bailey, 1990, 1991; Ozturk *et al.*, 1992; Lüdeman *et al.*, 1994; Newland *et al.*, 1994; Ryll *et al.*, 1994; Cruz *et*

al., 2000b). The addition of ammonium results in the accumulation of UDP-*N*-acetylhexosamine nucleotides and alters intracellular pH (Madshus, 1988; Doyle & Butler, 1990; McQueen & Bailey, 1990, 1991; Borys *et al.*, 1993, 1994; Martinelle & Häggström, 1993; Ryll *et al.*, 1994; Martinelle *et al.*, 1995; Schneider *et al.*, 1996; Barnabé & Butler, 1998; Barnabé, 1998; Zanghi *et al.*, 1998a, 1998b; Cruz *et al.*, 2000b).

The effects of ammonium on glycosylation appear to biosynthetic as result of these altered nucleotide pools and/or intracellular pH (Borys *et al.*, 1993, 1994; Andersen & Goochee, 1995; Pels Rijcken *et al.*, 1995; Gawlitzek *et al.*, 1998, 1999, 2000; Grammatikos *et al.*, 1998; Zanghi *et al.*, 1998a, 1998b; Yang, 2000; Yang & Butler, 2000a). These changes are generally manifested as increases in the antennarity and decreases in terminal glycosylation (*i.e.* galactosylation and sialylation) of the glycans. However, other effects have been observed. For example, the addition of ammonium to CHO cell cultures resulted in a reduction in the overall number of O-linked glycans on erythropoietin (EPO) and their level of sialylation (Yang & Butler, 2000a). There was also a reduction in the branching and sialylation of the N-linked glycans (Yang & Butler, 2000a, 2000b).

For antibodies, reductions in the galactosylation and sialylation of immunoglobulins from plasma cells (Thorens & Vassalli, 1986), and a recombinant IgG fusion protein (Gawlitzek *et al.*, 2000), were observed upon addition of ammonium or glucosamine. These changes were attributed to the affect of an increase in intracellular (*trans*-Golgi) pH on glycosyltransferase activities and not changes in nucleotide sugar pools. However, incorporation of radiolabelled ammonium into glycoprotein glycans has also been reported (Gawlitzek *et al.*, 1999).

In serum-free batch cultures of a NS0 cell line producing a mAb, additions of *N*-acetylmannosamine and glucosamine did not affect antennarity or sialylation of Fc N-glycans, but did cause the proportion of agalactosyl glycans

to increase (Hills *et al.*, 1999). In serum-free batch cultures of the CC9C10 hybridoma, addition of ammonium was found to result in decreases in the cell growth rate and increases in specific mAb production, without affecting the extent of glycosylation site occupancy (Barnabé & Butler, 1998; Barnabé, 1998). However, the mAb glycan heterogeneity was not examined.

In the work reported here, no significant variations in steady-state glutamine or ammonia concentrations, specific glutamine utilization, or specific ammonia production were observed in 10-100% DO in either the LH or NBS bioreactor (Petch 1994; Jan *et al.*, 1997). The effect of DO on galactosylation in the two bioreactors does not appear to be a result of altered ammonium concentration and related effects.

4.5.3 Post-secretion degradation by glycosidases

The potential for extracellular degradation of glycoprotein oligosaccharides in cultures has been studied (Gramer & Goochee, 1993, 1994a, 1994b; Warner *et al.*, 1993; Gramer *et al.*, 1994, 1995; Munzert *et al.*, 1996; Gawlitzek *et al.*, 1999, 2000). In batch cultures of CHO, NS0, and hybridoma cells, a number of glycosidases, including sialidases, fucosidase, and β-galactosidase, were present in the supernatant. The concentrations of secreted glycosidases increased with culture duration and were in some cases shown to affect glycosylation of the glycoprotein products. However, chemostat cultures are established at steady-state and the constant dilution with fresh medium would minimize glycosidase accumulation and mitigate their effect. Indeed, in many cases, even in batch culture, the changes observed in glycosylation were determined to be biosynthetic rather than degradative (Zanghi *et al.*, 1998b; Gawlitzek *et al.*, 1999, 2000; Yang, 2000; Yang & Butler, 2000a).

4.6 Potential mechanisms by which DO affects galactosylation

The mechanisms by which DO results in decreased galactosylation of the mAb are unclear. An obvious line of reasoning suggests a dearth of the UDP-Gal nucleotide sugar donor at the site of glycosylation, which might arise for a variety of reasons (Figure 4-5). Lower DO, and the consequent shortage of oxygen supply to the mitochondria for oxidative phosphorylation, may result in a reduction of the ATP needed for production of UDP-Gal. Since the energy derived from oxidative phosphorylation does not appear to be limiting to cell growth until below 1% DO (Miller *et al.*, 1987; Ozturk & Palsson, 1990, 1991c), it may be that the hybridoma cell has an intrinsic priority sequence as to where ATP is spent. At times of reduced ATP availability, energy may be preferentially channelled to necessary housekeeping, and such 'luxury' functions as glycosylation may be curtailed. However, the construction of the initial Dol-PP-linked oligosaccharide precursor, which is transferred to the protein in the ER, requires nucleotide sugar donors, as do all the other oligosaccharide elongation reactions in the Golgi. It would then be expected that any shortage of ATP would affect synthesis of all nucleotide sugars, and therefore the respective monosaccharide transfers, in a blanket-like fashion. This was not observed in the experiments reported in this work. However, it is entirely conceivable that the specific production or transport of UDP-Gal is especially susceptible to lower DO concentration and/or the concomitant ATP levels.

In the absence of Gal, the production of UDP-Gal requires the action of the enzyme UDP-Gal-4-epimerase, which catalyzes the conversion of UDP-Glc to UDP-Gal (Krieger *et al.*, 1989; Martin *et al.*, 1998; Bülter & Elling, 1999). Perhaps this enzyme is particularly affected by DO. In a mutant CHO cell line lacking this epimerase activity, the synthesis, intracellular sorting, and function of glycoproteins were affected (Krieger *et al.*, 1989). Addition of Gal to the culture medium, thereby circumventing the defect, rapidly corrected these effects.

Cognately, the possibility exists that a deficiency in UDP-Gal transport from the cytosol to the Golgi lumen is the cause of the observed effect at low and high DO. Although neither ATP nor ionic gradients appear directly involved in this transport, a specific UDP-Gal/UMP antiport has been demonstrated and cloned (Cecchelli *et al.*, 1986; Miura *et al.*, 1996). While similar antiports for the other nucleotide sugars lead to the formation of intralumenal pools of these sugar donors, such a pool has not been found for UDP-Gal, which would be utilized as soon as transported (Cacan *et al.*, 1984; Verbert *et al.*, 1987). Thus, while some glycosyltransferases would have an intralumenal pool of donors at their disposal, the activity of GalTs would depend more strictly upon the activity of the transport mechanism and upon the presence of the required nucleotide sugar in the cytoplasm. This is supported by the demonstration of CHO cell mutants which lack the UDP-Gal transport capability, and consequently undergalactosylate even though GalTs are present (Deutscher & Hirschberg, 1986; Oelmann *et al.*, 2001).

Among other possibilities are that varying DO concentration perturbs IgG protein folding and disulfide bond formation directly or indirectly (Sections 4.6.1, 4.6.1.1, & 4.6.1.2), or that the expression and/or activity of β1,4-GalT is affected (Section 4.6.2).

Figure 4-5. Postulated sites for the observed DO effect on galactosylation.

1. synthesis of initial nucleotide sugar (formation of UDP-Glc)
2. UDP-Gal availability (formation from UDP-Glc)
3. UDP-Gal availability (antiport into Golgi lumen)
4. IgG glycan acceptor accessibility (protein folding, disulfide bonding)
5. β1,4-GalT activity (phosphorylation, glycosylation, disulfide bonding)

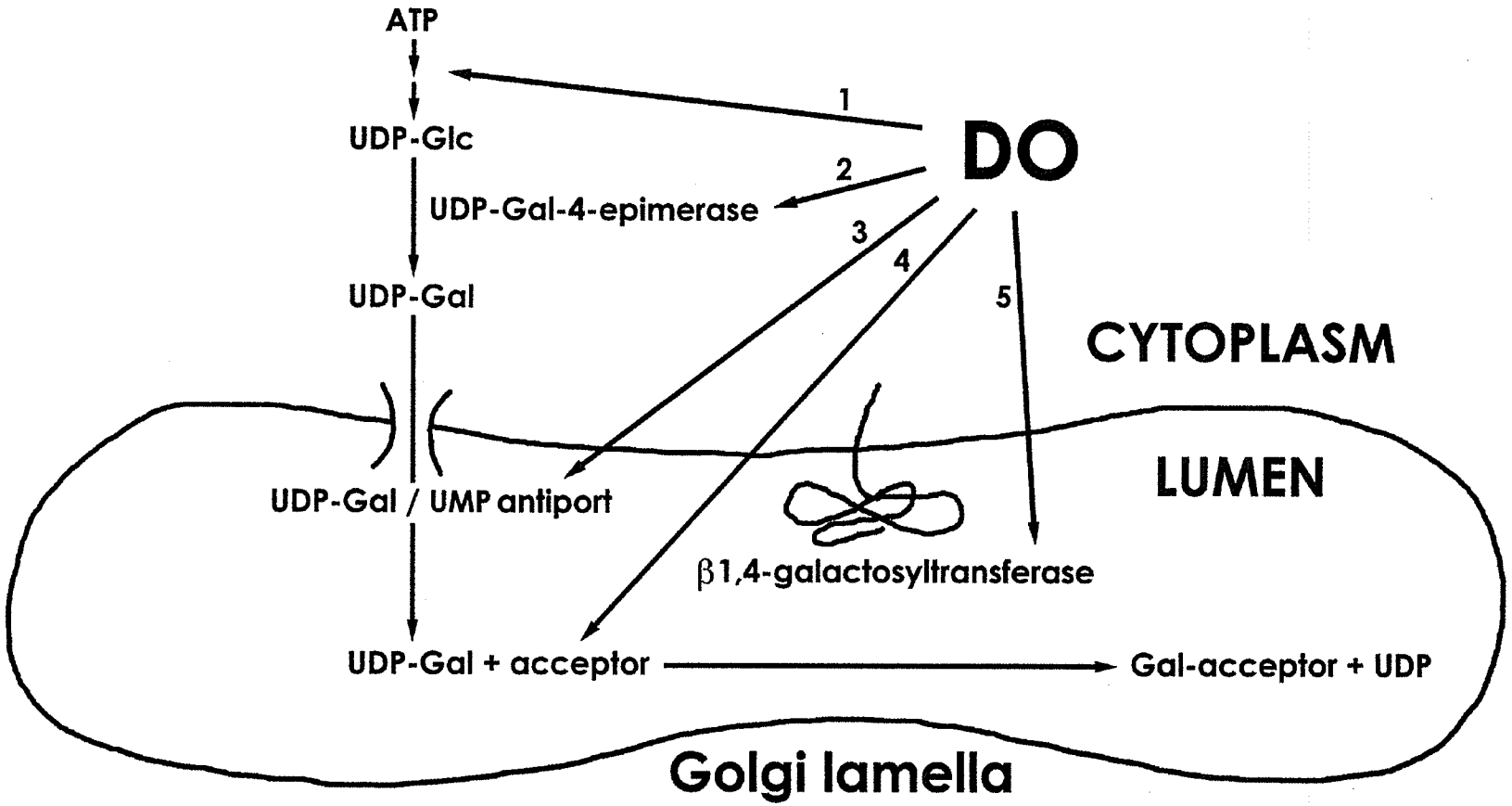
ATP
UDP-Glc
UDP-Gal-4-epimerase
UDP-Gal
DO
1
2
3
4
5
CYTOPLASM
LUMEN
UDP-Gal / UMP antiport
β1,4-galactosyltransferase
UDP-Gal + acceptor
Gal-acceptor + UDP
Golgi lamella

4.6.1 IgG protein folding and disulfide bond formation

Unlike other immunoglobulins, the rates of IgG assembly, intracellular transport, and secretion are not grossly affected by the absence or extent of glycosylation (Weitzman & Scharff, 1976; Hickman & Kornfeld, 1978; Sidman, 1981; Thorens & Vassalli, 1986; Hashim & Cushley, 1987; Barnabé & Butler, 1998; Barnabé, 1998). However, the converse may not entirely hold, and glycosylation may be affected by the rate of mAb protein synthesis, folding, and maturation. It is well established that during biosynthesis the conformation of the nascent protein may, in part, direct the extent of oligosaccharide processing (Schachter, 1986, 1991a, 1991b; Yet *et al.*, 1988; Yet & Wold, 1990; Baenziger, 1994; Do *et al.*, 1994). This is certainly true for IgG (Savvidou *et al.*, 1981, 1984; Fujii *et al.*, 1990; Lee *et al.*, 1990; Wright *et al.*, 1991; Jefferis *et al.*, 1992; Endo *et al.*, 1995; Lund *et al.*, 1996, 2000; White *et al.*, 1997). Thermal unfolding experiments of IgG-Fc and a series of truncated IgG peptide-deletion mutants have also revealed structural and functional differences correlated to the level of glycosylation, galactosylation, and sialylation of the Fc glycans (Ghirlando *et al.*, 1999; Lund *et al.*, 2000; Mimura *et al.*, 2000, 2001).

Assembly of the IgG heavy and light chain proteins, co-translational transfer of the initial oligosaccharide precursor to Asn-297 of each heavy chain, and limited trimming and processing of these oligosaccharide precursors takes place in the ER. Further glycan processing continues in the *cis-*, *medial-*, and *trans*-Golgi. β1,4-GalT is located predominantly in the *medial-* and *trans*-Golgi (Kornfeld & Kornfeld, 1985; Roth, 1987; Paulson & Colley, 1989; Cummings, 1992; Rabouille *et al.*, 1995; Colley, 1997; Varki *et al.*, 1999). Initial disulfide bond formation takes place in the ER but is often incorrect. The correct disulfide bond pairs are obtained by shuffling and this is facilitated by various chaperones and enzymes in the ER and Golgi. The precise location where a fully and properly folded IgG molecule is completed is dependent on several factors including the

species, tissue origin, and subclass of the IgG (Sutherland *et al.*, 1970, 1972; Petersen & Dorrington, 1974; Bergman & Kuehl, 1979; Roth & Koshland, 1981). Therefore, the intracellular events of peptide, disulfide, and glycosyl bond formation involved in the biosynthesis of IgG are not discrete events, but are temporally intertwined. It has been proposed that the timing and rate of formation of the inter-heavy chain disulfide bonds in the hinge region determine the level of IgG-Fc oligosaccharide galactosylation (Rademacher *et al.*, 1995, 1996).

Biosynthetic time-course studies and kinetic analysis of reoxidation experiments have shown that interchain disulfide bond formation in IgG proceeds through one major, and one or two minor, pathways (Scharff & Laskov, 1970; Sutherland *et al.*, 1970, 1972; Baumal *et al.*, 1971; Petersen & Dorrington, 1974; Sears *et al.*, 1975, 1977a). Pathway 1 involves disulfide bond formation first between the heavy chains, followed by consecutive addition of the two light chains (Figure 4-6). Pathways 2 and 3 begin with disulfide bond formation between heavy and light chains. However, while pathway 2 continues by the bonding of two heavy-light chain complexes to form the complete IgG, pathway 3 progresses through the consecutive additions of a heavy, and then light, chain to the initial heavy-light chain complex.

In vitro reoxidation experiments have shown that the rate of disulfide bond formation could be increased by increased pH, temperature, or by the addition of glutathione or cupric ion, and that there was a reticence to switch from one assembly pathway to another, except under non-physiologic conditions (Petersen & Dorrington, 1974). In contrast to these results, it has been established that pathways 1 and 2 are dominant *in vivo*, with little contribution from pathway 3 (Sutherland *et al.*, 1970, 1972; Bergman & Kuehl, 1979). In addition, IgG from different species and tissues demonstrated pathway preferences.

Figure 4-6. Three pathways of interchain disulfide bond formation in IgG.

Pathway 1: low galactosylation

Pathway 2: high galactosylation

Pathway 3:

H, heavy chain; L, light chain; •, disulfide bond

(Adapted from Baumal *et al.*, 1971; Petersen & Dorrington, 1974; and Rademacher *et al.*, 1995, 1996.)

Pathway 1	Pathway 2	Pathway 3
L H H L	L H H L	L H H L
L H • H L	L H H • L	L H H • L
L H • H • L	L • H H • L	L H • H • L
L • H • H • L	L • H • H • L	L • H • H • L
$H + H \rightarrow H_2$	$H + L \rightarrow HL$	$H + L \rightarrow HL$
$H_2 + L \rightarrow H_2L$	$2\ HL \rightarrow H_2L_2$	$HL + H \rightarrow H_2L$
$H_2L + L \rightarrow H_2L_2$		$H_2L + L \rightarrow H_2L_2$

IgG has been shown to be a substrate for thioredoxin (Magnusson *et al.*, 1997). Several different myeloma IgGs consistently showed that the interchain disulfides (H•H and H•L) were relatively susceptible to reduction compared to the buried intrachain disulfides, which were nearly impervious to reduction. This is in contrast to reduction by dithiothreitol (DTT), which showed no preferences in the relative susceptibility of disulfide bonds (Sears *et al.*, 1977b). This may simply reflect the differences in accessibility between the larger thioredoxin molecule and smaller DTT molecule to the various disulfide sites.

Most interesting, however, was that IgG processing intermediates assembled via pathway 2 showed an exceptional preference for galactosylation over those assembled via pathway 1 (Sutherland *et al.*, 1972). Thus, the addition of Gal is impeded by the formation of the inter-heavy chain disulfide bond. In the absence of inter-heavy chain disulfide bond formation, the oligosaccharides are fully accessible to the glycosyltransferases and processing enzymes. Formation of this bond sequesters the glycans between the CH2 domains by changes in tertiary and quaternary structure, and limits their accessibility to glycosyltransferases. Fab-associated glycans, if present, are not subject to these controls. In this way, protein structure effects related to the internal nature of the Fc glycans, and the relationship between interchain disulfide bond formation and glycan acquisition, provide a mechanism for the site-specific oligosaccharide processing at Asn-297.

It has therefore been proposed that pathways 1 and 2 correspond to low and high galactosylation pathways, respectively (Rademacher *et al.*, 1995, 1996) (Figure 4-6). It was further suggested that the partitioning of IgG molecules through these pathways might be influenced by a variety of factors, and any alterations in this partitioning would result in a shift in the final Gal heterogeneity of the Fc glycans. Accordingly, the variation in galactosylation of Asn-297 oligosaccharides with changes in DO concentration described in this report may

reflect a perturbation in the oxidizing environment of the ER and/or Golgi. Certainly, the formation and shuffling of disulfide bonds is extremely sensitive to the redox state of the cell. This disturbance may result in a change in the major pathway of disulfide bond formation, as a consequence of reduced rates of formation in the alternate pathways.

As previously discussed (Section 4.5.2), increases in intracellular pH as a result of ammonium or glucosamine addition resulted in decreases in galactosylation and sialylation of immunoglobulin G, and this was attributed to decreases in glycosyltransferase activity. However, increases in pH have also be shown to increase the rate of reoxidation of disulfide bonds (Peterson & Dorrington, 1974; Percy *et al.*, 1976). Overall, the combination of these two effects would appear to synergistically deter the galactosylation of Fc glycans.

4.6.1.1 Chaperones and enzymes assist folding and quality control

The initial transfer of oligosaccharide to the nascent protein, and formation of disulfide bonds, is co-translational in the ER. However, further processing of the oligosaccharide continues through the ER and Golgi. The disulfide bonds formed initially are often incorrect and the protein is misfolded. The action of several important chaperone proteins and other molecules in the ER and Golgi assist the correct reformation of disulfide bonds and protein refolding. In addition, as previously discussed, glycoprotein folding is specifically assisted by two chaperones, the membrane-bound calnexin and its soluble homolog calreticulin. The lectin-like interactions of calnexin and calreticulin with nascent glycoproteins provide access to a folding pathway, and allow the recruitment of certain other enzymes that facilitate disulfide bond formation and chaperones which assist the assembly of subunits.

Immunoglobulin heavy chain binding protein (BiP) is a chaperone that transiently binds to exposed hydrophobic segments and prevents them from

misfolding or forming aggregates, and thus enhances their ability to fold into the proper conformation. The rearrangement, or shuffling, of disulfide bond pairs is accelerated and facilitated by three members of the thioredoxin superfamily: protein disulfide isomerase (PDI), endoplasmic reticulum protein 57 kD (ERp57), and ERp72. Please note that BiP and the thiol oxidoreductases PDI, ERp57, and ERp72 are also known by several other names and acronyms. The names used in this work are the ones most commonly and currently in use. Many other chaperones and enzymes have been identified in assisted protein folding, and many more await discovery (Freedman *et al.*, 1995; Gilbert, 1997; Ruddon & Beddows, 1997; Ferrari & Söling, 1999). However, these four are known to assist protein folding and disulfide bond formation in immunoglobulin G.

ERp57 does not interact with non-glycosylated proteins, but only assists in disulfide bond shuffling of glycoproteins indirectly via interactions with calnexin and calreticulin (Trombetta & Helenius, 1998; Ferrari & Söling, 1999; Molinari & Helenius, 1999; Oliver *et al.*, 1999; Rudd *et al.*, 2001). Therefore, the specific modulation of folding and quality control of glycoproteins is at least the tale of the three chaperones calnexin, calreticulin, and ERp57 (High *et al.*, 2000). PDI, on the other hand, interacts with proteins independently of their glycosylation status. Expression of PDI is critical for the formation of the proper disulfide bonds in immunoglobulins, and increased synthesis of antibodies is correlated to increased synthesis of PDI (Roth & Koshland, 1981). Whether or not a glycoprotein interacts with BiP, and whether this is before or after interaction with calnexin and calreticulin, appears to depend on the location of the glycosylation site in relation to the N-terminus (Molinari & Helenius, 2000). However, BiP and PDI act synergistically in the proper folding and disulfide bond formation of antibodies (Mayer *et al.*, 2000). ERp72 appears to interact with proteins via interactions with BiP and PDI; also independently of calnexin and calreticulin.

Mathematical models in the metabolic control analysis of mAb synthesis have incorporated the action of BiP and PDI with some success (Bibila & Flickinger, 1991; Flickinger & Bibila, 1992; Gonzalez *et al.*, 2001). The probability of formation of each disulfide bond pair in the disulfide bond shuffling pathways, and the levels of BiP and PDI, were modelled to be dependent variables (but independent of each other), and were not expected to be the same under different growth or nutritional conditions. The latter study also incorporated parameters for the addition of oligosaccharides by OST (Gonzalez *et al.*, 2001). However, this study only modelled glycosylation site occupancy and did not take into account further glycan processing. A general mathematical model of N-linked glycoform biosynthesis has been presented (Umaña & Bailey, 1997). Future models will no doubt endeavour to incorporate these approaches.

The tripeptide glutathione is the major thiol-containing molecule in eukaryotic cells. It is highly abundant, found in millimolar amounts, and serves two important functions. The first is a major role in the cellular antioxidant defense mechanisms against free radical damage; the second is to prevent formation of disulfide bonds in the cytosol and to catalyze their formation in the ER. Glutathione shuttles between the reduced form, GSH, and the oxidized form, GSSG. A glutathione redox buffer of reduced to oxidized glutathione (GSH:GSSG of approximately 3:1) holds the redox state of the ER and Golgi more oxidizing than that of the cytosol (GSH:GSSG of approximately 50:1) to allow disulfides to form and rearrange (Gilbert, 1997). Conditions that would perturb or alter the intralumenal and/or cytosolic levels of glutathione, or the GSH:GSSG ratio, would influence the redox state and therefore affect disulfide bond formation.

In this work, maximum galactosylation of the IgG-Fc glycans was observed in 100% DO. There was a trend below and above 100% DO for galactosylation to decrease. Interestingly, the changes in the level of

galactosylation observed in 10-150% DO followed a similar trend for the levels of the intracellular antioxidant enzymes glutathione S-transferase and glutathione peroxidase, but not the extracellular antioxidant enzyme superoxide dismutase – which continued to be increasingly secreted by the hybridoma cells with increasing DO (Jan *et al.*, 1997). This is particularly remarkable considering that the former two enzymes are also intimately involved in the homestasis of the GSH:GSSG ratio.

4.6.1.2 Interdependency between protein folding and glycosylation

The observation that localized folding events on the nascent protein chain, including disulfide bond formation, can affect glycosylation by blocking the access of various glycan attachment and processing enzymes is not unique to IgG. Neither is the conclusion that the presence of the oligosaccharides themselves can assist in directing protein folding and can have a significant stabilizing effect on large regions of the backbone structure (Imperiali, 1997; O'Connor & Imperiali, 1998; Imperiali & O'Connor, 1999; Wormald & Dwek, 1999; O'Connor *et al.*, 2001). The interrelationship between glycosylation and protein folding will become a popular area of research, and a number of different examples have been reported recently.

The formation of a particular disulfide bond in the hemagglutinin-neuraminidase glycoprotein of Newcastle disease virus has been shown to block the usage of one of the potential glycosylation sites (McGinnes & Morrison, 1997). Although the site is not occupied in the normal protein, when either one of the cysteine residues involved in the disulfide bond was mutated, the site was glycosylated. The opposite effect was observed in a rotaviral glycoprotein, where the presence of glycans facilitated proper protein folding and disulfide bond formation, and their absence resulted in incorrect disulfide bond formation and misfolding (Mirazimi & Svensson, 1998). Similarly, a panel of vesicular

stomatitis virus glycoproteins with altered glycosylation sites were subject to aberrant disulfide bonding, misfolding, and aggregation (Machamer & Rose, 1988).

Tissue-type plasminogen activator (t-PA) contains seventeen disulfide bonds and is secreted as a mixture two functionally distinct types that differ in the extent of their glycosylation site occupancy. Type I t-PA is glycosylated at Asn-117, Asn-184, and Asn-448; type II is identical except it lacks glycosylation at Asn-184. Deterrence of disulfide bond formation led to complete glycosylation of Asn-184, in a sequon that is otherwise only variably occupied (Allen *et al.*, 1995). This demonstrated that folding and disulfide bond formation of t-PA determines, in part, the extent of occupancy of Asn-184 and the ratio of types I and II t-PA.

Chorionic gonadotropin (CG) and luteinizing hormone (LH) are members of a family of four heterodimeric αβ-glycoprotein hormones that contain a common α-subunit, but differ in their hormone-specific β-subunits. There is considerable homology between the β-subunits, which is most apparent at the conserved positions of the twelve cysteine residues which form six disulfide bonds. CGβ and LHβ are both glycosylated at Asn-30. However, CGβ also contains an additional occupied glycosylation site at Asn-13. Removal of either one or both N-glycosylation sites of the CG β-subunit resulted in impaired secretion and degradation, indicating that the presence of N-linked glycans facilitate correct disulfide bond pairing (Feng *et al.*, 1995). Conversely, disruption of three of the six disulfide bond pairs induced alterations in the attached oligosaccharide structures as a result of a change in protein conformation (Moriwaki *et al.*, 1997). As was suggested above for IgG, it was proposed that changes that cause alterations in the disulfide bond formation and shuffling pathways can affect glycosylation (Moriwaki *et al.*, 1997).

The LHβ subunit is particularly prone to misfolding and aggregation as a consequence of inappropriate disulfide bond formation, while the CGβ subunit is

not as sensitive. The addition of a glycosylation site to Asn-13 of LHβ rescued it from this susceptibility (Suzuki *et al.*, 2000). In contrast, removal of the Asn-13 site in CGβ instigated misfolding and aggregation. Therefore, the glycan at Asn-13 plays an important role in correct protein folding of both CGβ and LHβ subunits by directing the shuffling and final pairing of disulfide bonds (Suzuki *et al.*, 2000).

Disulfide bond formation and N-glycan processing also regulates the folding and maturation of tyrosinase-related protein-1 (TRP-1). TRP-1 has six potential glycosylation sites, four of which are occupied. The glycosylation sites are mostly associated with complex glycans, but there is also a significant contribution of high-mannose glycans, presumably from those sites which become inaccessible to glycan processing enzymes during the folding regimen. The folding of TRP-1 thus affects glycan processing (Branza-Nichita *et al.*, 2000; Negroiu *et al.*, 2000). There are also seventeen cysteines available for disulfide bond formation in TRP-1 in well-conserved positions in two cysteine-rich domains.

As described for IgG and the αβ-glycoprotein hormones, the final disulfide bonds of TRP-1 form by shuffling through different pathways of disulfide bond pairs, and the flux through these pathways can be perturbed. The glycan occupancies of each glycosylation site make variable contributions to TRP-1 folding and activity (Branza-Nichita *et al.*, 2000; Negroiu *et al.*, 2000). An array of primary and alternate disulfide bonding pathways has also been observed for insulin-like growth factor-I and an engineered analog (Milner *et al.*, 1999).

The above observations bolster the signficance of the interdependency between protein folding, disulfide bond formation, and the acquisition and processing of glycans.

Establishment of the proper folding of IgG and other glycoproteins is clearly a very complicated and convoluted process, requiring many iterations and the assistance of a number of facilitating chaperones and enzymes. The interactions of these chaperones and enzymes with their substrates are variously

and variably dependent on pH, temperature, redox state, NADPH, ATP, *etc.* This results in a significant potential for the disruption of glycoprotein maturation in any of these complex and synergistic interactions.

The organized and orchestrated fashion in which these chaperones and enzymes appear to work also allows much potential for disruption. Whether or not these chaperones and enzymes are able to interact with the glycoprotein, and their order of association, have been shown to be affected by the inhibition of glycosylation and/or disulfide bond formation (Mirazimi & Svensson, 1998; Branza-Nichita *et al.*, 2000; Negroiu *et al.*, 2000; Rudd *et al.*, 2001). It is certainly possible that the expression and/or activity of one or more of these chaperones or enzymes is disturbed by changes in the DO concentration. This may in turn perturb the timing and rate of formation of the disulfide bonds and/or the process of mAb protein folding, and ultimately affect glycosylation.

4.6.2 Activity of β1,4-galactosyltransferase is unaltered

The β1,4-galactosylation of N-glycans is a complex process (Furukawa & Sato, 1999). At least six homologous β1,4-GalT genes have recently been identified in humans, with the 'classical' enzyme being β1,4-GalT1 (Lo *et al.*, 1998; Lee *et al.*, 2001). In spite of their homology, the substrate specificities of β1,4-GalTs appear to be different from each other (Furukawa & Sato, 1999; Lee *et al.*, 2001). However, study of the detailed acceptor specificities of individual β1,4-GalTs has just begun. The expression levels of individual β1,4-GalT transcripts are highly variable among human tissues and the localization of each β1,4-GalT in cells appears more important for their functions that their *in vitro* acceptor specificities (Furukawa & Sato, 1999). Transfection of human B cells with the classical β1,4-GalT1 was shown to be enough to increase the galactosylation of IgG (Keusch *et al.*, 1998a). It is certainly possible that the expanding β1,4-GalT

gene family will furnish 'galactosyltransferases for all functions' (Amado *et al.*, 1999).

The average specific β1,4-GalT activity of the cellular protein in the CC9C10 hybridoma cells was 232 ± 8 pmol/mg/h. This compares well with the specific β1,4-GalT activity of cultures of a human lymphoblastic leukemia B-cell line, which was found to be 100-700 pmol/mg/h with macromolecular acceptors (Furukawa *et al.*, 1990). In contrast, transformation of B-lymphocyte cell lines with EBV results in more variable changes in β1,4-GalT activities (Furukawa *et al.*, 1990; Wilson *et al.*, 1993; Kumpel *et al.*, 1994). Thus, as previously discussed, the nature of the transformation, and each transformation event itself, may result in altered glycosylation profiles.

Unlike RA, however, this work has disqualified alterations in β1,4-GalT activity as a potential cause of the observed DO effect on galactosylation. The level of β1,4-GalT activity was consistent at all DO concentrations (Figure 3-25; Table 3-10). Interestingly, another report also failed to show any correlation between β1,4-GalT activity and the efficiency of galactosylation of mAbs as a result of changes in cell culture conditions (Kumpel *et al.*, 1994). So, as previously discussed for RA, it appears that decreased *in vitro* β1,4-GalT activity is not the primary cause of decreased IgG galactosylation.

However, DO may cause an indirect increase in intracellular (*trans*-Golgi) pH and reduce GalT activity *in vivo*. Increases in intracellular pH have been reported to decrease the galactosylation and sialylation of immunoglobulins from plasma cells (Thorens & Vassalli, 1986) and a recombinant IgG fusion protein (Gawlitzek *et al.*, 2000). In the latter report, the reductions in terminal glycosylation were attributed to decreases in glycosyltransferase activities due to an increase in intracellular pH as a result of ammonium accumulation. This effect would not have been observed in the *in vitro* GalT assays described in this work, but may well have occurred *in vivo*.

4.7 Further notes on the methods utilized in this work

4.7.1 Deglycosylation methods

The polyclonal IgGs and mAbs were subjected to deglycosylation by PNGase F digestion and/or hydrazinolysis. Chemical deglycosylation methods are touted as having advantages over enzymatic methods due to their innate nonselectivity (Patel *et al.*, 1993; Patel & Parekh, 1994). Enzymatic methods can prove unreliable since enzyme specificity and glycan inaccessibility may lead to incomplete and selective recovery of glycans. For example, differences were reported in the N-glycan pools recovered from α_1-AGP by PNGase F digestion and hydrazinolysis (Hermentin *et al.*, 1992b). This is particularly relevant in the removal of high-mannose and hybrid structures which tend to occur in areas of the protein inaccessible to the enzyme (Chu, 1986; Mussar *et al.*, 1989).

While PNGase F has been shown to release a broad range of N-linked oligosaccharides from native glycoproteins, denaturation or limited proteolysis prior to PNGase F digestion is advised (Tarentino *et al.*, 1985, 1989; Chu, 1986; Alexander & Elder, 1989; Nuck *et al.*, 1990). For example, α_1-AGP could not be rendered susceptible to PNGase F digestion unless denaturated with both SDS and 2-mercaptoethanol (Alexander & Elder, 1989; Nuck *et al.*, 1990). On the other hand, PNGase F is unlike other oligosaccharide-cleaving enzymes in that complete deglycosylation in many cases may be achieved on native glycoproteins in the absence of detergents (Tarentino *et al.*, 1985; Tarentino & Plummer, Jr., 1987). However, the removal of glycans from native glycoproteins requires higher levels of the enzyme. There is a large range in susceptibility of glycoproteins to complete deglycosylation by PNGase F and the amount of enzyme required must be determined empirically (Tarentino *et al.*, 1985; Tarentino & Plummer, Jr., 1987).

All attempts to denature the polyclonal IgGs and mAbs by the use of heat and/or the addition of 2-mercaptoethanol and/or SDS to the digestion

buffer resulted in complete aggregation and precipitation of the IgGs. Immunoglobulin G is notorious for being unstable to heat and it is recommended that denaturation with 2-mercaptoethanol and SDS is done at room temperature. However, this also resulted in complete precipitation. Therefore, all PNGase F digestions were performed with native IgGs and mAbs without denaturation prior to enzymatic deglycosylation. Interestingly, for SDS-PAGE, the mAbs were stable to heat in the presence of SDS, with and without 2-mercaptoethanol. The mAbs were undoubtedly stabilized by the presence of glycerol and a high concentration of Tris buffer instead of a low concentration of phosphate buffer.

For a 'hypothetical standard glycoprotein' of 50 kDa with four glycosylation sites, a substrate concentration of 1 mg/mL and an enzyme concentration of 500 mU/mL for native substrate or 100 mU/mL for denatured substrate is recommended. This yields an enzyme-to-substrate ratio of 500 mU/mg for native substrate or 100 mU/mg for denatured substrate. Translated into a 'standard IgG' of 150 kDa and two glycosylation sites, this is an enzyme concentration of 80 mU/mL for native IgG or 15 mU/mL for denatured IgG, and an enzyme-to-IgG ratio of 80 mU/mg for native IgG or 15 mU/mg for denatured IgG.

Native IgG was used as the substrate for all PNGase F digestions. Enzyme concentrations were 100 mU/mL in FACE and 40 mU/mL in HPAEC and MS experiments (approximately equal to the recommended level). Substrate IgG concentration was 20 mg/mL (about twenty times greater than recommended). This yielded enzyme-to-substrate ratios of 5 mU/mg for FACE (about fifteen times less than recommended) and 2 mU/mg (about forty times less than recommended) for HPAEC and MS experiments. However, the decrease in the enzyme-to-substrate ratio was mitigated by the increase in the substrate concentration.

The possibility that the absence of a denaturation step prior to the PNGase F digestion of the mAb samples might hinder deglycosylation was a concern, especially considering the sequestered nature of the Fc glycans, and the proximity of Asn-297 to the disulfide bonds linking the heavy chains in the hinge region. Despite this, there were no noticeable differences in the N-linked oligosaccharides released from the IgGs and mAbs by PNGase F digestion and hydrazinolysis – which yielded results essentially identical to each other in both FACE and HPAEC-PAD. The failure to detect any residual glycans on the mAb following PNGase F digestion (Barnabé & Butler, 1998; Barnabé, 1998) also suggested complete and quantitative deglycosylation by PNGase F digestion. Similar results for deglycosylation by PNGase F and hydrazinolysis have been found for human polyclonal IgG and a humanized monoclonal IgG (Lines, 1996).

Hydrazinolysis has the disadvantage that O-linked oligosaccharides, if any are present, are recovered with the N-linked glycans (Patel *et al.*, 1993; Patel & Parekh, 1994). However, as previously noted, no evidence for O-linked glycosylation of the mAb was observed.

PNGase F proved to be a very effective method for releasing IgG N-glycans, both in terms of quantitivity and the nonselectivity of removal. This somewhat surprising result shows that this enzyme, used under the conditions described here, can be reliably used to prepare N-linked oligosaccharides from IgG. Quantitative and nonselective release of glycans from IgG by PNGase F without denaturation has also been reported elsewhere (Frears *et al.*, 1999).

4.7.2 Glycan analysis methods

Methods for the analysis of glycoprotein glycans have recently been compared and reviewed (Higgins & Bernasconi, 1997; Routier *et al.*, 1998; Taverna *et al.*, 1998; Merry, 1999; Anumula, 2000; Raju, 2000). FACE and HPAEC-PAD are among the most facile, practical, and informative methods. They are

routinely used for determination of the nature and consistency of recombinant protein glycosylation (Spellman, 1990; Weitzhandler *et al.*, 1994; Friedman & Higgins, 1995; Masada *et al.*, 1995; McGuire *et al.*, 1996; Routier *et al.*, 1997; Anumula, 2000; Raju, 2000), and for correlating oligosaccharide content with culture conditions, and the activity and pharmacokinetics of glycosylated pharmaceuticals (Flesher *et al.*, 1995; Lifely *et al.*, 1995; Kloth *et al.*, 1999).

In this work, glycosylation analysis of the polyclonal IgG and mAb samples by FACE and HPAEC-PAD, which separate and detect glycans according to different principles, provided complementary and corroborating qualitative information. The two methods were also cross-validated by the remarkable quantitative agreement between them.

FACE and HPAEC-PAD are especially effective when used in conjunction with other orthogonal techniques, such as MS. There are several advantages in the MS methods employed in this work as compared to previous MALDI analyses of IgG and mAb glycosylation (Ashton *et al.*, 1995b; Kroon *et al.*, 1995; Küster *et al.*, 1997; Raju *et al.*, 2000). Derivatization of the glycans with PMP allowed for the detection of both neutral and sialylated glycans in the positive-ion mode, instead of neutral glycans in positive-ion mode and sialylated glycans in negative-ion mode. This was particularly obvious in the spectra of the neutral and sialylated standard glycans. However, because of the low degree of branching and sialylation of IgG glycans, a better practical test of the MALDI-QqTOF-MS of PMP-labelled acidic glycans would be the glycosylation analysis of a more typical serum glycoprotein, such as EPO, in which the majority of oligosaccharides are fully sialylated triantennary and tetraantennary structures. The use of the tandem-quadrupole MALDI equipped with an ion mirror allowed for much greater resolution and mass accuracy than one with linear TOF. However, because isomeric oligosaccharides are common and have identical molecular masses, the information from MS alone is not enough to

unequivocably identify the glycans. In this work, this assurance was obtained from the concurrence of the results from all three methods. Further collisional experiments in MS/MS mode have been conducted to obtain greater structural information by fragmentation of the glycans.

4.8 Future studies

Many questions suggest avenues for further examination. What is/are the preferred *in vivo* and *in vitro* pathway(s) of disulfide bond (re)formation for this mAb in this cell line? Is the reduction pathway different than the reoxidation pathway? Are nucleotide sugar levels, particularly UDP-Glc and UDP-Gal, or intracellular energy state, perturbed by alterations in DO concentration? Does DO affect intracellular (ER/Golgi) pH and alter disulfide bond formation and/or *in vivo* GalT activity? Does DO affect the intralumenal redox environment and the GSH:GSSG (reduced to oxidized glutathione) ratio? Do incremental additions of DTT result in increased galactosylation of the mAb? Are the expression and/or activity levels of calnexin and calreticulin, BiP, PDI, and ERp57 and ERp72, *etc.* affected by DO concentration? Is the DO effect observed in other IgG_1 mAbs and mAbs of other classes and subclasses? For example, is the effect observed in IgA, where the Fc glycosylation sites are surface accessible, and the glycans normally more completely processed than those of IgG with no evidence of RA-associated changes. Is the DO effect observed in other glycoproteins with glycosylation sites near a disulfide bond (*e.g.* EPO, t-PA, $\alpha\beta$-glycohormones, *etc.*), or is the effect unique to IgG?

Chapter 5 – Conclusions

The work presented in this thesis has resulted in the following conclusions:

- deglycosylation of the mAb by enzymatic (PNGase F) and chemical (hydrazinolysis) methods yielded identical results
- glycan analysis by FACE and HPAEC-PAD provided corroborating quantitative information
- glycan analysis by MALDI-QqTOF-MS confirmed glycan assignment
- the mAbs produced in different DO concentrations in both the LH and NBS bioreactors all possessed the same types of biantennary N-glycans, but the relative proportions of the oligosaccharides were affected by culture conditions
- increasing the steady-state concentration from 100-150% DO (*i.e.* 100, 125, & 150% DO) in chemostat culture resulted in a moderate decrease in galactosylation of the mAb
- decreasing the steady-state concentration from 100-1% DO (*i.e.* 100, 50, 25, 10, 5, 2, & 1% DO) in chemostat culture dramatically affected glycosylation of the mAb, with a marked decrease in galactosylation at the lower DO concentrations
- the optimum DO concentration for maximum galactosylation of the mAb glycans was 100% DO
- there appeared to be a threshold below 25% DO for minimum galactosylation of the mAb glycans
- the DO effects on galactosylation occurred in both LH and NBS chemostat bioreactors and was therefore not bioreactor-specific, but was influenced by the bioreactor type, being less pronounced in the NBS bioreactor
- the DO effect on galactosylation was not a result of alterations in β1,4-GalT activity, which was unaffected by DO concentration

- DO may affect galactosylation of the mAb by influencing the rate and timing of interchain disulfide bond formation through perturbation of pH or the oxidizing environment of the ER and/or Golgi
- DO may affect galactosylation of the mAb by altering the expression levels of one or more of the relevant chaperone proteins or thiol oxidoreductases

The majority of manufactured recombinant proteins are glycoproteins derived from animal cells, and it is essential to characterize and, if possible, control the glycosylation profile of these products. The fact that culture conditions can affect the glycosylation of glycoprotein biopharmaceuticals and, as a consequence, their immunological functions and other aspects of their efficacy *in vitro* and *in vivo*, has obvious implications for the development and production of mAbs for diagnostic and therapeutic use. In this work it was reported that the N-linked oligosaccharide structures of the mAb were strongly dependent on the DO concentration and, to a lesser extent, the production bioreactor. There are likely other significant cell culture parameters in the production of mAbs and other clinically useful glycoproteins that require consideration and investigation in order to ensure that structural features of the oligosaccharides are consistently reproducible and either correspond to those of the native molecule or a desired glycoform profile.

Glycosylation analysis is relevant during all stages of the development and production of recombinant glycoproteins and mAbs. The principal benefits of glycan analysis are:

- to determine fundamental structure-function relationships
- to allow structural comparison of the recombinant and native forms
- to make a preliminary assessment of the presence of glycans that could render a glycoprotein immunogenic/antigenic or reduce its circulatory lifetime without having to resort to *in vivo* studies

- to validate a production process with respect to the biochemical consistency of the product and improve the ease of purification
- to ensure lot-to-lot consistency
- to provide post-translational information required by the regulatory agencies and for patent protection purposes
- to determine the desired glycosylation profiles for improved or customized activity and biodistribution

The issue of the importance of the glycosylation of proteins, and their structure-function relationships, remains a significant and exciting challenge. The growing understanding of the biological roles of oligosaccharides has provided a future for both basic research and pharmaceutical development in glycobiology. It is clear that glycobiology is a crack in the door to one of the last great frontiers of biochemistry.

Relevant refereed publications

Kunkel, J.P., Jan, D.C.H., Jamieson, J.C., Butler, M. Dissolved oxygen concentration in serum-free continuous culture affects N-linked glycosylation of a monoclonal antibody. *J. Biotechnol.* **1998**, *62*, 55-71.

Kunkel, J.P., Jan, D.C.H., Butler, M., Jamieson, J.C. Comparisons of the glycosylation of a monoclonal antibody produced under nominally identical cell culture conditions in two different bioreactors. *Biotechnol. Prog.* **2000**, *16*, 462-470.

Saba, J.A., Kunkel, J.P., Jan, D.C.H., Ens, W.E., Standing, K.G., Butler, M., Jamieson, J.C., Perreault, H. A study of IgG glycosylation in monoclonal and polyclonal species using electrospray and matrix-assisted laser desorption/ionization mass spectrometry. *Anal. Biochem.* **2002**, *in press*.

Kunkel, J.P., Jamieson, J.C. Inexpensive quantitation of fluorophore-assisted carbohydrate electrophoresis gels: comparison with results from high-pH anion-exchange chromatography with pulsed amperometric detection. *Anal. Biochem.* **2002**, *in preparation*.

Kunkel, J.P., Yan, W.Y., Butler, M., Jamieson, J.C. Decreased monoclonal IgG_1 galactosylation at reduced dissolved oxygen concentrations is not a result of lowered galactosyltransferase activity *in vitro*. *Glycobiology* **2002**, *in preparation*.

Relevant non-refereed publications

Butler, M., Kunkel, J., Jan, D., Huzel, N., Jamieson, J. The glycosylation of immunoglobulin (IgG) in bioreactors. *Adv. Modern Biotechnol.*, Vol. V; **1999**, *O36*.

Saba, J.A., Kunkel, J.P., Bromirski, M.P., Ens, W., Standing, K.G., Jamieson, J.C., Perreault, H. Development of ESI-MS and MALDI-QqTOF-MS methods for the analysis of PMP-labelled N-linked oligosaccharides from polyclonal IgG standards: comparison with HPAEC-PAD analysis. *Proceedings of the 49th American Society for Mass Spectrometry Conference on Mass Spectrometry and Allied Topics*, **2001**.

Kunkel, J.P., Saba, J.A., Bromirski, M.P., Ens, W., Standing, K.G., Perreault, H., Jamieson, J.C. Comparative ESI, MALDI, HPAEC-PAD, and FACE studies of N-linked oligosaccharides from a monoclonal antibody produced in continuous culture: effect of dissolved oxygen concentration. *Proceedings of the 49th American Society for Mass Spectrometry Conference on Mass Spectrometry and Allied Topics*, **2001**.

Relevant conference presentations

Kunkel, J.P., Jamieson, J.C., Jan, D.C.H., Butler, M. Varying dissolved oxygen concentration in continuous culture affects glycosylation of a monoclonal antibody: determination by HPAEC-PAD and FACE. *80th Canadian Society for Chemistry Conference & Exhibition*; Windsor, ON, Canada; June 1-4, **1997**. Talk.

Kunkel, J.P., Jan, D.C.H., Jamieson, J.C., Butler, M. Dissolved oxygen concentration in serum-free continuous culture affects N-linked glycosylation of a monoclonal antibody. *Glycobiology 1997: The Society for Glycobiology 25th Conference*; Long Beach, CA, USA; November 1-4, **1997**. Poster.

Kunkel, J.P., Jan, D.C.H., Jamieson, J.C., Butler, M. The dissolved oxygen in a culture affects the glycosylation of a monoclonal antibody. *International GlycoBioTechnology Symposium*; Braunschweig, Germany; May 3-8, **1998**. Poster.

Butler, M., Jan, D.C.H., Huzel, N., Kunkel, J.P., Jamieson, J.C. Hybridomas grown at various levels of dissolved oxygen show altered metabolic profiles and antibody glycosylation. *216th American Chemical Society National Meeting*; Boston, MA, USA; August 23-27, **1998**. Invited talk.

Kunkel, J.P., Butler, M., Jamieson, J.C. Does dissolved oxygen concentration in cell culture affect IgG glycosylation by influencing the timing and rate of interchain disulfide bond formation? *Glycobiology '98: 3rd Annual Conference of The Society for Glycobiology*; Baltimore, MD, USA; November 11-14, **1998**. Poster.

Butler, M., Kunkel, J.P., Jan, D.C.H., Huzel, N., Jamieson, J.C. Factors that may affect the glycosylation of an immunoglobulin (IgG). *42nd Annual Meeting of the Canadian Federation of Biological Societies*; Winnipeg, MB, Canada; June 2-5, **1999**. Poster.

Kunkel, J.P., Jan, D.C.H., Butler, M., Jamieson, J.C. Comparisons of the glycosylation of a monoclonal antibody produced under nominally identical steady-state conditions in two different bioreactors. *Glycobiology '99: 4th Annual Conference of The Society for Glycobiology*; San Francisco, CA, USA; October 30 - November 2, **1999**. Poster.

Butler, M., Kunkel, J., Jan, D., Huzel, N., Jamieson, J. The glycosylation of immunoglobulin (IgG) in bioreactors. *Biotecnología Habana '99: 8th International Scientific Congress on Medical Applications of Modern Biotechnology*; Havana, Cuba; November 28 - December 3, **1999**. Invited talk.

Perreault, H., Saba, J.A., Kunkel, J.P., Williams, T.T.J., Jamieson, J.C. New strategies involving mass spectrometry for the determination of composition and structure of oligosaccharides derived from glycoproteins. *84th Canadian Society for Chemistry Conference & Exhibition*; Montréal, PQ, Canada; May 26-30, **2001**. Invited talk.

Saba, J.A., Kunkel, J.P., Bromirski, M.P., Ens, W., Standing, K.G., Jamieson, J.C., Perreault, H. Development of ESI-MS and MALDI-QqTOF-MS methods for the analysis of PMP-labelled N-linked oligosaccharides from polyclonal IgG standards: comparison with HPAEC-PAD analysis. *American Society for Mass Spectrometry 49th Conference on Mass Spectrometry and Allied Topics*; Chicago, IL, USA; May 27-31, **2001**. Poster.

Kunkel, J.P., Saba, J.A., Bromirski, M.P., Ens, W., Standing, K.G., Perreault, H., Jamieson, J.C. Comparative ESI, MALDI, HPAEC-PAD, and FACE studies of N-linked oligosaccharides from a monoclonal antibody produced in continuous culture: effect of dissolved oxygen concentration. *American Society for Mass Spectrometry 49th Conference on Mass Spectrometry and Allied Topics*; Chicago, IL, USA; May 27-31, **2001**. Poster.

Saba, J.A., Kunkel, J.P., Jan, D.C.H., Ens, W.E., Standing, K.G., Butler, M., Jamieson, J.C., Perreault, H. A study of IgG glycosylation in a monoclonal antibody by electrospray and matrix-assisted laser desorption/ionization mass spectrometry. *Glycobiology 2001: 6th Annual Conference of The Society for Glycobiology*; San Francisco, CA, USA; November 14-17, **2001**. Poster.

Other relevant presentations

Kunkel, J.P. Dissolved oxygen concentration in continuous culture affects glycosylation of a monoclonal antibody. *Novopharm Biotech Inc.*; Winnipeg, MB, Canada; May 22, **1998**. Invited talk.

Kunkel, J.P. The structural and functional relevance of glycosylation in several glycoproteins of clinical interest. *Department of Chemistry Ph.D. Colloquium*; Winnipeg, MB, Canada; October 5, **2000**. Talk.

Kunkel, J.P., Jan, D.C.H., Butler, M., Jamieson, J.C. Comparisons of the glycosylation of a monoclonal antibody produced under nominally identical steady-state conditions in two different bioreactors. *University of Manitoba Faculties of Science and Engineering Showcase 2001*; Winnipeg, MB, Canada; March 1, **2001**. Poster.

References

Abadeh, S., Church, S., Dong, S., Lund, J., Goodall, M., Jefferis, R. Remodelling the oligosaccharide of human IgG antibodies: effects on biological activities. *Biochem. Soc. Trans.* **1997**, *25*, S661.

Abbadi, A., Mcharfi, M., Aubry, A., Prémilat, S., Boussard, G., Marraud, M. Involvement of side functions in peptide structures: the Asx turn: occurrence and conformational aspects. *J. Am. Chem. Soc.* **1991**, *113*, 2729-2735.

Abeijon, C., Hirschberg, C.B. Topography of glycosylation reactions in the endoplasmic reticulum. *Trends Biochem.* **1992**, *17*, 32-36.

Abeijon, C., Mandon, E.C., Hirschberg, C.B. Transporters of nucleotide sugars, nucleotide sulfate and ATP in the Golgi apparatus. *Trends Biochem. Sci.* **1997**, *22*, 203-207.

Adler, Y., Lamour, A., Jamin, C., Menez, J.F., Le Coree, R., Shoenfeld, Y., Youinou, P. Impaired binding capacity of asialyl and agalactosyl IgG to Fc gamma receptors. *Clin. Exp. Rheumatol.* **1995**, *13*, 315-319.

Alavi, A., Axford, J. β1,4-galactosyltransferase variations in rheumatoid arthritis. *Adv. Exp. Med. Biol.* **1995a**, *376*, 185-192.

Alavi, A., Axford, J. Evaluation of β1,4-galactosyltransferase in rheumatoid arthritis and its role in the glycosylation network associated with this disease. *Glycoconjugate J.* **1995b**, *12*, 206-210.

Alavi, A., Axford, J.S. The glycosyltransferases. In: *Abnormalities of IgG Glycosylation and Immunological Disorders*; Isenberg, D.A., Rademacher, T.W., Eds.; John Wiley & Sons, **1996**; pp 149-169.

Alavi, A., Axford, J.S. Serum galactosylatransferase as a marker of disease activity in rheumatoid arthritis. *Biochem. Soc. Trans.* **1997**, *25*, 313S.

Alavi, A., Axford, J.S., Hay, F.C., Jones, M.G. Tissue-specific galactosyltransferase abnormalities in an experimental model of rheumatoid arthritis. *Ann. Med. Interne* **1998**, *149*, 251-260.

Alavi, A., Arden, N., Spector, T.D., Axford, J.S. Immunoglobulin G glycosylation and clinical outcome in rheumatoid arthritis during pregnancy. *J. Rheumatol.* **2000**, *27*, 1379-1385.

Alexander, S., Elder, J.H. Endoglycosidases from Flavobacterium meningo-septicum: application to biological problems. *Methods Enzymol.* **1989**, *179*, 505-518.

Allen, S., Naim, H.Y., Bulleid, N.J. Intracellular folding of tissue-type plasminogen activator: effects of disulfide bond formation on N-linked glycosylation and

secretion. *J. Biol. Chem.* **1995**, *270*, 4797-4804.

Amado, M., Almeida, R., Schwientek, T., Clausen, H. Identification and characterization of large galactosyltransferase gene families: galactosyltransferases for all functions. *Biochim. Biophys. Acta* **1999**, *1473*, 35-53.

Anderson, C.L. Human IgG Fc receptors. *Clin. Immunol. Immunopathol.* **1989**, *53*, S63-S71.

Andersen, D.C., Goochee, C.F. The effect of cell-culture conditions on the oligosaccharide structures of secreted glycoproteins. *Curr. Opin. Biotechnol.* **1994**, *5*, 546-549.

Andersen, D.C., Goochee, C.F. The effect of ammonia on the O-linked glycosylation of granulocyte colony-stimulating factor produced by Chinese hamster ovary cells. *Biotechnol. Bioeng.* **1995**, *47*, 96-105.

Anumula, K.R. High-sensitivity and high-resolution methods for glycoprotein analysis. *Anal. Biochem.* **2000**, *283*, 17-26.

Arvieux, J., Willis, A.C., Williams, A.F. MRC OX-45 antigen: a leucocyte/ endothelium rat membrane glycoprotein of 45,000 molecular weight. *Mol. Immunol.* **1986**, *23*, 983-990.

Ashton, D.S., Beddel, C.R., Cooper, D.J., Craig, S.J., Lines, A.C., Oliver, R.W., Smith, M.A. Mass spectrometry of the humanized monoclonal antibody CAMPATH 1H. *Anal. Chem.* **1995a**, *67*, 835-842.

Ashton, D.S., Beddell, C.R., Cooper, D.J., Lines, A.C. Determination of carbohydrate heterogeneity in the humanised antibody CAMPATH 1H by liquid chromatography and matrix-assisted laser desorption ionisation mass spectrometry. *Anal. Chim. Acta* **1995b**, *306*, 43-48.

Ashwell, G., Harford, J. Carbohydrate-specific receptors of the liver. *Annu. Rev. Biochem.* **1982**, *51*, 531-554.

Atkinson, D.E. The energy charge of the adenylate pool as a regulatory parameter: interaction with feedback modifiers. *Biochemistry* **1968**, *7*, 4030-4034.

Atkinson, D.E. Regulation of enzyme function. *Annu. Rev. Microbiol.* **1969**, *23*, 47-68.

Atkinson, D.E. *Cellular Energy Metabolism and its Regulation*. Academic Press, **1977**.

Axford, J.S., MacKenzie, L., Lydyard, P.M., Hay, F.C., Isenberg, D.A., Roitt, I.M. Reduced B-cell galactosyltransferase activity in rheumatoid arthritis. *Lancet II*, **1987**, 1486-1488.

Axford, J.S. Decreased B-cell galactosyltransferase activity in rheumatoid arthritis. *Br. J. Rheumatol.* **1988**, *27(suppl II)*, 170.

Axford, J.S., Sumar, N., Alavi, A., Isenberg, D.A., Young, A., Bodman, K.B., Roitt, I.M. Changes in normal glycosylation mechanisms in autoimmune rheumatic disease. *J. Clin. Invest.* **1992**, *89*, 1021-1031.

Axford, J.S., Alavi, A., Bond, A., Hay, F.C. Differential B lymophocyte galactosyltransferase activity in the MRL mouse model of rheumatoid arthritis. *Autoimmunity* **1994**, *17*, 157-163.

Axford, J.S. Glycosylation and rheumatic disease. *Biochim. Biophys. Acta* **1999**, *1455*, 219-229.

Baenziger, J.U. Protein-specific glycosyltransferases: how and why they do it! *FASEB J.* **1994**, *8*, 1019-1025.

Barnabé, N., Butler, M. Effect of temperature on nucleotide pools and monoclonal antibody production in a mouse hybridoma. *Biotechnol. Bioeng.* **1994**, *44*, 1235-1245.

Barnabé, N. The relationship between intracellular nucleotides and hybridoma cell culture productivity and viability. *Ph.D. Thesis* **1998**, Department of Microbiology, University of Manitoba.

Barnabé, N., Butler, M. The relationship between intracellular UDP-*N*-acetyl hexosamine pool and monoclonal antibody production in a mouse hybridoma. *J. Biotechnol.* **1998**, *60*, 67-80.

Basa, L.J., Spellman, M.W. Analysis of glycoprotein-derived oligosaccharides by high-pH anion-exchange chromatography. *J. Chromatogr.* **1990**, *499*, 205-220.

Baumal, R., Potter, M., Scharff, M.D. Synthesis, assembly, and secretion of gamma globulin by mouse myeloma cells III: assembly of the three subclasses of IgG. *J. Exp. Med.* **1971**, *134*, 1316-1334.

Bause, E., Legler, G. The role of hydroxy amino acid in the triplet sequence Asn-Xaa-Thr(Ser) for the N-glycosylation step during glycoprotein biosynthesis. *Biochem. J.* **1981**, *195*, 639-644.

Bause, E. Structural requirements of N-glycosylation of proteins: studies with proline peptides as conformational probes. *Biochem. J.* **1983**, *209*, 331-336.

Bayer, E.A., Ben-Hur, H., Wilchek, M. Analysis of proteins and glycoproteins on blots. *Methods Enzymol.* **1990a**, *184*, 415-427.

Bayer, E.A., Ben-Hur, H., Wilchek, M. Direct labeling of blotted glycoconjugates. *Methods Enzymol.* **1990b**, *184*, 427-429.

Bergeron, J.J.M., Brenner, M.B., Thomas, D.Y., Williams, D.B. Calnexin: a membrane-bound chaperone of the endoplasmic reticulum. *Trends Biochem. Sci.* **1994**, *19*, 124-128.

Bergeron, J.J.M., Zapun, A., Ou, W.-J., Hemming, R., Parlati, F., Cameron, P.H., Thomas, D.Y. The role of the lectin calnexin in conformation independent binding to N-linked glycoproteins and quality control. *Adv. Exp. Med. Biol.* **1998**, *435*, 105-116.

Bergman, L.W., Kuehl, W.M. Formation of intermolecular disulfide bonds on nascent immunoglobulin polypeptides. *J. Biol Chem.* **1979**, *254*, 5690-5694.

Bergwerff, A.A., Stroop, C.J.M., Murray, B., Holtorf, A.P., Pluschke, G., Van Oostrum, J., Kamerling, J.P., Vliegenthart, J.F.G. Variation in N-linked carbohydrate chains in different batches of two chimeric monoclonal IgG_1 antibodies produced by different murine SP2/0 transfectoma cell subclones. *Glycoconjugate J.* **1995**, *12*, 318-330.

Bibila, T., Flickinger, M.C. A structured model for monoclonal antibody synthesis in exponentially growing and stationary phase hybridoma cells. *Biotechnol. Bioeng.* **1991**, *37*, 210-226.

Bibila, T.A., Robinson, D.K. In pursuit of the optimal fed-batch process for monoclonal antibody production. *Biotechnol. Prog.* **1995**, *11*, 1-13.

Birch, J.R., Bonnerjea, J., Flatman, S., Vranch, S. The production of monoclonal antibodies. In: *Monoclonal Antibodies: Principles and Applications*; Birch, J.R., Lennox, E.S., Eds.; Wiley-Liss, **1995**; pp 231-265.

Bjare, U., Serum-free cell culture. *Pharm. Ther.* **1992**, *53*, 355-374.

Black, D.J., Barford, J.P., Harbour, C., Packen, N., Fletcher, A. Serum content affects the structure and activity of the antibody produced by animal cells in culture. In: *Animal Cell Technology: Developments Towards the 21st Century*; Beuvery, E.C., Griffiths, J.B., Zeiljemaker, W.P., Eds.; Kluwer, **1995**; pp 365-369.

Bodman, K.B., Sumar, N., MacKenzie, L.E., Isenberg, D.A., Hay, F.C., Roitt,.I.M., Lydyard, P.M. Lymphocytes from patients with rheumatoid arthritis produce agalactosylated IgG *in vitro*. *Clin. Exp. Immunol.* **1992**, *88*, 420-423.

Bodman, K.B., Hutchings, P.R., Jeddi, P.A., Delves, P.J., Rook, G.A.W., Sumar, N., Roitt, I.M., Lydyard, P.M. IgG glycosylation in autoimmune-prone strains of mice. *Clin. Exp. Immunol.* **1994**, *95*, 103-107.

Bodman-Smith, K., Sumar, N., Sinclair, H., Roitt, I., Isenberg, D., Young, A. Agalactosyl IgG [Gal(0)]: an analysis of its clinical utility in the long-term follow-up of patients with rheumatoid arthritis. *Br. J. Rheumatol.* **1996**, *35*, 1063-1066.

Bond, A., Cooke, A., Hay, F.C. Glycosylation of IgG, immune complexes and IgG

subclasses in the MRL-lpr/lpr mouse model of rheumatoid arthritis. *Eur. J. Immunol.* **1990**, *20*, 2229-2233.

Bond, A., Jones, M.G., Hay, F.C. Human IgG preparations isolated by ion-exchange or protein G affinity chromatography differ in their glycosylation profiles. *J. Immunol. Methods* **1993**, *166*, 27-33.

Borys, M.C., Linzer, D.I.H., Papoutsakis, E.T. Culture pH affects expression rates and glycosylation of recombinant mouse placental lactogen proteins by Chinese hamster ovary (CHO) cells. *Biotechnology (NY)* **1993**, *11*, 720-724.

Borys, M.C., Linzer, D.I.H., Papoutsakis, E.T. Ammonia affects the glycosylation patterns of recombinant mouse placental lactogen-I by Chinese hamster ovary cells in a pH-dependent manner. *Biotechnol. Bioeng.* **1994**, *43*, 505-514.

Boyd, P.N., Lines, A.C., Patel, A.K. The effect of the removal of sialic acid, galactose and total carbohydrate on the functional activity of Campath-1H. *Mol. Immunol.* **1995**, *32*, 1311-1318.

Bradford, M.M. A rapid and sensitive method for the quantitation of microgram quantities of protein utilising the principle of protein-dye binding. *Anal. Biochem.* **1976**, *72*, 248-254.

Branza-Nichita, N., Petrescu, A.J., Negroiu, G., Dwek, R.A., Petrescu, S.M. N-Glycosylation processing and glycoprotein folding: lessons learned from the tyrosinase-related proteins. *Chem. Rev.* **2000**, *100*, 4697-4711.

Brew, K., Vanaman, T.C., Hill, R.L. The role of α-lactalbumin and the A protein in lactose synthetase: a unique mechanism for the control of a biological reaction. *Proc. Natl. Acad. Sci. USA* **1968**, *59*, 491-497.

Brockhausen, I., Narasimhan, S., Schachter, H. The biosynthesis of highly branched N-glycans: studies on the sequential pathway and functional role of *N*-acetylglucosaminyltransferases I, II, II, IV, V and VI. *Biochimie* **1988**, *70*, 1521-1533.

Brockhausen, I. Clinical aspects of glycoprotein synthesis. *Crit. Rev. Clin. Lab. Sci.* **1993**, *30*, 65-151.

Bülter, T., Elling, L. Enzymatic synthesis of nucleotide sugars. *Glycoconjugate J.* **1999**, *16*, 147-159.

Burton, D.R. Structure and function of antibodies. In: *Molecular Genetics of Immunoglobulin*; Calabi, F., Neuberger, M.S., Eds.; Elsevier, **1987**; pp 1-50.

Butler, M. Processes with animal cell and tissue cultures. In: *Biotechnology: A Comprehensive Treatise in 8 Volumes*, Vol. 6b; Rehm, H.-J., Reed, C., Eds.; VCH, **1988**; pp 249-316.

Cacan, R., Cecchelli, R., Hoflack, B., Verbert, A. Intralumenal pool and transport of CMP-*N*-acetylneuraminic acid, GDP-fucose and UDP-galactose: study with plasma-membrane-permeabilized mouse thymocytes. *Biochem. J.* **1984**, *224*, 277-284.

Cacan, R., Verbert, A. Transport of free and N-linked oligomannoside species across the rough endoplasmic reticulum membranes. *Glycobiology* **2000**, *10*, 645-648.

Cacan, R., Duvet, S., Labiau, O., Verbert, A., Krag, S.S. Monoglucosylated oligomannosides are released during the degradation process of newly synthesized glycoproteins. *J. Biol. Chem.* **2001**, *276*, 22307-22312.

Cant, D., Barford, J., Harbour, C., Fletcher, A., Packer, N., Gooley, A. Glycosylation and functional activity of anti-D secreted by two human lymphoblastoid cell lines. *Cytotechnology* **1994**, *15*, 223-228.

Capasso, J.M., Hirschberg, C.M. Mechanisms of glycosylation and sulfation in the Golgi apparatus: evidence for nucleotide sugar/nucleoside monophosphate and nucleotide sulfate/nucleoside monophosphate antiports in the Golgi apparatus membrane. *Proc. Natl. Acad. Sci. USA* **1984**, *81*, 7051-7055.

Cecchelli, R., Cacan, R., Verbert, A. Mechanism of UDP-sugar transport into intracellular vesicles: occurrence of UDP-GlcNAc/UDP and UDP-Gal/UDP antiports. *FEBS Lett.* **1986**, *208*, 407-412.

Center for Biologics Evaluation and Research. Points to consider in the manufacture and testing of monoclonal antibody products for human use. *Food and Drug Administration*; Rockville, MD, USA, **1997**.

Cherry, R.S., Papoutsakis, E.T. Fluid-mechanical injury of cells in bioreactors. In: *Animal Cell Biotechnology*, Vol. 4; Spier, R.E., Griffiths, J.B., Eds.; Academic Press, **1990**; pp 71-121.

Chiu, M.H., Tamura, T., Wadhwa, M.S., Rice, K.G. *In vivo* targeting function of N-linked oligosaccharides with terminating galactose and *N*-acetylgalactosamine residues. *J. Biol. Chem.* **1994**, *269*, 16195-16202.

Chotigeat, W., Watanapokasin, Y., Mahler, S., Gray, P.P. Role of environmental conditions on the expression levels, glycoform pattern and levels of sialyltransferase for hFSH produced by recombinant CHO cells. *Cytotechnology* **1994**, *15*, 217-221.

Chou, H.-H., Takematsu, H., Diaz, S., Iber, J., Nickerson, E., Wright, K.L., Muchmore, E.A., Nelson, D.L., Warren, S.T., Varki, A. A mutation in human CMP-sialic acid hydroxylase occurred after the Homo-Pan divergence. *Proc. Natl. Acad. Sci. USA* **1998**, *95*, 11751-11756.

Chu, F.K. Requirements of cleavage of high mannose oligosaccharides in glycoproteins by peptide-N-glycosidase F. *J. Biol. Chem.* **1986**, *261*, 172-177.

Clark, M.R. IgG effector mechanisms. *Chem. Immunol.* **1997**, *65*, 88-110.

Cole, C.R., Smith, C.A., Butler, M. Specific activities of glycosyltransferase enzymes vary with monoclonal antibody productivity in murine hybridomas. *Biotechnol. Lett.* **1993**, *15*, 553-558.

Colley, K. Golgi localization of glycosyltransferases: more questions than answers. *Glycobiology* **1997**, *7*, 1-13.

Costello, C.E., Perreault, H., Ngoka, L.C. Mass spectrometric and tandem mass spectrometric approaches to the analysis of glycoconjugates. In: *Mass Spectrometry in the Biological Sciences*; Burlingame, A.L., Carr, S.A., Eds.; Humana Press, **1996**; pp 365-384.

Cruz, H.J., Conradt, H.S., Peixoto, C.M., Alves, P.M., Nimtz, M., Dias, E.M., Santos, H., Moreira, J.L., Carrondo, M.J.T. Glycosylation patterns of a rec-fusion protein expressed in BHK cells at different metabolic states. In: *Animal Cell Technology: Products from Cells, Cells as Products*; Bernard, A., Griffiths, B., Noé, W., Wurm, F., Eds.; Kluwer, **1999a**; pp 241-243.

Cruz, H.J., Ferreira, A.S., Freitas, C.M., Moreira, J.L., Carrondo, M.J.T. Metabolic responses to different glucose and glutamine levels in baby hamster kidney cell culture. *Appl. Microbiol. Biotechnol.* **1999b**, *51*, 579-585.

Cruz, H.J., Moreira, J.L., Carrondo, M.J.T. Metabolic shifts by nutrient manipulation in continuous cultures of BHK cells. *Biotechnol. Bioeng.* **1999c**, *66*, 104-113.

Cruz, H.J., Peixoto, C.M., Nimtz, M., Alves, P.M., Dias, E.M., Moreira, J.L., Carrondo, M.J.T. Metabolic shifts do not influence the glycosylation patterns of a recombinant fusion protein expressed in BHK cells. *Biotechnol. Bioeng.* **2000a**, *69*, 129-139.

Cruz, H.J., Freitas, C.M., Alves, P.M., Moreira, J.L., Carrondo, M.J.T. Effects of ammonia and lactate on growth, metabolism, and productivity of BHK cells. *Enzyme Microb. Technol.* **2000b**, *27*, 43-52.

Cumming, D.A. Glycosylation of recombinant protein therapeutics: control and functional implications. *Glycobiology* **1991**, *1*, 115-130.

Cummings, R.D. Synthesis of asparagine-linked oligosaccharides: pathways, genetics, and metabolic regulation. In: *Glycoconjugates: Composition, Structure, and Function*; Allen, H.J., Kisailus, E.C., Eds.; Marcel Dekker, **1992**; pp 333-360.

Dauchez, M., Mazurier, J., Montreuil, J., Spik, G., Vergoten, G. Molecular dynamics simulations of a monofucosylated biantennary glycan of the *N*-acetyllactosamine type: the human lactotransferrin glycan. *Biochimie* **1992**, *74*, 63-74.

Deisenhofer, J., Colman, P.M., Epp, O., Huber, R. Crystallographic structural studies of a human Fc fragment. *Hoppe Seylers Z. Physiol. Chem.* **1976**, *357*, 1421-1434.

Deisenhofer, J. Crystallographic refinement and atomic models of a human Fc fragment and it complex with fragment B of protein A from Staphylococcus aureus at 2.9- and 2.8-Å resolution. *Biochemistry* **1981**, *20*, 2361-2370.

Deutscher, S.L., Hirschberg, C.B. Mechanism of galactosylation in the Golgi apparatus: a Chinese hamster ovary cell mutant deficient in translocation of UDP-galactose across Golgi vesicle membranes. *J. Biol. Chem.* **1986**, *261*, 96-100.

deZengotita, V.M., Kimura, R., Miller, W.M. Effects of CO_2 and osmolality on hybridoma cells: growth, metabolism, and monoclonal antibody production. *Cytotechnology* **1998**, *28*, 213-227.

Dinter, A., Berger, E.G. The regulation of cell- and tissue-specific expression of glycans by glycosyltransferases. *Adv. Exp. Med. Biol.* **1995**, *376*, 53-82.

Do, K.-Y., Fregien, N., Pierce, M., Cummings, R.D. Modification of glycoproteins by *N*-acetylglucosaminyltransferase V is greatly influenced by accessibility of the enzyme to oligosaccharide acceptors. *J. Biol. Chem.* **1994**, *269*, 23456-23464.

Dong, X., Storkus, W.J., Salter, R.D. Binding and uptake of agalactosyl IgG by mannose receptor on macrophages and dendritic cells. *J. Immunol.* **1999**, *163*, 5427-5434.

Doyle, C., Butler, M. The effect of pH on the toxicity of ammonia to a murine hybridoma. *J. Biotechnol.* **1990**, *9*, 346-352.

Dwek, R.A., Lellouch, A.C., Wormald, M.R. Glycobiology: 'the function of sugar in the IgG molecule'. *J. Anat.* **1995**, *187*, 279-292.

Elbein, A.D. Inhibitors of the biosynthesis and processing of N-linked oligosaccharide chains. *Annu. Rev. Biochem.* **1987a**, *56*, 497-534.

Elbein, A.D. Glycosylation inhibitors for N-linked glycoproteins. *Methods Enzymol.* **1987b**, *138*, 661-709.

Elbein, A.D. Glycosidase inhibitors: inhibitors of N-linked oligosaccharide processing. *FASEB J.* **1991a**, *5*, 3055-3063.

Elbein, A.D. The role of N-linked oligosaccharides in glycoprotein function. *Trends Biotechnol.* **1991b**, *9*, 33-39.

Endo, T., Kochibe, N., Kobata, A. Structural study of the carbohydrate moieties of two human immunoglobulin subclasses (IgG_2 and IgG_4). *Glycoconjugate J.* **1989**, *6*, 57-66

Endo, T., Wright, A., Morrison, S.L., Kobata, A. Glycosylation of the variable region of immunoglobulin G: site specific maturation of the sugar chains. *Mol. Immunol.* **1995**, *32*, 931-940.

Ey, P.L., Prowse, S.J., Jenkin, C.R. Isolation of pure IgG_1, IgG_{2a} and IgG_{2b} immunoglobulins from mouse serum using protein A-sepharose. *Immunochemistry* **1978**, *15*, 429-436.

Feizi, T., Childs, R.A. Carbohydrates as antigenic determinants of glycoproteins. *Biochem. J.* **1987**, *245*, 1-11.

Feng, W., Matzuk, M.M., Mountjoy, K., Bedows, E., Ruddon, R.W., Boime, I. The asparagine-linked oligosaccharides of human chorionic gonadotropin β subunit facilitate correct disulfide bond pairing. *J. Biol. Chem.* **1995**, *270*, 11851-11859.

Ferrari, D.M., Söling, H.-D. The protein disulphide-isomerase family: unravelling a string of folds. *Biochem. J.* **1999**, *339*, 1-10.

Field, M.C., Amatayakul-Chantler, S., Rademacher, T.W., Rudd, P.M., Dwek, R.A. Structural analysis of the N-glycans from human immunoglobulin A_1: comparison of normal human serum immunoglobulin A_1 with that isolated from patients with rheumatoid arthritis. *Biochem. J.* **1994**, *299*, 261-275.

Flesher, A.R., Marzowski, J., Wang, W.-C., Raff, H.V. Fluorophore-labeled carbohydrate analysis of immunoglobulin fusion proteins: correlation of oligosaccharide content with *in vivo* clearance profile. *Biotechnol. Bioeng.* **1995**, *46*, 399-407.

Flickinger, M.C., Bibila, T. Modeling the regulation of antibody synthesis and assembly in a murine hybridoma. *Frontiers in Bioprocessing II*; Todd, P., Sikdar, S.K., Bier, M., Eds.; American Chemical Society, USA; **1992**; pp 241-257.

Fraser, I.H., Mookerjea, S. Studies on the purification and properties of UDP-galactose-glycoprotein galactosyltransferase from rat liver and serum. *Biochem. J.* **1976**, *156*, 347-355.

Frears, E.R., Axford, J.S. Fluorophore-labelled carbohydrate electrophoresis distinguishes rheumatoid arthritis from healthy individuals. *Biochem. Soc. Trans.* **1997**, *25*, S662.

Frears, E.R., Merry, A.H., Axford, J.S. Screening neutral and acidic IgG N-glycans by high density electrophoresis. *Glycoconjugate J.* **1999**, *16*, 283-290.

Freedman, R.B., Greenall, C., Jenkins, N., Tuite, M.F. Protein folding in the secretory pathway of animal cells. In: *Animal Cell Technology: Developments Towards the 21st Century*; Beuvery, E.C., Griffiths, J.B., Zeiljemaker, W.P., Eds.; Kluwer, **1995**; pp 371-376.

Friedman, Y., Higgins, E.A. A method for monitoring the glycosylation of recombinant glycoproteins from conditioned medium, using fluorophore-assisted carbohydrate electrophoresis. *Anal. Biochem.* **1995**, *228*, 221-225.

Fu, D., O'Neill, R.A. Monosaccharide composition analysis of oligosaccharides and glycoproteins by high-performance liquid chromatography. *Anal. Biochem.* **1995**, *227*, 377-384.

Fujii, S., Nishiura, T., Nishikawa, A., Miura, R., Taniguchi, N. Structural heterogeneity of sugar chains in immunoglobulin G: conformation of immunoglobulin G molecule and substrate specificities of glycosyltransferases. *J. Biol. Chem.* **1990**, *265*, 6009-6018.

Furukawa, K., Matsuta, K., Takeuchi, F., Kosuge, E., Miyamoto, T., Kobata, A. Kinetic study of a galactosyltransferase in the B cells of patients with rheumatoid arthritis. *Int. Immunol.* **1990**, *2*, 105-112.

Furukawa, K., Kobata, A. IgG galactosylation: its biological significance and pathology. *Mol. Immunol.* **1991**, *28*, 1333-1340.

Furukawa, K., Sato, T. β-1,4-Galactosylation of N-glycans is a complex process. *Biochim. Biophys. Acta* **1999**, *1473*, 54-66.

Gagneux, P., Varki, A. Evolutionary considerations in relating oligosaccharide diversity to biological function. *Glycobiology* **1999**, *9*, 747-755.

Galili, U., Clark, M.R., Shohet, S.B., Buehler, J., Macher, B.A. Evolutionary relationship between the natural anti-Gal antibody and the Galα1-3Gal epitope in primates. *Proc. Natl. Acad. Sci. USA* **1987**, *84*, 1369-1373.

Galili, U., Shohet, S.B., Kobrin, E., Stults, C.L.M., Macher, B.A. Man, apes, and Old World monkeys differ from other mammals in the expression of α-galactosyl epitopes on nucleated cells. *J. Biol. Chem.* **1988**, *263*, 17755-17762.

Galili, U. Abnormal expression of α-galactosyl epitopes in man: a trigger for autoimmune processes? *Lancet II*, **1989**, 358-361.

Galili, U. Evolution and pathophysiology of the human natural anti-α-galactosyl IgG (anti-Gal) antibody. *Springer Sem. Immunopathol.* **1993**, *15*, 155-171.

Gauny, S.S., Andya, J., Thomson, J., Young, J.D., Winkelhake, J.L. Effect of production method on the systemic clearance rate of a human monoclonal antibody in the rat. *Hum. Antibod. Hybridomas* **1991**, *2*, 33-38.

Gavel, Y., Von Heijne, G. Sequence differences between glycosylated and non-glycosylated Asn-X-Thr/Ser acceptor sites: implications for protein engineering. *Protein Eng.* **1990**, *3*, 433-442.

Gawlitzek, M., Conradt, H.S., Wagner, R. Effect of different cell culture conditions on the polypeptide integrity and N-glycosylation of a recombinant model glycoprotein. *Biotechnol. Bioeng.* **1995a**, *46*, 536-544.

Gawlitzek, M., Valley, U., Nimtz, M., Wagner, R., Conradt, H.S. Characterization of changes in the glycosylation pattern of recombinant proteins from BHK-21 cells due to different culture conditions. *J. Biotechnol.* **1995b**, *42*, 117-131.

Gawlitzek, M., Valley, U., Wagner, R. Ammonium ion and glucosamine dependent increases of oligosaccharide complexity in recombinant glycoproteins secreted from cultivated BHK-21 cells. *Biotechnol. Bioeng.* **1998**, *57*, 518-528.

Gawlitzek, M., Papac, D.I., Sliwkowski, M.B., Ryll, T. Incorporation of ^{15}N from ammonium into the N-linked oligosaccharides of an immunoadhesin glycoprotein expressed in Chinese hamster ovary cells. *Glycobiology* **1999**, *9*, 125-131.

Gawlitzek, M., Ryll, T., Lofgren, T., Sliwkowski, M.B. Ammonium alters N-glycan structures of recombinant TNFR-IgG: degradative versus biosynthetic mechanisms. *Biotechnol. Bioeng.* **2000**, *68*, 637-646.

Ghirlando, R., Lund, J., Goodall, M., Jefferis, R. Glycosylation of human IgG-Fc: influences on structure revealed by differential scanning micro-calorimetry. *Immunol. Lett.* **1999**, *68*, 47-52.

Gilbert, H.F. Protein disulfide isomerase and assisted protein folding. *J. Biol. Chem.* **1997**, *272*, 29399-29402.

Glassy, M.C., Tharakan, J.P., Chau, P.C. Serum-free media in hybridoma culture and monoclonal antibody production. *Biotechnol. Bioeng.* **1988**, *32*, 1015-1028.

Gonzalez, R., Asenjo, J.A., Andrews, B.A. Metabolic control analysis of monoclonal antibody synthesis. *Biotechnol. Prog.* **2001**, *17*, 217-226.

Goochee, C.F., Monica, T. Environmental effects on protein glycosylation. *Biotechnology (NY)* **1990**, *8*, 421-427.

Goochee, C.F., Gramer, M.J., Andersen, D.C., Bahr, J.B., Rasmussen, J.R. The oligosaccharides of glycoproteins: bioprocess factors affecting oligosaccharide structure and their effect on glycoprotein properties. *Biotechnology (NY)* **1991**, *9*, 1347-1355.

Goochee, C.F. Bioprocess factors affecting glycoprotein oligosaccharide structure. *Dev. Biol. Stand.* **1992**, *76*, 95-104

Goochee, C.F., Gramer, M.J., Andersen, D.C., Bahr, J.B., Rasmussen, J.R. The oligosaccharides of glycoproteins: factors affecting their synthesis and their influence on glycoprotein properties. *Frontiers in Bioprocessing II*; Todd, P., Sikdar, S.K., Bier, M., Eds.; American Chemical Society, **1992**; pp 199-240.

Grabenhorst, E., Schlenke, P., Pohl, S., Nimtz, M., Conradt, H.S. Genetic engineering of recombinant glycoproteins and the glycosylation pathway in mammalian host cells. *Glycoconjugate J.* **1999**, *16*, 81-97.

Gramer, M.J., Goochee, C.F. Glycosidase activities in Chinese hamster ovary cell lysate and cell culture supernatant. *Biotechnol. Prog.* **1993**, *9*, 366-373.

Gramer, M.J., Goochee, C.F. Glycosidase activities of the 293 and NS0 cell lines, and of an antibody-producing hybridoma cell line. *Biotechnol. Bioeng.* **1994a**, *43*, 423-428.

Gramer, M.J., Goochee, C.F. Glycosidase activities in Chinese hamster ovary cells. *Biotechnol. Prog.* **1994b**, *10*, 121-124.

Gramer, M.J., Schaffer, D.V., Sliwkowski, M.B., Goochee, C.F. Purification and characterization of a fucosidase from Chinese hamster ovary cell culture supernatant. *Glycobiology* **1994**, *4*, 611-616.

Gramer, M.J., Goochee, C.F., Chock, V.Y., Brousseau, D.T., Sliwkowski, M.B. Removal of sialic acid from a glycoprotein in CHO cell culture supernatant by action of an extracellular CHO cell sialidase. *Biotechnology (NY)* **1995**, *13*, 692-698.

Grammatikos, S.I., Valley, U., Nimtz, M., Conradt, H.S., Wagner, R. Intracellular UDP-*N*-acetylhexosamine pool affects N-glycan complexity: a mechanism of ammonium action on protein glycosylation. *Biotechnol. Prog.* **1998**, *14*, 410-419.

Gray, D.R., Chen, S., Howarth, W., Inlow, D., Maiorella, B.L. CO_2 in large-scale and high-density CHO cell perfusion culture. *Cytotechnology* **1996**, 22, 65-78.

Griffiths, J.B. Overview of cell culture systems and their scale-up. In: *Animal Cell Biotechnology*, Vol. 3; Spier, R.E., Griffiths, J.B., Eds.; Academic Press, **1988**; pp 179-220.

Gross, V., Heinrich, P.C., vom Berg, D., Steube, K., Andus, T., Tran-Thi, T.-A., Decker, K., Gerok, W. Involvement of various organs in the initial plasma clearance of differently glycosylated rat liver secretory proteins. *Eur. J. Biochem.* **1988**, *173*, 653-659.

Gross, V., Steube, K., Tran-Thi, T.-A., Gerok, W., Heinrich, P.C. Role of N-glycosylation for the plasma clearance of rat liver secretory glycoproteins. *Biochem. Soc. Trans.* **1989**, *17*, 21-23.

Hamako, J., Matsui, T., Ozeki, Y., Mizuochi, T., Titani, K. Comparative studies of asparagine-linked sugar chains of immunoglobulin G from eleven mammalian species. *Comp. Biochem. Physiol. B* **1993**, *106*, 949-954.

Hames, B.D. One-dimensional polyacrylamide gel electrophoresis. In: *Gel Electrophoresis of Proteins: A Practical Approach*, 2nd ed.; Hames, B.D., Rickwood, D., Eds.; Oxford University Press, **1990**; pp 1-147.

Hammond, C., Braakman, I., Helenius, A. Role of N-linked oligosaccharide recognition, glucose trimming and calnexin during glycoprotein folding in the endoplasmic reticulum. *Proc. Natl. Acad. Sci. USA* **1994**, *91*, 913-917.

Handa-Corrigan, A. Oxygenating animal cell cultures: the remaining problems. In: *Animal Cell Biotechnology*, Vol. 4; Spier, R.E., Griffiths, J.B., Eds.; Academic Press, **1990**; pp 123-132.

Hansen, J.E., Lund, O., Tolstrup, N., Gooley, A.A., Williams, K.L., Brunak, S. NetOglyc: prediction of mucin type O-glycosylation sites based on sequence context and surface accessibility. *Glycoconjugate J.* **1998**, *15*, 115-130.

Harbour, C., Fletcher, A. Hybridomas: production and selection. In: *Mammalian Cell Biotechnology: A Practical Approach*; Butler, M., Ed., Oxford University Press, **1991**; pp 109-138.

Hardy, M.R., Townsend, R.R. Separation of positional isomers of oligosaccharides and glycopeptides by high-performance anion-exchange chromatography with pulsed amperometric detection. *Proc. Natl. Acad. Sci. USA* **1988**, *85*, 3289-3293.

Hardy, M.R., Townsend, R.R. Separation of fucosylated oligosaccharides using high-pH anion-exchange chromatography with pulsed-amperometric detection. *Carbohydr. Res.* **1989**, *188*, 1-7.

Hardy, M.R., Townsend, R.R. High-pH anion-exchange chromatography of glycoprotein-derived carbohydrates. *Methods Enzymol.* **1994**, *230*, 208-225.

Harris, J.L., Spier, R.E. Physical and chemical parameters: measurement and control. In: *Animal Cell Biotechnology*, Vol. 1; Spier, R.E., Griffiths, J.B., Eds.; Academic Press, **1985**; pp 283-319.

Harris, L.J., Skaletsky, E., McPherson, A. Crystallographic structure of an intact IgG_1 monoclonal antibody. *J. Mol. Biol.* **1998**, *275*, 861-872.

Harvey, D.J. Matrix-assisted laser desorption/ionisation mass spectrometry of oligosaccharides and glycoconjugates. *J. Chromatogr. A* **1996**, *720*, 429-446.

Harvey, D.J., Küster, B., Naven, T.J.P. Perspectives in the glycosciences: matrix-assisted laser desorption/ionization (MALDI) mass spectrometry of carbohydrates. *Glycoconjugate J.* **1998**, *15*, 333-338.

Hashim, O.H., Cushley, W. Role of processing of N-linked oligosaccharides in control of immunoglobulin secretion from rat hybridomas. *Mol. Immunol.* **1987**, *24*, 1087-1096.

Helenius, A. How N-linked oligosaccharides affect glycoprotein folding in the endoplasmic reticulum. *Mol. Biol. Cell* **1994**, *5*, 253-265.

Helenius, A., Trombetta, E.S., Hebert, D.N., Simons, J.F. Calnexin, calreticulin and the folding of glycoproteins. *Trends Cell. Biol.* **1997**, *7*, 193-200.

Helenius, A., Aebi, M. Intracellular functions of N-linked glycans. *Science* **2001**, *291*, 2364-2369.

Hermentin, P., Witzel, R., Vliegenthart, J.F.G., Kamerling, J.P., Nimtz, M., Conradt, H.S. A strategy for the mapping of N-glycans by high-pH anion-exchange chromatography with pulsed amperometric detection. *Anal. Biochem.* **1992a**, *203*, 281-289.

Hermentin, P., Witzel, R., Doenges, R., Bauer, R., Haupt, H., Patel, T., Parekh, R.B., Brazel, D. The mapping by high-pH anion-exchange chromatography with pulsed amperometric detection and capillary electrophoresis of the carbohydrate moieties of human plasma α_1-acid glycoprotein. *Anal. Biochem.* **1992b**, *206*, 419-429.

Hickman, S., Kornfeld, S. Effect of tunicamycin on IgM, IgA, and IgG secretion by mouse plasmacytoma cells. *J. Immunol.* **1978**, *121*, 990-996.

Higgins, E., Bernasconi, R. A comparison of oligosaccharide profiling methods. In: *Techniques in Glycobiology*; Townsend, R.R., Hotchkiss, Jr., A.T., Eds.; Marcel Dekker, **1997**; pp 431-442.

High, S., Lecomte, F.J., Russell, S.J., Abell, B.M., Oliver, J.D. Glycoprotein folding in the endoplasmic reticulum: a tale of three chaperones? *FEBS Lett.* **2000**, *476*, 38-41.

Hillenkamp, F., Karas, M., Beavis, R.C., Chait, B.T. Matrix-assisted laser desorption/ionization mass spectrometry of biopolymers. *Anal. Chem.* **1991**, *63*, 1193A-1203A.

Hills, A.E., Patel, A.K., Boyd, P.N., James, D.C. Control of therapeutic monoclonal antibody glycosylation. In: *Animal Cell Technology: Products from Cells, Cells as Products*; Bernard, A., Griffiths, B., Noé, W., Wurm, F., Eds.; Kluwer, **1999**; pp 255-257.

Hirani, S., Bernasconi, R.J., Rasmussen, J.R. Use of *N*-glycanase to release asparagine-linked oligosaccharides for structural analysis. *Anal. Biochem.* **1987**, *162*, 485-492.

Hirschberg, C.B., Snider, M.B. Topography of glycosylation in the rough endoplasmic reticulum and Golgi apparatus. *Annu. Rev. Biochem.* **1987**, *56*, 63-87.

Hirschberg, C.B., Robbins, P.W., Abeijon, C. Transporters of nucleotide sugars, ATP, and nucleotide sulfate in the endoplasmic reticulum and Golgi apparatus. *Annu. Rev. Biochem.* **1998**, *67*, 49-69.

Homans, S.W. Conformation and dynamics of oligosaccharides in solution. *Glycobiology* **1993**, *3*, 551-555.

Honda, S., Akao, E., Suzuki, S., Okuda, M., Kakehi, K., Nakamura, J. High-performance liquid chromatography of reducing carbohydrates as strongly ultraviolet-absorbing and electrochemically sensitive 1-phenyl-3-methyl-5-pyrazolone derivatives. *Anal. Biochem.* **1989**, *180*, 351-357.

Honda, S., Suzuki, S., Nose, A., Yamamoto, K., Kakehi, K. Capillary zone electrophoresis of reducing mono- and oligo-saccharides as the borate complexes of their 3-methyl-1-phenyl-2-pyrazolin-5-one derivatives. *Carbohydr. Res.* **1991**, *215*, 193-198.

Hounsell, E.F., Michael, J.D., Renouf, D.V. O-linked protein glycosylation structure and function. *Glycoconjugate J.* **1996**, *13*, 19-26.

Hu, G.-F. Fluorophore-assisted carbohydrate electrophoresis: technology and applications. *J. Chromatog. A* **1995**, *705*, 89-103.

Huber, R., Deisenhofer, J., Colman, P.M., Matsushima, M., Palm, W. Crystallographic structure studies of an IgG molecule and an Fc fragment. *Nature* **1976**, *264*, 415-420.

Hymes, A.J., Mullinax, G.L., Mullinax, F. Immunoglobulin carbohydrate requirement for formation of an IgG-IgG complex. *J. Biol. Chem.* **1979**, *254*, 3148-3151.

Imperiali, B., Shannon, K.L. Differences between Asn-Xaa-Thr-containing peptides: a comparison of solution conformation and substrate behaviour with oligosaccharyltransferase. *Biochemistry* **1991**, *30*, 4373-4380.

Imperiali, B. Protein glycosylation: the clash of the titans. *Acc. Chem. Res.* **1997**, *30*, 452-459.

Imperiali, B., O'Connor, S.E. Effect of N-linked glycosylation on glycopeptide and glycoprotein structure. *Curr. Opin. Chem. Biol.* **1999**, *3*, 643-649.

Irie, A., Koyama, S., Kozutsumi, Y., Kawasaki, T., Suzuki, A. The molecular basis for the absence of *N*-glycolylneuraminic acid in humans. *J. Biol. Chem.* **1998**, *273*, 15866-15871.

Jackson, P. The use of polyacrylamide-gel electrophoresis for the high-resolution separation of reducing saccharides labelled with the fluorophore 8-aminonaphthalene-1,3,6-trisulphonic acid: detection of picomolar quantities by an imaging system based on a cooled charged-coupled device. *Biochem. J.* **1990**, *270*, 705-713.

Jackson, P., Williams, G.R. Polyacrylamide gel electrophoresis of reducing saccharides labeled with the fluorophore 8-aminonapthalene-1,3,6-trisulphonic acid: application to the enzymological structural analysis of oligosaccharides. *Electrophoresis* **1991**, *12*, 94-96.

Jackson, P. Fluorophore-assisted carbohydrate electrophoresis: a new technology for the analysis of glycans. *Biochem. Soc. Trans.* **1993**, *21*, 121-125.

Jackson, P. The analysis of fluorophore-labeled glycans by high-resolution polyacrylamide gel electrophoresis. *Anal. Biochem.* **1994a**, *216*, 243-252.

Jackson, P. High-resolution polyacrylamide gel electrophoresis of fluorophore-labeled reducing saccharides. *Methods Enzymol.* **1994b**, *230*, 250-265.

Jackson, P. The analysis of fluorophore-labeled carbohydrates by polyacrylamide gel electrophoresis. *Mol. Biotechnol.* **1996**, *5*, 101-123.

Jackson, P. Polyacrylamide gel electrophoresis of fluorophore-labelled reducing saccharides: a review. In: *A Laboratory Guide to Glycoconjugate Analysis*, BioMethods, Vol. 9; Jackson, P., Gallagher, J.T., Eds.; Birkhäuser Verlag, **1997**; pp 113-139.

Jackson, P. Fluorophore-labelled saccharide electrophoresis for the analysis of glycoproteins. In: *Gel Electrophoresis of Proteins: A Practical Approach*, 3rd ed.; Hames, B.D., Ed.; Oxford University Press, **1998**; pp 269-292.

James, K. Therapeutic monoclonal antibodies: their production and application. In: *Animal Cell Biotechnology*, Vol. 4; Spier, R.E., Griffiths, J.B., Eds.; Academic Press, **1990**; pp 205-255.

Jan, D.C.H., Petch, D.A., Huzel, N., Butler, M. The effect of dissolved oxygen on the metabolic profile of a murine hybridoma grown in serum-free medium in continuous culture. *Biotechnol. Bioeng.* **1997**, *54*, 153-164.

Jassal, R., Jenkins, N. Remodelling glycans on IgG by genetic re-engineering. *Biochem. Soc. Trans.* **1998**, *26*, S113.

Jassal, R., Jenkins, N., Charlwood, J., Camilleri, P., Jefferis, R., Lund, J. Sialylation of human IgG-Fc carbohydrate by transfected rat α2,6-sialyltransferase. *Biochem. Biophys. Res. Commun.* **2001**, *286*, 243-249.

Jeddi, P.A., Bodman-Smith, K.B., Lund, T., Lydyard, P.M., Mengle-Gaw, L., Isenberg, D.A., Youinou, P., Delves, P.J. Agalactosyl IgG and β-1,4-

galactosyltransferase gene expression in rheumatoid arthritis patients and in the arthritis-prone MRL lpr/lpr mouse. *Immunology* **1996**, *87*, 654-659.

Jeddi, P.A., Keusch, J., Lydyard, P.M., Delves, P.J. The stability of lymphocytic β1,4-galactosyltransferase expression during pregnancy and lactation. *Scand. J. Immunol.* **1997**, *45*, 145-150.

Jefferis, R., Lund, J., Mizutani, H., Nakagawa, H., Kawazoe, Y., Arata, Y., Takahashi, N. A comparative study of the N-linked oligosaccharide structures of human IgG subclass proteins. *Biochem. J.* **1990**, *268*, 529-537.

Jefferis, R. Structure-function relationships of human immunoglobulins. *Neth. J. Med.* **1991**, *39*, 188-198.

Jefferis, R., Takahashi, N., Lund, J., Tyler, R., Hindley, S. Does an antibody molecule act as a template directing (determining) its glycosylation? *Biochem. Soc. Trans.* **1992**, *20*, 228S.

Jefferis, R. The glycosylation of antibody molecules: functional significance. *Glycoconjugate J.* **1993**, *10*, 357-361.

Jefferis, R., Pound, J., Lund, J., Goodall, M. Effector mechanisms activated by human IgG subclass antibodies: clinical and molecular aspects. *Ann. Biol. Clin.* **1994**, *52*, 57-65.

Jefferis, R., Lund, J., Goodall, M. Recognition sites on human IgG for $Fc\gamma$ receptors: the role of glycosylation. *Immunol. Lett.* **1995**, *44*, 111-117.

Jefferis, R., Lund, J., Goodall, M. Modulation of $Fc\gamma R$ and human complement activation by IgG_3-core oligosaccharide interactions. *Immunol. Lett.* **1996**, *54*, 101-104.

Jefferis, R., Lund, J. Glycosylation of antibody molecules: structural and functional significance. *Chem. Immunol.* **1997**, *65*, 111-128.

Jefferis, R., Lund, J., Pound, J.D. IgG-Fc-mediated effector functions: molecular definition of interaction sites for effector ligands and the role of glycosylation. *Immunol. Rev.* **1998**, *163*, 59-76.

Jenkins, N., Curling, E.M.A. Glycosylation of recombinant proteins: problems and prospects. *Enzyme Microb. Technol.* **1994**, *16*, 354-364.

Jenkins, N. Monitoring and control of recombinant glycoprotein heterogeneity in animal cell cultures. *Biochem. Soc. Trans.* **1995**, *23*, 171-175.

Jenkins, N., Parekh, R.B., James, D.C. Getting the glycosylation right: implications for the biotechnology industry. *Nature Biotechnol.* **1996**, *14*, 975-981.

Jentoft, N. Why are proteins O-glycosylated? *Trends Biochem. Sci.* **1990**, *15*, 291-

294.

Karas, M., Hillenkamp, F. Laser desorption ionization of proteins with molecular masses exceeding 10 000 Daltons. *Anal. Chem.* **1988**, *60*, 2299-2301.

Kasturi, L., Chen, H., Shakin-Eshleman, S.H. Regulation of N-linked core glycosylation: use of a site-directed mutagenesis approach to identify Asn-Xaa-Ser/Thre sequons that are poor oligosaccharide acceptors. *Biochem. J.* **1997**, 323, 415-419.

Kaushal, G.P., Elbein, A.D. Glycosidase inhibitors in study of glycoconjugates. *Methods Enzymol.* **1994**, *230*, 316-329.

Kawakita, M., Ishida, N., Miura, N., Sun-Wada, G.-H., Yoshioka, S. Nucleotide sugar transporters: elucidation of their molecular identity and its implication for future studies. *J. Biochem. (Tokyo)* **1998**, *123*, 777-785.

Keusch, J., Lydyard, P.M., Delves, P.J. The effect on IgG galactosylation of altering β1,4-galactosyltransferase-1 activity in B cells. *Glycobiology* **1998a**, *8*, 1215-1220.

Keusch, J., Lydyard, P.M., Berger, E.G., Delves, P.J. B lymphocyte galactosyl-transferase protein levels in normal individuals and in patients with rheumatoid arthritis. *Glycoconjugate J.* **1998b**, *15*, 1093-1097.

Khatra, B.S., Herries, D.G., Brew, K. Some kinetic properties of human-milk galactosyl transferase. *Eur. J. Biochem.* **1974**, *44*, 537-560.

Kilburn, D.G., Webb, F.C. The cultivation of animal cells at controlled dissolved oxygen partial pressure. *Biotechnol. Bioeng.* **1968**, *10*, 801-814.

Kilburn, D.G., Lilly, M.D., Self, D.A., Webb, F.C. The effect of dissolved oxygen partial pressure on the growth and carbohydrate metabolism of mouse LS cells. *J. Cell. Sci.* **1969**, *4*, 25-37.

Kimura, R., Miller, W.M. Effects of elevated pCO_2 and/or osmolality on the growth and recombinant tPA production of CHO cells. *Biotechnol. Bioeng.* **1996**, *52*, 152-160.

Kimura, R., Miller, W.M. Glycosylation of CHO-derived recombinant tPA produced under elevated pCO_2. *Biotechnol. Prog.* **1997**, *13*, 311-317.

Kimura, S., Numaguchi, M., Kaizu, T., Kim, D., Takagi, Y., Gomi, K. High galactosylation of oligosaccharides in umbilical cord blood IgG, and its relationship to placental function. *Clin. Chim. Acta* **2000**, *299*, 169-177.

Kitagawa, H., Paulson, J.C. Differential expression of five sialyltransferase genes in human tissues. *J. Biol. Chem.* **1994**, *269*, 17872-17878.

Klock, J.C., Starr, C.M. Polyacrylamide gel electrophoresis of fluorophore-labeled carbohydrates from glycoproteins. In: *Glycoanalysis Protocols*, 2nd ed.; Methods in Molecular Biology, Vol. 76; Hounsell, E.F., Ed.; Humana Press, **1998**; pp 115-129.

Kloth, C., Leibiger, H., Valley, U., Yalcin, E., Buchholz, R., Emmrich, F., Marx, U. Glycosylation analysis of nanomolar amounts of glycoprotein combining in-gel enzymatic digestion and FACE. In: *Animal Cell Technology: Products from Cells, Cells as Products*; Bernard, A., Griffiths, B., Noé, W., Wurm, F., Eds.; Kluwer, **1999**; pp 237-239.

Kobata, A. Function and pathology of the sugar chains of human immunoglobulin G. *Glycobiology* **1990**, *1*, 5-8.

Köhler, G., Milstein, C. Continuous cultures of fused cells secreting antibody of predefined specificity. *Nature* **1975**, *256*, 495-497.

Köhler, C., Milstein, C. Derivation of specific antibody-producing tissue culture and tumor lines by cell fusion. *Eur. J. Immunol.* **1976**, *6*, 511-519.

Koide, N., Nose, M., Muramatsu, T. Recognition of IgG by Fc receptor and complement: effects of glycosidase digestion. *Biochem. Biophys. Res. Commun.* **1977**, *75*, 838-844.

Kornfeld, R., Kornfeld, S. Assembly of asparagine-linked oligosaccharides. *Annu. Rev. Biochem.* **1985**, *54*, 631-664.

Krieger, M., Reddy, P., Kozarsky, K., Kingsley, D., Hobbie, L., Penman, M. Analysis of the synthesis, intracellular sorting, and function of glycoproteins using a mammalian cell mutant with reversible glycosylation defects. *Methods Cell Biol.* **1989**, *32*, 57-84.

Kroon, D.J., Freedy, J., Burinsky, D.J., Sharma, B. Rapid profiling of carbohydrate glycoforms in monoclonal antibodies using MALDI/TOF mass spectrometry. *J. Pharm. Biomed. Anal.* **1995**, *13*, 1049-1054.

Kumpel, B.M., Rademacher, T.W., Rook, G.A.W., Williams, P.J., Wilson, I.B.H. Galactosylation of human IgG monoclonal anti-D produced by EBV-transformed B-lymphoblastoid cell lines is dependent on culture method and affects Fc receptor-mediated functional activity. *Hum. Antibod. Hybridomas* **1994**, *5*, 143-151.

Küster, B., Wheeler, S.F., Hunter, A.P., Dwek, R.A., Harvey, D.J. Sequencing of N-linked oligosaccharides directly from protein gels: in-gel deglycosylation followed by matrix-assisted laser desorption/ionization mass spectrometry and normal-phase high-performance liquid chromatography. *Anal. Biochem.* **1997**, *250*, 82-101.

Laemmli, U.K. Cleavage of structural proteins during the assembly of the head of bacteriophage T4. *Nature* **1970**, *227*, 680-685.

Lammers, G., Jamieson, J.C. The role of a cathepsin D-like activity in the release of Galβ1-4GlcNAc α2-6 sialyltransferase from rat liver Golgi membranes during the acute phase response. *Biochem. J.* **1988**, *256*, 623-631.

Lammers, G., Jamieson, J.C. Cathepsin D-like activity in the release of Galβ1-4GlcNAc α2-6 sialyltransferase from mouse and guinea pig liver Golgi membranes during the acute phase response. *Comp. Biochem. Physiol. B* **1990**, *95*, 327-334.

Lastra, G.C., Thompson, S.J., Lemonidis, A.S., Elson, C.J. Changes in the galactose content of IgG during humoral immune responses. *Autoimmunity* **1998**, *28*, 25-30.

Lavery, M., Kearns, M.J., Price, D.G., Emery, A.N., Jefferis, R., Nienow, A.W. Physical conditions during batch culture of hybridomas in laboratory scale stirred tank reactors. *Dev. Biol. Stand.* **1985**, *60*, 199-206.

Leader, K.A., Lastra, G.C., Kirwan, J.R., Elson, C.J. Agalactosyl IgG in aggregates from the rheumatoid joint. *Br. J. Rheum.* **1996**, *35*, 335-341.

Leatherbarrow, R.J., Dwek, R.A. The effect of aglycosylation on the binding of mouse IgG to staphylococcal protein A. *FEBS Lett.* **1983**, *164*, 227-230.

Leatherbarrow, R.J., Rademacher, T.W., Dwek, R.A., Woof, J.M., Clark, A., Burton, D.R., Richardson, N., Feinstein, A. Effector functions of a monoclonal aglycosylated mouse IgG_{2a}: binding and activation of complement component C1 and interaction with human monocyte Fc receptor. *Mol. Immunol.* **1985**, *22*, 407-415.

Lee, J., Sundaram, S., Shaper, N.L., Raju, T.S., Stanley, P. Chinese hamster ovary (CHO) cells may express six β4-galactosyltransferases (β4GalTs): consequences of the loss of functional β4GalT-1, β4GalT-6, or both in CHO glycosylation mutants. *J. Biol. Chem.* **2001**, *276*, 13924-13934.

Lee, S.-O., Connolly, J.M., Ramirez-Soto, D., Poretz, R.D. The polypeptide of immunoglobulin G influences its galactosylation *in vivo*. *J. Biol. Chem.* **1990**, *265*, 5833-5839.

Lee, Y.C. High-performance anion-exchange chromatography for carbohydrate analysis. *Anal. Biochem.* **1990**, *189*, 151-162.

Leibiger, H., Wünstner, D., Stigler, R.-D., Marx, U. Variable domain-linked oligosaccharides of a human monoclonal IgG: structure and influence on antigen binding. *Biochem. J.* **1999**, *338*, 529-538.

Lemoine, J., Chirat, F., Domon, B. Structural analysis of derivatized oligosaccharides using post-source decay matrix-assisted laser desorption/ionization mass spectrometry. *J. Mass Spectrom.* **1996**, *31*, 908-912.

Lifely, M.R., Hale, C., Boyce, S., Keen, M.J., Phillips, J. Glycosylation and biological activity of CAMPATH-1H expressed in different cell lines and grown under different culture conditions. *Glycobiology* **1995**, *5*, 813-822.

Lin, A.A., Kimura, R., Miller, W.M. Production of tPA in recombinant CHO cells under oxygen-limited conditions. *Biotechnol. Bioeng.* **1993**, *42*, 339-350.

Lines, A.C. High-performance liquid chromatographic mapping of the oligosaccharides released from the humanised immunoglobulin, CAMPATH 1H. *J. Pharm. Biomed. Anal.* **1996**, *14*, 601-608.

Lis, H., Sharon, N. Protein glycosylation: structural and functional aspects. *Eur. J. Biochem.* **1993**, *218*, 1-27.

Lo, N.W., Shaper, J.H., Pevsner, J., Shaper, N.L. The expanding β4-galactosyltransferase gene family: messages from the databanks. *Glycobiology* **1998**, *8*, 517-526.

Loboda, A.V., Krutchinsky, A.N., Bromirski, M., Ens, W., Standing, K.G. A tandem quadrupole/time-of-flight mass spectrometer with a matrix-assisted laser desorption/ionization source: design and performance. *Rapid Commun. Mass Spectrom.* **2000**, *14*, 1047-1057.

Lowry, O.H., Rosebrough, N.J., Farr, A.L., Randall, R.J. Protein measurement with the Folin phenol reagent. *J. Biol. Chem.* **1951**, *193*, 265-275.

Lüdeman, I., Pörtner, R., Märkl, H. Effect of NH_3 on the cell growth of a hybridoma cell line. *Cytotechnology* **1994**, *14*, 11-20.

Lund, J., Tanaka, T., Takahashi, N., Sarmay, G., Arata, Y., Jefferis, R. A protein structural change in aglycosylated IgG_3 correlates with loss of huFcγRI and huFcγRIII binding and/or activation. *Mol. Immunol.* **1990**, *27*, 1145-1153.

Lund, J., Takahashi, N., Hindley, S., Tyler, R., Goodall, M., Jefferis, R. Glycosylation of human IgG subclass and mouse IgG_{2b} heavy chains secreted by mouse J558L transfectoma cell lines as chimeric antibodies. *Hum. Antibod. Hybridomas* **1993a**, *4*, 20-25.

Lund, J., Takahashi, N., Nakagawa, H., Goodall, M., Bentley, T., Hindley, S.A., Tyler, R., Jefferis, R. Control of IgG/Fc glycosylation: a comparison of oligosaccharides from chimeric human/mouse and mouse subclass immunoglobulin Gs. *Mol. Immunol.* **1993b**, *30*, 741-748.

Lund, J., Takahashi, N., Pound, J.D., Goodall, M., Nakagawa, H., Jefferis, R. Oligosaccharide-protein interactions in IgG can modulate recognition by Fcγ receptors. *FASEB J.* **1995**, *9*, 115-119.

Lund, J., Takahashi, N., Pound, J.D., Goodall, M., Jefferis, R. Multiple interactions of IgG with its core oligosaccharide can modulate recognition by complement

and human Fcγ receptor I and influence the synthesis of its oligosaccharide chains. *J. Immunol.* **1996**, *157*, 4963-4969.

Lund, J., Takahashi, N., Popplewell, A., Goodall, M., Pound, J.D., Tyler, R., King, D.J., Jefferis, R. Expression and characterization of truncated forms of humanized L243 IgG_1: architectural features can influence synthesis of its oligosaccharide chains and affect superoxide production triggered through human Fcγ receptor I. *Eur. J. Biochem.* **2000**, *267*, 7246-7256.

Ma, S., Nashabeh, W. Carbohydrate analysis of a chimeric recombinant monoclonal antibody by capillary electrophoresis with laser-induced fluorescence detection. *Anal. Chem.* **1999**, *71*, 5185-5192.

MacGillivray, A.J., Iwobi, M., Fernandes, L., Papasavvas, G. Oligosaccharides of IgG in rheumatoid arthritis. *Biochem. Soc. Trans.* **1995**, *23*, 163S.

Machamer, C.E., Rose, J.K. Vesicular stomatitis virus G proteins with altered glycosylation sites display temperature-sensitive intracellular transport and are subject to aberrant intermolecular disulfide bonding. *J. Biol. Chem.* **1988**, *203*, 5955-5960.

Madshus, I.H. Regulation of intracellular pH in eukaryotic cells. *Biochem. J.* **1988**, *250*, 1-8.

Magnusson, C.G., Bjornstedt, M., Holmgren, A. Human IgG is substrate for the thioredoxin system: differential cleavage pattern of interchain disulfide bridges in IgG subclasses. *Mol. Immunol.* **1997**, *34*, 709-717.

Maiorella, B.L., Winkelhake, J., Young, J., Moyer, B., Bauer, R., Hora, M., Andya, J., Thompson, J., Patel, T., Parekh, R. Effect of culture conditions on IgM antibody structure, pharmacokinetics and activity. *Biotechnology (NY)* **1993**, *11*, 387-392.

Maley, F., Trimble, R.B., Tarentino, A.L., Plummer, T.H., Jr. Characterization of glycoproteins and their associated oligosaccharides through the use of endoglycosidases. *Anal. Biochem.* **1989**, *180*, 195-204.

Malhotra, R., Wormald, M.R., Rudd, P.M., Fischer, P.B., Dwek, R.A., Sim, R.B. Glycosylation changes of IgG associated with rheumatoid arthritis can activate complement via the mannose-binding protein. *Nature Med.* **1995**, *1*, 237-243.

Marino, M., Corti, A., Ippolito, A., Cassani, G., Fassina, G. Effect of bench-scale culture conditions on murine IgG heterogeneity. *Biotechnol. Bioeng.* **1997**, *54*, 17-25.

Martin, A., Rambal, C., Berger, V., Perier, S., Louisot, P. Availability of specific sugars for glycoconjugate biosynthesis: a need for further investigations in man. *Biochimie* **1998**, *80*, 75-86.

Martin, K., Talukder, R., Hay, F.C., Axford, J.S. Characterization of changes in IgG

associated oligosaccharide profiles in rheumatoid arthritis, psioratic arthritis, and ankylosing spondylitis using fluorophore linked carbohydrate electrophoresis. *J. Rheumatol.* **2001**, *28*, 1531-1536.

Martinelle, K., Häggström, L. Mechanisms of ammonia and ammonium ion toxicity in animal cells: transport across cell membranes. *J. Biotechnol.* **1993**, *30*, 339-350.

Martinelle, K., Westlund, A., Häggström, L. Ammonium transport in myeloma and hybridoma cells. In: *Animal Cell Technology: Developments Towards the 21st Century*; Beuvery, E.C., Griffiths, J.B., Zeiljemaker, W.P., Eds.; Kluwer, **1995**; pp 241-245.

Masada, R.I., Hague, C., Seid, R., Ho, S., McAlister, S., Pigiet, V., Starr, C.M. Fluorophore-assisted-carbohydrate-electrophoresis (FACE) for determining the nature and consistency of recombinant protein glycosylation. *Trends Glycosci. Glycotechnol.* **1995**, *7*, 133-147.

Masuda, K., Yamaguchi, Y., Kato, K., Takahashi, N., Shimada, I., Arata, Y. Pairing of oligosaccharides in the Fc region of immunoglobulin G. *FEBS Lett.* **2000**, *473*, 349-357.

Matsuda, H., Nakamura, S., Ichikawa, Y., Kozai, K., Takano, R., Nose, M., Endo, S., Nishimura, Y., Arata, Y. Proton nuclear magnetic resonance studies of the structure of the Fc fragment of human immunoglobulin G_1: comparisons of native and recombinant proteins. *Mol. Immunol.* **1990**, *27*, 571-579.

Matsumoto, A., Shikata, K., Takeuchi, F., Kojima, N., Mizuochi, T. Autoantibody activity of IgG rheumatoid factor increases with decreasing levels of galactosylation and sialylation. *J. Biochem. (Tokyo)* **2000**, *128*, 621-628.

Mattu, T.S., Pleass, R.J., Willis, A.C., Kilian, M., Wormald, M.R., Lellouch, A.C., Rudd, P.M., Woof, J.M., Dwek, R.A. The glycosylation and structure of human serum IgA_1, Fab, and Fc regions and the role of N-glycosylation on Fcα receptor interactions. *J. Biol. Chem.* **1998**, *273*, 2260-2272.

Mayer, M., Kies, U., Kammermeier, R., Buchner, J. BiP and PDI cooperate in the oxidative folding of antibodies *in vitro*. *J. Biol. Chem.* **2000**, *275*, 29421-29425.

Mazurier, J., Dauchez, M., Vergoten, G., Montreuil, J., Spik, G. Molecular modeling of a disialylated monofucosylated biantennary glycan of the *N*-acetyllactosamine type. *Glycoconjugate J.* **1991**, *8*, 390-399.

McCaffrey, G., Jamieson, J.C. Evidence for the role of a cathepsin D-like activity in the release of Galβ1-4GlcNAc α2-6 sialyltransferase from rat and mouse liver in whole-cell systems. *Comp. Biochem. Physiol. B* **1993**, *104*, 91-94.

McGinnes, L.W., Morrison, T.G. Disulfide bond formation is a determinant of glycosylation site usage in the hemagglutinin-neuraminidase glycoprotein of

Newcastle disease virus. *J. Virol.* **1997**, *71*, 3083-3089.

McGuire, J.M., Douglas, M., Smith, K.D. The resolution of the neutral N-linked oligosaccharides of IgG by high pH anion-exchange chromatography. *Carbohydr. Res.* **1996**, *292*, 1-9.

McQueen, A., Bailey, J.E. Effect of ammonium ion and extracellular pH on hybridoma cell metabolism and antibody production. *Biotechnol. Bioeng.* **1990**, *35*, 1067-1077.

McQueen, A., Bailey, J.E. Growth inhibition of hybridoma cells by ammonium ion: correlation with effects on intracellular pH. *Bioprocess Eng.* **1991**, *6*, 49-61.

Mellquist, J.L., Kasturi, L., Spitalnik, S.L., Shakin-Eshleman, S.H. The amino acid following an Asn-X-Ser/Thr sequon is an important determinant of N-linked core glycosylation efficiency. *Biochemistry* **1998**, *37*, 6833-6837.

Merry, T. Current techniques in protein glycosylation analysis: a guide to their application. *Acta Biochim. Pol.* **1999**, *46*, 303-314.

Merten, O.-W. Production and use of non-therapeutic monoclonal antibodies. In: *Animal Cell Biotechnology*, Vol. 4; Spier, R.E., Griffiths, J.B., Eds.; Academic Press, **1990**; pp 257-315.

Michalak, M., Corbett, E.F., Mesaeli, N., Nakamura, K., Opas, M. Calreticulin: one protein, one gene, many functions. *Biochem. J.* **1999**, *344*, 281-292.

Miller, W.M., Wilke, C.R., Blanch, H.W. Effects of dissolved oxygen concentration on hybridoma growth and metabolism in continuous culture. *J. Cell Physiol.* **1987**, *132*, 524-530.

Milner, S.J., Carver, J.A., Ballard, F.J., Francis, G.L. Probing the disulfide folding pathway of insulin-like growth factor-I. *Biotechnol. Bioeng.* **1999**, *62*, 693-703.

Mimura, Y., Church, S., Ghirlando, R., Ashton, P.R., Dong, S., Goodall, M., Lund, J., Jefferis, R. The influence of glycosylation on the thermal stability and effector function expression of human IgG_1-Fc: properties of a series of truncated glycoforms. *Mol. Immunol.* **2000**, *37*, 697-706.

Mimura, Y., Sondermann, P., Ghirlando, R., Lund, J., Young, S.P., Goodall, M., Jefferis, R. Role of oligosaccharide residues of IgG_1-Fc in $Fc\gamma$RIIb binding. *J. Biol. Chem.* **2001**, *276*, 45539-45547.

Mirazimi, A., Svensson, L. Carbohydrates faciliate correct disulfide bond formation and folding of rotavirus VP7. *J. Virol.* **1998**, *72*, 3887-3892.

Miura, N., Ishida, N., Hoshino, M., Yamauchi, M., Hara, T., Ayusawa, D., Kawakita, M. Human UDP-galactose translocator: molecular cloning of a complementary DNA that complements the genetic defect of a mutant cell line

deficient in UDP-galactose translocator. *J. Biochem. (Tokyo)* **1996**, *120*, 236-241.

Mizuochi, T., Taniguchi, T., Shimizu, A., Kobata, A. Structural and numerical variations of the carbohydrate moiety of immunoglobulin G. *J. Immunol.* **1982**, *129*, 2016-2020.

Mizuochi, T., Hamako, J., Titani, K. Structures of the sugar chains of mouse immunoglobulin G. *Arch. Biochem. Biophys.* **1987**, *257*, 387-394.

Mizuochi, T., Hamako, J., Nose, M., Titani, K. Structural changes in the oligosaccharide chains of IgG in autoimmune MRL/lp-lpr/lpr mice. *J. Immunol.* **1990**, *145*, 1794-1798.

Mohan, S.B., Chohan, S.R., Eade, J., Lyddiatt, A. Molecular integrity of monoclonal antibodies produced by hybridoma cells in batch culture and in continuous-flow culture with integrated product recovery. *Biotechnol. Bioeng.* **1993**, *42*, 974-986.

Mohr, M.D., Bornsen, K.O., Widmer, H.M. Matrix-assisted laser desorption/ionization mass spectrometry: improved matrix for oligosaccharides. *Rapid Commun. Mass Spectrom.* **1995**, *9*, 809-814.

Molinari, M., Helenius, A. Glycoproteins form mixed disulphides with oxido-reductases during folding in living cells. *Nature* **1999**, *402*, 90-93.

Molinari, M., Helenius, A. Chaperone selection during glycoprotein translocation into the endoplasmic reticulum. *Science* **2000**, *288*, 331-333.

Monica, T.J., Goochee, C.F., Maiorella, B.L. Comparative biochemical characterization of a human IgM produced in both ascites and *in vitro* cell culture. *Biotechnology (NY)* **1993**, *11*, 512-515.

Monod, J. La technique de culture continue: théorie et applications. *Ann. Inst. Pasteur (Paris)* **1950**, *79*, 390-410.

Moran, E.B., McGowan, S.T., McGuire, J.M., Frankland, J.E., Oyebade, I.A., Waller, W., Archer, L.C., Morris, L.O., Pandya, J., Nathan, S.R., Smith, L., Cadette, M.L., Michalowski, J.T. A systematic approach to the validation of process control parameters for monoclonal antibody production in fed-batch culture of a murine myeloma. *Biotechnol. Bioeng.* **2000**, *69*, 242-255.

Morell, A.G., Irvine, R.A., Sternlieb, I., Scheinberg, I.H., Ashwell, G. Physical and chemical studies on ceruloplasmin: V. metabolic studies on sialic acid-free ceruloplasmin *in vivo*. *J. Biol. Chem.* **1968**, *243*, 155-159.

Moremen, K.W., Trimble, R.B., Herscovics, A. Glycosidases of the asparagine-linked oligosaccharide processing pathway. *Glycobiology* **1994**, *4*, 113-125.

Moriwaki, T., Suganuma, N., Furuhashi, M., Kikkawa, F., Tomoda, Y., Boime, I., Nakata, M., Mizuochi, T. Alteration of N-linked oligosaccharide structures of human chorionic gonadotropin β-subunit by disruption of disulfide bonds. *Glycoconjugate J.* **1997**, *14*, 225-229.

Muchmore, E.A., Milewski, M., Varki, A., Diaz, S. Biosynthesis of *N*-glycolylneuraminic acid: the primary site of hydroxylation of *N*-acetylneuraminic acid is the cytosolic sugar nucleotide pool. *J. Biol. Chem.* **1989**, *264*, 20216-20223.

Muchmore, E.A., Diaz, S., Varki, A. A biochemical difference between humans and great apes: absence of a single oxygen atom on sialic acids. *Glycobiology* **1997**, *7*, 1038.

Muchmore, E.A., Diaz, S., Varki, A. A structural difference between the cell surface of humans and the great apes. *Am. J. Phys. Anthropol.* **1998**, *107*, 187-198.

Mullinax, F., Mullinax, G.L. Abnormality of IgG structure in rheumatoid arthritis and systemic lupus erythematosus. *Arthritis Rheum.* **1975**, *18*, 417-418.

Mullinax, F., Hymes, A.J., Mullinax, G.L. Molecular site and enzymatic origin of IgG galactose deficiency in rheumatoid arthritis and SLE. *Arthritis Rheum.* **1976**, *19*, 813.

Munzert, E., Müthing, J., Büntemeyer, H., Lehmann, J. Sialidase activity in culture fluid of Chinese hamster ovary cells during batch culture and its effect on recombinant human antithrombin III integrity. *Biotechnol. Prog.* **1996**, *12*, 559-563.

Murhammer, D.W., Goochee, C.F. Structural features of nonionic polyglycol polymer molecules responsible for the protective effect in sparged animal cell bioreactors. *Biotechnol. Prog.* **1990a**, 6, 142-148.

Murhammer, D.W., Goochee, C.F. Sparged animal cell bioreactors: mechanism of cell damage and Pluronic F-68 protection. *Biotechnol. Prog.* **1990b**, 6, 391-397.

Mussar, K.J., Murray, G.J., Martin, B.M., Viswanatha, T. Peptide: N-glycosidase F: studies on the glycoprotein aminoglycan amidase from Flavobacterium meningosepticum. *J. Biochem. Biophys. Methods* **1989**, *20*, 53-68.

Nahrgang, S., Kragten, E., De Jesus, M., Bourgeois, M., Déjardin, S., Von Stockar, U., Marison, I.W. The effect of cell line, transfection procedure and reactor conditions on the glycosylation of recombinant human anti-rhesus D IgG_1. In: *Animal Cell Technology: Products from Cells, Cells as Products*; Bernard, A., Griffiths, B., Noé, W., Wurm, F., Eds.; Kluwer, **1999**; pp 259-261.

Narasimhan, S., Freed, J.C., Schachter, H. Control of glycoprotein synthesis: bovine milk UDPgalactose: *N*-acetylglucosamine β-4-galactosyltransferase catalyzes the preferential transfer of galactose to the GlcNAcβ1,2Manα1,3-

branch of both bisected and nonbisected complex biantennary asparagine-linked oligosaccharides. *Biochemistry* ***1985***, *24*, 1694-1700.

Negroiu, G., Dwek, R.A., Petrescu, S.M. Folding and maturation of tyrosinase-related protein-1 are regulated by post-translational formation of disulfide bonds and N-glycan processing. *J. Biol. Chem.* **2000**, *275*, 32200-32207.

Neuberger, A., Wilson, B.M. The separation of glycosides on a strongly basic ion-exchange resin: an interpretation in terms of acidity. *Carbohydr. Res.* **1971**, *17*, 89-95.

Newkirk, M.M. Fc glycosylation and rheumatoid factors. In: *Abnormalities of IgG Glycosylation and Immunological Disorders*; Isenberg, D.A., Rademacher, T.W., Eds.; John Wiley & Sons, **1996**; pp 119-130.

Newland, M., Nazlee Kamal, M., Greenfield, P.F., Nielsen, L.K. Ammonia inhibition of hybridomas propagated in batch, fed-batch, and continuous culture. *Biotechnol. Bioeng.* **1994**, *43*, 434-438.

Noguchi, A., Mukuria, C.J., Suzuki, E., Naiki, M. Immunogenicity of *N*-glycolylneuraminic acid-containing carbohydrate chains of recombinant human erythropoietin in Chinese hamster ovary cells. *J. Biochem. (Tokyo)* **1995**, *117*, 59-62.

Nose, M., Wigzell, H. Biological significance of carbohydrate chains on monoclonal antibodies. *Proc. Natl. Acad. Sci. USA* **1983**, *80*, 6632-6636.

Novick, A., Szilard, L. Experiments with the chemostat on spontaneous mutations of bacteria. *Proc. Natl. Acad. Sci. USA* **1950**, *36*, 708-719.

Nuck, R., Zimmerman, M., Sauvageot, D., Josic, D., Reutter, W. Optimized deglycosylation of glycoproteins by peptide-N^4-(*N*-acetyl-β-glucosaminyl)-asparagine amidase from Flavobacterium meningosepticum. *Glycoconjugate J.* **1990**, *7*, 279-286.

O'Connor, S.E., Imperiali, B. A molecular basis for glycosylation-induced conformation switching. *Chem. Biol.* **1998**, *5*, 427-437.

O'Connor, S.E., Pohlmann, J., Imperiali, B., Saskiawan, I., Yamamato, K. Probing the effect of the outer saccharide residues of N-linked glycans on peptide conformation. *J. Am. Chem. Soc.* **2001**, *123*, 6187-6188.

Oelmann, S., Stanley, P., Gerardy-Schahn, R. Point mutations identified in Lec8 Chinese hamster ovary glycosylation mutants that inactivate both the UDP-galactose and CMP-sialic acid transporters. *J. Biol. Chem.* **2001**, *276*, 26291-26300.

Ogawa, T., Kamihira, M., Yoshida, H., Iijima, S., Kobayashi, T. Effect of dissolved oxygen concentration on monoclonal antibody production in hybridoma cell cultures. *J. Ferment. Bioeng.* **1992**, *74*, 372-378.

Oh, S.K.W., Vig, P., Chua, F., Teo, W.K., Yap, W.G.S. Substantial overproduction of antibodies by applying osmotic pressure and sodium butyrate. *Biotechnol. Bioeng.* **1993**, *42*, 601-610.

Oliver, J.D., Roderick, H.L., Llewellyn, D.H., High, S. ERp57 functions as a subunit of specific complexes formed with the ER lectins calreticulin and calnexin. *Mol. Biol. Cell* **1999**, *10*, 2573-2582.

Oller, A.R., Buser, C.W., Tyo, M.A., Thilly, W.G. Growth of mammalian cells at high oxygen concentrations. *J. Cell. Sci.* **1989**, *14*, 43-49.

O'Neill, R.A. Glycotechnology: an emerging field in biochemistry, cell biology, and pharmaceutical development. *Am. Biotechnol. Lab.* **1994**, *January*, 12-13.

Ou, W.-J., Cameron, P.H., Thomas, D.Y., Bergeron, J.J.M. Association of folding intermediates of glycoproteins with calnexin during protein maturation. *Nature* **1993**, *364*, 771-776.

Ozturk, S.S., Palsson, B.Ø. Effects of dissolved oxygen on hybridoma cell growth, metabolism, and antibody production kinetics in continuous culture. *Biotechnol. Prog.* **1990**, *6*, 437-446.

Ozturk, S.S., Palsson, B.O. Physiological changes during the adaptation of hybridoma cells to low serum and serum-free media. *Biotechnol. Bioeng.* **1991a**, *37*, 35-46.

Ozturk, S.S., Palsson, B.O. Effect of medium osmolarity on hybridoma growth, metabolism, and antibody production. *Biotechnol. Bioeng.* **1991b**, *37*, 989-993.

Ozturk, S.S., Palsson, B.O. Growth, metabolic, and antibody production kinetics of hybridoma cell culture: 2. effects of serum concentration, dissolved oxygen concentration, and medium pH in a batch reactor. *Biotechnol. Prog.* **1991c**, *7*, 481-494.

Ozturk, S.S., Palsson, B.O. Examination of serum and bovine serum albumin as shear protective agents in agitated cultures of hybridoma cells. *J. Biotechnol.* **1991d**, *18*, 13-28.

Ozturk, S.S., Riley, M.R., Palsson, B.O. Effects of ammonia and lactate on hybridoma growth, metabolism, and antibody production. *Biotechnol. Bioeng.* **1992**, *39*, 418-431.

Padlan, E.A. Anatomy of the antibody molecule. *Mol. Immunol.* **1994**, 31, 169-217.

Papac, D.I., Wong, A., Jones, A.J. Analysis of acidic oligosaccharides and glycopeptides by matrix-assisted laser desorption/ionization time-of-flight mass spectrometry. *Anal. Chem.* **1996**, *68*, 3215-3223.

Papac, D.I., Jones, A.J., Basa, L.J. Matrix-assisted laser desorption/ionization time-of-flight mass spectrometry of oligosaccharides separated by high pH anion-exchange chromatography. In: *Techniques in Glycobiology*; Townsend, R.R., Hotchkiss, Jr., A.T., Eds.; Marcel Dekker, **1997**; pp 33-52.

Pâquet, M.R., Narasimhan, S., Schachter, H., Moscarello, M.A. Branch specificity of purified rat liver Golgi UDP-galactose: *N*-acetylglucosamine β-1,4-galactosyltransferase: preferential transfer of galactose on the GlcNAcβ1,2-Manα1,3-branch of a complex biantennary Asn-linked oligosaccharide. *J. Biol. Chem.* **1984**, *259*, 4716-4721.

Parekh, R.B., Dwek, R.A., Sutton, B.J., Fernandes, D.L., Leung, A., Stanworth, D., Rademacher, T.W., Mizuochi, T., Taniguchi, T., Matsuta, K., Takeuchi, F., Nagano, Y., Miyamoto, T., Kobata, A. Association of rheumatoid arthritis and primary osteoarthritis with changes in the glycosylation pattern of total serum IgG. *Nature* **1985**, *316*, 452-457.

Parekh, R.B., Tse, A.G.D., Dwek, R.A., Williams, A.F., Rademacher, T.W. Tissue-specific N-glycosylation, site-specific oligosaccharide patterns and lentil lectin recognition of rat Thy-1. *EMBO J.* **1987**, *6*, 1233-1244.

Parekh, R.B., Dwek, R.A., Rademacher, T.W. Rheumatoid arthritis as a glycosylation disorder. *Br. J. Rheumatol.* **1988a**, *27*, 162-169.

Parekh, R., Roitt, I., Isenberg, D., Dwek, R., Rademacher, T. Age-related galactosylation of the N-linked oligosaccharides of human serum IgG. *J. Exp. Med.* **1988b**, *167*, 1731-1736.

Parekh, R.B., Isenberg, D.A., Ansell, B.A., Roitt, I.M., Dwek, R.A., Rademacher, T.W. Galactosylation of IgG associated oligosaccharides: reduction in patients with adult and juvenile onset rheumatoid arthritis and relation to disease activity. *Lancet II*, **1988c**, 966-969.

Parekh, R., Isenberg, D., Rook, G., Roitt, I., Dwek, R., Rademacher, T. A comparative analysis of disease-associated changes in galactosylation of serum IgG. *J. Autoimmun.* **1989**, *2*, 101-114.

Parekh, R.B. Mammalian cell gene expression: protein glycosylation. *Curr. Opin. Biotechnol.* **1991**, *2*, 730-734.

Parekh, R.B. Gene expression: glycosylation. *Biologicals* **1994a**, *22*, 113-119.

Parekh, R.B. Glycoform analysis of glycoproteins. *Methods Enzymol.* **1994b**, *230*, 340-348.

Parodi, A. The quality control of glycoprotein folding in the endoplasmic reticulum: a trip from trypanosomes to mammals. *Braz. J. Med. Biol. Res.* **1998**, *31*, 601-614.

Parodi, A. Reglucosylation of glycoproteins and quality control of glycoprotein folding in the endoplasmic reticulum of yeast cells. *Biochim. Biophys. Acta* **1999**, *1426*, 287-295.

Parodi, A. Protein glucosylation and its role in protein folding. *Annu. Rev. Biochem.* **2000a**, *69*, 69-93.

Parodi, A. Role of N-oligosaccharide endoplasmic reticulum processing reactions in glycoprotein folding and degradation. *Biochem. J.* **2000b**, *348*, 1-13.

Patel, T.P., Parekh, R.B., Moellering, B.J., Prior, C.P. Different culture methods lead to differences in glycosylation of a murine IgG monoclonal antibody. *Biochem. J.* **1992**, *285*, 839-845.

Patel, T., Bruce, J., Merry, A., Bigge, C., Wormald, M., Jaques, A., Parekh, R. Use of hydrazine to release in intact and unreduced form both N- and O-linked oligosaccharides from glycoproteins. *Biochemistry* **1993**, *32*, 679-693.

Patel, T.P., Parekh, R.B. Release of oligosaccharides from glycoproteins by hydrazinolysis. *Methods Enzymol.* **1994**, *230*, 57-66.

Patterson, M.K. Measurement of growth and viability of cells in culture. *Methods Enzymol.* **1979**, *58*, 141-152.

Paulson, J.C., Colley, K.J. Glycosyltransferases: structure, localization, and control of cell type-specific glycosylation. *J. Biol. Chem.* **1989**, *264*, 17615-17618.

Pels Rijcken, W.R., Overdijk, B., Van den Eijnden, D.H., Ferwerda, W. The effect of increasing nucleotide-sugar concentrations on the incorporation of sugars into glycoconjugates in rat hepatocytes. *Biochem. J.* **1995**, *305*, 865-870.

Percy, M.E., Baumal, R., Dorrington, K.J., Percy, J.R. Covalent assembly of mouse immunoglobulin G subclasses *in vitro*: application of a theoretical model for interchain disulfide bond formation. *Can. J. Biochem.* **1976**, *54*, 675-687.

Pérez, S. Theoretical aspects of oligosaccharide conformation. *Curr. Opin. Struct. Biol.* **1993**, *3*, 675-680.

Petch, D.A. A metabolic analysis of glucose and glutamine utilization in hybridoma CC9C10. *M.Sc. Thesis* **1994**, Department of Microbiology, University of Manitoba.

Petersen, J.G.L., Dorrington, K.J. An *in vitro* system for studying the kinetics of interchain disulfide bond formation in immunoglobulin G. *J. Biol. Chem.* **1974**, *249*, 5633-5641.

Petrescu, A.J., Petrescu, S.M., Dwek, R.A., Wormald, M.R. A statistical analysis of N- and O-glycan linkage conformations from crystallographic data. *Glycobiology* **1999**, *9*, 343-352.

Pfeiffer, G., Geyer, H., Geyer, R., Kalsner, I., Wendorf, P. Separation of glycoprotein-N-glycans by high-pH anion-exchange chromatography. *Biomed. Chromatogr.* **1990**, *4*, 193-199.

Pilkington, C., Wang, Y., Rook, G.A.W. The disease distribution and pathogenetic significance of a raised percentage of agalactosyl IgG. In: *Abnormalities of IgG Glycosylation and Immunological Disorders*; Isenberg, D.A., Rademacher, T.W., Eds.; John Wiley & Sons, **1996**; pp 201-219.

Pollack, L., Atkinson, P.H. Correlation of glycosylation forms with position in amino acid sequence. *J. Cell Biol.* **1983**, *97*, 293-300.

Pound, J.D., Lund, J., Jefferis, R. Aglycosylated chimaeric human IgG_3 can trigger the human phagocytic respiratory burst. *Mol. Immunol.* **1993**, *30*, 233-241.

Price, P.J. Hybridoma technology. In: *Advances in Cell Culture*, Vol. 4; Maramorosch, K., Ed.; Academic Press, **1985**; pp 157-177.

Putnam, F.W. Immunoglobulins: structure, function, and genes. In: *The Plasma Proteins*, Vol. V, 3rd ed.; Putnam, F.W., Ed.; Academic Press, **1987**; pp 49-140.

Qasba, P.K., Balaji, P.V., Rao, V.S.R. Conformational analysis of Asn-linked oligosaccharides: implications in biological processes. *J. Mol. Struct. (Theochem)* **1997**, *395-396*, 333-360.

Quintero, O., Montesino, R., Cremata, J.A. Two-dimensional mapping of 8-amino-1,3,6-naphthalene trisulfonic acid derivatives of N-linked neutral and sialyloligosaccharides. *Anal. Biochem.* **1998**, *256*, 23-32.

Rabouille, C., Hui, N., Hunte, F., Kieckbusch, R., Berger, E.G., Warren, G., Nilsson, T. Mapping the distribution of Golgi enzymes involved in the construction of complex oligosaccharides. *J. Cell Sci.* **1995**, *108*, 1617-1627.

Radaev, S., Sun, P.D. Recognition of IgG by $Fc\gamma$ receptor: the role of Fc glycosylation and the binding of peptide inhibitors. *J. Biol. Chem.* **2001**, *276*, 16478-16483.

Rademacher, T.W., Homans, S.W., Parekh, R.B., Dwek, R.A. Immunoglobulin G as a glycoprotein. *Biochem. Soc. Symp.* **1986**, *51*, 131-148.

Rademacher, T.W., Parekh, R.B., Dwek, R.A. Glycobiology. *Annu. Rev. Biochem.* **1988a**, *57*, 785-838.

Rademacher, T.W., Parekh, R.B., Dwek, R.A., Isenberg, D., Rook, G., Axford, J.S.,

Roitt, I. The role of IgG glycoforms in the pathogenesis of rheumatoid arthritis. *Springer Semin. Immunopathol.* **1988b**, *10*, 231-249.

Rademacher, T.W. Network theory of glycosylation-etiologic and pathogenic implications of changes in IgG glycoform levels in autoimmunity. *Semin. Cell. Biol.* **1991**, *2*, 327-337.

Rademacher, T.W. Glycosylation as a factor affecting product consistency. *Biologicals* **1993**, *21*, 103-104.

Rademacher, T.W. Monitoring and control of glycosylation. In: *Animal Cell Biotechnology*, Vol. 6; Spier, R.E., Griffiths, J.B., Eds.; Academic Press, **1994**; pp 5-22.

Rademacher, T.W., Williams, P., Dwek, R.A. Agalactosyl glycoforms of IgG autoantibodies are pathogenic. *Proc. Natl. Acad. Sci. USA* **1994**, *91*, 6123-6127.

Rademacher, T.W., Jones, R.H.V., Williams, P.J. Significance and molecular basis for IgG glycosylation changes in rheumatoid arthritis. *Adv. Exp. Med. Biol.* **1995**, *376*, 193-204.

Rademacher, T.W., Jaques, A., Williams, P.J. The defining characteristics of immunoglobulin glycosylation. In: *Abnormalities of IgG Glycosylation and Immunological Disorders*; Isenberg, D.A., Rademacher, T.W., Eds.; John Wiley & Sons, **1996**; pp 1-44.

Rahman, M.A.A., Isenberg, D.A. Glycosylation of IgG in rheumatic diseases. In: *Abnormalities of IgG Glycosylation and Immunological Disorders*; Isenberg, D.A., Rademacher, T.W., Eds.; John Wiley & Sons, **1996**; pp 101-118.

Raju, T.S., Nayak, N., Briggs, J., O'Connor, J.V., Lerner, L. A convenient microscale colorimetric method for terminal galactose on immunoglobulins. *Biochem. Biophys. Res. Commun.* **1999**, *261*, 196-201.

Raju, T.S. Electrophoretic methods for the analysis of N-linked oligosaccharides. *Anal. Biochem.* **2000**, *283*, 125-132.

Raju, T.S., Briggs, J.B., Borge, S.M., Jones, A.J.S. Species-specific variation in glycosylation of IgG: evidence for the species-specific sialylation and branch-specific galactosylation and importance for engineering recombinant glycoprotein therapeutics. *Glycobiology* **2000**, *10*, 477-486.

Raju, T.S., Briggs, J.B., Chamow, S.M., Winkler, M.E., Jones, A.J. Glycoengineering of therapeutic glycoproteins: *in vitro* galactosylation and sialylation of glycoproteins with terminal *N*-acetylglucosamine and galactose residues. *Biochemistry* **2001**, *40*, 8868-8876.

Rendleman, Jr., J.A. Ionization of carbohydrates in the presence of metal hydroxides and oxides. *Adv. Chem. Ser.* **1971**, *117*, 51-69.

Reuveny, S., Velez, D., Macmillan, J.D., Miller, L. Factors affecting cell growth and monoclonal antibody production in stirred reactors. *J. Immunol. Methods* **1986**, *86*, 53-59.

Reuveny, S., Velez, D., Macmillan, J.D., Miller, L. Factors affecting monoclonal antibody production in culture. *Dev. Biol. Stand.* **1987**, *66*, 169-175.

Rice, K.G., Wu, P., Brand, L., Lee, Y.C. Experimental determination of oligosaccharide three-dimensional structure. *Curr. Opin. Struct. Biol.* **1993**, *3*, 669-674.

Richardson, K., Jamieson, J.C. Release of sialyltransferases from rat liver Golgi membranes by a cathepsin D-like proteinase: comparison of the release of Galβ1-4GlcNAc α2-6 sialyltransferase, Galβ1-3(4)GlcNAc α2-3 sialyltransferase and lactosylceramide α2-3 sialyltransferase (SAT-1). *Comp. Biochem. Physiol. B Biochem. Mol. Biol.* **1995**, *110*, 445-450.

Robinson, D.K., Chan, C.P., Yu Ip, C., Tsai, P.K., Tung, J., Seamans, T.C., Lenny, A.B., Lee, D.K., Irwin, J., Silberklang, M. Characterization of a recombinant antibody produced in the course of a high yield fed-batch process. *Biotechnol. Bioeng.* **1994**, *44*, 727-735.

Rocklin, R.D., Pohl, C.A. Determination of carbohydrates by anion exchange chromatography with pulsed amperometric detection. *J. Liq. Chromatogr.* **1983**, *6*, 1577-1590.

Rohrer, J.S. Separation of asparagine-linked oligosaccharides by high-pH anion-exchange chromatography with pulsed amperometric detection: empirical relationships between oligosaccharide structure and chromatographic retention. *Glycobiology* **1995**, *5*, 359-363.

Rook, G.A.W., Steele, J., Brealey, R., Whyte, A., Isenberg, D., Sumar, N., Nelson, J.L., Bodman, K.B., Young, A., Roitt, I.M., Williams, P., Scragg, I., Edge, C.J., Arkwright, P.D., Ashford, D., Wormald, M., Rudd, P., Redman, C.W.G., Dwek, R.A., Rademacher, T.W. Changes in IgG glycoform levels are associated with remission of arthritis during pregnancy. *J. Autoimmun.* **1991**, *4*, 779-794.

Roth, J. Subcellular organization of glycosylation in mammalian cells. *Biochim. Biophys. Acta* **1987**, *906*, 405-436.

Roth, R.A., Koshland, M.E. Role of disulfide interchange enzyme in immunoglobulin synthesis. *Biochemistry* **1981**, *20*, 6594-6599.

Rothman, R.J., Warren, L., Vliegenthart, J.F.G., Härd, K.J. Clonal analysis of the glycosylation of immunoglobulin G secreted by murine hybridomas. *Biochemistry* **1989**, *28*, 1377-1384.

Routier, F.H., Davies, M.J., Bergemann, K., Hounsell, E.F. The glycosylation pattern of a humanized IgG_1 antibody (D1.3) expressed in CHO cells. *Glycoconjugate*

J. **1997**, *14*, 201-207.

Routier, F.H., Hounsell, E.F., Rudd, P.M., Takahashi, N., Bond, A., Hay, F.C., Alavi, A., Axford, J.S., Jefferis, R. Quantitation of the oligosaccharides of human serum IgG from patients with rheumatoid arthritis: a critical evaluation of different methods. *J. Immunol. Methods* **1998**, *213*, 113-130.

Rudd, P.M., Leatherbarrow, R.J., Rademacher, T.W., Dwek, R.A. Diversification of the IgG molecule by oligosaccharides. *Mol. Immunol.* **1991**, *28*, 1369-1378.

Rudd, P., Fortune, F., Lehner, T., Parekh, R., Patel, T., Wormald, M., Malhotra, R., Sim, R., Dwek, R. Lectin-carbohydrate interactions in disease: T-cell recognition of IgA and IgD; mannose binding protein recognition of IgG0. *Adv. Exp. Med. Biol.* **1995**, *376*, 147-152.

Rudd, P.M., Dwek, R.A. Glycosylation: heterogeneity and the 3D structure of proteins. *Crit. Rev. Biochem. Mol. Biol.* **1997**, *32*, 1-100.

Rudd, P.M., Elliott, T., Cresswell, P., Wilson, I.A., Dwek, R.A. Glycosylation and the immune system. *Science* **2001**, *291*, 2370-2376.

Ruddon, R.W., Bedows, E. Assisted protein folding. *J. Biol. Chem.* **1997**, *272*, 3125-3128.

Ryll, T., Wagner, R. Intracellular ribonucleotide pools as a tool for monitoring the physiological state of *in vitro* cultivated mammalian cells during production processes. *Biotechnol. Bioeng.* **1992**, *40*, 934-946.

Ryll, T., Valley, U., Wagner, R. Biochemistry of growth inhibition by ammonium ions in mammalian cells. *Biotechnol Bioeng.* **1994**, *44*, 184-193.

Saba, J.A., Shen, X., Jamieson, J.C., Perreault, H. Effect of 1-phenyl-3-methyl-5-pyrazolone labeling on the fragmentation behaviour of asialo and sialylated N-linked glycans under electrospray ionization conditions. *Rapid Commun. Mass Spectrom.* **1999**, *13*, 704-711.

Saba, J.A., Shen, X., Jamieson, J.C., Perreault, H. Investigation of different combinations of derivatization, separation methods and electrospray ionization mass spectrometry for standard oligosaccharides and glycans from ovalbumin. *J. Mass Spectrom.* **2001**, *36*, 563-574.

Saba, J.A., Kunkel, J.P., Jan, D.C.H., Ens, W.E., Standing, K.G., Butler, M., Jamieson, J.C., Perreault, H. A study of IgG glycosylation in monoclonal and polyclonal species using electrospray and matrix-assisted laser desorption/ionization mass spectrometry. *Anal. Biochem.* **2002**, *in press*.

Savvidou, G., Klein, M., Horne, C., Hofmann, T., Dorrington, K.J. A monoclonal immunoglobulin G_1 in which some molecules possess glycosylated light chains: 1. site of glycosylation. *Mol. Immunol.* **1981**, *18*, 793-805.

Savvidou, G., Klein, M., Grey, A.A., Dorrington, K.J., Carver, J.P. Possible role for peptide-oligosaccharide interactions in differential oligosaccharide processing at asparagine-107 of the light chain and asparagine-297 of the heavy chain in a monoclonal IgG_1 kappa. *Biochemistry* **1984**, *23*, 3736-3740.

Sayle, R.A., Milner-White, E.J. RASMOL: biomolecular graphics for all. *Trends Biochem. Sci.*, **1995**, *20*, 374.

Schachter, H., Narasimhan, S., Gleeson, P., Vella, G. Control of branching during the biosynthesis of asparagine-linked oligosaccharides. *Can. J. Biochem. Cell Biol.* **1983**, *61*, 1049-1066.

Schachter, H. Biosynthetic controls that determine the branching and microheterogeneity of protein-bound oligosaccharides. *Biochem. Cell Biol.* **1986**, *64*, 163-181.

Schachter, H., Brockhausen, I. The biosynthesis of branched O-glycans. *Symp. Soc. Exp. Biol.* **1989**, *43*, 1-26.

Schachter, H. Enzymes associated with glycosylation. *Curr. Opin. Struct. Biol.* **1991a**, *1*, 755-765.

Schachter, H. The 'yellow brick road' to branched complex N-glycans. *Glycobiology* **1991b**, *1*, 453-461.

Schaffner, G., Haase, M., Giess, S. Criteria for the investigation of the product equivalence of monoclonal antibodies for therapeutic and *in vivo* diagnostic use in case of introduction of changes in the manufacturing process. *Biologicals* **1995**, *23*, 253-259.

Scharff, M.D., Laskov, R. Synthesis and assembly of immunoglobulin polypeptide chains. *Prog. Allergy* **1970**, *14*, 37-80.

Schneider, M., Marison, I.W., von Stockar, U. The importance of ammonia in mammalian cell culture. *J. Biotechnol.* **1996**, *46*, 161-185.

Schroer, J.A., Bender, T., Feldman, R.J., Kim, K.J. Mapping epitopes on the insulin molecule using monoclonal antibodies. *Eur. J. Immunol.* **1983**, *13*, 693-700.

Schwartz, B.A., Gray, G.R. Proteins containing reductively aminated disaccharides: synthesis and chemical characterization. *Arch. Biochem. Biophys.* **1977**, *181*, 542-549.

Schweikart, F., Jones, R., Jaton, J.-C., Hughes, G.J. Rapid structural characterisation of a murine monoclonal IgA α chain: heterogeneity in the oligosaccharide structures at a specific site in samples produced in different bioreactor systems. *J. Biotechnol.* **1999**, *69*, 191-201.

Sears, D.W., Mohrer, J., Beychok, S. A kinetic study *in vitro* of the reoxidation of interchain disulfide bonds in a human immunoglobulin $IgG_{1\kappa}$: correlation between sulfhydryl disappearance and intermediates in covalent assembly of H_2L_2. *Proc. Natl. Acad. Sci. USA* **1975**, *72*, 353-357.

Sears, D.W., Kazin, A.R., Mohrer, J., Friedman, F., Beychok, S. Acquisition of covalent quaternary structure of an immunoglobulin G molecule: reoxidative assembly *in vitro*. *Biochemistry* **1977a**, *16*, 2016-2025.

Sears, D.W., Mohrer, J., Beychok, S. Relative susceptibilities of the interchain disulfides of an immunoglobulin G molecule to reduction by dithiothreitol. *Biochemistry* **1977b**, *16*, 2031-2035.

Shacter, E. Serum-free media for bulk culture of hybridoma cells and the preparation of monoclonal antibodies. *Trends Biotechnol.* **1989**, *7*, 248-253.

Shah, P., Reece-Ford, M., Dong, S., Goodall, M., Pidaparthi, S., Jefferis, R., Jenkins, N. Physiological influences on recombinant IgG glycosylation. *Biochem. Soc. Trans.* **1998**, *26*, S114.

Shakin-Eshleman, S.H., Spitalnik, S.L., Kasturi, L. The amino acid at the X position of an Asn-X-Ser sequon is an important determinant of N-linked core-glycosylation efficiency. *J. Biol. Chem.* **1996**, *271*, 6363-6366.

Sheeley, D.M., Merrill, B.M., Taylor, L.C.E. Characterization of monoclonal antibody glycosylation: comparison of expression systems and identification of terminal α-linked galactose. *Anal. Biochem.* **1997**, *247*, 102-110.

Shen, X., Perreault, H. Characterization of carbohydrates using a combination of derivatization, high-performance liquid chromatography and mass spectrometry. *J. Chromatogr. A* **1998**, *811*, 47-59.

Shen, X., Perreault, H. Electrospray ionization mass spectrometry of 1-phenyl-3-methyl-5-pyrazolone derivatives of neutral and *N*-acetylated oligosaccharides. *J. Mass Spectrom.* **1999**, *34*, 502-510.

Shi, Q., Jackowski, G. One-dimensional polyacrylamide gel electrophoresis. In: *Gel Electrophoresis of Proteins: A Practical Approach*, 3rd ed.; Hames, B.D., Ed.; Oxford University Press, **1998**; pp 1-52.

Shikata, K., Yasuda, T., Takeuchi, F., Konishi, T., Nakata, M., Mizuochi, T. Structural changes in the oligosaccharide moiety of human IgG with aging. *Glycoconjugate J.* **1998**, *15*, 683-689.

Shulman, M., Wilde, C.D., Köhler, G. A better cell line for making hybridomas secreting specific antibodies. *Nature* **1978**, *276*, 269-270.

Sichel, F., Malas, J.-P., Gauduchon, P., Aubert, M., Bar, E., Le Talaër, J.-Y. A simple serum galactosyltransferase assay method suitable for routine use. *Clin. Chim. Acta* **1990**, *188*, 49-58.

Sidman, C. Differing requirements for glycosylation in the secretion of related glycoproteins is determined neither by the producing cell nor by the relative number of oligosaccharide units. *J. Biol. Chem.* **1981**, *256*, 9374-9376.

Silberstein, S., Gilmore, R. Biochemistry, molecular biology, and genetics of the oligosaccharyltransferase. *FASEB J.* **1996**, *10*, 849-858.

Silverton, E.W., Navia, M.A., Davies, D.R. Three-dimensional structure of an intact human immunoglobulin. *Proc. Natl. Acad. Sci. USA* **1977**, *74*, 5140-5144.

Smith, P.K., Krohn, R.I., Hermanson, G.T., Mallia, A.K., Gartner, F.H., Provenzano, M.D., Fujimoto, E.K., Goeke, N.M., Olson, B.J., Klenk, D.C. Measurement of protein using bicinchoninic acid. *Anal. Biochem.* **1985**, *150*, 76-85.

Soltys, A.J., Hay, F.C., Bond, A., Axford, J.A., Jones, M.G., Randen, I., Thompson, K.M., Natvig, J.B. The binding of synovial tissue-derived human monoclonal immunoglobulin M rheumatoid factor to immunoglobulin G preparations of differing galactose content. *Scand. J. Immunol.* **1994**, *40*, 135-143.

Soltys, A.J., Bond, A., Westwood, O.M.R., Hay, F.C. The effects of altered glycosylation of IgG on rheumatoid factor-binding and immune complex formation. *Adv. Exp. Med. Biol.* **1995**, *376*, 155-160.

Spellman, M.W. Carbohydrate characterization of recombinant glycoproteins of pharmaceutical interest. *Anal. Chem.* **1990**, *62*, 1714-1722.

Stack, R.J., Sullivan, M.T. Electrophoretic resolution and fluorescence detection of N-linked glycoprotein oligosaccharides after reductive amination with 8-aminonaphthalene-1,3,6-trisulphonic acid. *Glycobiology* **1992**, *2*, 85-92.

Stanley, P. Glycosylation mutants of animal cells. *Annu. Rev. Genet.* **1984**, *18*, 525-552.

Stanley, P. Biochemical characterization of animal cell glycosylation mutants. *Methods Enzymol.* **1987**, *138*, 443-458.

Stanley, P. Chinese hamster ovary cell mutants with multiple glycosylation defects for production of glycoproteins with minimal carbohydrate heterogeneity. *Mol. Cell. Biol.* **1989**, *9*, 377-383.

Stanley, P. Glycosylation engineering. *Glycobiology* **1992**, *2*, 99-107.

Stanley, P., Ioffe, E. Glycosyltransferase mutants: key to new insights in glycobiology. *FASEB J.* **1995**, *9*, 1436-1444.

Starr, C.M., Masada, R.I., Hague, C., Skop, E., Klock, J.C. Fluorophore-assisted carbohydrate electrophoresis in the separation, analysis, and sequencing of carbohydrates. *J. Chromatog. A* **1996**, *720*, 295-321.

Stoscheck, C.M. Quantitation of protein. *Methods Enzymol.* **1990**, *182*, 50-68.

Strang, A.-M. "Additional" empirical relationships between oligosaccharide structure and high pH anion exchange chromatography. *Glycobiology* **1998**, *8*, iii.

Stuike-Prill, R., Meyer, B. A new force-field program for the calculation of glycopeptides and its application to a heptocosapeptide-decasaccharide of immunglobulin G_1: importance of 1-6-glycosidic linkages in carbohydrate-peptide interactions. *Eur. J. Biochem.* **1990**, *194*, 903-919.

Sumar, N., Bodman, K.B., Rademacher, T.W., Dwek, R.A., Williams, P., Parekh, R.B., Edge, J., Rook, G.A.W., Isenberg, D.A., Hay, F.C., Roitt, I.M. Analysis of glycosylation changes in IgG using lectins. *J. Immunol. Methods* **1990**, *131*, 127-136.

Sutherland III, E.W., Zimmerman, D.H., Kern, M. Synthesis and secretion of γ-globulin by lymph node cells VIII: order of synthesis of the interchain disulfide linkages of immunoglobulins. *Proc. Natl. Acad. Sci. USA* **1970**, *66*, 987-994.

Sutherland III, E.W., Zimmerman, D.H., Kern, M. Synthesis and secretion of gammaglobulin by lymph node cells: the acquisition of carbohydrate residues of immunoglobulin in relation to interchain disulfide bond formation. *Proc. Natl. Acad. Sci. USA* **1972**, *69*, 167-171.

Sutton, B.J., Phillips, D.C. The three-dimensional structure of the carbohydrate within the Fc fragment of immunoglobulin G. *Biochem. Soc. Trans.* **1983**, *11*, 130-132.

Sutton, B.J., Corper, A.J., Sohi, M.K., Jefferis, R., Beale, D., Taussig, M.J. The structure of a human rheumatoid factor bound to IgG Fc. *Adv. Exp. Med. Biol.* **1998**, *435*, 41-50.

Suzuki, S., Furuhashi, M., Suganuma, N. Additional N-glycosylation at Asn(13) rescues the human LHβ-subunit from disulfide-linked aggregation. *Mol. Cell. Endocrinol.* **2000**, *160*, 157-163.

Suzuki, T., Yan, Q., Lennarz, W.J. Complex, two-way traffic of molecules across the membrane of the endoplasmic reticulum. *J. Biol. Chem.* **1998a**, *273*, 10083-10086.

Suzuki, T., Park, H., Kitajima, K., Lennarz, W.J. Peptides glycosylated in the endoplasmic reticulum of yeast are subsequently deglycosylated by a soluble peptide N-glycanase activity. *J. Biol. Chem.* **1998b**, *273*, 21526-21530.

Suzuki, T., Lennarz, W.J. In yeast the export of small glycopeptides from the endoplasmic reticulum into the cytosol is not affected by the structure of their oligosaccharide chains. *Glycobiology* **2000**, *10*, 51-58.

Tachibana, H., Taniguchi, K., Ushio, Y., Teruya, K., Osada, K., Murakami, H. Changes of monosaccharide availability of human hybridoma lead to alteration of biological properties of human monoclonal antibody. *Cytotechnology* **1994**, *16*, 151-157.

Tachibana, H., Jiyoun, K., Taniguchi, K., Ushio, Y., Teruya, K., Osada, K., Inoue, Y., Shirahata, S., Murakami, H. Modified antigen-binding of human antibodies with glycosylation variations of the light chains produced in sugar-limited human hybridoma cultures. *In Vitro Cell. Dev. Biol. Anim.* **1996**, *32*, 178-183.

Takahashi, N., Ishii, I., Ishihara, H., Mori, M., Tejima, S., Jefferis, R., Endo, S., Arata, Y. Comparative structural study of the N-linked oligosaccharides of human normal and pathological immunoglobulin G. *Biochemistry* **1987**, *26*, 1137-1144.

Takasaki, S., Mizuochi, T., Kobata, A. Hydrazinolysis of asparagine-linked sugar chains to produce free oligosaccharides. *Methods Enzymol.* **1982**, *83*, 263-268.

Tandai, M., Endo, T., Sasaki, S., Masuho, Y., Kochibe, N., Kobata, A. Structural study of the sugar moieties of monoclonal antibodies secreted by human-mouse hybridoma. *Arch. Biochem. Biophys.* **1991**, *291*, 339-348.

Tao, M., Morrison, S.L. Studies of aglycosylated chimeric mouse-human IgG: role of carbohydrate in the structure and effector functions mediated by the human IgG constant region. *J. Immunol.* **1989**, *143*, 2595-2601.

Tarentino, A.L., Gómez, C.M., Plummer, T.H., Jr. Deglycosylation of asparagine-linked glycans by peptide:N-glycosidase F. *Biochemistry* **1985**, *24*, 4665-4671.

Tarentino, A.L., Plummer, T.H., Jr. Peptide-N^4-(*N*-acetyl-β-glucosaminyl)asparagine amidase and endo-β-*N*-acetylglucosaminidase from Flavobacterium meningosepticum. *Methods Enzymol.* **1987**, *138*, 770-778.

Tarentino, A.L., Trimble, R.B., Plummer, T.H., Jr. Enzymatic approaches for studying the structure, synthesis and processing of glycoproteins. *Methods Cell Biol.* **1989**, *32*, 111-139.

Tarentino, A.L., Plummer, T.H., Jr. Enzymatic deglycosylation of asparagine-linked glycans: purification, properties, and specificity of oligosaccharide-cleaving enzymes from Flavobacterium meningosepticum. *Methods Enzymol.* **1994**, *230*, 44-57.

Taverna, M., Thuy Tran, N., Merry, T., Horvath, E., Ferrier, D. Electrophoretic methods for process monitoring and the quality assessment of recombinant glycoproteins. *Electrophoresis* **1998**, *19*, 2572-2594.

Thompson, S.J., Hitsumoto, Y., Zhang, Y.W., Rook, G.A.W., Elson, C.J. Agalactosyl IgG in pristane-induced arthritis: pregnancy affects the incidence and severity of arthritis and the glycosylation status of IgG. *Clin. Exp. Immunol.* **1992**, *89*, 434-438.

Thompson, S.J., Leader, K.A., Lastra, G.C., Elson, C.J. The role of agalactosyl IgG in rodent models of autoimmune disease and in the pathgenesis of rheumatoid arthritis. In: *Abnormalities of IgG Glycosylation and Immunological Disorders*; Isenberg, D.A., Rademacher, T.W., Eds.; John Wiley & Sons, **1996**; pp 131-148.

Thorens, B., Vassalli, P. Chloroquine and ammonium chloride prevent terminal glycosylation of immunoglobulins in plasma cells without affecting secretion. *Nature* **1986**, *321*, 618-620.

Tomana, M., Schrohenloher, R.E., Koopman, W.J., Alarcón, G.S., Paul, W.A. Abnormal glycosylation of serum IgG from patients with chronic inflammatory diseases. *Arthritis Rheum.* **1988**, *31*, 333-338.

Tomana, M., Schrohenloher, R.E., Bennett, P.H., del Puente, A., Koopman, W.J. Occurrence of deficient galactosylation of serum IgG prior to the onset of rheumatoid arthritis. *Rheumatol. Int.* **1994**, *13*, 217-220.

Tovey, M.G. The cultivation of animal cells in continuous-flow culture. In: *Animal Cell Biotechnology*, Vol. 1; Spier, R.E., Griffiths, J.B., Eds.; Academic Press, **1985**; pp 195-210.

Towbin, H., Staehelin, T., Gordon, J. Electrophoretic transfer of proteins from polyacrylamide gels to nitrocellulose sheets: procedure and some applications. *Proc. Natl. Acad. Sci. USA* **1979**, *76*, 4350-4354.

Townsend, R.R., Hardy, M.R., Hindsgaul, O., Lee, Y.C. High-performance anion-exchange chromatography of oligosaccharides using pellicular resins and pulsed amperometric detection. *Anal. Biochem.* **1988**, *174*, 459-470.

Townsend, R.R., Hardy, M.R., Cumming, D.A., Carver, J.P., Bendiak, B. Separation of branching sialylated oligosaccharides using high-pH anion-exchange chromatography with pulsed amperometric detection. *Anal. Biochem.* **1989a**, *182*, 1-8.

Townsend, R.R., Hardy, M.R., Lee, Y.C. Separation of oligosaccharides using high-performance anion-exchange chromatography with pulsed amperometric detection. *Methods Enzymol.* **1989b**, *179*, 65-76.

Townsend, R.R., Hardy, M.R. Analysis of glycoprotein oligosaccharides using high-pH anion exchange chromatography. *Glycobiology* **1991**, *1*, 139-147.

Tretter, V., Altmann, F., März, L. Peptide-N^4-(*N*-acetyl-β-glucosaminyl)asparagine amidase F cannot release glycans with fucose attached α1,3 to the asparagine-linked *N*-acetylglucosamine residue. *Eur. J. Biochem.* **1991**, *199*, 647-652.

Trombetta, E.S., Helenius, A. Lectins as chaperones in glycoprotein folding. *Curr. Opin. Struct. Biol.* **1998**, *8*, 587-592.

Trombetta, E.S., Helenius, A. Conformational requirements for glycoprotein reglucosylation in the endoplasmic reticulum. *J. Cell. Biol.* **2000**, *148*, 1123-1129.

Tsuchiya, N., Endo, T., Matsuta, K., Yoshinoya, S., Aikawa, T., Kosuge, E., Takeuchi, F., Miyamoto, T., Kobata, A. Effects of galactose depletion from oligosaccharide chains on immunological activities of human IgG. *J. Rheumatol.* **1989**, *16*, 285-290.

Umaña, P., Bailey, P.E. A mathematical model of N-linked glycoform biosynthesis. *Biotechnol. Bioeng.* **1997**, *55*, 890-908.

Umaña, P., Jean-Mairet, J., Moudry, R., Amstutz, H., Bailey, J.E. Engineered glycoforms of an antineuroblastoma IgG_1 with optimized antibody-dependent cellular cytotoxic activity. *Nature Biotechnol.* **1999**, *17*, 176-180.

Vandamme, V., Cazlaris, H., Le Marer, N., Laudet, V., Lagrou, C., Verbert, A., Delannoy, P. Comparison of sialyl- and α1,3-galactosyltransferase activity in NIH3T3 cells transformed with ras oncogene: increased β-galactoside α-2,6-sialyltransferase. *Biochimie* **1992**, *74*, 89-100.

van den Eijnden, D.H., Joziasse, D.H. Enzymes associated with glycosylation. *Curr. Opin. Struct. Biol.* **1993**, *3*, 711-721.

Van den Steen, P., Rudd, P.M., Dwek, R.A., Opdenakker, G. Concepts and principles of O-linked glycosylation. *Crit. Rev. Biochem. Mol. Biol.* **1998**, *33*, 151-208.

van der Valk, P., Gille, J.J.P., Oostra, A.B., Roubos, E.W., Sminia, T., Joenje, H. Characterization of an oxygen-tolerant cell line derived from Chinese hamster ovary. *Cell Tissue Res.* **1985**, *239*, 61-68.

van Sommeren, A.P.G., Marchielsen, P.A.G.M., Gribnau, T.C.J. Effects of temperature, flow rate and composition of binding buffer on adsorption of mouse monoclonal IgG_1 antibodies to protein A Sepharose 4 Fast Flow. *Prep. Biochem.* **1992**, *22*, 135-149.

Van Zeben, D., Rook, G.A.W., Hazes, J.M.W., Zwinderman, A.H., Zhang, Y., Ghelani, S., Rademacher, T.W., Breedveld, F.C. Early agalactosylation of IgG is associated with a more progressive disease course in patients with rheumatoid arthritis: results of a follow-up study. *Br. J. Rheumatol.* **1994**, *33*, 36-42.

Varki, A. Biological roles of oligosaccharides: all of the theories are correct. *Glycobiology* **1993**, *3*, 97-130.

Varki, A. Factors controlling the glycosylation potential of the Golgi apparatus.

Trends Cell Biol. **1998**, *8*, 34-40.

Varki, A., Cummings, R., Esko, J., Freeze, H., Hart, G., Marth, J., Eds. *Essentials of Glycobiology*. Cold Spring Harbor Laboratory Press, **1999**.

Vassilakos, A., Michalak, M., Lehrman, M.A., Williams, D.B. Oligosaccharide binding characteristics of the molecular chaperones calnexin and calreticulin. *Biochemistry* **1998**, *37*, 3480-3490.

Verbert, A., Cacan, R., Cecchelli, R. Membrane transport of sugar donors to the glycosylation sites. *Biochimie* **1987**, *69*, 91-99.

Walker, M.R., Lund, J., Thompson, K.M., Jefferis, R. Aglycosylation of human IgG_1 and IgG_3 monoclonal antibodies can eliminate recognition by human cells expressing $Fc\gamma$ RI and/or $Fc\gamma$ RII receptors. *Biochem. J.* **1989**, *259*, 347-353.

Wallick, S.C., Kabat, E.A., Morrison, S.L. Glycosylation of a V_H residue of a monoclonal antibody against α(1-6) dextran increases its affinity for antigen. *J. Exp. Med.* **1988**, *168*, 1099-1109.

Wang, J., Hata, M., Park, Y.S., Iijima, S., Kobayashi, T. Effects of dissolved oxygen concentration on anchorage-dependent animal cell growth and erythropoietin production. *J. Ferment. Bioeng.* **1994**, *78*, 321-326.

Wang, J., Honda, H., Watanabe, H., Kobayashi, T. Enhancement of tPA production under hyperoxic conditions by BHK cells in serum-free and serum-containing cultures. *J. Ferment. Bioeng.* **1995**, *79*, 579-584.

Ware, F.E., Vassilakos, A., Peterson, P.A., Jackson, M.R., Lehrman, M.A., Williams, D.B. The molecular chaperone calnexin binds $Glc_1Man_9GlcNAc_2$ oligo-saccharide as an initial step in recognizing unfolded glycoproteins. *J. Biol. Chem.* **1995**, *270*, 4697-4704.

Warner, T.G., Chang, J., Ferrari, J., Harris, R., McNerney, T., Bennett, G., Burnier, J., Sliwkowski, M.B. Isolation and properties of a soluble sialidase from the culture fluid of Chinese hamster ovary cells. *Glycobiology* **1993**, *3*, 455-463.

Watson, M., Rudd, P.M., Bland, M., Dwek, R.A., Axford, J.S. Sugar printing rheumatic diseases: a potential method for disease differentiation using immunoglobulin G oligosaccharides. *Arthritis Rheum.* **1999**, *42*, 1682-1690.

Weikert, S., Papac, D., Briggs, J., Cowfer, D., Tom, S., Gawlitzek, M., Lofgren, J., Mehta, S., Chisholm, V., Modi, N., Eppler, S., Carroll, K., Chamow, S., Peers, D., Berman, P., Krummen, L. Engineering Chinese hamster ovary cells to maximize sialic acid content of recombinant glycoproteins. *Nature Biotechnol.* **1999**, *17*, 1116-1121.

Weitzhandler, M., Hardy, M., Co, M.S., Avdalovic, N. Analysis of carbohydrates on IgG preparations. *J. Pharm. Sci.* **1994**, *83*, 1670-1675.

Weitzman, S., Scharff, M.D. Mouse myeloma mutants blocked in the assembly, glycosylation and secretion of immunoglobulin. *J. Mol. Biol.* **1976**, *102*, 237-252.

White, K.D., Cummings, R.D., Waxman, F.J. Ig N-glycan orientation can influence interactions with the complement system. *J. Immunol.* **1997**, *158*, 426-435.

Williams, P.J., Arkwright, P.D., Rudd, P., Scragg, I.G., Edge, C.J., Wormald, M.R., Rademacher, T.W. Selective placental transport of maternal IgG to the fetus. *Placenta* **1995**, *16*, 749-756.

Wilson, I.B.H., Gavel, Y., von Heijne, G. Amino acid distributions around O-linked glycosylation sites. *Biochem. J.* **1991**, *275*, 529-534.

Wilson, I.B.H., Platt, F.M., Isenberg, D.A., Rademacher, T.W. Aberrant control of galactosyltransferase in peripheral B lymphocytes and Epstein-Barr virus transformed B-lymphoblasts from patients with rheumatoid arthritis. *J. Rheumatol.* **1993**, *20*, 1282-1287.

Wilson, I.B.H., Harthill, J.E., Mullin, N.P., Ashford, D.A., Altmann, F. Core α1,3-fucose is a key part of the epitope recognized by antibodies reacting against plant N-linked oligosaccharides and is present in a wide variety of plant extracts. *Glycobiology* **1998**, *8*, 651-661.

Wilson, I.B.H., Zeleny, R., Kolarich, D., Staudacher, E., Stroop, C.J.M., Kamerling, J.P., Altmann, F. Analysis of Asn-linked glycans from vegetable foodstuffs: widespread occurrence of Lewis a, core α1,3-linked fucose and xylose substitutions. *Glycobiology* **2001**, *11*, 261-274.

Winkelhake, J.L. Immunoglobulin structure and effector functions. *Immunochemistry* **1978**, *15*, 695-714.

Wormald, M.R., Rudd, P.M., Harvey, D.J., Chang, S.-C., Scragg, I.G., Dwek, R.A. Variations in oligosaccharide-protein interactions in immunoglobulin G determine the site-specific glycosylation profiles and modulate the dynamic motion of the Fc oligosaccharides. *Biochemistry* **1997**, 36, 1370-1380.

Wormald, M.R., Dwek, R.A. Glycoproteins: glycan presentation and protein-fold stability. *Structure* **1999**, *7*, R155-R160.

Wright, A., Tao, M., Kabat, E.A., Morrison, S.L. Antibody variable region glycosylation: position effects on antigen binding and carbohydrate structure. *EMBO J.* **1991**, *10*, 2717-2723.

Wright, A., Morrison, S.L. Antibody variable region glycosylation: biochemical and clinical effects. *Springer Semin. Immunopathol.* **1993**, *15*, 259-273.

Wright, A., Morrison, S.L. Effect of altered CH2-associated carbohydrate structure in the functional properties and *in vivo* fate of chimeric mouse-human

immunoglobulin G_1. *J. Exp. Med.* **1994**, *180*, 1087-1096.

Wright, A., Morrison, S.L. Effect of glycosylation on antibody function: implications for genetic engineering. *Trends Biotechnol.* **1997**, *15*, 26-32.

Wright, A., Morrison, S.L. Effect of C2-associated carbohydrate structure on IgG effector function: studies with chimeric mouse-human IgG_1 antibodies in glycosylation mutants of Chinese hamster ovary cells. *J. Immunol.* **1998**, *160*, 3393-3402.

Wright, A., Sato, Y., Okada, T., Hee Chang, K., Endo, T., Morrison, S.L. *In vivo* trafficking and catabolism of IgG_1 antibodies with Fc associated carbohydrates of differing structure. *Glycobiology* **2000**, *10*, 1347-1355.

Yamada, E., Tsukamoto, Y., Sasaki, R., Yagyu, R., Takahashi, N. Structural changes of immunoglobulin G oligosaccharides with age in healthy human serum. *Glycoconjugate J.* **1997**, *14*, 401-405.

Yamaguchi, Y., Kato, K., Shindo, M., Aoki, S., Furusho, K., Koga, K., Takahashi, N., Arata, Y., Shimada, I. Dynamics of the carbohydrate chains attached to the Fc portion of immunoglobulin G as studied by NMR spectroscopy assisted by selective ^{13}C labeling of the glycans. *J. Biomol. NMR* **1998**, *12*, 385-394.

Yang, M. Ammonia effects on CHO cell growth, metabolism, erythropoietin production and glycosylation. *Ph.D. Thesis* **2000**, Department of Microbiology, University of Manitoba.

Yang, M., Butler, M. Effects of ammonia on CHO cell growth, erythropoietin production, and glycosylation. *Biotechnol. Bioeng.* **2000a**, *68*, 370-380.

Yang, M., Butler, M. Effect of ammonia on the glycosylation of human recombinant erythropoietin in culture. *Biotechnol. Prog.* **2000b**, *16*, 751-759.

Yeh, J.-C., Cummings, R.D. Differential recognition of glycoprotein acceptors by terminal glycosyltransferases. *Glycobiology* **1997**, *7*, 241-251.

Yet, M.-G., Shao, M.-C., Wold, F. Effects of the protein matrix on glycan processing in glycoproteins. *FASEB J.* **1988**, 2, 22-31.

Yet, M.-G., Wold, F. The distribution of glycan structures in individual N-glycosylation sites in animal and plant glycoproteins. *Arch. Biochem. Biophys.* **1990**, *278*, 356-364.

Zanghi, J.A., Mendoza, T.P., Schmelzer, A.E., Knop, R.H., Miller, W.M. Role of nucleotide sugar pools in the inhibition of NCAM polysialylation by ammonia. *Biotechnol. Prog.* **1998a**, *14*, 834-844.

Zanghi, J.A., Mendoza, T.P., Knop, R.H., Miller, W.M. Ammonia inhibits neural cell adhesion molecule polysialylation in Chinese hamster ovary and small cell lung

cancer cells. *J. Cell. Physiol.* **1998b**, *177*, 248-263.

Zanghi, J.A., Schmelzer, A.E., Mendoza, T.P., Knop, R.H., Miller, W.M. Bicarbonate concentration and osmolality are key determinants in the inhibition of CHO cell polysialylation under elevated pCO_2 or pH. *Biotechnol. Bioeng.* **1999**, *65*, 182-191.